THE CONTROL OF CHROMOSOME SEGREGATION IN MOUSE OOCYTES

Simon I.R. Lane BSc (Hons I)

PhD Thesis

April 2012

The thesis contains no material which has been accepted for the award of any other degree or diploma in any university or other tertiary institution and, to the best of my knowledge and belief, contains no material previously published or written by another person, except where due reference has been made in the text. I give consent to this copy of my thesis, when deposited in the University Library, being made available for loan and photocopying subject to the provisions of the Copyright Act 1968.

Simon Lane, 2nd April 2012

I hereby certify that the work embodied in this thesis contains published papers of which I am a joint author. I have included as part of the thesis a written statement, endorsed by my supervisor, attesting to my contribution to the joint publications (Appendix I).

Simon Lane, 2nd April 2012

This page is dedicated to Dr. C. K. Mercer

Acknowledgements

My sincerest thanks to Prof. Keith Jones for his tireless supervision and guidance, and for all the sound advice he has offered throughout my PhD.

I want to thank my family, who have been very understanding and supportive through my student years. In particular, Mum, for her endless encouragement, support and belief, and Dad too for his unique mix of wisdom and humour.

Thank you to the members of the Jones' lab; Janet, Jessica, Julie, Keith, Kyra, Michelle, Phoebe, Sophia, Suzanne, Wai and Yan, who made my PhD such an enjoyable experience.

Lastly I thank Charlene, for sticking by me through the good times and the trying times and for making every day worthwhile.

TABLE OF CONTENTS

Table of contents 5
Abstract 11
Table of Figures 12
List of commonly used abreviations 13
1 Introduction 15
1.1.1 Aims of this introduction 15
1.2 Cell cycle machinery 15
1.2.1 Cyclin dependent kinase 1 15
1.2.2 The anaphase promoting complex 16
1.2.3 The spindle assembly checkpoint 17
1.2.4 Molecular basis for the spindle assembly checkpoint 19
1.3 Meiosis I 22
1.3.1 Meiosis overview: Two divisions, two arrests 22
1.3.2 Primordial germ cell differetiation 25
1.3.3 Recombination 25
1.3.4 Germinal vesicle arrest 26
1.3.5 Follicle recruitment and growth 28
1.3.6 Resumption of meiosis I 29
1.3.7 Early prometaphase I: Spindle assembly 29
1.3.8 Late prometaphase: The SAC 30
1.3.9 Sister mono-orientation 32
1.3.10 Kinetochore capture and error correction 32
1.3.11 Checkpoint criteria 33
1.3.12 Metaphase 34
1.3.13 Anaphase 35
1.3.14 Exit from meiosis I 36
1.3.15 Aneuploidy in oocytes 37
1.4 Thesis Aims 38
1.4.1 The spindle assembly checkpoint in mouse oocytes 38
1.4.2 Meiosis I checkpoint criteria 38
1.4.3 The SAC role of aurora kinases in meiosis 38
1.4.4 Timing of meiosis I exit 38
2 Methods and Materials 40
2.1 Mouse handling and dissection 40
2.1.1 Ethics 40
2.1.2 Breeding 40
2.1.3 Hormonal priming 40
2.1.4 Dissection 40

2.2 Oocyte collection and handling 41
2.2.1 Handling pipette manufacture 41
2.2.2 Oocyte collection 41
2.3 Oocyte culture 41
2.3.1 M2 media 41
2.3.2 MEM media 42
2.3.3 Preparation and addition of drugs to culture media 42
2.3.4 Milrinone and oocyte synchronization 42
2.4 Western Blot 44
2.4.1 Sample preparation 44
2.4.2 Gel loading and protein separation 44
2.4.3 Protein transfer 44
2.4.4 Immunolabelling and chemiluminescence 45
2.5 Cloning 45
2.5.1 Plasmid design and cloning strategy 45
2.5.2 Gene amplification 46
2.5.3 Restirction digest 46
2.5.4 Ligation 46
2.5.5 Transformation of competent cells 49
2.5.6 PCR screening 49
2.5.7 Plasmid preparation 49
2.5.8 DNA Sequencing 50
2.6 mRNA synthesis 50
2.6.1 Linearisation and DNA preparation 50
2.6.2 RNA polymerase reaction 52
2.6.3 RNA purification and preparation 52
2.7 Oocyte fixation 54
2.7.1 General techniques 54
2.7.2 Fixing for kinetochore counting 54
2.7.3 Fixing to preserve stable microtubules 54
2.8 Immunofluorescence 54
2.8.1 General principles 54
2.8.2 Antibodies used in this thesis 55
2.9 Microinjection 56
2.9.1 Injection pipette preparation 56
2.9.2 Loading pipette preparation 56
2.9.3 Inverted microscope customisation 56
2.9.4 Microinjection 58
2.10 imaging Systems 61

2.10.1 General principles 61
2.10.2 Fluorchromes and light sources 61
2.10.3 Dichroic mirrors and optics 64
2.10.4 Objectives 64
2.10.5 Cameras/detectors 64
2.11 Oocyte imaging 65
2.11.1 Imaging of fixed samples 65
2.11.2 Inverted microscopy 65
2.11.3 Confocal microscopy 65
2.12 Image analysis and figure preparation 66
2.12.1 Mad2/CREST kinetochore analysis 66
2.12.2 Analysis of bivalents 67
2.12.3 Figure preparation 67
2.12.4 Calculating spindle dimensions 68
2.12.5 Densitometric Analyisis 68
2.12.6 Cyclin B1-GFP analysis 68
3 The SAC in meiosis I 71
3.1 Introduction 71
3.2 Progression of meiosis I in mouse oocytes 72
3.2.1 Development of the MI spindle. 72
3.2.2 Bivalent arrangement during maturation 73
3.2.3 Formation of kinetochore and non-kinetochore microtubule fibres during prometaphase I. 76
3.2.4 Destruction of endogenous cyclin B1 and securin in prometaphase I. 84
3.2.5 Destruction of exogenous cyclin B1-GFP in prometaphase I. 84
3.2.6 Loss of exogenous Mad2 from chromosomes during prometaphase I 87
3.2.7 Timing of loss of endogenous Mad2 from kinetochores and APC activation. 87
3.3 Movie Figure legends 92
3.4 Discussion 92
3.4.1 Initial spindle formation and bivalent organisation 92
3.4.2 Spindle polarisation and bivalent alignment, orientation and stretching. 93
3.4.3 The timing of k-fibre formation, SAC satisfaction and APC activation in meiosis I. 94
3.4.4 Cyclin B1 destruction and exit from meiosis I 96
3.4.5 Comparing relative timings 97
3.4.6 Summary 97
4 Non-aligned bivalents in meiosis I 100
4.1 Introduction 100
4.2 Results 101

4.2.1 Non-aligned chromosomes are a common feature of metaphase I. 101
4.2.2 Non-aligned chromosomes are bivalents 101
4.2.3 Non-aligned bivalents recruit Mad2 103
4.2.4 Non-aligned bivalents have microtubule attachments 108
4.2.5 Live imaging of non-aligned bivalents 112
4.2.6 Non-aligned bivalents do not inhibit the APC. 113
4.2.7 The fate of non-aligned bivalents 116

4.3 Movie Figure Legends 118

4.4 Discussion 120
4.4.1 Non alignment is a common phenomenon in oocytes, but not somatic cells 120
4.4.2 Non-aligned bivalents, Mad2, tension, inter-kinetochore distance and microtubule attachment 121
4.4.3 A model for chromosome alignment 122
4.4.4 Non-alignment, APC activity and aneuploidy 122
4.4.5 Non-alignment as a relevant mechanism for generating aneuploidy 125
4.4.6 Summary 126

5 The effects of the pan-Aurora inhibitor ZM447439 on meiosis I 127

5.1 Introduction 127

5.2 The effects of ZM447439 on oocyte meiosis I 129
5.2.1 Dose determination for the use of ZM447439 and nocodazole 129
5.2.2 ZM447439 addition in prophase does not block GVBD 129
5.2.3 ZM447439 addition from GVBD onward caused an aborted polar body extrusion 131
5.2.4 Prometaphase addition of ZM447439 accelerates PBE 135
5.2.5 Incubation with ZM447439 prevents formation of a metaphase II spindle. 139
5.2.6 ZM447439 effect depends on timing of addition 139
5.2.7 ZM447439 can overcome nocodazole induced arrest in MI oocytes. 142
5.2.8 Addition of ZM447439 reverses nocodazole inhibition of the APC. 145
5.2.9 ZM447439 treatment causes an increase in aneuploidy 148

5.3 Discussion 151
5.3.1 Auroras are not required for GVBD but are required for maturation. 151
5.3.2 Inhibition of Auroras throughout prometaphase blocks oocyte maturation. 151
5.3.3 Auroras have temporally distinct roles during maturation. 152
5.3.4 Aurora Kinase inhibition in early prometaphase shortens meiosis I. 153
5.3.5 Aurora Kinases are required to correct kinetochore microtubule attachments 154
5.3.6 Aurora Kinases reduce aneuploidy 155
5.3.7 Is Aurora SAC function direct or indirect? 156
5.3.8 Summary 156

6 Control of anaphase timing and exit from meiosis I 158

6.1 Introduction 158

6.2 Cdk1 in exit from meiosis I 159
6.2.1 CDK inhibition causes premature anaphase onset 159
6.2.2 Timing of anaphase depends on timing of CDK inhibition 159
6.2.3 Timing of anaphase can be modified by cyclin B1 levels 161

6.3 APC activity and exit from meiosis I 165
6.3.1 CDK activity prevents maximal APC activity 165
6.3.2 Aurora Kinase activity prevents maximal APC activity 167

6.4 Discussion 169
6.4.1 CDK inhibition hastens anaphase 170
6.4.2 Could cyclin B1 levels determine the timing of anaphase? 171
6.4.3 The mitotic exit network 171
6.4.4 The APC is not maximally active following SAC satisfaction in MI 173
6.4.5 Cyclin B1 destruction is incomplete in meiosis I 174
6.4.6 An evolutionary perspective 174
6.4.7 Summary 175

7 General discussion 176

7.1 Summary 176

7.2 Discussion 176
7.2.1 Aneuploidy in oocytes 176
7.2.2 APC activity 177

8 Appendix 180

8.1 Published works contained in this thesis 180
Appendix I. Declaration of Authorship 180

8.2 Buffers and solutions 181

Notes 181
Appendix II. PMSG 181
Appendix III. M2 Media 181
Appendix IV. MEM Media 182
Appendix V. General Buffering solutions 182
Appendix VI. Western Blotting solutions 182
Appendix VII. Fixation solutions 183
Appendix VIII. Immunofluorescence Solutions 184
Appendix IX. Microinjection Solutions 185

8.3 Imaging and fluorochrome information 185
Appendix X. Spectral information for common Fluorochromes 185

8.4 Image J macros 185

Appendix XI. Mad2 / CREST measurment macro 185
Appendix XII. Bivalent measurement macro 188

Bibliography 193

ABSTRACT

This thesis explores the first meiotic division in mouse oocytes, using imaging of fluorescent chimeras by confocal and epifluorescence microscopy in real time and of fixed specimens following immunocytochemistry. The activities of the spindle assembly checkpoint (SAC) and the anaphase promoting complex (APC) are examined with respect to the timing of germinal vesicle breakdown, spindle formation, chromosome alignment, and polar body extrusion. The activation of the APC, an event that in mitosis is prevented until proper attachment of all chromosomes is achieved, is shown not to be strictly coupled to bivalent alignment in prometaphase I. Instead the metaphase to anaphase transition is begun following the attachment of the majority of kinetochores and is characterised by sub-optimal activity of the APC. It is shown that this uncoupling of the SAC and chromosome alignment has the potential to generate aneuploidy. These findings have implications for the high aneuploidy rates deriving from the first meiotic division, which are often responsible for miscarriage in humans.

TABLE OF FIGURES

Figure 1.1 The role of the APC in controlling anaphase onset 18
Figure 1.2 - Overview of progression from prophase arrest through to metaphase II arrest. 23
Figure 1.3 - Chromosome attachment and segregation in meiosis I and II 24
Figure 1.4 - Formation of crossovers during prophase of meiosis I 27
Figure 2.1 - Timing of GVBD after release from milrinone arrest. 43
Figure 2.2 - Map of the pMDL vector. 47
Figure 2.3 - Inverted microscope customized for microinjection 57
Figure 2.4 - Microinjection of mouse oocytes 60
Figure 2.5 - Light path through an inverted microscope with an excitation filter and a dichroic mirror pair for imaging GFP. 62
Figure 2.6 - Analysis of fluorescent protein intensity during meiosis I 69
Figure 3.1 - The formation of the MI spindle. 74
Figure 3.2 Bivalent behaviour during meiosis I 77
Figure 3.3 - Spindle formation occurs early in prometaphase but stable k-fibres do not form until 4-5 h. 79
Figure 3.4 - Kinetochores are not connected by microtubule fibres at 4 h. 81
Figure 3.5 - Kinetochores are connected by microtubule fibres at 5 h. 82
Figure 3.6 - The majority of kinetochores acquire microtubule attachment 4-5 h. 83
Figure 3.7 - Degradation of endogenous cyclin B1 and securin during prometaphase I. 85
Figure 3.8 - Degradation of cyclin B1-GFP during meiosis I. 86
Figure 3.9 - Loss of Mad2-YFP from chromosomes during prometaphase I. 88
Figure 3.10 - Loss of endogenous Mad2 from kinetochores is coincident with APC activation. 89
Figure 3.11 - Overview of the timing of events in meiosis I 98
Figure 4.1 - Non aligned chromosomes can be observed following APC activation 102
Figure 4.2 - Non-aligned chromosomes are identified as bivalents 104
Figure 4.3 - Non-aligned bivalents recruit more Mad2 than aligned bivalents 106
Figure 4.4 - Non-aligned bivalents form microtubule attachments 110
Figure 4.5 - Live imaging of a non-aligned bivalent using CenpC-EGFP to visualise kinetochores 114
Figure 4.6 - Non-aligned bivalents do not delay anaphase 115
Figure 4.7 - Non-aligned bivalents can persist until anaphase and result in non-disjunction. 117
Figure 4.8 - Possible mechanism by which non-aligned bivalents achieve alignment and orientation. 123
Figure 5.1 - Percentage PBE following addition of 3-30µM ZM447439. 130
Figure 5.2 - ZM447439 addition at the time of GVBD results in a block to PBE. 132

Figure 5.3 - ZM447439 addition from GVBD disrupts chromosome congression and segregation. 134
Figure 5.4 - Percentage of PBE after addition of ZM447439 between 0-4 h. 136
Figure 5.5 - ZM447439 addition at 2 h causes resorption of polar bodies. 137
Figure 5.6 - Aurora Kinase inhibition in early prometaphase quickens meiosis I. 138
Figure 5.7 - Aurora Kinase inhibition increases non-alignment and lagging chromosomes. 140
Figure 5.8 - Oocytes treated with ZM447439 from 4 h fail to assemble a normal metaphase II spindle. 141
Figure 5.9 - Effect of ZM447439 addition for the first two h of maturation or after 6 h of maturation on PBE timing. 143
Figure 5.10 - Aurora Kinase inhibition can overcome the SAC. 144
Figure 5.11 - Effects of ZM447439 and nocodazole on spindle formation. 146
Figure 5.12 - ZM447439 addition initiates cyclin B1 degradation in nocodazole arrested oocytes. 147
Figure 5.13 - The effect of monastrol treatment on a mouse oocyte spindles. 149
Figure 5.14 - ZM447439 addition increases aneuploidy in mouse oocytes. 150
Figure 6.1 - The effect of various doses of roscovitine on GVBD 160
Figure 6.2 - The effect of roscovitine addition to oocytes at various times during Meiosis I 162
Figure 6.3 - Anaphase in oocytes with high levels of cyclin B1-GFP following roscovitine addition 163
Figure 6.4 - The effect of roscovitine on APC activity 166
Figure 6.5 - The effect of ZM447439 on APC activity 168
Figure 7.1 - Possible effect of aging on chromosome cohesion and microtubule attachment 178

LIST OF COMMONLY USED ABREVIATIONS

APC – Anaphase Promoting Complex

CDK – Cyclin Dependent Kinase

CPC – Chromosomal Passenger Complex

GVBD – Germinal Vesicle Breakdown

ICC – Immunocytochemistry

MCC – Mitotic Checkpoint Complex

MI – Meiosis I

MII – Meiosis II

PBE – Polar Body Extrusion

PGC – Primordial Germ Cell

SAC – Spindle Assembly Checkpoint

SC – Synaptonemal Complex

1 INTRODUCTION

Meiosis is a highly specialised set of cell divisions which fulfils a unique role in sexually reproducing species. It forms the precarious link between one generation and the next where the entire future organism is contained in just two cells, the spermatozoon and the oocyte. The fusion of these two cells allows for the creation of new combinations of alleles. This in turn maintains genetic diversity within a species.

In readiness for fertilisation where the DNA content of the resulting cell will double, each gamete must have only a half complement of chromosomes. The purpose of the meiotic divisions therefore is to produce a gamete cell, which is highly specialised for the purposes of fertilization, and contains only one copy, instead of the normal two copies, of each chromosome. This thesis is concerned only with the female gamete, and this introduction will address some of the specialisations that the oocyte acquires as it goes through the first meiotic division.

1.1.1 AIMS OF THIS INTRODUCTION

This introduction aims to provide an overview of the first meiotic division. The oocyte is highly differentiated for conducting the two meiotic divisions, fertilisation and the subsequent embryonic divisions; the specialisations it possesses to allow it to achieve these unique events are too numerous to list. Therefore this introduction is only concerned with providing sufficient background for the major events and activities during the first division, which will form the basis of this thesis.

Before discussing the oocyte however, it is necessary to introduce some of the relevant cell cycle machinery in the context of mitosis, in which most of the detailed research on these components has been conducted. Later in the introduction the first division in the oocyte will be discussed which, despite being highly specialised, utilises much the same mechanisms found in mitosis.

1.2 CELL CYCLE MACHINERY

1.2.1 CYCLIN DEPENDENT KINASE 1

Cyclin Dependant Kinase 1 (Cdk1) is a kinase that requires a binding partner for its activity. Its predominant binding partner is cyclin B1, so called because of its cyclic

emergence once per cell cycle in mitosis (Moreno et al., 1989). Cdk1 is a master regulator of the events of mitosis; its activity being implicated in almost every major process (Enserink and Kolodner, 2010). Importantly, a rise in Cdk1 activity drives cells into mitosis and is required for many events, such as nuclear envelope breakdown, chromosome condensation and spindle assembly. Conversely a decline in Cdk1 activity is responsible for mitotic exit.

Regulation of Cdk1 is therefore a key feature of both entry into and exit from the cell cycle. Entry into mitosis is restricted until completion of DNA repair and replication by low levels of cyclin B1, but also by inhibitory phosphorylation on Cdk1 (Lindqvist et al., 2009). To ensure proper exit from mitosis Cdk1 is inactivated by destruction of cyclin B1 (Wolf et al., 2006), which is discussed below, and again by regulation of Cdk1 phosphorylation (Potapova et al., 2009).

1.2.2 THE ANAPHASE PROMOTING COMPLEX

The anaphase promoting complex (APC) is a large, multi-subunit, E3 ubiquitin ligase that specifically targets proteins based on the presence of sequence motifs (Peters, 2006). Many APC target motifs have been categorised, and most are variants of the D-box and KEN box motifs (Pines, 2011). Recognition by the APC allows the proteins to be labelled by poly-ubiquitin chains, marking the proteins and permitting their degradation by the 26S proteosome (Bedford et al., 2010). The APC has been found to have two activating subunits, Cdh1 and Cdc20, which also act as adaptors, recognising and presenting substrates to the APC (Thornton et al., 2006). The binding of the APC to one of these two subunits allows the substrate specificity of the APC to be temporally regulated. Cdc20 predominantly binds the APC during mitosis, switching to Cdh1 after anaphase (Hagting et al., 2002). Both Cdc20 and Cdh1 recognise the D box, whilst Cdh1 can also recognise the KEN box (Pfleger and Kirschner, 2000). During prometaphase and metaphase Cdc20 is the main APC activator, and this appears to be due to high Cdk1 activity, providing activating phosphorylation to the APC, which then favours Cdc20 binding over Cdh1 (Kraft et al., 2003; Rudner and Murray, 2000; Shteinberg et al., 1999).

APC activity, as its name suggests, is critical for anaphase because it regulates the activity of an enzyme termed separase. During mitosis, separase is the key activity that must be restrained to prevent premature anaphase, as its activation provides the final,

non-reversible action required for anaphase. Its primary function is to cleave the cohesin complexes that are holding chromosomes together. It is APC^{Cdc20} activity that activates separase by targeting two critically regulated proteins, cyclin B1 and securin, for destruction (Figure 1.1). Both cyclin B1 and securin have a role to play in inhibiting separase and their destruction is sufficient and required for proper anaphase onset (Chang et al., 2003; Clute and Pines, 1999; Thornton and Toczyski, 2003).

Separase is held in an inactive state because it is bound to securin, its inhibitory chaperone. APC mediated destruction of securin resolves this complex, freeing separase. However its activity is also prevented by additional means, as even in the absence of securin, premature anaphase onset is prevented (Stemmann et al., 2001). This second mechanism was shown to be phosphorylation of separase by Cdk1. The other critical APC target, cyclin B1, is required for Cdk1 activity. Its destruction therefore decreases Cdk1 activity, reducing inhibitory phosphorylation of separase. Further to this the Cdk1/Cyclin B1 heterodimer can bind phosphorylated separase, which also acts to inhibit it (Gorr et al., 2005). Thus the APC, by promoting destruction of two key proteins, cyclin B1 and securin, is central to promoting separase activity and therefore anaphase (Figure 1.1).

In spite of its name, the anaphase promoting complex has functions throughout the cell cycle, and not only at the metaphase to anaphase transition. Its destruction of cyclin B1 and securin is its most predominant role as far as this thesis is concerned, but it is worth noting that regulation of the APC is also critical during the G2-M transition. APC activity during the equivalent transition in oocytes is very important as will be discussed later.

1.2.3 THE SPINDLE ASSEMBLY CHECKPOINT

Before successful segregation can occur, chromosomes must first be attached to the mitotic spindle. This is a bi-polar structure comprising of microtubule arrays generates the forces needed to separate chromosome from each other at anaphase. Each sister chromatid attaches to the spindle via a kinetochore, a large protein complex comprising of many subunits, that allows microtubules in the spindle to become tethered to chromosomes (Cheeseman et al., 2006; Musacchio and Salmon, 2007). The process of attaching chromosomes to the spindle takes a variable length of time due to the

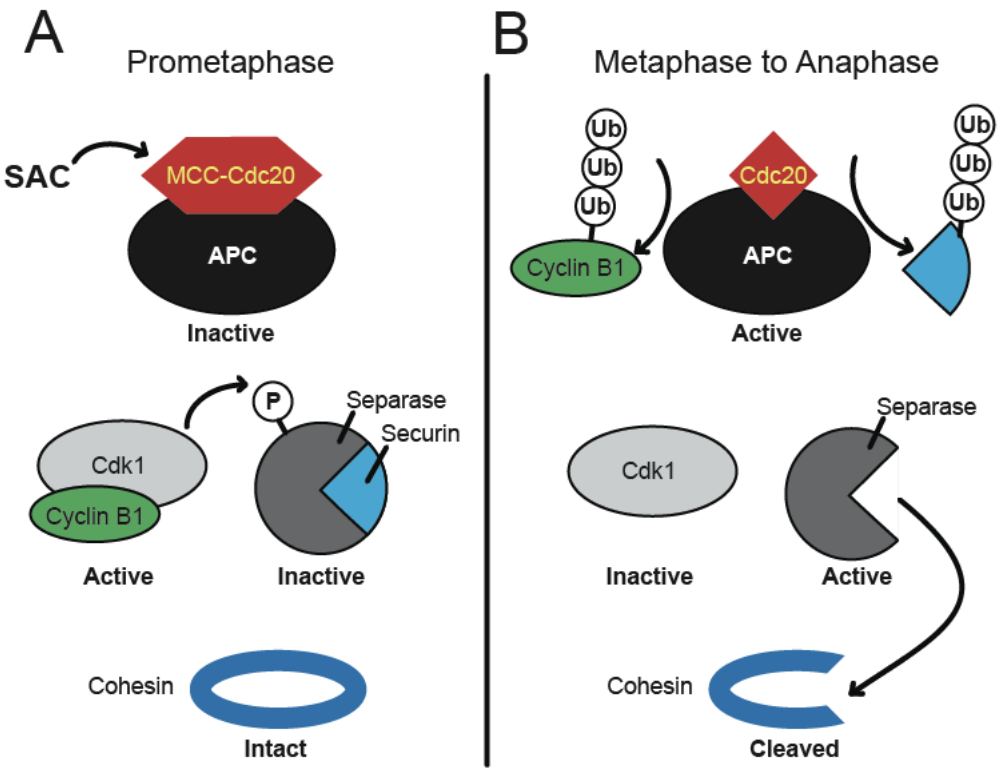

Figure 1.1 The role of the APC in controlling anaphase onset

(A)During prometaphase the APC is inactive towards cyclin B1 and separase. Separase is inhibited both by the presence of securin and by phosphorylation from active Cdk1/cyclin B1. Cohesin therefore remains intact due to the inactivity of separase. (B) Following activation of the APC both cyclin B1 and securin are targeted for destruction due to addition of ubiquitin molecules by APC^{Cdc20}*.This inactivates Cdk1, thus allowing removal of phosphorylation from separase resulting in its activation. Active separase then cleaves cohesin residues, permitting anaphase onset.*

stochastic nature of microtubules capturing kinetochores (Kotwaliwale and Biggins, 2006). Additionally there is no guarantee that initial microtubule-kinetochore attachments will be correct ones (Cimini et al., 2006). Therefore, the timing of anaphase must be controlled so that it occurs only after the correct attachment of all chromosomes to the spindle. The mechanism employed to do this is the spindle assembly checkpoint (SAC). As mentioned above, it is the APC that drives cells into anaphase, it therefore makes a logical target for the SAC. More specifically, it is the APC activator, Cdc20 that is regulated by the SAC (Fang et al., 1998; Sudakin et al., 2001).

In mitosis the efficacy of the SAC is high. Somatic cells rarely make errors when undergoing mitosis and this is due to their sensitivity to a single unaligned chromosome. Proof of a checkpoint that co-ordinates the attachment of the chromosomes to the spindle with anaphase came from direct observation of chromosomes in live cells (Rieder et al., 1994). In these experiments the duration of mitosis was proportional to the time for which unattached kinetochores persisted. Following attachment of the final kinetochore however, the time taken to anaphase was very consistent, providing strong evidence for a checkpoint that responded to kinetochore attachment. Proof that this signal is produced by the kinetochore came from experiments in which the last unattached kinetochore in a living cell was destroyed by laser irradiation. The cell then completed anaphase with normal timing, indicating that along with the kinetochore the checkpoint signal had been ablated (Rieder et al., 1995). Thus the role of microtubule attachment in satisfying the SAC was established.

1.2.4 MOLECULAR BASIS FOR THE SPINDLE ASSEMBLY CHECKPOINT

Even before the SAC was demonstrated to be a kinetochore derived signal in the mid 1990s, many components of the SAC had already been identified in screens for yeast mutants that failed to arrest following spindle disruption. Different core SAC proteins including members of the Mad (Mitotic arrest deficient) and Bub (Budding uninhibited by benzimidazoles) families were first identified in 1991 (Hoyt et al., 1991; Li and Murray, 1991) and Mps1 in 1996 (Weiss and Winey, 1996).

The SAC signal is initiated on unattached kinetochores (Li and Nicklas, 1995; Rieder et al., 1995; Rieder et al., 1994) as discussed above, and so it is not surprising that the

SAC proteins and their target the APC activator Cdc20, and the APC itself are all found to localise there (Acquaviva et al., 2004; Chan et al., 2005; Howell et al., 2000; Johnson et al., 2004; Kallio et al., 2002; Shah et al., 2004). The SAC components that inhibit Cdc20 are collectively called the mitotic checkpoint complex (MCC) and comprise of Mad2, BubR1 and Bub3, of which Mad2 and BubR1 directly bind Cdc20 (Kulukian et al., 2009; Sudakin et al., 2001). By binding Cdc20 this complex reduces Cdc20 mediated activation of the APC. MCC-Cdc20 binds and inhibits the APC, preventing ubiquitination of cyclin B1 and securin, in addition, Cdc20 itself is processed for degradation during this process and the MCC components are released to be re-used (Mansfeld et al., 2011). Once the SAC signal ceases following complete attachment of all kinetochores to the spindle cyclin B1 directed APC^{Cdc20} activity begins (Clute and Pines, 1999).

The formation of MCC involves many SAC proteins, but centres around Mad2. Mad2 has two conformations known as ‘open’ and ‘closed’, and is able to bind either Mad1 or Cdc20 (De Antoni et al., 2005). The closed conformation of Mad2 facilitates MCC formation and APC inhibition through sequestration of Cdc20. Conversion from open to closed Mad2 requires Mad1 (Fava et al., 2011; Luo et al., 2004). Mad1 is recruited to unattached kinetochores where it binds Mad2 in the closed form (Sironi et al., 2002), this complex then appears to act as a template for the formation of Mad2-Cdc20 (Luo et al., 2004) which forms the basis of the soluble APC inhibitor. Mad1 is recruited to kinetochores in response to phosphorylation of certain residues on the outer kinetochore plate (Wei et al., 2011) and recruitment of Mad1 and Mad2 requires the activity of the upstream SAC components Bub1 and Mps1 (Farr and Hoyt, 1998; Hardwick et al., 1996) and Polo-like Kinase 1 (Chi et al., 2008). For a good overview of MCC formation see Kulukian et al., (2009).

The protein Bub1 appears to have a less direct role in the SAC response, however it is among the first proteins to be recruited to the kinetochore where its presence is required for further recruitment of several other SAC (Bub3, BubR1 and Mad2) and centromere (CENP-E, CENP-F) proteins to the kinetochore/centromere (Jablonski et al., 1998; Johnson et al., 2004). Bub1 appears to be a stable component of the kinetochore and is therefore thought to act as a scaffold, providing a platform for checkpoint signalling (Rischitor et al., 2007). Its kinase activity is not required for this scaffold function, nor is it required for checkpoint signalling in human cell lines (Perera

and Taylor, 2010; Perera et al., 2007). The Bub1 kinase domain can however phosphorylate Cdc20 in vitro, and mutant Cdc20 which is resistant to phosphorylation weakens the checkpoint response (Tang et al., 2004a). Bub1 therefore appears to have an essential kinase independent function and a non-essential kinase function in the SAC. The Bub1 kinase is also important for non-SAC functions; its phosphorylation of centromere proteins is required for the localisation of Shugoshins and PP2A (Protein Phosphatase 2A) (Boyarchuk et al., 2007; Kitajima et al., 2005; Perera and Taylor, 2010; Tang et al., 2004b) the importance of which are discussed in 1.3.13.

BubR1 has an essential role in generating MCC as mentioned above. Following generation of Mad2-Cdc20 additional binding of BubR1 occurs (Kulukian et al., 2009). However its role in binding Cdc20 and inhibiting the APC does not require its kinase domain (Zhang et al., 2007b). BubR1 is recruited to unattached kinetochores, where its presence is required for the localisation of other checkpoint proteins such as Mad1, Mad2, Bub1 and Bub3 as well as CenpE (Chen, 2002). BubR1 is highly implicated in chromosome alignment and regulating microtubule kinetochore attachment (Ditchfield et al., 2003; Elowe et al., 2007), and may act to counter the microtubule destabilising activity of the Aurora B kinase (Lampson and Kapoor, 2005).

The Mps1 kinase is an upstream kinase essential to the SAC. It is recruited to vacant kinetochores and its activity is required for the kinetochore recruitment of BubR1, Bub1, Mad1 and Mad2 (Abrieu et al., 2001; Hewitt et al., 2010; Ito et al., 2011; Jelluma et al., 2010; Tighe et al., 2008; Zich et al., 2012). Mps1, when tethered to kinetochores, recruits SAC proteins and can maintain the checkpoint signal independently of kinetochore attachment status (Jelluma et al., 2010). Its own activity and that of Aurora B kinase appears to be reciprocal with each activating the other (Jelluma et al., 2008; Saurin et al., 2011) and like Aurora B, experiments in budding yeast suggest that Mps1 is required for correction of erroneous microtubule attachments that do not result in tension across the centromere (Maure et al., 2007).

Aurora B is a member of the chromosomal passenger complex (CPC), comprising of Aurora B, Borealin, Survivin and INCENP. Its localisation changes throughout the cell cycle as it performs widely differing roles from spindle assembly to cytokinesis (Carmena et al., 2009). However here I am only interested in discussing its role in the SAC. It was demonstrated to recruit BubR1, Mad2 and Mps1 proteins to the kinetochore (Ditchfield et al., 2003; Saurin et al., 2011). However, more recently

evidence has accumulated suggesting a direct role for Aurora B in SAC signalling (Maldonado and Kapoor, 2011; Santaguida et al., 2011).

In summary, the interactions of the SAC proteins are complex with many components depending on each other for recruitment and activity. Although many of the details of this network are still emerging, as a whole the SAC in mitosis efficiently detects the presence of microtubule attachment errors and generates a signal that can robustly inhibit the APC for prolonged periods.

1.3 MEIOSIS I

1.3.1 MEIOSIS OVERVIEW: TWO DIVISIONS, TWO ARRESTS

To arrive in a 'fertilisation ready' form the oocyte must undergo two divisions and also achieve two distinct periods of arrest. Primordial germ cells first enter meiosis in foetal life, where the newly replicated sister chromosomes, held together by cohesin, pair with their homologous partners. These homologous pairs are then physically linked by exchange of their DNA in a process called recombination, and are then termed bivalents. Following this the oocyte enters the first arrest, in prophase I (Figure 1.2). This arrest is extremely protracted, lasting for months in mice, and potentially for several decades in humans. Finally, the arrest is broken in response to hormonal cues and oocytes can re-enter meiosis I. This begins with oocytes entering prometaphase, which is seen morphologically as the breaking down of the nuclear membrane, termed the 'germinal vesicle' in oocytes, (Germinal Vesicle Breakdown, GVBD) and marks the start of oocyte maturation. During the first meiotic division the homologous chromosome pairs within the bivalents are separated in a reductional fashion whilst the sister chromatids within each homologous pair remain tethered together (Figure 1.3). This requires that only the arm cohesin is cleaved, leaving the centromeric cohesin to keep the sister chromatids attached together in readiness for sister segregation at meiosis II. Completion of the first division is marked by cytokinesis, which is highly asymmetrical, resulting in the extrusion of a small cell termed a polar body. This polar body plays no further role in meiosis. Following the first division the oocyte enters meiosis II without an intervening S-phase. Here the oocyte assembles a metaphase II spindle and arrests for a period potentially lasting many hours. This time the arrest is released by the contribution of Phospholipase Cζ (PLCζ) from the sperm upon

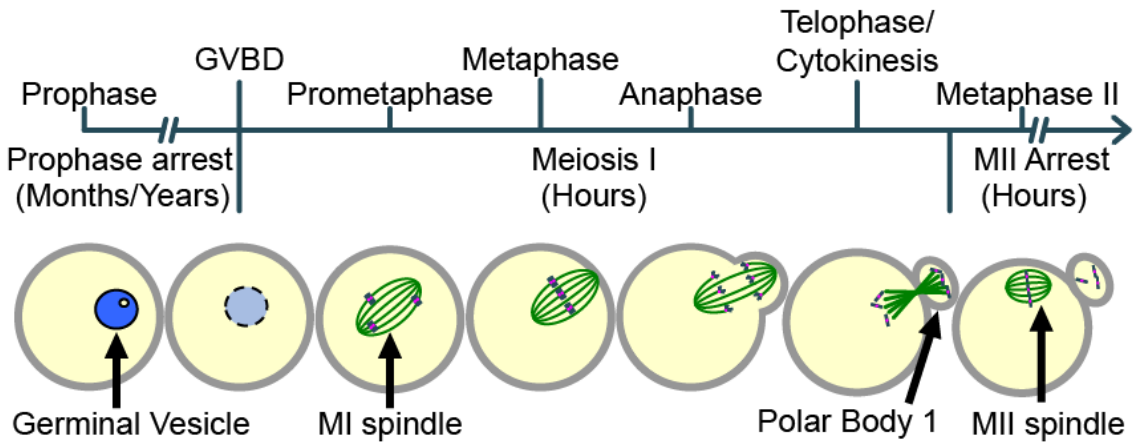

Figure 1.2 - Overview of progression from prophase arrest through to metaphase II arrest.

Oocytes arrest in prophase of meiosis I for long periods of time. Resumption of meiosis is morphologically evident by the breaking down of the germinal vesicle (GVBD). The oocyte then assembles a bipolar spindle (MI spindle) and segregates bivalent chromosomes. The cytokinesis is asymmetrical, resulting in the extrusion of a small polar body (Polar body 1) which marks the end of meiosis I. Oocytes then assemble a second, smaller spindle (MII spindle) and arrest, awaiting fertilisation.

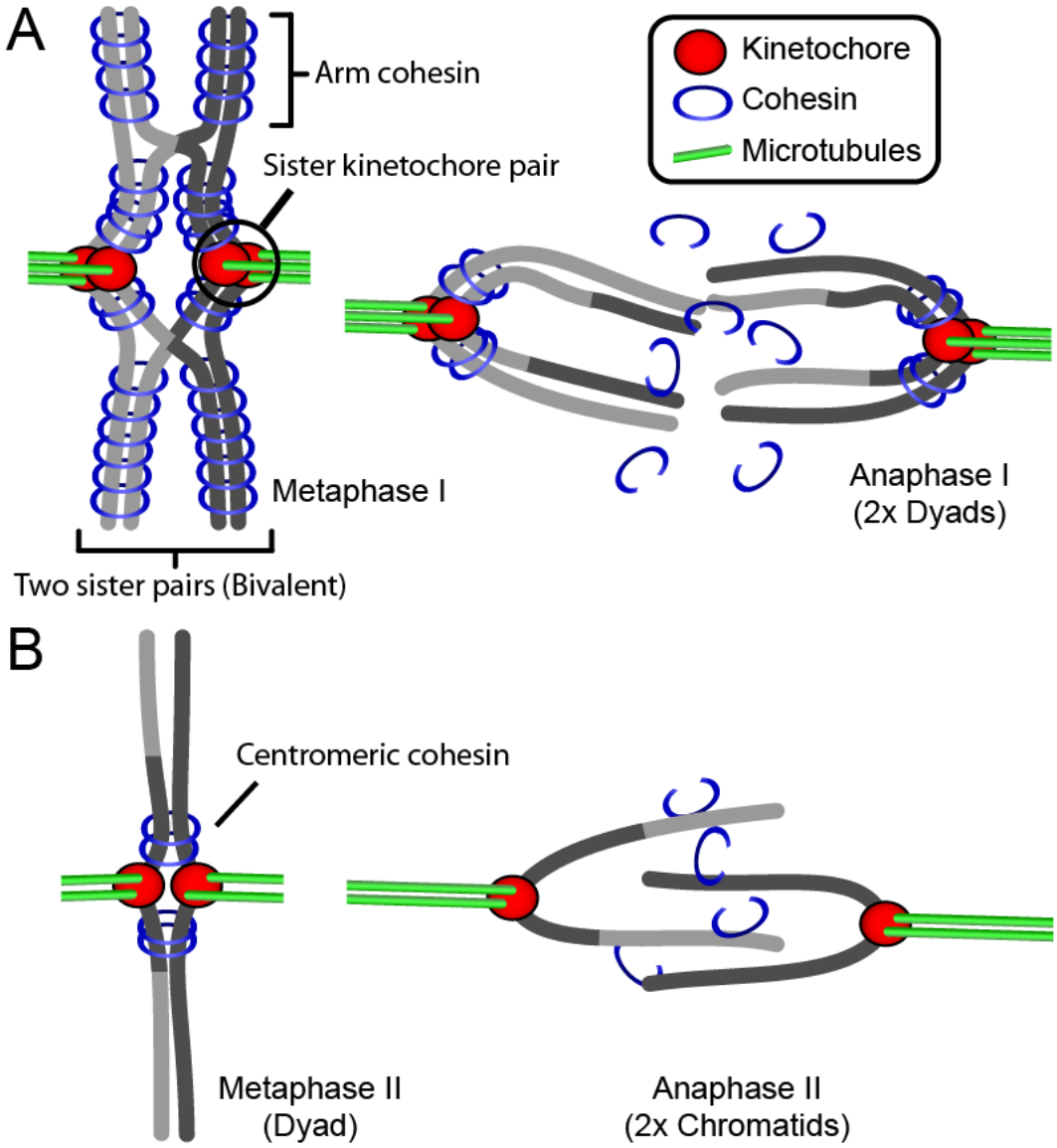

Figure 1.3 - Chromosome attachment and segregation in meiosis I and II

In Meiosis I sister kinetochores mono-orientate, attaching to the same pole, subsequently homologous chromosomes are segregated at anaphase. Note that the centromeric cohesin is protected from separase and thus it serves to tether the sister chromatids together during metaphase II. In Metaphase II sister chromatids bi-orientate, attaching to opposite poles. The remaining cohesin is cleaved at the MII-AII transition allowing their segregation.

fertilization (Cox et al., 2002). Fertilization sets off calcium oscillations in the oocyte, which drive the cellular events causing the second meiotic division, the formation of pronuclei and finally entry into mitotic cell divisions.

In the subsequent sections only the events of meiosis I will be addressed in more detail, as this thesis does not explore events occurring after first polar body extrusion.

1.3.2 PRIMORDIAL GERM CELL DIFFERETIATION

Germ cell progenitors have been identified in the foetus at around 7.2 days post coitum in the epiblast adjacent to the extraembryonic ectoderm. These small number of cells(<50) expand their numbers whilst migrating along the hindgut and reach what will become the genital ridge by day 11.5 (McLaren, 2000; McLaren, 2003). Mitotic divisions continue resulting in >24,000 Primordial Germ Cells (PGCs) by 13.5 days post coitum (McLaren, 2000; Tam and Snow, 1981). The transition from mitosis to meiosis is dependent on Retinoic Acid (RA) synthesised by the neighbouring mesonephros, which is a foetal specific structure that is part of the early developing kidney (Baltus et al., 2006). Sex specific regulation of the RA leads to the mitosis to meiosis transition during foetal life in females, whereas males delay this transition until after birth (Bowles et al., 2006). In males continued metabolism of RA by cyp26b1 prevents its accumulation in the germ cells, preventing them entering meiosis. However, in the female gonad, expression of cyp26b1 declines at around day 12.5. RA accumulation then stimulates changes in gene expression allowing the PGCs to leave mitotic cycles and enter prophase of meiosis I. At their peak the germ cells number around 21,000 (McClellan et al., 2003).

1.3.3 RECOMBINATION

Upon entering leptotene of prophase the chromosomes begin to condense and an axial element (a protein structure, incorporating the cohesin rings) forms along the chromosome length (Page and Hawley, 2004). Homologous chromosomes then align in pairs, initially in short segments and finally along their entire lengths. The mechanism behind this has been shown to require double stranded breaks in many, but not all, species and is likely to be based on a homology search of DNA sections freed by the double stranded breaks, called axial associations (Tesse et al., 2003). Homolog alignment defines the zygotene stage of prophase and is followed by the formation of the synaptonemal complex (SC), a protein structure linking the two axial elements of

the homologous chromosomes together (Schramm et al., 2011). Initially SC formation occurs at locations of axial association between the homologs but later encompasses the entire length of the chromosomes (Baltus et al., 2006). Completion of SC formation marks pachytene of prophase and occurs at around 15 days pc.

During pachytene DNA interactions between homologs are formed. Successful interactions (resulting in physical linkage between homologs) occur as follows: double stranded breaks are formed by the topoisomerase enzyme, spo11 (Keeney and Neale, 2006; Tesse et al., 2003). This allows single strand invasion into the complementary region on the homologous chromosome. The invading strand extends and DNA ligase enzymes rejoin the ends to create a double holiday junction. Asymmetric cleavage of the double holiday junction then results in a complete crossover event (Page and Hawley, 2004). The two homologous chromosomes are now physically linked together by the exchange between their DNA. Recombination between homologous chromosomes generates what are termed ‘bivalents’ in meiosis I. The recombination serves to increase genetic variation within a population, but also has a crucial role in tethering homologs together until anaphase I.

Following formation of crossover events on each chromosome the synaptonemal complex is disassembled and oocytes enter diplotene, arresting with their chromosomes decondensed around 20 days into embryonic development (Figure 1.4). With recombination complete, the oocyte enters a quiescent state until meiosis is resumed at a later time in response to hormonal cues.

1.3.4 GERMINAL VESICLE ARREST

The nature of Germinal Vesicle (GV) arrest is interesting, because it must be sustained for such a long period of time from completion of recombination in the foetus, until an increase in Follicle Stimulating Hormone causes granulosa cells to lower levels of cAMP in the oocyte, resulting in oocyte maturation as discussed below. Prior to the surge in lutinising hormone (LH), which signals ovulation, oocytes are tightly regulated to maintain GV arrest by multiple partially redundant mechanisms, the downstream target of which is Cdk1 (Han and Conti, 2006). These multiple pathways will be discussed briefly.

Firstly Cdk1 inhibitory phosphorylation on Thr14/Tyr15 is maintained by high kinase activity and low phosphatase activity. The phosphorylation is maintained by Wee1B

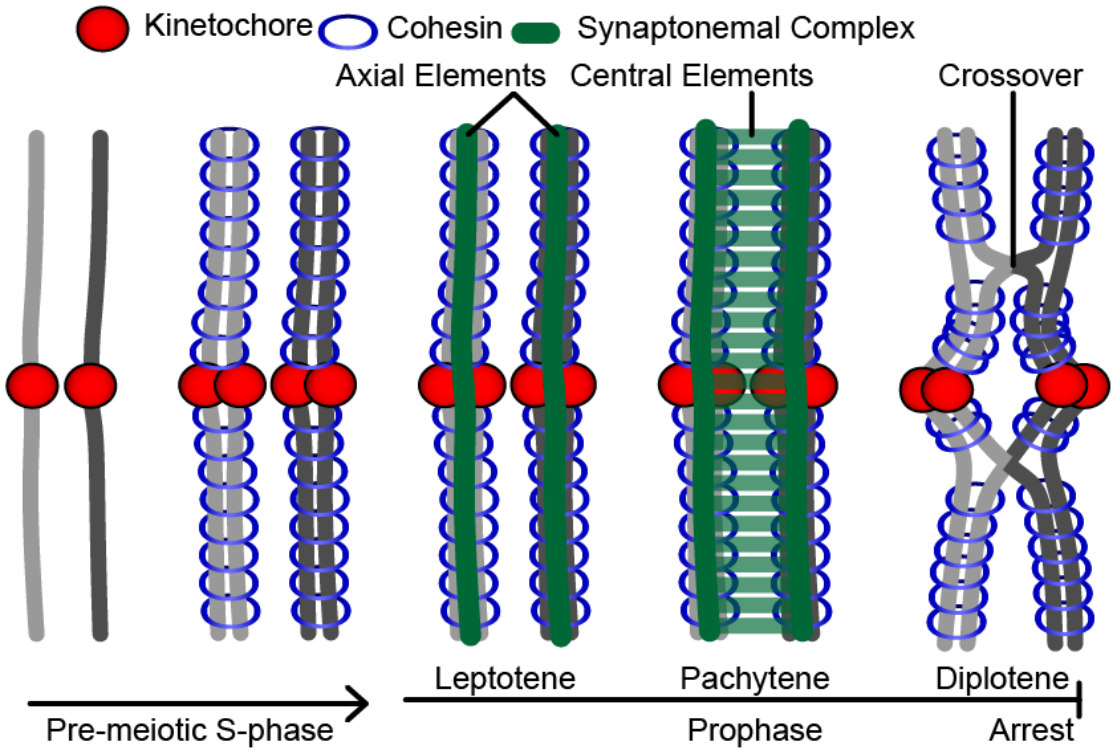

Figure 1.4 - Formation of crossovers during prophase of meiosis I

Replication of chromatids occurs in pre-meiotic S-phase, where cohesin is loaded onto chromosome arms. In leptotene maternal and paternal chromosomes have aligned and axial elements form along the length of each chromatid pair. In Pachytene central elements temporarily hold homologous chromosomes together. Following formation of crossovers the synaptonemal complex dissolves and newly formed bivalents arrest in diplotene.

kinase, and removed by the phosphatase Cdc25B. Wee1B and Cdc25B are both regulated (Wee1B positively and Cdc25B negatively) by phosphorylation by Protein Kinase A (PKA, Han and Conti, 2006). PKA activity in turn is reliant on cAMP concentrations (Han and Conti, 2006). Therefore, for GV arrest to be maintained, cAMP levels must be kept high. cAMP is produced by constituently active G-proteins located on the oocyte plasma membrane, however it is also broken down by phosphodiesterase 3A activity (Masciarelli et al., 2004). The phosphodiesterase activity is inhibited by cGMP supplied to the oocyte by the granulosa cells (Norris et al., 2009).

Secondly, cyclin B1, the Cdk1 binding partner, is prevented from accumulating at high levels by the activity of the Anaphase Promoting Complex (APC). Cyclin B1 levels are kept in check by the activity of the APC and its activator Cdh1. Loss of Cdh1 causes premature GVBD, suggesting this mechanism is essential for maintaining GV arrest (Holt et al., 2011; Reis et al., 2006).

Thirdly, there exists a spatial separation of key proteins by the nuclear envelope. Active Cdk1 is prevented from accumulating in the GV because cyclin B1 is predominantly cytoplasmic. In addition, Wee1B is nuclear, whilst Cdc25 is cytoplasmic. Finally, APC Cdh1 is nuclear, degrading cyclin B1 in the nucleus. These discrete spatial distributions of various activities all contribute to preventing GVBD in the oocyte and many proteins appear to be transported across the nuclear envelope at the time of GVBD to facilitate a rapid transition into prometaphase (Holt et al., 2010; Marangos and Carroll, 2004; Oh et al., 2010; Reis et al., 2006; Solc et al., 2008).

1.3.5 FOLLICLE RECRUITMENT AND GROWTH

Each arrested oocyte within the ovary is contained within a primordial follicle which comprises of a layer of granulosa cells. At this stage the oocyte is around 20µm in diameter. The cytoplasm of the granulosa cells are continuous with that of the oocyte due to gap junctions between the two (Matzuk et al., 2002). Proliferation of the granulosa cells occurs, to give multiple layers around the oocyte that denotes development into secondary follicles. Further growth to form an antral follicle is dependent on gonadotrophic hormones, and finally attainment of pre-ovulatory follicles depends on the LH surge (Fortune, 2003).

It is during the growth of the follicle that the oocyte acquires competence, that is the ability to resume meiosis I. Competence is associated with, but not dependent on, the

growth of the oocyte, (Wickramasinghe et al., 1991). It is more likely to do with acquisition of a suitable level of Cdk1 (Kanatsu-Shinohara et al., 2000).

1.3.6 RESUMPTION OF MEIOSIS I

Meiosis resumes following stimulation of the granulosa cells by LH just prior to ovulation of the oocyte. LH binds its receptor on the granulosa cells inducing the closure of the gap junctions and blocking the supply of cGMP to the oocyte. This relieves the inhibition on the phosphodiesterase A3 (PDE3A) allowing cAMP levels to fall. PKA activity falls as a consequence and changes the balance of Cdc25B and Wee1B activity (Norris 2009). Oocytes are then induced to undergo GVBD as Cdc25B activity exceeds that of Wee1B, removing inhibitory phosphorylation of Cdk1.

1.3.7 EARLY PROMETAPHASE I: SPINDLE ASSEMBLY

The first step towards segregating the chromosomes in meiosis I (MI), as in other divisions, is the building of a bipolar spindle. Many spindles use centrosomes which act as centres from which microtubules are organised, however oocytes assemble a spindle in the absence of centrosomes, using the inherent properties of microtubules and motor proteins to self-assemble a bipolar spindle (Brunet et al., 1999; Schuh and Ellenberg, 2007). Such a process can also occur in somatic cells when the centrosomes are removed (Hornick et al., 2011). During spindle assembly in oocytes microtubule organising centres (MTOCs) form throughout the cytoplasm in large numbers, and as meiosis I progresses they aggregate, finally forming a ball of microtubules around 1 h after GVBD. The interaction of this microtubule structure with the chromosomes is of importance, as it begins the process of organising the bivalents by pushing them outwards onto the periphery of the ball, resulting in a rosette arrangement. The MTOCs then emit multiple poles (1-2 h after GVBD), which coalesce to form two dominant poles (2-3 h after GVBD). Subsequent separation of the two poles in a process dependent of the motor protein Kinesin 5 finally gives rise to a bipolar spindle 3-4 h after GVBD, (Schuh and Ellenberg, 2007). The oocyte spindle bipolarisation is therefore very slow, lasting several hours as opposed to <30 minutes for somatic cells (Kapoor et al., 2000). Interestingly, bipolar spindles can assemble in mouse oocytes, albeit with lower efficiency, in the absence of chromosomes, suggesting chromatin or kinetochores, although not essential, facilitate the process of bipolar spindle formation (Brunet et al., 1998).

1.3.8 LATE PROMETAPHASE: THE SAC

The existence of the spindle assembly checkpoint in mouse oocytes has been questioned in the past, because aneuploidy rates from this division were so high compared to mitotic cells and evidence suggested that oocytes were unable to respond to univalent chromosomes during meiosis I (XO mouse). Since then all the SAC proteins have been investigated, and all were found to be present. Furthermore they appeared to be functional, as their knockdown invariably resulted in an increase in aneuploidy and a shortening of the duration of meiosis I, both indicative of an abrogation of the SAC.

Mad1 and Mad2 proteins are found to localise to unattached kinetochores in either unperturbed prometaphase oocytes or in oocytes in which spindle poisons are applied (Waters et al., 1998; Zhang et al., 2004; Zhang et al., 2007a). Further to this Mad2 manipulation by knockdown or partial knockout (Homer et al., 2005a; Niault et al., 2007) or by expression of a dominant negative construct (Wassmann et al., 2003) prevented SAC inhibition of the APC, accelerating MI, whilst its overexpression caused MI arrest (Niault et al., 2007; Wassmann et al., 2003). Depletion of Mad2 was also accompanied by an increase in aneuploidy in meiosis II (MII) eggs (Homer et al., 2005b).

Bub1 is also present and functional in oocytes, as its knockout prevents prometaphase inhibition of the APC, disrupts proper bi-orientation, causes premature loss of centromeric cohesin and increases aneuploidy (McGuinness et al., 2009). Additionally, expression of a dominant negative Bub1 or injection of an antibody to disrupt Bub1 function accelerates passage through meiosis I, consisted with abrogation of the SAC (Tsurumi et al., 2004; Yin et al., 2006).

Knockdown of BubR1 demonstrates that it too is required for normal meiosis I progression. Unlike knockdown of other SAC proteins, knockdown of BubR1 was not associated with an acceleration of meiosis I, but instead blocked oocytes in MI (Homer et al., 2009). This seems to be due to a dependence of the APC activator Cdh1 on BubR1 for its own stability. Depletion of BubR1 caused loss of Cdh1 which allowed securin levels to rise unchecked during prophase. The elevated securin levels appeared to cause the MI arrest and so was independent of BubR1s SAC function (Homer et al., 2009). The BubR1 checkpoint function was however demonstrated in

oocytes by injection of a dominant negative BubR1 construct, which accelerated meiosis I (Tsurumi et al., 2004). A role for BubR1 in regulating kinetochore attachments was also established in MI as following its knockdown there is a loss of k-fibre formation (Homer et al., 2009; Wei et al., 2010). This is consistent with the proposed role of BubR1 in antagonising the microtubule destabilising actions of Aurora B (Lampson and Kapoor, 2005).

The role of the checkpoint kinase Mps1 has also been addressed in mouse oocytes. In mice lacking the N terminal of Mps1, a deletion that prevents kinetochore localisation, aneuploidy is raised and meiosis I is accelerated. Additionally these oocytes fail to arrest in response to nocodazole, and can segregate chromosomes without first achieving proper alignment (Hached et al., 2011). Oocytes also have mis-localised Aurora B/C following loss of Mps1 on kinetochores. Together these findings indicate an essential checkpoint, and an Aurora kinase recruitment role for Mps1 is conserved in mouse meiosis I.

In meiosis I the Aurora B kinase appears to be replaced with the meiosis specific expression of the highly related Aurora C; the two proteins share 78% sequence homology (Tseng et al., 1998). mRNA for both Auroras are found in oocytes (Shuda et al., 2009; Swain et al., 2008; Yang et al., 2010), however studies using Aurora B and C specific antibodies suggests that only Aurora C protein is found (Shuda et al., 2009; Yang et al., 2010), therefore translation of Aurora B mRNA may specifically be blocked. Aurora C is found located on chromosomes and centromeres during prometaphase and metaphase, and translocates to the spindle midzone consistent with its predicted movement as a member of the chromosomal passenger complex (Ruchaud et al., 2007). As with other SAC proteins, its role appears to be conserved in meiosis, however a role specifically in the SAC has not been demonstrated. Inhibition of Auroras disrupts MI spindle formation and chromosome condensation (Swain et al., 2008; Vogt et al., 2009) and oocytes typically fail to reach MII (Swain et al., 2008; Vogt et al., 2009). Oocytes injected with a kinase dead Aurora C construct did however have an accelerated meiosis I, suggesting that this kinase may have a conserved SAC function (Yang et al., 2010).

1.3.9 SISTER MONO-ORIENTATION

Once bipolarisation of the spindle is complete the bivalents start interacting with the spindle by forming microtubule attachments via their kinetochores. Each sister chromatid has a kinetochore, however, bivalents comprise of four chromatids arranged as two sister kinetochore pairs. Importantly in meiosis I, each pair behaves as having one functional kinetochore (Figure 1.3 A). The grouping of two sister kinetochores into one functional unit is an important feature of meiosis I, as it allows correct segregation of homologous chromosomes at anaphase. Both Aurora B and the monopolin complex are required for co-orientation of sister kinetochore pairs in budding yeast (Monje-Casas et al., 2007), but proteins that play the equivalent role in higher eukaryotes are not known. Additionally, the presence of the chiasmata also favours the attachment of the two sisters to one pole (Hirose et al., 2011; Sakuno et al., 2011), as does the presence of centromeric cohesin (Sakuno et al., 2009).

1.3.10 KINETOCHORE CAPTURE AND ERROR CORRECTION

During prometaphase the chromosomes start interacting with the spindle, and the SAC functions to delay anaphase, permitting enough time for all chromosomes to make correct attachments. Initially, kinetochores must be captured by microtubules. Ideally this would occur such that sister kinetochore pairs are attached to opposing poles.

Direct interaction of microtubules and kinetochores has not been visualised in live mouse oocytes, however in mitotic cells microtubules were observed to capture kinetochores in live cells as early as 1990 (Hayden et al., 1990; Rieder and Alexander, 1990). In this study microtubules emanating from spindle poles were seen to interact with chromosomes, capturing them and pulling them poleward. Since then work in yeast has identified the major steps in kinetochore capture as being i) side-on attachment of kinetochore to microtubules ii) poleward movement of kinetochore along the microtubule iii) conversion from lateral to end-on attachment iv) attachment of sister kinetochore via a similar mechanism to establish bi-orientation (Tanaka et al., 2007; Tanaka et al., 2010). In budding yeast the kinetochore and microtubule binding apparatus is substantially different from higher eukaryotes where alternative methods may also come into play. Observations in both somatic cells and in oocytes and plants which lack centrioles suggest that both ‘search and capture’ of kinetochores by astral microtubules and a microtubule self-assembly from kinetochores may be important

(Rieder, 2005). Additional methods are probably required to make both search and capture and kinetochore derived microtubules more efficient. One possible mechanism is the stabilizing of microtubules in the vicinity of the chromosomes by a RanGTP gradient (Wollman et al., 2005) and its associated effectors (Meunier and Vernos, 2011). Such a gradient also exists in mouse oocytes, however it does not appear to be critical for meiosis I spindle formation or chromosome segregation (Dumont et al., 2007).

1.3.11 CHECKPOINT CRITERIA

In mitosis a debate as to what conditions satisfy the SAC has been ongoing for several years. The checkpoint responds to attachment; however tension has also long been cited as a requisite for checkpoint satisfaction. A role for tension in this checkpoint was implicated because use of taxol, a microtubule stabilizing drug, to reduce tension without disrupting attachment, causes a delay to anaphase (Rieder et al., 1994). Chromosomes with both kinetochores attached to the spindle were found to exhibit higher inter-kinetochore distances, an indication of tension (Waters et al., 1996) and the application of tension using a micromanipulator to the last non-aligned chromosome led to anaphase (Li and Nicklas, 1995). Tension was therefore initially proposed as being a requirement for the checkpoint. However, this idea has been questioned because several systems have been established in which SAC satisfaction is established in the absence of tension. For example MUG (mitosis with unreplicated genome) cells have chromosomes in mitosis that are single chromatids and thus cannot establish tension across centromeres, but which nonetheless proceed through mitosis with normal timing (O'Connell et al., 2008). Additionally, under experimental conditions using low doses of spindle poisons that prevent tension generation, without disrupting attachment, the SAC is satisfied (Maresca and Salmon, 2009; Uchida et al., 2009; Waters et al., 1998).

The XO mouse is an interesting case that highlights the dilemma of what constitutes the checkpoint criteria in oocytes. The XO mouse only has one X chromosome and so enters meiosis I with a univalent (i.e. one pair of sister chromatids). The presence of the univalent in meiosis I does not delay anaphase despite a tendency to remain non-aligned on the meiotic spindle, suggesting that it does not activate the SAC (LeMaire-Adkins et al., 1997). In around two-thirds of oocytes the univalent segregates intact, suggesting that it is not bi-orientated and thus should not have been able to generate

tension across its centromere. Therefore, in the XO mouse lack of tension across the single X chromosome appears insufficient to activate the SAC. Similarly, the presence of multiple univalents, which also have the option of making mono-polar or bi-polar attachments in meiosis I seem unable to generate a robust SAC signal, although this is the case only in certain strains (Nagaoka et al., 2011; Woods et al., 1999).

1.3.12 METAPHASE

Metaphase is defined in terms of its morphological appearance, in which all chromosomes are aligned on a 'metaphase plate'. Attainment of this state is usually concomitant with particular biochemical events, such as the onset of cyclin B1 and securin destruction, implying that the SAC has been satisfied and the APC activated. In mitosis, where the SAC is effective, there is little difference in timing between the attainment of the metaphase plate and APC activation (~3 minutes, Clute and Pines, 1999), but in oocytes this has not been thoroughly investigated. I am therefore going to be discussing metaphase in the context of satisfaction of the SAC.

Following satisfaction of the SAC the APC must be activated in order to push the cell into anaphase. For this reason MCC production must cease. This has not been investigated mechanistically in oocytes other than observations that concentrations of SAC proteins such as Mad1 (Zhang et al., 2005), Mad2 (Wassmann et al., 2003), BubR1 (Homer et al., 2009) or Bub3 (Li et al., 2009) decline at kinetochores prior to anaphase.

One interesting possibility for which evidence exists in mitosis is that upon microtubule attachment to kinetochores, SAC proteins are transported along microtubules to the spindle pole. The loss of SAC proteins coincides with the attachment of microtubules (Hoffman et al., 2001; Waters et al., 1998), therefore this seems a convenient solution. This does in fact appear to occur for Mad1 and Mad2 in somatic cells (Basto et al., 2004; Howell et al., 2000) and may also be correct for Bub3 as well as Cdc20 (Howell et al., 2004). This transport likely depends on a Rod/Zw10 dynein complex, which accumulates on unattached outer kinetochores and can travel along microtubules (Basto et al., 2004; Gassmann et al., 2010). Dynein recruitment to kinetochores in turn depends on Spindly, whose knockdown generates metaphase arrest in Drosophila (Griffis et al., 2007) and human cells (Gassmann et al., 2010). Additionally, BubR1 kinase activity is inhibited by microtubule attachment to CenpE in vivo (Mao et al.,

2005) but this remains to be demonstrated in an in-vitro complete-kinetochore environment.

Other SAC silencing mechanisms appear to exist besides those that are a direct result of attachment. Protein phosphatase activity probably plays a large role in silencing the SAC, for instance recruitment of Protein Phosphatase I (PP1) to kinetochores is required for cyclin destruction in fission and budding yeast (Pinsky et al., 2009; Vanoosthuyse and Hardwick, 2009). Furthermore, in human cells PP1 recruitment to the outer kinetochore is necessary for removal of Aurora B phosphorylation (Liu et al., 2010).

Finally, there appears to be at least 3 routes by which Cdc20 is released from assembled MCC, thus helping to activate the APC by making more Cdc20 available. Firstly, proteolysis of an unknown protein appears essential for the dissociation of the Mad2-Cdc20 complex via an as yet unidentified phosphatase (Visconti et al., 2010). Secondly, the protein $p31^{comet}$ binds to the MCC and appears to remove Mad2 from this complex (Westhorpe et al., 2011). p31 overexpression abrogates the checkpoint and its knockdown prolongs mitosis (Hagan et al., 2011). Thirdly, auto-ubiquitination of Cdc20 promotes its dissociation from the MCC (Jia et al., 2011), a process that depends on the APC subunit APC15 (Mansfeld et al., 2011).

The culmination of the above processes, and possibly others still to be defined, results in the activation of the APC towards cyclin B1 and securin, ensuring anaphase follows shortly afterwards. However, in oocytes regulation of the APC during metaphase may be quite different, as both cyclin B1 destruction (and Cdk1 activity) decline gradually as anaphase approaches (Hampl and Eppig, 1995; Winston, 1997). Therefore the processes occurring during metaphase in oocytes still require further investigation.

1.3.13 ANAPHASE

Following activation of the APC, both cyclin B1 and securin are degraded, resulting in the release of active separase which is responsible for cleaving the cohesin rings holding chromosome arms together. Due to the need to separate only homologous chromosomes in meiosis I (Figure 1.3 A), whilst reserving the ability to separate sister chromatids in meiosis II (Figure 1.3 B), cleavage of cohesin is spatially regulated in meiosis I.

Mitotic cohesin contains two structural maintenance of chromosome subunits (SMC1 and 3) as well as SCC3, and an additional kleisin subunit, the target of separase, RAD21. Cleavage of RAD21 is sufficient for sister chromatid resolution (Oliveira et al., 2010). In meiosis, RAD21 is largely replaced with Rec8, which can also be cleaved by separase (Klein et al., 1999; Watanabe and Nurse, 1999) and its artificial cleavage by TEV protease is sufficient for complete cohesin dissolution, causing loss of cohesion between both bivalents and sisters in meiosis I (Tachibana-Konwalski et al., 2010). Under normal conditions, it is cleavage of Rec8 that permits bivalent (meiosis I) or sister (meiosis II) separation (Buonomo et al., 2000; Kitajima et al., 2003; Kudo et al., 2006). Centromeric cohesion, which remains following meiosis I is therefore not preserved by use of an alternative cohesin subunit set, but by preventing separase from cleaving Rec8 specifically in the centromeric region.

The above preservation is due to the activities of the meiosis specific Sgo2 (Shugoshin 2) and the protein phosphatase PP2A-B (Kitajima et al., 2004; Kitajima et al., 2006). Sgo localises PP2A-B to the centromeric region (Kitajima et al., 2006), and once tethered there the phosphatase protects centromeric Rec8 from separase, by preventing its phosphorylation (Katis et al., 2010; Riedel et al., 2006). This was shown by using a phospho-mimic Rec8 mutant, which results in cleavage of all Rec8 and precocious loss of sister chromatid cohesion in meiosis I (Katis et al., 2010). Therefore Sgo2 and PP2A-B are critical for maintenance of chromosome integrity during anaphase.

1.3.14 EXIT FROM MEIOSIS I

Exit from meiosis is associated with a decline in Cdk1 activity brought about at least in part by the APC mediated degradation of cyclin B1 (Hampl and Eppig, 1995). The decline in Cdk1 activity is essential as non-degradable cyclin B1 causes metaphase I arrest (Herbert et al., 2003). Phosphatase activity also appears important for proper exit, as Cdc14A antibody injection delays completion of MI (Schindler and Schultz, 2009). It is not clear though if this is by inhibiting Cdk1 itself or by dephosphorylation of Cdk1 substrates.

In mitosis there appear to be multiple additional pathways that act to remove the activating phosphorylation on Cdk1 (Chow et al., 2011; Potapova et al., 2009; Tumurbaatar et al., 2011). The loss of Cdk1 activity facilitates the transition into G1, the

disassembly of the spindle apparatus, the assembly of the nuclear envelope and chromosome decondensation. However, after meiosis I, oocytes proceed straight into meiosis II without an intervening interphase or S-phase. It is possible therefore that exit from meiosis I is regulated quite differently. Indeed, there is only a transient period of interkinesis before MII is entered (Jones, 2008). Entry into meiosis II follows meiosis I, so there is no complete decondensation of chromosomes or assembly of a nuclear lamina.

1.3.15 ANEUPLOIDY IN OOCYTES

Aneuploidy occurs when a cell receives an incorrect chromosome complement. The strongest risk factor for embryonic aneuploidy in humans is the age of the mother (Hassold and Hunt, 2001) and the most common source is the first meiotic division in the oocyte (Kuliev et al., 2005; Kuliev et al., 2011; Rosenbusch, 2004). Unlike spermatozoa, which are produced continuously in males post puberty, oocytes are made in foetal life and then arrest, only to resume meiosis many years later (Jones, 2008). Aneuploidy in human oocytes is estimated at >40% (Kuliev et al., 2011). This is based on analysis of specimens from women undergoing IVF, and is therefore likely to be an overestimate of the general population. Human aneuploidy is present at relatively high rates, even in young women however (Hassold and Hunt, 2001), suggesting that there are age-independent causes of human aneuploidy as well.

This aneuploidy is categorised by two main errors types. The first is non-disjunction, where both pairs of homologous chromosomes segregate to the same pole. The second is premature sister chromatid separation (termed PSCS or ‘pre-division’). In this event, separation of sister chromatids, occurs prior to MII, generating individual chromatids. It is worth noting that either of these errors has the potential to be corrected in the second meiotic division, but correction is beyond the control of the oocyte and depends on stochastic segregation of chromosomes.

The potential for aneuploidy can be created even before MI. For several chromosomes aneuploidy has been found to be caused by a failure to recombine in prophase, generating two univalents in meiosis I (Bugge et al., 1998; Hassold et al., 1995; Lamb et al., 1997b; Lamb et al., 1996; Robinson et al., 1998; Thomas et al., 2001; Warren et al., 1987). Failure to recombine has also been observed directly in prophase arrested human oocytes (Tease et al., 2002).

Aside from age, certain environmental factors have been demonstrated to influence aneuploidy in mice. Exposure of mice to man-made estrogenic compounds can cause increased aneuploidy (Hunt et al., 2003; Muhlhauser et al., 2009). And calorie restriction can lower aneuploidy in aged mice, an effect that may act through ATP levels (Selesniemi et al., 2011; Wang et al., 2009). In summary the events of recombination as well as environmental factors are likely to contribute to aneuploidy. Additionally the reduced ability of oocytes to arrest in response to certain chromosomal errors in meiosis I increases the chances of aneuploidy in embryos.

1.4 THESIS AIMS

1.4.1 THE SPINDLE ASSEMBLY CHECKPOINT IN MOUSE OOCYTES

The timing of some major events in meiosis I relative to each other are still unknown. Events in mitosis take place in rapid succession, however equivalent events are drawn out over many hours in meiosis I. It remains to be established if the same temporal relationships exist between events such as kinetochore-microtubule attachment, SAC satisfaction, APC activation and anaphase. This will be addressed in Chapter 3.

1.4.2 MEIOSIS I CHECKPOINT CRITERIA

High rates of meiosis I derived aneuploidy prompt the questions of what causes and what permits chromosome errors to occur. The ability of the SAC to inhibit the APC in mouse oocytes will therefore be investigated to test its sensitivity to certain types of chromosome alignment errors. This is examined in Chapter 4.

1.4.3 THE SAC ROLE OF AURORA KINASES IN MEIOSIS

On commencing my PhD research, little was known about the roles of the Aurora kinases in meiosis I with regards to their role in the SAC. Previous studies had not investigated the effects of Auroras on certain aspects of the first meiotic division such as the SAC, possibly due to Aurora kinase inhibition causing cytokinesis failure. I will therefore address the effect of Aurora inhibition on SAC function in meiosis I, and this is examined in Chapter 5.

1.4.4 TIMING OF MEIOSIS I EXIT

Questions such as ‘why is meiosis I so long?’ and ‘what determines the timing of anaphase?’ have not been addressed in mouse oocytes. I will investigate the role of Cdk1 and the APC during exit from meiosis I in Chapter 6.

2 METHODS AND MATERIALS

Detailed lists of constituents and procedures for the preparation of media and various solutions used have been compiled in the Appendix.

2.1 MOUSE HANDLING AND DISSECTION

2.1.1 ETHICS

All procedures were completed in compliance with the Australian Code of Practice for the Care and Use of Animals for Scientific Purposes and were approved by the University of Newcastle Animal Care and Ethics Committee.

2.1.2 BREEDING

All experiments detailed in this thesis were performed using young (4-6 weeks) female F1 mice produced from a C57BL6 (female) x CBA (male) cross. Mice were bred by the University of Newcastle's Animal Services Unit.

2.1.3 HORMONAL PRIMING

To increase oocyte yield and reduce the number of animals required for experiments mice were hormonally primed before use. Mice were injected with 5-10 International Units of PMSG (Pregnant Mare Serum Gonadotrophin, Invitrogen, New Zealand; Appendix II) 48 hours before use. For injections, mice were held by the loose skin of the back and inverted then injected in the peritoneal cavity with 0.1-0.2ml of the PMSG solution (5-10 IU). Mice were checked shortly after and 24 hours after injection for signs of discomfort.

2.1.4 DISSECTION

Mice were killed by cervical dislocation. The abdominal skin was briefly washed with 75% ethanol and cut open with scissors. The ovaries were removed using small dissecting scissors to cut away the oviduct, connective tissue and surrounding fat. The ovaries were briefly brushed against a lint free tissue (KimTech, Kimberly Clarke Professional, USA) to remove blood before transfer into a Petri dish containing pre-warmed M2 media (Appendix III) supplemented with 1mM milrinone (Sigma-Aldrich,

Australia). The ovaries were then viewed on a stereo microscope and repeatedly punctured using a 30 gauge, ½ inch needle to release the cumulus-oocyte-complexes (COCs) into the media. This procedure was completed within 2-3 minutes.

2.2 OOCYTE COLLECTION AND HANDLING

2.2.1 HANDLING PIPETTE MANUFACTURE

Handling of oocytes required the use of glass pipettes that were manufactured in the lab. 150mm glass pipettes (Kimble-Chase/Lomb Direct, Australia) were heated in a Bunsen burner pilot flame melting the region just below the shoulder. Once soft the glass was then moved from the flame and pulled quickly to draw out the glass into a fine pipette. The glass was the broken approximately 10cm from the shoulder and stored. Before use the pipettes were broken again approximately 3-4 cm from the shoulder until the desired internal diameter with a clean break had been achieved.

2.2.2 OOCYTE COLLECTION

Oocyte collection was performed on a stereomicroscope with a x80 variable zoom (SZ51, Olympus, Japan) and a transmitted illumination attachment (SZ2-ILA, Olympus, Japan). A heated stage (MATS-U4020WF, Tokai Hit, Japan) was also used to help maintain a 37°C environment for oocytes during collection. To collect the oocytes from the media containing the COCs a glass handling pipette was broken to give an internal tip diameter slightly greater than that of an oocyte (~85µm) and mounted into a pipette apparatus. Gentle pressure was applied to draw COCs in and out of the pipette to dislodge the cumulus cells. Typically 3-4 movements were required to remove the cumulus cells. Denuded oocytes were then collected in a larger handling pipette (internal diameter ~ 200µm) and washed into clean media. This procedure was done as quickly as possible in a darkened room, minimizing the oocytes exposure to light as much as possible.

2.3 OOCYTE CULTURE

2.3.1 M2 MEDIA

M2 media (Appendix III) was used for oocyte collection, microinjection, short term incubation and some imaging experiments. Although M2 is considered a handling

media, and not suitable for long term culture, if carefully handled greater than 90% of GV arrested oocytes could mature to metaphase II arrest in M2 media, even after microinjection and imaging. M2 media was therefore used for any experiments where there was no option of providing a 5% CO_2 atmosphere, such as those performed on inverted microscopes. M2 media was made in the lab every two weeks from individual components as described in the Solutions and Media section.

2.3.2 MEM MEDIA

MEM media (Appendix IV) was bought in powdered sachets (Gibco/Invitrogen, Australia) and made fresh every 2 weeks. MEM media is HCO_3 buffered so to attain physiological pH was incubated for several hours in a humidified incubator with 5% CO_2 in air. In addition any mineral oil used to overlay MEM during experiments was also pre-incubated in 5% CO_2.

2.3.3 PREPARATION AND ADDITION OF DRUGS TO CULTURE MEDIA

In experiments where a drug was to be added to the media at a specific timepoint a stock was first prepared by suspending in DSMO (Sigma-Aldrich, Australia), typically at a concentration 1000 times that of the desired final concentration. The stock was divided into 1µl aliquots in 0.5ml Eppendorfs and stored at -20°C. To add the drug during an experiment, the stage of the microscope was set up so that the imaging chamber contained 900µl of media (M2 or MEM). 100µl of warmed media was then rapidly added to an aliquot of the drug to be used and mixed to ensure the drug was dissolved. Addition of the dissolved drug to the imaging chamber was completed between two consecutive images.

2.3.4 MILRINONE AND OOCYTE SYNCHRONIZATION

From the time of collection oocytes were usually kept in media containing milrinone (0.5-1mM). After 1 hour arrest the oocytes were washed through 5 droplets of milrinone-free media. Following washout oocytes were then transferred to the stage of the microscope dependent on the experiment being performed. Oocytes with unusually late times of GVBD were excluded from any analysis but following this synchronization the majority (>80%) of oocytes were found to undergo GVBD within 20 minutes of each other (Figure 2.1).

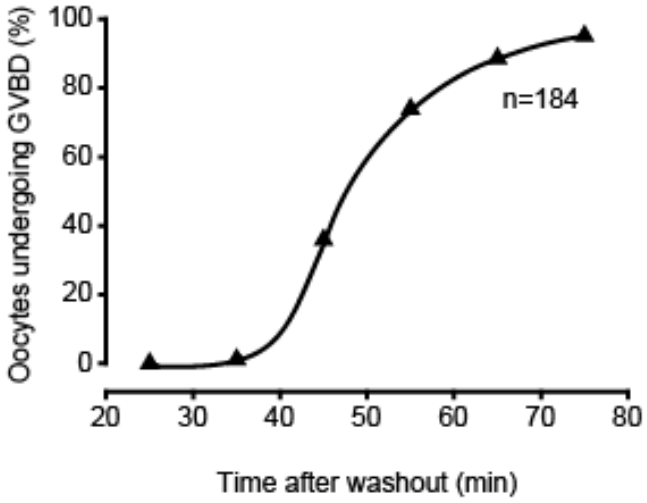

Figure 2.1 - Timing of GVBD after release from milrinone arrest.

The synchrony of oocytes undergoing GVBD was established by plotting GVBD (%) against time (min) following the complete washout of the oocytes from milrinone containing media. Oocytes were checked for GVBD at 10 minute intervals.

2.4 WESTERN BLOT

2.4.1 SAMPLE PREPARATION

Oocytes were washed out of M2 media by washing briefly through 3 drops of PBS (Appendix V) supplemented with 1% PVP (PBS-PVP, Appendix V), then transferred by handling pipette in as small a volume as possible to the side of a 1.5ml Eppendorf tube. This tube was positioned under a stereomicroscope such that the oocytes remained in focus. The pipette was then used to withdraw the PBS buffer, leaving the oocytes in a minimal volume. Five µl of 1 x sample buffer (NuPage LDS, Invitrogen, Australia) was then added on top of the oocytes and the tube was closed. The oocytes were left for several minutes to dissolve into the sample buffer. Samples were centrifuged briefly (10,000g) and incubated at 95°C for 5 minutes. The sample was then used or stored at -80°C.

2.4.2 GEL LOADING AND PROTEIN SEPARATION

The XCell SureLock Mini-Cell tank apparatus (Invitrogen, Australia) was set up according to the manufacturer's instructions and filled with MOPS running buffer (NuPage/Invitrogen, Australia) in the lower chamber and MOPS running buffer supplemented with antioxidant (also NuPage) in the upper chamber. A 10% Bis-Tris SDS-PAGE gel (NuPage/Invitrogen, Australia) was used for separation of the proteins. After removing air bubbles samples were loaded into the wells and a BenchMark protein ladder (NuPage/Invitrogen, Australia) was used for size markers (10 to 220 kDa). The gel was run at 200V for 60 minutes.

2.4.3 PROTEIN TRANSFER

The gel was removed from the tank and arranged into the XCell II Blot Module (Invitrogen, Australia) with blotting pads, a PVDF membrane (Millipore, USA) and transfer buffer (NuPage/Invitrogen, Australia) supplemented with 10% methanol according to the manufacturer's instructions. The protein transfer was then performed by applying 30V across the tank apparatus for 60 minutes.

2.4.4 IMMUNOLABELLING AND CHEMILUMINESCENCE

Firstly the protein ladder was labelled by staining the membrane with Ponceau S stain (0.1%w/v in 5% acetic acid). The membrane was placed on a light box and the ladder marked with a pencil. The Ponceau S stain was then washed from the membrane by repeated washes in ddH_2O.

Membranes were then incubated overnight at 4°C in PBST-BSA (PBS, 0.1% Tween-20, 3% BSA, Appendix V). This solution was also used to dilute the primary antibodies in which the membrane was incubated overnight at 4°C. Following overnight incubation, the membrane was washed by 5 x 20 min washes in PBST and the secondary (HPR conjugated) antibody was applied for 1 hour at room temperature in PBST-BSA. The membrane was again washed 5 x for 20 min each in PBST and the blot developed onto ECL film (GE Healthcare, UK) using ECL Plus (GE Healthcare, UK). Films were exposed for 1, 2 and 5 minutes to obtain the best exposure for each protein. The primary antibodies used were, mouse anti-Securin (ab3305, Abcam, UK, at a dilution of 1:200), mouse anti-Cyclin B1 (ab72, Abcam, UK, 1:500), mouse anti-Actin (ab3280, Abcam, UK, 1:400). The secondary antibody was goat anti-mouse IgG (P0447, DAKO, UK, 1:1000).

2.5 CLONING

2.5.1 PLASMID DESIGN AND CLONING STRATEGY

The plasmids used in this thesis (pMDL) were designed by Dr. Mark Levassuer (University of Newcastle, UK) to be used with the T3 mMessage RNA polymerase kit (T3 Message Machine High Yield Transcription Kit, Life Technologies/Invitrogen, Australia)(McDougall and Levasseur, 1998). The plasmid, modified from pRN3 incorporates a T3 promotor followed by two cassettes located between between three restriction sites. The first cassette, between Bgl II and Sal I restriction sites is for gene insertion. The second cassette, between Sal I and Not I restriction sites contains the fluorescent protein such as Cerulean Fluorescent Protein (CeFP), Green Fluorescent Protein (GFP), Venus, Yellow Fluorescent Protein (YFP) or mCherry. In addition, a further 2 restriction sites (Pst I and Kpn I) are present 3' of the fluorescent protein. These enable the plasmid to be linearised for the production of mRNA. Finally the plasmid contains an ampicillin resistance gene to facilitate selection of bacteria

containing the plasmid during cloning. It is important that the stop codon of the gene of interest is omitted, so that premature termination of the construct does not happen when it is translated in the oocyte (Figure 2.2).

2.5.2 GENE AMPLIFICATION

The coding sequence of the gene of interest was amplified from a cDNA library using PCR. PCR primers were designed to incorporate a 3' SalI and 5' BglII restriction sites such that the gene could ultimately be inserted into the pMDL plasmid 'in-frame' with the fluorescent protein. Primers were ordered from Geneworks, Australia. The PCR reaction was set up using the Accuprime PCR kit (Invitrogen, Australia, Table 2.1) and cycled in an automated PCR machine as shown in Table 2.2. The PCR product was cleaned and its size checked by separation on a 1% agarose gel, followed by recovery on a column DNA gel purification kit (Promega, Australia) and elution into 50µl nuclease free water (Gibco/Invitrogen, Australia).

2.5.3 RESTIRCTION DIGEST

A restriction digest was then performed on the PCR product using Sal I and Bgl II restriction enzymes (Promega, Australia) which both worked effectively in buffer D (Promega, Australia, Table 2.3). At the same time, the pMDL vector containing the fluorescent protein of choice was also digested using the same enzymes (Figure 2.2). Both the digested PCR product and vector were run on a 1% agarose gel to separate the cut fragments and restriction enzymes from the DNA. The DNA was then captured using a column gel DNA purification kit (Wizard SV Gel and PCR clean-up System, Promega, Australia) and eluted into 30µl of nuclease free water.

2.5.4 LIGATION

One µl of both the DNA backbone and PCR product were run on an agarose gel to quantify their concentration. The two were then added to T4 ligation reactions (Promega, Australia) in molar ratios of 3:1, 1:1 and 1:3 calculated as shown in Equation 1. The reaction was performed according to the manufacturer's protocol.

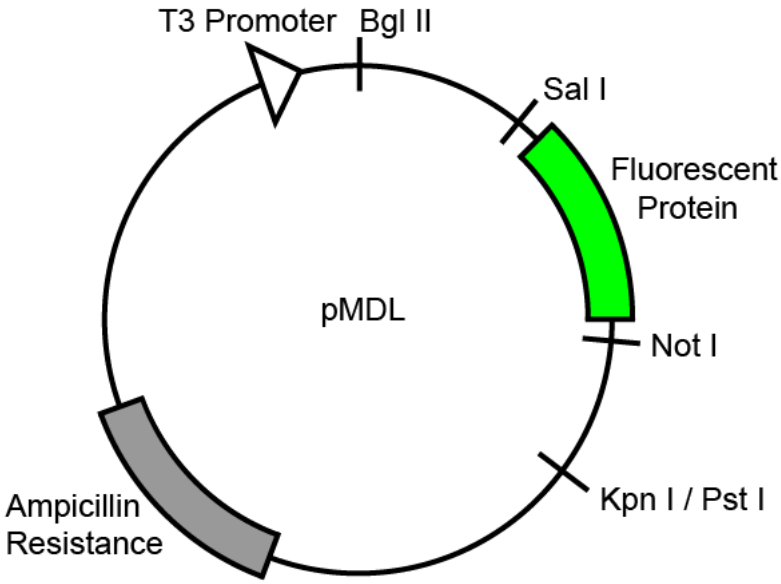

Figure 2.2 - Map of the pMDL vector.

The pRN3 modified plasmid, incorporates a cassette for gene insertion between Bgl II and Sal I restriction sites. The plasmid also has extra restriction sites for linearization, a T3 promoter and a fluorescent protein insert to allow for expression of the gene as a fluorescent fusion protein and an ampicillin resistance gene to facilitate the cloning process.

Reagent	Volume
Accuprime pfx 10X buffer with MgSO4 + dNTP's	5µl
Primer mix (10µM each)	1.5µl
cDNA (1:50 dilution)	1µl
Nuclease free water	42µl
pfx DNA polymerase	0.5µl
TOTAL	50µl

Table 2.1 - Acuprime PCR reaction assembly for gene amplification

Stage	Temp (°C)	Duration	No. of cycles
Initial denaturation	95	2m 0s	1
Denaturation	95	0m 15s	
Annealing	55-64	0m 30s	25-35
Extension	68	1min per kb	
Final extension	68	5m 0s	1
Hold	4	HOLD	

Table 2.2 - PCR amplification temperature cycle

Reagent	Volume
Buffer D (10x)	2µl
PCR/ plasmid DNA	2µl
BSA (10x)	2µl
Sal I	0.5µl
Bgl II	0.5µl
Nuclease free water	13µl
TOTAL	20µl

Table 2.3 - Double restriction digest reaction

$$\frac{\text{ng of vector x size of insert (kb)}}{\text{size of vector (kb)}} \times \text{molar ratio (insert/vector)} = \text{ng of insert}$$

Equation 1 – Calculation of required moles of reactants for ligation

2.5.5 TRANSFORMATION OF COMPETENT CELLS

Two µl from each ligation reaction (1:3, 1:1 and 3:1) were then mixed with 50µl of DH5α competent cells (Invitrogen/Life Technologies, Australia) which were gently thawed on ice. After 30 min the cells were heat shocked by 45s incubation at 42°C and then a 2 min incubation on ice. The cells were then supplemented with 950µl SOC broth and incubated for 1 hour at 37°C in a shaking incubator. These cultures were then each spread onto agar plates supplemented with 100µg/ml ampicillin and incubated overnight at 37°C to select for transformed bacteria.

2.5.6 PCR SCREENING

The ampicillin plates were examined the following day for colonies. Individual colonies were picked from the plate and used as a template for a PCR reaction containing a 5' T3 primer and 3' primer of the gene of interest. This combination of primers reduces the false positive rate of the PCR reaction, which could be caused by residual PCR product still present but unincorporated into the plasmid from the original ligation reaction.

The GoTaq PCR system was used (Promega, Australia) for low fidelity PCR screening and a 10 reaction master mix was set up according to the manufacturer's instructions (20µl per reaction). Colonies were picked from the plate with a sterile pipette tip and mixed with a 20µl PCR reaction. The same tip was then used to transfer the colony to a fresh ampicillin containing agar plate. In this way, any positive PCR results could be traced to the relevant bacterial colony on this plate. A separate reaction was also prepared with a different gene as a template to act as a negative control and one reaction as a positive control by adding 5' and 3' primers and the PCR product of the gene of interest.

2.5.7 PLASMID PREPARATION

Based on successful PCR reactions the bacteria containing the plasmid with the gene of interest were transferred into 5ml vials of LB broth containing ampicillin and cultured overnight (12-16 hours) at 37°C in a shaking incubator. Of these cultures, 500µl were then mixed with autoclaved glycerol (1:1), labelled and stored at -80°C. The remaining culture was centrifuged to produce a pellet and the supernatant discarded. The pellet was re-suspended and the DNA harvested using the SV Wizard miniprep kit (Promega,

Australia) according to the manufacturer's protocol. The plasmid DNA was eluted into 30µl of nuclease free water and stored at -20°C.

2.5.8 DNA SEQUENCING

Plasmid preparation concentration was assessed by photospectrometry and then a reaction was assembled for sequencing as shown in Table 2.4. Samples were sent to the Australian Genome Research Facility, Brisbane, Australia for sequencing.

Each primer yielded around 800 bases of sequence information. Depending on the length of the gene of interest, different numbers of primers were needed to cover up to the 5'-end of the fluorescent protein sequence. The sequences were then aligned using CLC sequence viewer (CLC bio A/S, Denmark) and checked against the known sequence for that gene (Pubmed). Silent mutations were accepted, but if the sequence generated amino acid substitutions, or other coding errors, that plasmid was discarded. Plasmids were also checked to make sure they were in frame with the fluorescent protein. Once a plasmid with the correct sequence was found other plasmids and glycerol stocks were discarded.

2.6 MRNA SYNTHESIS

2.6.1 LINEARISATION AND DNA PREPARATION

Correctly sequenced plasmid was prepared for mRNA synthesis by linearization followed by purification. Firstly, the linearization reaction was set up as in Table 2.5 using the Sfi I restriction enzyme and buffer (Takara, Japan). This reaction was run overnight at 50°C.

If the gene of interest contained an Sfi I digest site then a similar reaction with Kpn I could be used instead. The reaction was terminated by a 10 minute incubation at 80°C. One µl DNA was run on an agarose gel to confirm the linearization reaction. Enzymes and other proteins were then inactivated and digested with the addition of Proteinase K (Invitrogen, Australia, Table 2.6). The reaction was incubated at 50°C for 30 minutes and DNA purified using Phenol/Chloroform Extraction. The volume of the sample was made up to 150µl with nuclease free water and mixed with 150µl of Phenol: Chloroform: Isoamly (25:24:1, Sigma-Aldrich, Australia). The mixture was vortexed and centrifuged at maximum power in a bench-top centrifuge for 10 minutes. The aqueous

Reagent	Amount
Plasmid DNA	200-500 ng
Primer (10µM)	1.12 µl
Nuclease free water	-
TOTAL	14 µl

Table 2.4 – DNA sequencing reaction

Reagent	Volume (µl)
DNA plasmid	10
Buffer M (10x, with BSA)	5
Sfi I	2
Nuclease free water	33
TOTAL	50µl

Table 2.5 – Linearasation of plasmid

Reagent	Volume (µl)
Linear DNA	49
Nuclease Free Water	45
Filtered 10%SDS	5
Proteinase K (20mg/ml)	1
TOTAL	100µl

Table 2.6 – Proteinase K treatment reaction

phase was transferred to a clean Eppendorf, without disturbing the interface. Chloroform (130µl) was added, vortexed and spun as before. The aqueous phase was transferred to a clean Eppendorf. The DNA in this sample was cleaned and concentrated by precipitation using the reaction in Table 2.7 at room temperature for 10 minutes. The Eppendorf was then centrifuged at maximum power for 5 minutes to pellet the DNA (visible as a pink pellet due to the pellet paint). The supernatant was then withdrawn and replaced with 500µl of 70% Ethanol (made using nuclease free water). The tube was vortexed to dislodge the pellet and allow any salts to dissolve into the solution. The tube was then centrifuged to pin the pellet to the bottom and the ethanol removed and replaced. This was repeated twice. Finally after removal of the 70% ethanol, the pellet was allowed to air dry and was finally re-suspended in 20µl of nuclease free water. The sample was then stored at -20°C.

2.6.2 RNA POLYMERASE REACTION

The concentration of linearised DNA was quantified by running one µl on a 1% agarose gel. The reaction in Table 2.8 was assembled according to the T3 mMessage High Yield Capped RNA Transcription Kit (Ambion / Invitrogen, Australia) protocol and run for 2 hours at 37°C. It was terminated by the addition of 30µl nuclease free water and 30µl LiCl precipitation solution. The solution was then chilled to -20°C for ~ 30 minutes and spun at 4°C for 15 minutes at maximum speed on a bench-top centrifuge. The RNA pellet was visualized by dislodging it from the bottom of the tube following vortexing.

2.6.3 RNA PURIFICATION AND PREPARATION

The RNA pellet was washed using the same technique as for the DNA pellet described above (Section 2.6.1, two washes using 70% ethanol in nuclease free water). Finally the pellet was briefly air dried and re-suspended in 20µl of nuclease free water. The RNA solution was divided into 0.5µl aliquots and stored at -80°C. One aliquot was used for photospectrometry to quantify the RNA concentration.

Reagent	Volume (µl)
Linear DNA	120
Pellet Paint (Merck)	2
Sodium Acetate (3M)	12
100% Ethanol	300
TOTAL	434µl

Table 2.7 – DNA precipitation reaction

Reagent	Volume (µl)
Nuclease free H20	to 20
2X NTP/CAP	10
10X Reaction buffer	2
Linear template DNA (~1ug)	-
Enzyme mix	2
TOTAL	20µl

Table 2.8 – mRNA transcription reaction

2.7 OOCYTE FIXATION

2.7.1 GENERAL TECHNIQUES

For fixation, the oocytes were briefly washed through 2 drops of PHEM-PVP (Pipes 60mM, Hepes 35mM, EGTA 25mM, $MgSO_4.7H_2O$ 4mM, 1% PVP, Appendix VII), and incubated with fixation buffer (Appendix VII) at room temperature in a humidified chamber for 40 minutes. This solution also contained Triton X-100 (0.5%) for permeabilization. Oocytes were washed three times in PBS-PVP (Appendix V) and were further washed overnight at 4°C. Oocytes could then be stored in this solution for up to two weeks at 4°C.

2.7.2 FIXING FOR KINETOCHORE COUNTING

In experiments where it was necessary to count the number of kinetochores in an oocyte the normal fixation protocol (2.7.1) was preceded by a 2-hour incubation in the presence of 500µM monastrol.

2.7.3 FIXING TO PRESERVE STABLE MICROTUBULES

A modified protocol was used for the fixation of oocytes where only the stable kinetochore microtubules were to be preserved. Oocytes were washed free of media as above and then incubated in calcium buffer (Appendix VII) for 90s at 37°C. Oocytes were then fixed in calcium fixation solution (Appendix VII) for 40 minutes and processed as for other fixed samples.

2.8 IMMUNOFLUORESCENCE

2.8.1 GENERAL PRINCIPLES

Following fixation, oocytes were typically labelled with primary antibodies to detect proteins of interest, which were then targeted by fluorescently conjugated secondary antibodies. In order to immunostain for multiple proteins simultaneously it was necessary to use primary antibodies derived from different species. In this way, species specific secondary antibodies could be used to target a particular fluorescent dye to each protein of interest.

Fixed oocytes (see section 2.7) were incubated in blocking solution (Appendix VIII) for 1 hour at room temperature and then with primary antibody diluted in blocking solution overnight at 4°C. Oocytes were washed 5 times in washing solution for 30 min each to remove any unbound primary antibody. If needed the procedure was repeated with another primary antibody. Oocytes were incubated with secondary antibodies each diluted 1:1000 in washing solution for 1 hour at room temperature in a darkened room. Oocytes were then washed 3 times with washing solution.

Chromatin was labelled by Hoechst 33258 (20µg/ml Hoechst in PBS-PVP). At the same time oocytes were diluted out of the washing solution and into a mounting solution by 20 minute incubations in above solution diluted 1:1 with Citifluor mounting agent (Citifluor Ltd., UK) and then mounting with Citifluor only.

The oocytes were mounted in small (~0.1µl) drops of Citifluor on a glass slide with pre-made wells. Oocytes were transferred to the Citifluor in as small a volume as possible and allowed to mix for several minutes as there is a large difference in density between the two solutions. Once the oocytes had settled into the Citifluor the excess mounting solution was removed by suction, leaving just enough solution to cover the oocytes. A thin glass coverslip was then placed over the glass slide and gently pressed into place. The edges of the slide were then sealed with nail varnish.

2.8.2 ANTIBODIES USED IN THIS THESIS

Kinetochores were labelled using antibodies derived from serum of patients with the auto-immune disorder CREST, where antibodies are produced against centromere proteins (Fitzgerald/Bioclone, Australia). CREST was detected using goat Alexa-555 anti human IgG (1:1000 dilution).

Microtubules were labelled using bovine anti-mouse α-tubulin (A11126, Molecular Probes/Invitrogen, Australia) and detected with goat Alexa-633 or Alexa-488 conjugated anti-bovine IgG.

Mad2 antibody (rabbit anti-Xenopus Mad2) was a kind gift from Dr. R.H. Chen (Taipei, Taiwan). Goat Alexa-488 conjugated anti-rabbit IgG was used for detection. All secondary antibodies were purchased from Invitrogen, Australia.

2.9 MICROINJECTION

2.9.1 INJECTION PIPETTE PREPARATION

Microinjection pipettes were pulled from borosilicate glass pipettes (1.5mm outer and 0.84mm inner diameter) with an internal filament (World Precision Instruments/ Coherent Scientific, Australia) using a P-97 Flaming-Brown pipette puller (Sutter Instruments, USA). The parameters of the pipette puller were adjusted to give a fine tip about 1cm from the shoulder of the glass. This tip was then carefully broken against the folded edge of a lint-free tissue (KimTech, Kimberly Clarke Professional, USA) and examined under a compound microscope using 400x magnification to assess the break. Pipettes with a cleanly broken tip of the correct diameter (determined empirically and learned by experience through repeated microinjection) were then stored in a pipette storage jar (World Precision Instruments/ Coherent Scientific, Australia) until needed to prevent accumulation of dust.

2.9.2 LOADING PIPETTE PREPARATION

Loading pipettes were manufactured from 1ml plastic syringes (Terumo, USA). The plunger was withdrawn and the syringe melted by rotating in the pilot light of a Bunsen burner. Once soft the syringe was withdrawn from the flame and smoothly pulled to draw the plastic into a fine tip around 50cm long. The syringe was then suspended and the plastic allowed to set. Finally the tip was cut with scissors 10cm from the shoulder and the plunger pushed back in to test if the tip had remained open. The syringe was stored in a clean, dust-free container until needed.

2.9.3 INVERTED MICROSCOPE CUSTOMISATION

A TE300 Nikon inverted microscope (Nikon, Japan) fitted with 10x and 20x objectives lens and 10x eyepieces, a heated culture chamber and left- and right-sided micromanipulators (Narashige, Japan) was used to perform microinjections (Figure 2.3). A pre-fabricated holding pipette (G32801, Cook Medical, USA), was prefilled with mineral oil (Sigma-Aldrich, Australia), and mounted on the left micromanipulator. The pressure in the holding pipette was controlled by an IM-5A hydraulic syringe (Narashige, Japan). The right micromanipulator held the microinjection pipette apparatus which was attached pneumatically to a PV820 picopump (World Precision

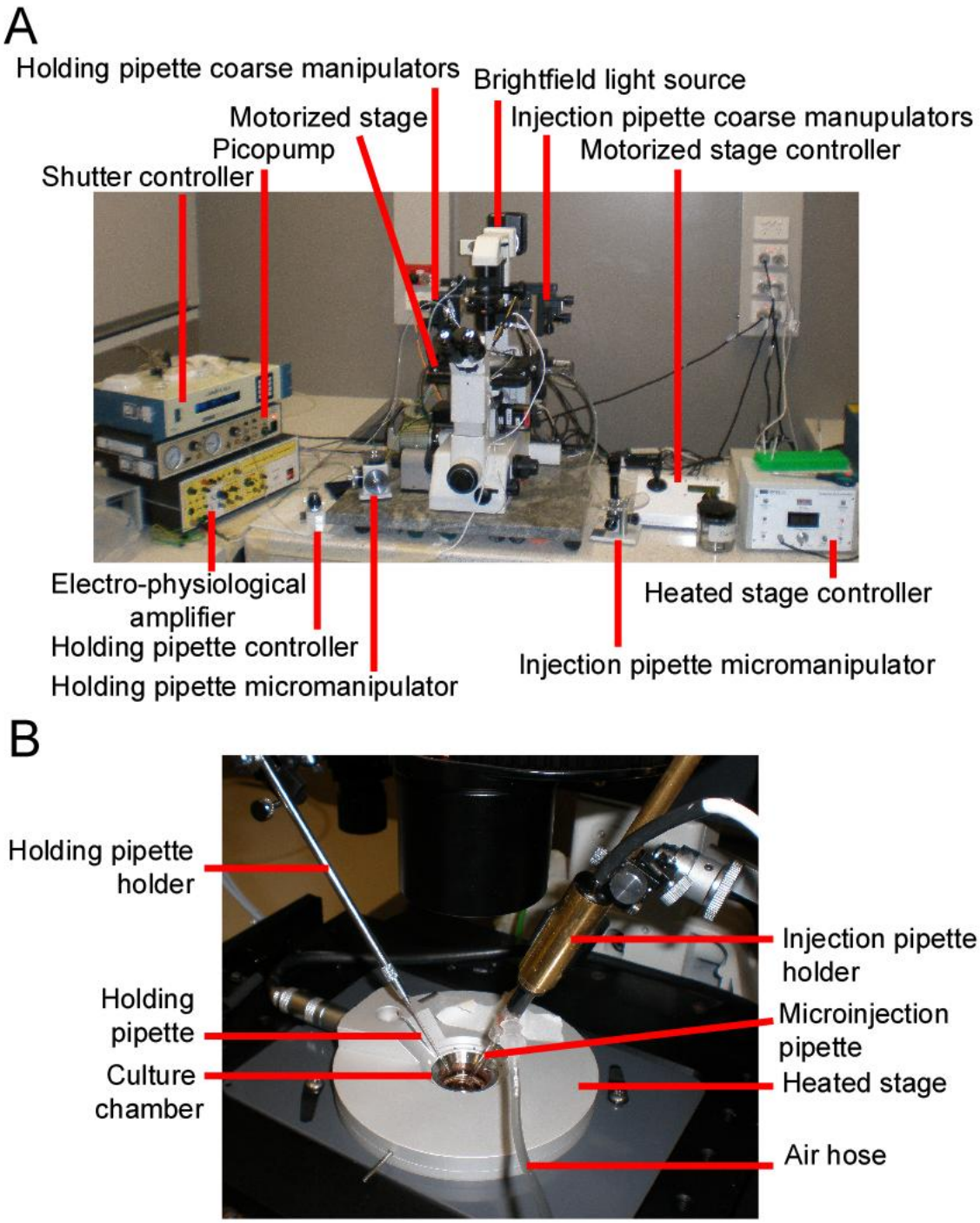

Figure 2.3 - Inverted microscope customized for microinjection

(A) A view of the whole microscope with ancillary devices. (B) The stage of the microscope setup with holding and injection pipettes.

Instruments/ Coherent Scientific, Australia) to control injection pressure and duration. Both micromanipulators were controlled hydraulically in x,y and z directions by MMN-1 coarse manipulators (Narashige, Japan) located to the sides of the microscope and fine control was given by MO-202U or MHW-3 joystick manipulators (Narashige, Japan) positioned next to the microscope. An ASI MS2000 motorized microscope stage was used and controlled by a joystick controller on the right of the microscope (ASI, USA). The imaging chamber was earthed to an Electro 705 Electrometer (World Precision Instruments/ Coherent Scientific, Australia), which has a negative capacitance function. The microscope setup is shown in Figure 2.3 A.

2.9.4 MICROINJECTION

The method for oocyte microinjection employed here has been described in many publications from the Jones laboratory (e.g. See Nixon et al., 2002). The imaging chamber was assembled around a cylindrical chamber with a 22mm diameter cover slip (thickness #1, ProSciTech, Australia) using soft petroleum jelly to seal the edges. The chamber was then filled with 1ml of pre-warmed M2 media, covered by a thin layer of mineral oil and allowed to equilibrate at 37°C. The 10x objective was focused onto the coverslip in the exact centre of the imaging chamber. At this point the earth connection used to complete the electronegative capacitance circuit was placed in the media at the side of the chamber.

The holding pipette was then introduced to the imaging chamber and positioned slightly left of centre in the field of view with its tip resting gently on the coverslip. The oocytes were placed into the centre of the imaging chamber using the mouth pipette apparatus fitted with a transfer pipette. In this step it was essential that the oocytes were not placed closer to one edge of the chamber as convection currents roll them towards that edge. Only enough oocytes for 5-10 minutes of injection were placed on the stage at any one time, to prevent oocytes being illuminated for too long. In addition, whenever not needed the illumination to the microscope was blocked.

The injection pipette was then assembled; the pipette holder was filled with a 120mM KCl, 20mM HEPES solution pH 7.4 using a loading pipette and then put aside whilst the injection pipette was prepared. Aliquots of cRNA were thawed and diluted as required in nuclease free water. The injection pipette was back-filled with a small amount of cRNA (<1ul) using a narrow-tipped loading pipette. The cRNA was forced

into the pipette tip by gentle flicking. The loaded pipette was inserted into the pipette holder which in turn was mounted onto the micromanipulator. The injection pipette was positioned next to the oocytes in the centre of the field of view. The angle of the injection pipette was made to be as steep as possible (~15° from being vertical) as this increased the survival rate of injected oocytes. Any air bubbles inside the tip of the injection pipette were forced out at this point by increasing the injection pressure on the picopump to ~60 psi and applying pressure for several seconds. Once this was achieved the pressure on the picopump was reduced to ~18 psi ready for injection. The objective lens was the switched from 10x to 20x and was focused on the centre of the oocytes.

An individual oocyte was captured using gentle suction from the holding pipette. The captured oocyte was moved slightly away from the other oocytes and the injection pipette positioned above the oocyte. The injection pipette was then lowered directly into the oocyte cytoplasm, either to the left or the right of the germinal vesicle (Figure 2.4). A good pipette tip can break through the zona pellucida with little resistance. This can be seen as the slight recoil of the zona. Following this, a short (~1s) negative capacitance current was delivered to the oocyte by the Electro 705 using its 'tickle' button, to transiently disrupt the plasma membrane, ensuring that the pipette tip had entered the oocyte proper. A timed pressure injection was then used to deliver cRNA into the oocyte. Having the tip of the injection pipette in focus at this point was important as it allows the size of the injection to be gauged. The size was then adjusted in subsequent injections by adjusting the pressure and duration of the injection on the picopump. To ensure consistency the size of the injection was adjusted so as to be the same as that of the nucleolus although oocytes are capable of tolerating much larger injections. By using a consistent injection size the amount of cRNA delivered could be reliably changed by either delivering multiple injections or by changing the dilution used when preparing the cRNA. The pipette was then withdrawn quickly from the injected oocyte and the procedure repeated on the remaining oocytes. Finally the oocytes were transferred from the inverted microscope to milrinone containing media and incubated in the dark on a heat block allowing them to recover for at least 15 minutes before further handling.

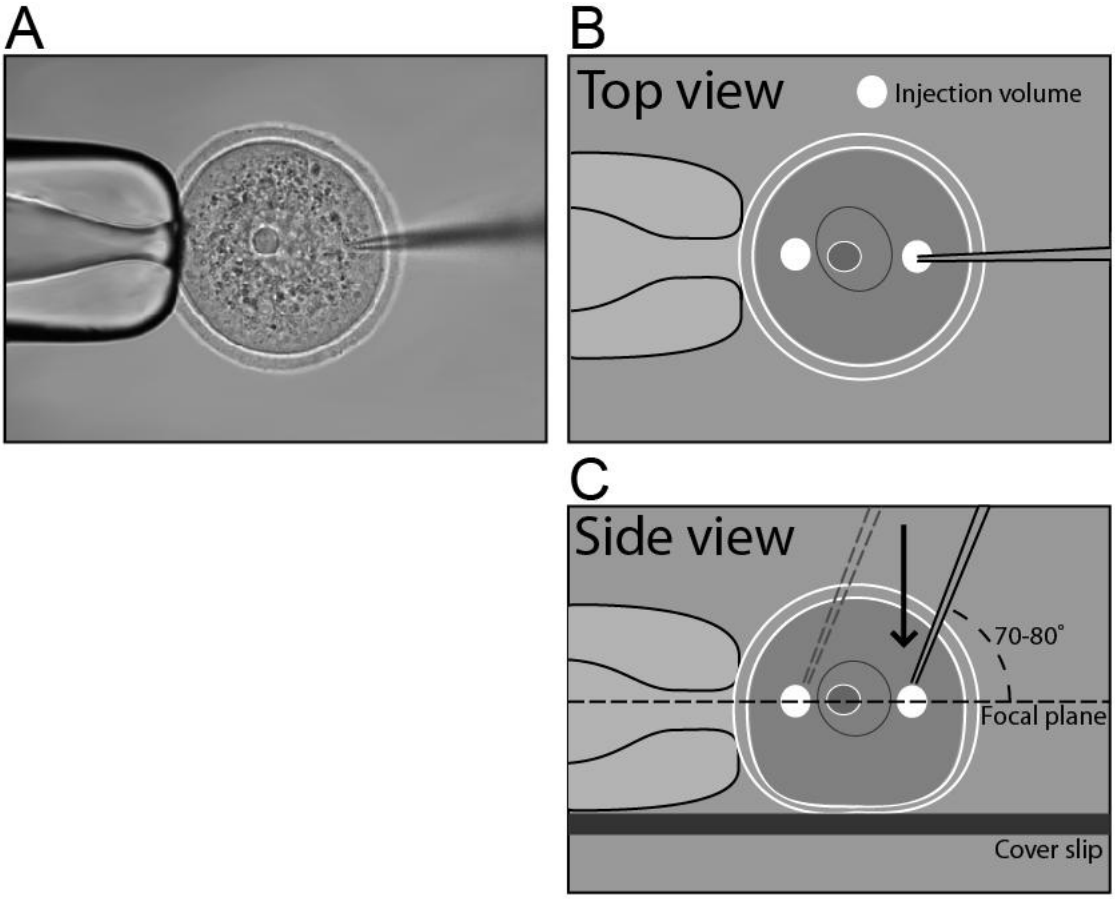

Figure 2.4 - Microinjection of mouse oocytes

(A) An image taken (20x) of an oocyte being secured by a holding pipette (left) and injected by a microinjection pipette (right). The tip of the injection pipette is in focus, however, due to the steep angle of the pipette, it mostly appears out of focus. (B) Schematic of (A) showing the two best places to inject. (C) side view of (B).

2.10 IMAGING SYSTEMS

The imaging experiments were conducted mostly using two systems. A TE2000-U inverted microscope capable of epi-fluorescence timelapse and an Olympus Fluoview FV1000 confocal microscope fitted with an environmental chamber heated to 37°C and perfused with humidified 5% CO_2. For a few experiments an IM Biostation (Nikon, Japan) was used, whose principles of operation are similar to the TE2000-U inverted microscope but which contained a humidified 5% CO_2 imaging chamber.

2.10.1 GENERAL PRINCIPLES

On an atomic scale light at a particular wavelength can excite electrons orbiting an atom into a more energetic orbital, and this excited electron can subsequently emit a photon of light at a higher wavelength (lower energy level – Stokes Law) when it falls back into a lower energy orbit. This basic principle is harnessed to image biological specimens that have been labelled with fluorescent dyes (e.g. Hoechst) or proteins (e.g. Enhanced Green Fluorescent Protein, EGFP). The ability to separate the excitation light from the emitted light allows a detailed image to be captured, accepting only light from the structure/compound of interest. This process is possible due to a dichroic mirror, which reflects higher energy low wavelength light but is designed to transmit lower energy higher wavelength light. The design of the dichroic mirror is dictated by the specific properties of the dye or protein being imaged. For example, EGFP is maximally excited at 488nm, and its peak emission is at 507nm. Therefore, if the specimen were excited with 488nm light a dichroic mirror specifically designed for EGFP would reflect to the microscope stage the excitation light but transmit the epi-fluorescence light (507+nm) from the specimen on the stage (Figure 2.5). This light could then be detected by an appropriate imaging device.

2.10.2 FLUORCHROMES AND LIGHT SOURCES

For epi-fluorescence a mercury lamp (200 Watts) was used. A filter wheel (Sutter Lambda 10-2, Sutter Instruments, CA, USA) was positioned between the Hg lamp and the inverted microscope and was used to insert different filters into the light path to control the wavelength reaching the sample (Table 2.9). For confocal microscopy 4 laser lines were used (Table 2.10).

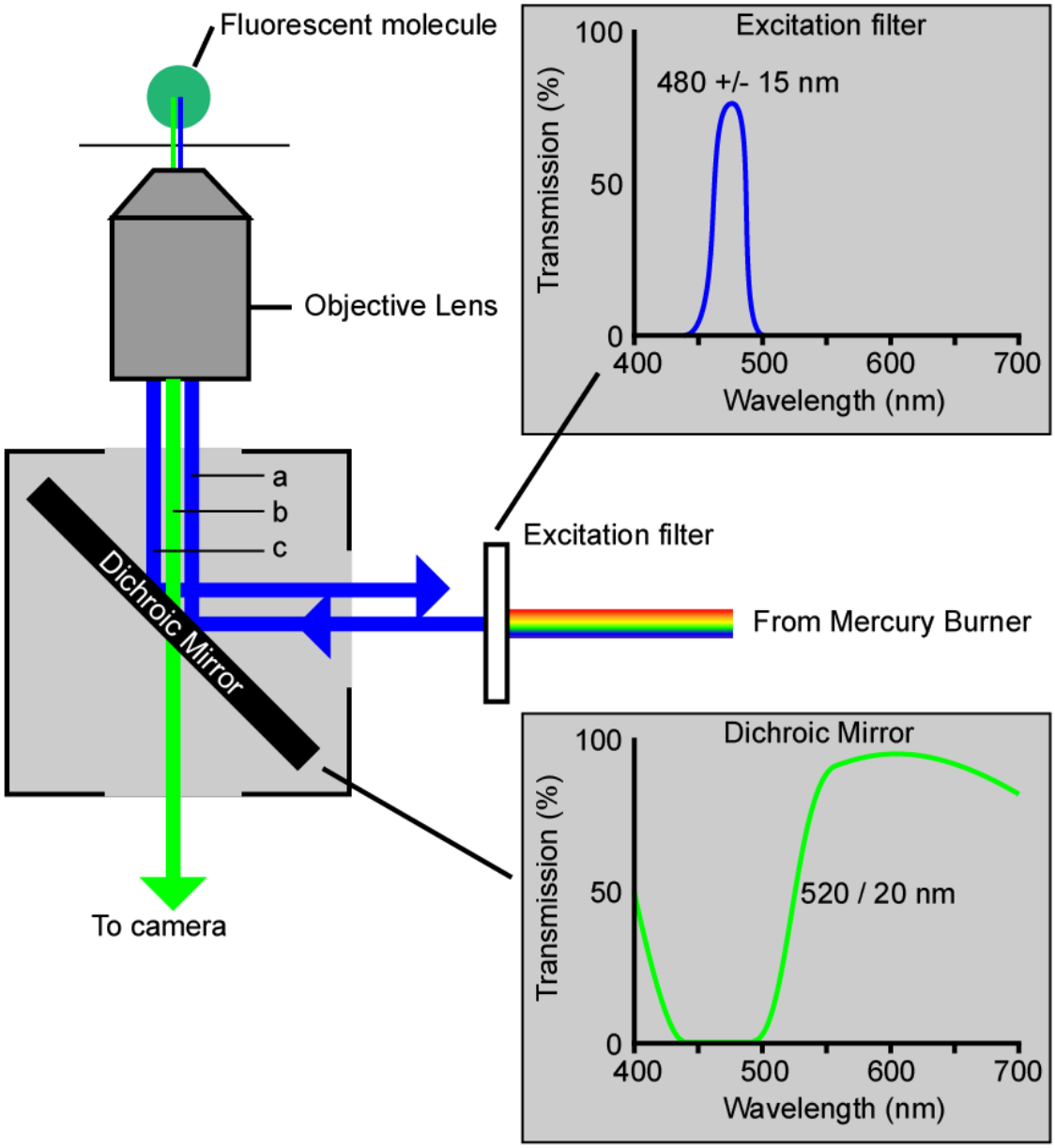

Figure 2.5 - Light path through an inverted microscope with an excitation filter and a dichroic mirror pair for imaging GFP.

'a' refers to the excitation light after it has passed through the excitation filter (480±15nm). 'b' refers to the light emitted by GFP (>505nm) which is able to pass through the dichroic mirror and 'c' refers to reflected light which is unable to pass through the dichroic mirror.

Laser wavelength (nm)	Live imaging
380	Hoechst
480±15	GFP
510±7.9	YFP/Venus
580±10	mCherry

Table 2.9 – Excitation wavelengths generated by filters for use with particular fluorochromes

Laser wavelength (nm)	Live imaging	Fixed samples
405		Hoechst
488	GFP, YFP, Venus	Alexa488
532	mCherry	Alexa555
633	-	Alexa633

Table 2.10 – Wavelengths of lasers used for excitation of particular fluorochromes

A variety of fluorochromes were used, including Hoechst, EGFP, Venus, YFP and mCherry. The excitation and emission properties of which are shown in Appendix X. The ideal fluorochromes were different for different imaging systems. On the confocal EGFP was favoured because it was highly excited by the 488nm laser line. Venus and YFP however were only 20% as bight when excited at this wavelength. On the inverted microscope Venus was a better choice than EGFP due to its higher relative brightness when excited at 510±7.9nm. mCherry was useful on either system because it was excited by longer wavelengths which are less damaging to oocytes.

2.10.3 DICHROIC MIRRORS AND OPTICS

Dichroic mirrors were selected to match the properties of the fluorochromes being imaged and the principle is the same for both confocal and epi-fluorescent imaging. Figure 2.5 shows an example where GFP is being imaged by epi-fluorescence in this case a Long-pass 505LP dichroic mirror is used (Chroma Technology Corp., USA). A 490±7.3nm excitation filter (Chroma Technology Corp., USA) is used to narrow the excitation wavelengths to a range suitable for exciting the GFP. This light is reflected to the objective lens and focused onto the specimen (a). Fluoresced light from GFP is channelled back to the dichroic mirror and because the emitted light is a longer wavelength it is able to pass through the mirror and onto to the camera (b).

2.10.4 OBJECTIVES

20x dry objectives with a 0.75 numerical aperture and a 1mm working distance were typically used for imaging on inverted microscopes and a 60x oil-immersion objective (with 1.35 numerical aperture and a 0.15mm working distance) used for confocal microscopy.

2.10.5 CAMERAS/DETECTORS

The inverted microscope was fitted with a MicroMax 5-MHz charge-coupled device camera (Princeton Instruments; UK) and the confocal with 3 photomultiplier detectors and 6 barrier filters (Olympus, Japan).

2.11 OOCYTE IMAGING

2.11.1 IMAGING OF FIXED SAMPLES

Fixed samples were imaged by confocal microscopy using the 60x oil immersion objective lens with 6x electronic zoom. Z-stacks were compiled with 0.5µm slice separation in the z-axis and an x and y resolution of at least 512 or 1024 pixels. Common arrangements for imaging included Hoechst with Alexa555 labelled CREST and either Mad2 or tubulin labelled with Alexa488 or Alexa633. The spectral separation of these fluorochromes never resulted in observable bleed-through between channels at the laser powers that were used.

During experiments where the fluorescent intensity was of importance (e.g. studying relative Mad2 levels at different timepoints; Figure 3.10) the laser power and other confocal parameters were not adjusted between acquisitions. Additionally, all oocytes were imaged on the same day to minimize any loss of fluorescence that might occur with time.

2.11.2 INVERTED MICROSCOPY

Inverted microscopy was used where 2D information would be sufficient. Typically this was when recording whole cell cyclin B1-Venus fluorescence. Its ease of use e.g. adding drugs to media and the ability to image large numbers of oocytes simultaneously (~30 at 20x) was advantageous. The inverted microscope was also used for many experiments where timing was important, for example anaphase timing in oocytes injected with H2B-mCherry. Additionally the camera fitted to the inverted microscope was sensitive enough to allow for individual non-aligned chromosomes to be resolved using the dry 20x objective lens.

2.11.3 CONFOCAL MICROSCOPY

Confocal microscopy has the advantage that out of focus light is blocked and only in focus light reaches the camera via a pin-hole. This makes images much clearer and structures as small as a kinetochore (~1µm) are easily discernible. Coupled with an automated microscope where the objective lens can be moved it is possible to capture images stacks that can later be assembled to give 3D information. This was very useful for imaging fixed specimens and also live oocytes. In fixed specimens where the

fluorescent signal is strong and resistant to bleaching (e.g. Alexa fluorochromes) time was not a constraint and detailed z-stacks could be captured. On live oocytes it was still possible to capture sufficient information to assemble 3D, high quality images; however the image quality was far less than that from fixed samples. Using a 60x objective 4 oocytes could be imaged simultaneously with a high resolution. This limited the usefulness of the confocal in situations where large numbers of observations were necessary.

2.12 IMAGE ANALYSIS AND FIGURE PREPARATION

2.12.1 MAD2/CREST KINETOCHORE ANALYSIS

The analysis of Mad2 levels on kinetochores was performed using an ImageJ macro that I wrote (Appendix XI). In this macro the user opens the confocal images in ImageJ as a virtual stack using the 'LOCI Bio-formats' plugin available from (http://loci.wisc.edu/bio-formats/imageJ). The macro displays the channels containing CREST and chromatin signals, and the user logs the positions of the kinetochores by clicking on them in pairs, so that both kinetochores of each bivalent are recorded consecutively. The macro then marks the image (using an overlay, not an actual change to the image) with an open circle which is displayed in all planes and a solid circle that is displayed in the plane in which the kinetochore is clicked. The circle is also numbered according to the number of the bivalent. In this way no kinetochore is logged twice, and kinetochores sitting above one another in the image stack can still be distinguished. For each kinetochore that was logged the macro uses a 12 pixel circle to calculate the intensity of the CREST and Mad2 signal on the kinetochore. Then a background measurement is made within 90 pixels of the kinetochore. Due to the likelihood of there being another kinetochore close by, the position of the area used for the background reading was automatically moved within this 90 pixel limit until an area was found that did not contain a strong kinetochore signal. A 90x90 pixel area was then used to take another CREST and Mad2 reading. The macro then performed a background subtraction (kinetochore – background signal) for both Mad2 and CREST and gave the ratio between the two (Mad2/CREST). All these data (kinetochore and background readings and ratios) along with the positions of the kinetochores and the inter kinetochore distances were automatically recorded to an excel spreadsheet.

For the recording of Mad2 in live experiments a similar method was used, only without the ratio against CREST (which was not available) being performed.

2.12.2 ANALYSIS OF BIVALENTS

To assess the extent of bivalent orientation, inter-kinetochore distance and alignment the Mad2-kinetochore analysis macro (2.12.1) was used to record 3D position data for all kinetochore pairs. These data were then presented to another ImageJ macro (Appendix XII) which performed calculations on these data. Firstly, this macro calculated the orientation of the plane which best fit the bivalents by trialling 1,000,000 different planes comprising of 100 increments of rotation in the x, y and z axis. For each plane the angle at which each bivalent intersected the proposed plane was calculated. The plane yielding the highest average angle of incidence was selected as giving the orientation (but not position) of the equatorial plane shown in Figure 3.2 E-F. Secondly the spindle midpoint was calculated by finding the centroid of all the kinetochores and transforming the plane generated previously so that it encompassed this central point to give the ‘equatorial plane’.

This equatorial plane was then used to calculate the alignment of each bivalent. To do this the mid-point between the two kinetochore pairs of each bivalent was calculated (bivalent midpoint). The shortest distance between each bivalent’s midpoint and the equatorial plane was then calculated to give the alignment distances shown in Figure 3.2 C-D. Finally the distance between each kinetochore pair is calculated for each bivalent and used to give the data shown in Figure 3.2 A-B.

The output from the macro was automatically entered into an excel spreadsheet. It was then manually copied into GraphPad Prism 5 (GraphPad software Inc.) to generate the graphs and statistical evaluations shown.

2.12.3 FIGURE PREPARATION

Data generated by various programs (e.g. ImageJ macro or metafluor) were saved in Microsoft Excel, then copied and pasted into GraphPad Prism 5 where graphs of the data and statistical evaluations were made. Graphs were then copied into Adobe Illustrator where they were assembled into figures and annotations were added.

Micrographs were copied directly from either Metafluor or ImageJ into Illustrator with scale data already marked onto the image. Scale bars were then added in Illustrator. Images were adjusted to improve colour contrast only where appropriate, and images within one experiment were treated equally.

2.12.4 CALCULATING SPINDLE DIMENSIONS

Spindle dimensions were measured by making multiple readings on spindles using the Mad2-kinetochore logging macro to obtain 3D point data of opposing points of the spindle. Distances were then calculated using 3D Pythagoras theorem.

2.12.5 DENSITOMETRIC ANALYISIS

Densitometric analysis of Western blots was performed using Metamorph (Universal Imaging, PA, USA). Films (with no saturated bands) were scanned on a flatbed scanner and images imported into Metamorph. Images were inverted and a constant-sized region used to define each of the bands. Total intensity measurements were taken for each region and background subtracted from a region just below the band.

2.12.6 CYCLIN B1-GFP ANALYSIS

Following experiments in which recordings were made of cyclin B1-GFP the image files were opened in Metafluor, if the experiment was saved as a Metafluor file format, or ImageJ ,if the experiment was performed on the confocal using the Olympus file format. In both cases the process of analysis is the same. Images were opened as a stack and the first image was used to mark the outline of the oocytes, defining a region in which the (fluorescence) intensity would be measured (Figure 2.6 A). The average intensity within the regions were then recorded for each timepoint in the series and the data exported to an excel spreadsheet. One region which was centred on an uninjected oocyte was also used to take a background reading. Using the brightfield images taken at the same time as the fluorescent images, the timing of GVBD for each oocyte was also recorded.

The data generated from the experiment were then processed stepwise. Firstly data from oocytes which did not undergo GVBD with normal timing were removed. Normal timing was considered as being within 20 minutes of the average time of GVBD. Secondly the background reading was subtracted (Figure 2.6 B→C, background is the

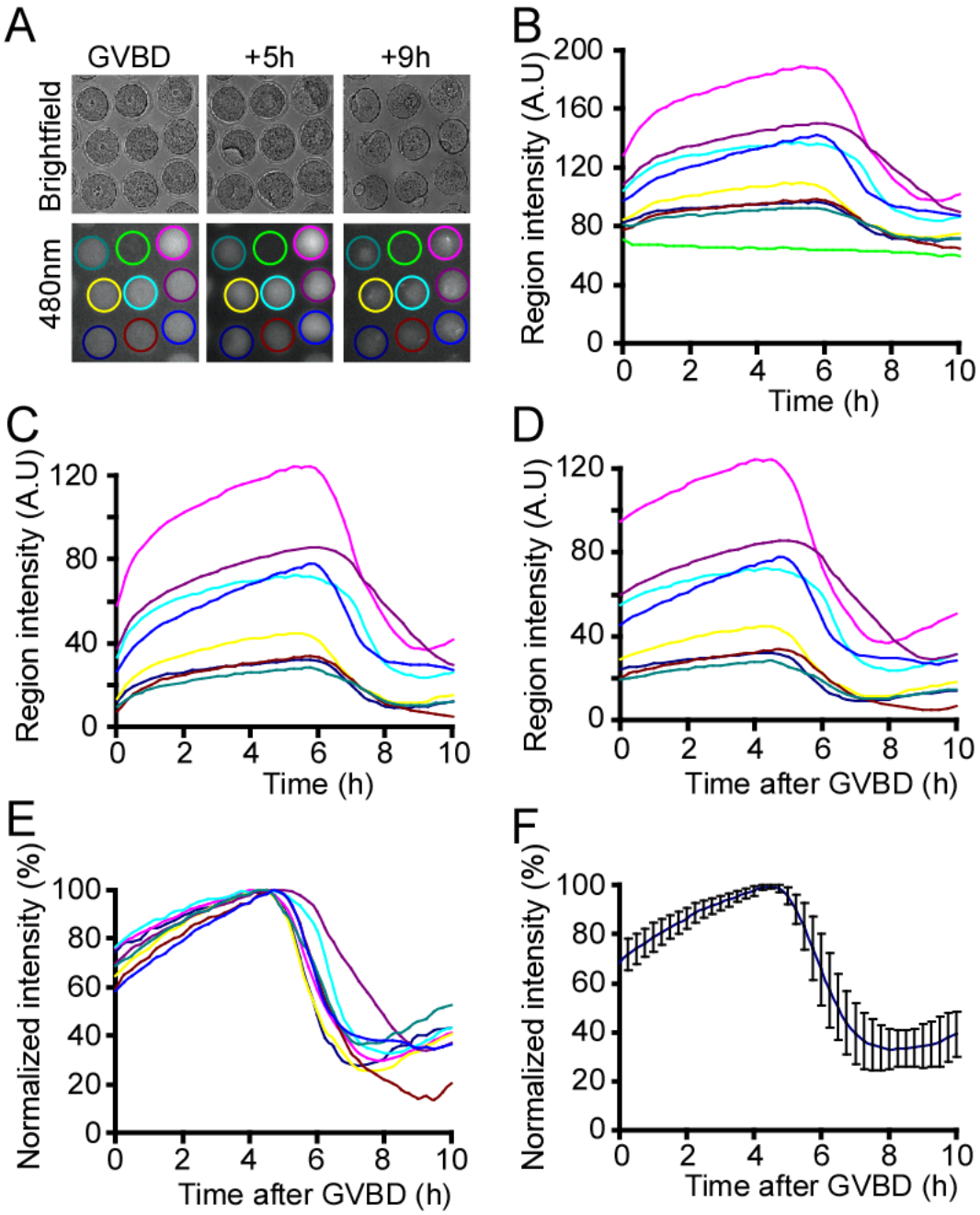

Figure 2.6 - Analysis of fluorescent protein intensity during meiosis I

(A) Brightfield and 480nm images of oocytes during the timelapse. The green circled oocyte is a background control. The circles show the positions of the regions used to record fluorescence intensity. (B) Traces of oocytes in 'A' over the course of maturation. (C) After subtraction of background. (D) After adjustment for the time of GVBD. (E) After normalization of maxima to 100%. (F) Mean values ± standard deviation.

green trace). Thirdly the traces were adjusted so that for each oocyte the time of GVBD was equal to time zero (Figure 2.6 C→D). Fourthly the traces were normalized such that the maximum fluorescence of each trace was set to 100 (Figure 2.6. D→E). Finally the mean and standard deviation were calculated for each timepoint (Figure 2.6 F).

3 THE SAC IN MEIOSIS I

3.1 INTRODUCTION

The function of cell division is to segregate the replicated chromosomes into two new cells. This must be done faithfully so that chromosomes are always divided equally, as errors can lead to tumorigenicity in somatic cells and to miscarriage or severe birth defects in oocytes. Therefore activities during mitosis or meiosis centre around 1) setting up the cell for the division of the chromosomes, 2) monitoring the chromosomes to prevent errors, and 3) once the correct preparations are made, dividing the chromosomes. These activities manifest as 1) the building of a spindle, and the attachment of the chromosomes to that spindle. The latter involves the formation of stable, end-on microtubule attachments to kinetochores, tethering the chromosomes to the spindle. 2) Monitoring is overseen by the Spindle Assembly Checkpoint, which prevents progression to anaphase until certain criteria are fulfilled. These criteria are of great interest but in principle may not be the same in oocytes as mitotic cells. 3) Following satisfaction of the checkpoint criteria the cell enters anaphase by activating the APC. These points have been studied extensively in mitosis where much is known about each. However, some details still remain elusive, such as the precise checkpoint criteria, which will be discussed in Section 4.4.4. In oocytes less is known and importantly the temporal relationship between the above points has not been as clearly defined as in somatic cells. Meiosis I in oocytes is a long process, lasting several hours, far longer than a somatic cell where the events of mitosis happen over tens of minutes. The long duration of the first division in oocytes therefore presents an interesting anomaly. For instance, it is not entirely clear at what point during the several hours of meiosis I the SAC become satisfied: is it towards the end of MI leading immediately to anaphase onset, or is it earlier, in which case why doesn't anaphase occur sooner?

MI spindle formation in eggs is achieved without centrioles and is a slow process taking place over the first few hours of maturation (Brunet and Maro, 2005; Schuh and Ellenberg, 2007). Following spindle assembly, the bivalents must then attach to the spindle so as to be separated at anaphase. The formation of k-fibres assessed by electron microscopy has been reported to occur during the final hour of maturation (Brunet et al., 1999). This may mean that the SAC is satisfied very late in MI, after k-

fibre formation, and before anaphase. This conflicts however with reports examining the localization of the SAC protein Mad2, which suggest a much earlier time for SAC satisfaction (Hached et al., 2011; Wassmann et al., 2003). The timing of the activation of the APC, also indicative of SAC satisfaction, has not previously been shown relative to either k-fibre formation or SAC satisfaction. Many groups have demonstrated the destruction of cyclin B1 or securin in oocytes, the timing of this destruction varying greatly between different strains of mouse. In MF1 oocytes APC activity is directed towards cyclin B1 and securin approximately between 8 and 11 hours after GVBD (Herbert et al., 2003; Homer et al., 2005a; Homer et al., 2005b; Madgwick et al., 2006), whereas the 129/SV C57/BL6 mixed background gives timings of around 6-9 hours (Hached et al., 2011) or 9-13 hours (McGuinness et al., 2009). The KE strain gives timings of 6-8 hours (Ledan et al., 2001), similar to the 6-9 hours given from the background C57BL6/Icrfa^{t} (Lister et al., 2010).

Given the variability in the timing of APC activation in differing strains, it is likely that other events such as k-fibre formation and SAC satisfaction also occur at different times. It is therefore difficult to relate the findings of the different studies examining k-fibre formation, SAC satisfaction to APC activation to each other. In this study I decided to perform experiments with an emphasis on timing, showing how these events were linked temporally in one strain of mouse resulting in an overall picture during MI. The strain of mouse used in this study is an F1 hybrid of C57BL6 females and CBA males. The oocytes of this hybrid give high rates of polar body following in vitro maturation and are very amenable to microinjection. They also have a very consistent timing of PB1, which is relatively early when compared to other strains, making this strain ideal for experiments where timing is critical.

3.2 PROGRESSION OF MEIOSIS I IN MOUSE OOCYTES

3.2.1 DEVELOPMENT OF THE MI SPINDLE.

All times in the results chapters of this thesis are measured with respect to GVBD, unless stated otherwise. Oocytes were synchronized by incubation in milrinone containing media and following its washout oocytes that had not undergone GVBD within 1 h were discarded or excluded from analysis. GVBD was either monitored manually at 10 minute intervals, or in the case of timelapse experiments was

determined from the brightfield images. The average time taken for an oocyte to complete meiosis I, was 8.1 ± 0.7 h (n=100).

In order to begin to understand the timing of major events of meiosis, oocytes were fixed at 2, 4, 6, 8 or 12 h, and fluorescently labelled for tubulin, CREST and chromatin (Figure 3.1 A). At 2 h, tubulin staining gave a ball-like microtubule structure which elongated significantly between 2 and 4 h (16.5±1.16µm, n=5 vs. 26.0±3.05µm n=6, P<0.001, ANOVA with Tukey's multiple comparison test, Figure 3.1 B-C) to form a barrel-like shape, typical of acentiolar spindles. After this time, no significant further increase was observed either between 4 and 6 h, or between 6 and 8 h (4 h, 26.0±3.05µm, n=6; 6 h, 27.5±2.17µm, n=5; 8 h, 27.8±3.13µm, n=5; ANOVA with Tukey's Multiple Comparison Test). During meiotic maturation no significant change was observed in the width of the spindle (2 h, 14.8±1.09µm, n=5; 4 h, 16.7±1.19µm, n=6; 6 h, 17.0±1.01µm, n=5; 8 h, 15.7±1.24µm, n=5; ANOVA with Tukey's Multiple Comparison Test). Additionally, between 4 and 6 h the spindle moved from a central position in the oocyte to the cortex, an event known as spindle migration which is necessary to facilitate the asymmetric division in MI (Verlhac et al., 2000). Finally by 8 h, around the time of PBE, oocytes could be observed in metaphase, anaphase or telophase (Figure 3.1 A).

3.2.2 BIVALENT ARRANGEMENT DURING MATURATION

During the process of spindle elongation and migration to the cortex the bivalents were seen to become progressively more organized. Between 2 and 4 h the distance separating the kinetochore pairs increased, the bivalents congressed towards the spindle centre and additionally became more parallel with the long spindle axis so that the bivalents were arranged with one kinetochore pair facing each of the spindle poles (Fig 3.1 B).

The above observations could be quantified by mapping the position of the kinetochore pairs for each bivalent in 3D. Algorithms were used (See methods section 2.12.2) to find an equatorial plane that best fits the bivalents based on their positions. Using the 3D data, it was possible to calculate the distances between the two kinetochore pairs for bivalents at distinct timepoints during maturation up to 8 h. This distance is a measure of the tension developed across the bivalent as a result of poleward microtubule pulling forces. Significant increases (P<0.001) in inter-kinetochore distance

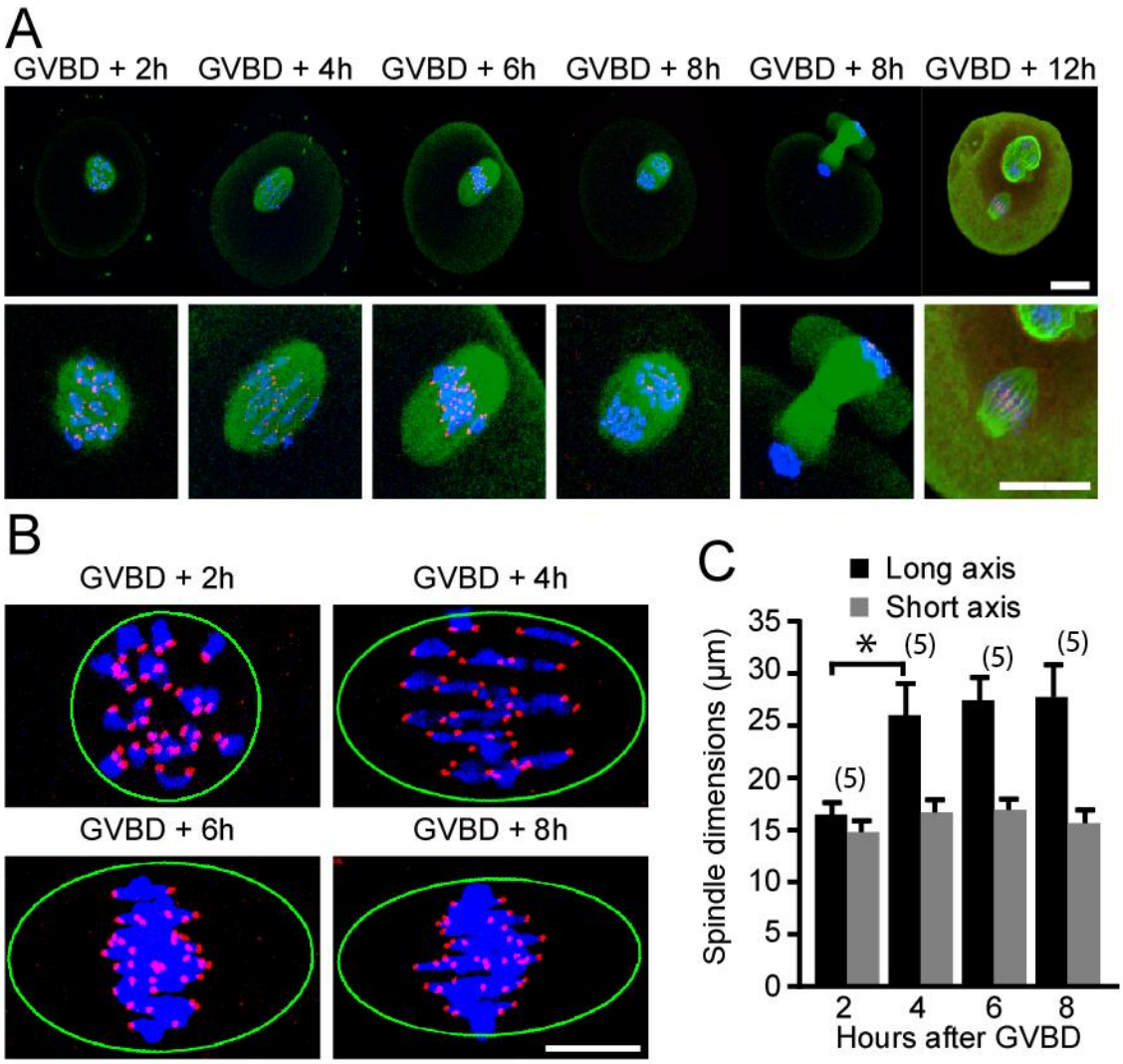

Figure 3.1 - The formation of the MI spindle.

(A) Images show representative z-projections of stacks generated by confocal microscopy. Oocytes were fixed at the times indicated after GVBD and processed by ICC for Tubulin (green), centromeres (red) and chromatin (blue). Whole oocyte (top row) and spindle (bottom row), n=10 oocytes per timepoint, scale bars represent 20µm. (B) Representative images showing the change in spindle shape, and chromosome alignment during meiosis I. Chromatin is indicated in blue, Centromeres in red and the outline of the spindle, derived from tubulin staining as in 'A', in green. Scale bar represents 10µm. (C) Spindle width and length were calculated as the shortest and longest distance passing through the spindle centre respectively, n=5 oocytes per timepoint, error bars represent S.D.

were observed between 2 and 4 h, between 4 and 5 h and between 6 and 8 h (2 h, 1.8+/-0.7µm, n=100; 4 h, 3.8±1.0µm, n=100; 5 h, 4.5±1.4µm, n=160; 6 h, 4.4±1.1µm, n=100; 8 h, 6.5±1.7µm, n=40; ANOVA with Tukey's Multiple Comparison Test; Figure 3.2 A-B), suggesting that tension increases at all stages of oocyte maturation but that the maximal increase is observed between 2 and 4 h (Fig 3.2. B).

In order to assess the congression of the bivalents during maturation, the midpoint of each bivalent was calculated as the centre point between its two kinetochore pairs. The distance of each bivalent from the equatorial plane was then calculated and these were used as a measure of congression (Figure 3.2 C). An oocyte achieving better congression would have a smaller mean bivalent displacement. There was a significant ($P<0.001$) decrease in the mean distance of bivalents from the spindle midzone between 2 and 4 h and between 5 and 6 h (2 h, 2.8±1.8µm, n=100; 4 h, 1.8±1.3µm, n=100; 5 h, 1.9±1.6µm, n=160; 8 h, 1.1±0.8µm, n=40; ANOVA with Tukey's Multiple Comparison Test; Figure 3.2 D). These changes mirrored the above changes in tension, such that bivalents became more congressed as their inter-kinetochore distances increased.

Finally, the 3D data were used to calculate the angle the bivalents made with the equatorial plane. For each bivalent the angle at which the line passing through both its kinetochore pairs intersected the equatorial plane was used to give θ (Figure 3.2 E). Thus in oocytes with most bivalents perpendicular to the equatorial plane the mean value of θ would be close to 90° with a small standard deviation, whilst oocytes with their bivalents arranged at random would be expected to have a mean θ value close to 45° with a large standard deviation. When oocytes fixed at different timepoints were assessed it was found that θ increased the as they matured. At 2 h, bivalents intersected the equatorial plane at angles covering almost the entire range from 0 to 90°, and as such had a large standard deviation and a mean angle close to 45° (mean: 44.1±22.2°; minimum: 0.6°; maximum 86.9°), all indicative of the bivalents being randomly arranged. Between 2 and 4 h there was a significant increase ($P<0.001$, ANOVA with Dunn's Multiple Comparison Test) in θ values, with the mean angle increasing and standard deviation narrowing and this trend continued (though not always significantly) throughout maturation (4 h, 78.7±12.2º; 5 h, 79,8±7.8º; 6 h, 84.1±4.2º; 8 h, 86.9±2.3º; Figure 3.2 F). Together the data in this figure suggest that during maturation the largest improvement in the organization of the bivalents occurs

between 2 and 4 h, with further, but more subtle improvements occurring during the remainder of meiosis I.

3.2.3 FORMATION OF KINETOCHORE AND NON-KINETOCHORE MICROTUBULE FIBRES DURING PROMETAPHASE I.

The above data suggested that the process of establishing a spindle and organising the chromosomes, although not complete appeared to be well underway by 4 h. This raised the question of at what point during MI the kinetochores first started to interact with the spindle microtubules directly. At 4 h chromosomes appeared to be stretched with each sister kinetochore pair facing one spindle pole (Figure 3.1 B, Figure 3.2 F) and had undergone an increase in inter-kinetochore distance (Figure 3.2 B). It seemed reasonable that this might be the result of kinetochore-microtubule interactions. To test this idea synchronized oocytes were fixed at hourly timepoints through the latter half of meiosis I (4-8 h). For each timepoint oocytes were either fixed directly after washout from the 37°C media, or were fixed likewise but after a 5 min incubation in 4°C media. Reducing the temperature causes microtubules to depolymerise, unless they are stabilized by attachment to kinetochores. Therefore after cold treatment, the only microtubules remaining should be the kinetochore-bound microtubules, also referred to as k-fibres (Amaro et al., 2010; DeLuca et al., 2006; Salmon and Begg, 1980; Toso et al., 2009). Using this method, it was possible to see that although a barrel-shaped spindle had been formed by 4 h (Figure 3.3 A) this spindle did not comprise of any k-fibres. The overall structure of the spindle did not change as meiosis progressed (37°C, Figure 3.3 A), however the proportion of this spindle that was comprised of k-fibres appeared to increase as the oocytes matured, such that by 8 h the spindle appeared relatively unchanged after cold treatment.

Attachment of kinetochores to microtubules is an important event during the cell cycle, as it relieves the cell of SAC inhibition, allowing it to proceed to anaphase. In mitosis the last remaining unattached kinetochore is thought to be able to prevent anaphase (Rieder et al., 1995). Therefore it is pertinent to discover at what time in oocytes all kinetochores are attached to microtubules. I sought to establish if at 5 h, when the cold-stable microtubules first appeared they contacted all, or just some of the kinetochores. Figure 3.3 B shows an expansion of the z sections of the 4°C, 5 h timepoint oocyte

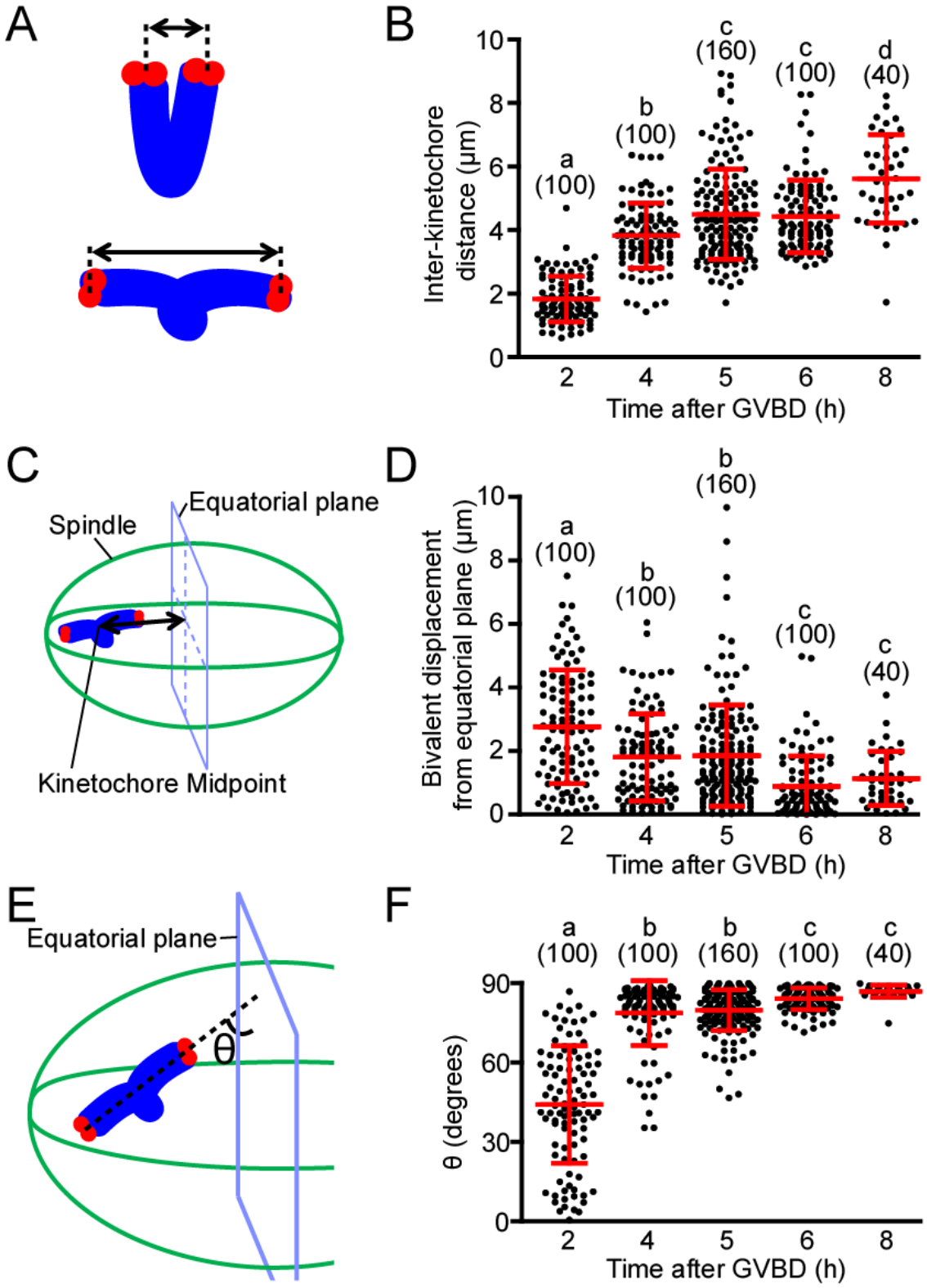

Figure 3.2 Bivalent behaviour during meiosis I

(A-B) Inter-kinetochore distance was calculated as shown 'A' and plotted for each timepoint in 'B'. (C-D) Bivalent alignment was calculated as shown in 'C' by measuring the distance from the centre of the bivalent to the nearest point on the equatorial plane. These data were plotted for each timepoint in 'D'. (E-F) The angle at which the line passing through both kinetochore pairs intersected the equatorial plane, denoted θ, as shown in 'E' was plotted for each timepoint in 'F'. (B,D,F) number of bivalents analyzed are indicated in parenthesis. Red lines indicate mean values and standard deviations. Different letters (a,b,c,d) indicate a significant difference between groups (P<0.001). (C,E) Equatorial plane was calculated based on algorithms described in the methods section, predicting the best fit with the bivalents.

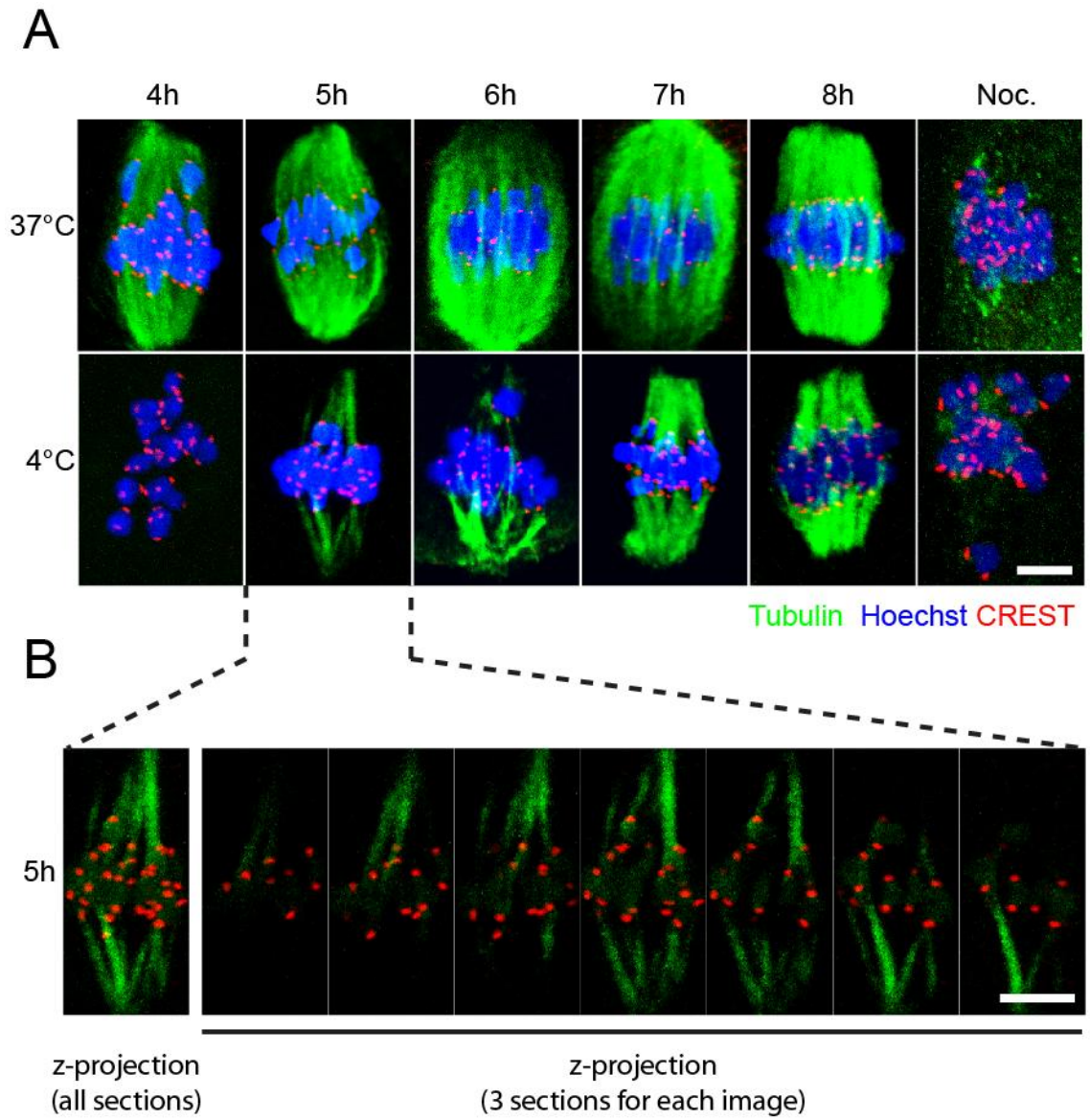

Figure 3.3 - Spindle formation occurs early in prometaphase but stable k-fibres do not form until 4-5 h.

(A) Synchronized oocytes were fixed at the indicated timepoints during meiosis I or after treatment with 400nM nocodazole for 30 min at 8 h. Oocytes were either fixed directly after culture at 37°C (top row) or after a 5 min incubation in media maintained at 4°C. Oocytes were fluorescently labelled for tubulin (green), CREST (red) and chromatin (blue) and displayed as a whole stack z-projection. (B) Enlarged view of the 5 h timepoint at 4°C showing both the whole-stack z-projection (left) and z-projections of 3 slices (right). (A-B) n=5-10 oocytes per group, scale bars represent 5µm.

displayed as a whole-stack projection (left), and projections of three consecutive slices (right). Most kinetochores did appear to be contacted by microtubules, although many

of the connections were extremely weak and whether these constituted kinetochore-microtubule attachments was uncertain. An alternative method of preserving only k-fibres is treatment in a Ca^{2+} containing buffer (DeLuca et al., 2006; Kitajima et al., 2011; Weisenberg and Deery, 1981). Synchronised oocytes fixed at 4 h in Ca^{2+} buffer confirmed that no stable k-fibres were present, as was the case after cold treatment (Figure 3.4 A). When the tubulin was examined a weak spindle shape was observed, but it did not comprise of fibre structures, only punctate and randomly distributed foci which were also present to a lesser extent in the neighbouring cytoplasm. Additionally, examination of individual kinetochores from 8 oocytes did not reveal any associated k-fibres (Figure 3.4 B). Therefore the residual tubulin after Ca^{2+} treatment did not constitute k-fibres.

When oocytes were fixed in Ca^{2+} buffer just one hour later, at 5 h, there was a clear difference in the tubulin staining observed (Figure 3.5 A-B). A barrel shaped spindle structure was present and the majority of microtubule fibres appeared to connect with kinetochores suggesting that the Ca^{2+} buffer method was removing non-kinetochore microtubules. To confirm this, oocytes were examined after fixation by an identical process only without the inclusion of Ca^{2+}. This resulted in more tubulin remaining after fixation (Figure 3.5 A, inset ii). Following examination of each individual kinetochore in 8 oocytes, it was possible to determine the attachment status of the vast majority (292/320, 91.3% Figure 3.6 A). Of those that were determinable, 241 were found to be attached to one spindle pole (mono-orientated, 82.5%), 42 were attached to both poles (biorientated, 14.4%) and 9 had no apparent attachment (3.1%). Therefore the vast majority (88.4 - 96.9%) of kinetochores had formed attachment, although not necessarily correct, by 5 h.

Together these data suggest that stable kinetochore fibres first form between 4 and 5 h. This appeared to differ from the timing with which the bivalents achieved bi-orientation, as biorientation was apparent in oocytes at 4 h (Figure 3.1 - Figure 3.4). Interestingly therefore the initial increase in θ and inter-kinetochore distance are possibly not the result of attachment of kinetochores by k-fibres, which occurs later than 4 h.

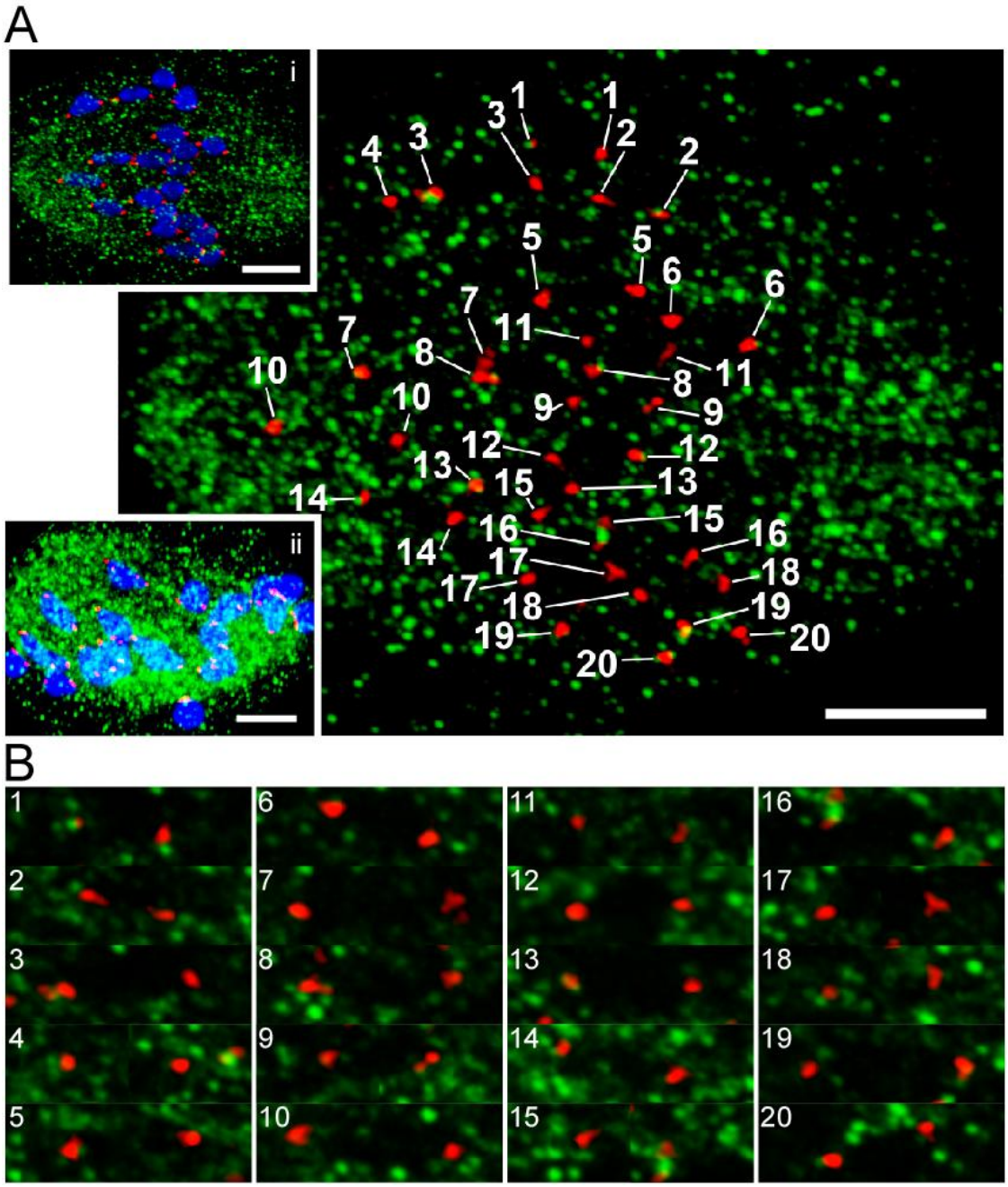

Figure 3.4 - Kinetochores are not connected by microtubule fibres at 4 h.

(A) A representative whole-stack projection of a fluorescently labelled oocyte treated in a Ca^{2+} containing buffer prior to fixation at 4 h. Kinetochores are shown in red and tubulin in green. Chromatin is shown in blue in inset i and a control oocyte treated without calcium is shown in inset ii. (B) Individual z-sections showing the kinetochores for each bivalent in the oocyte, numbers correspond to those in 'A'. (A-B) Scale bars represent 5µm.

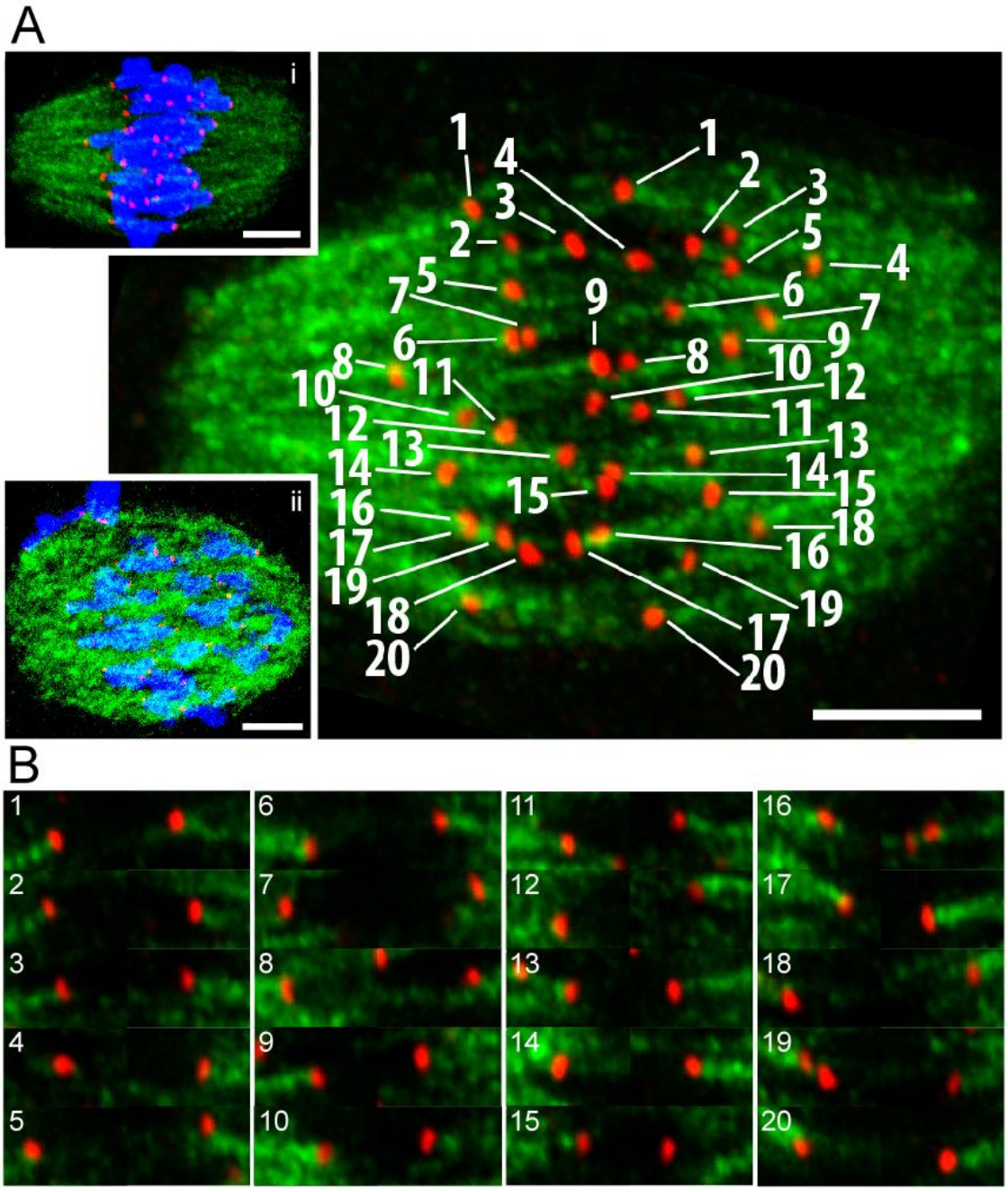

Figure 3.5 - Kinetochores are connected by microtubule fibres at 5 h.

(A) A representative whole-stack projection of a fluorescently labelled oocyte treated in a Ca^{2+} containing buffer prior to fixation at 5 h. Kinetochores are shown in red and tubulin in green. Chromatin is shown in blue in inset i and a control oocyte treated without calcium is shown in inset ii. (B) Individual z-sections showing the kinetochores for each bivalent in the oocyte, numbers correspond to those in 'A'. (A-B) Scale bars represent 5µm.

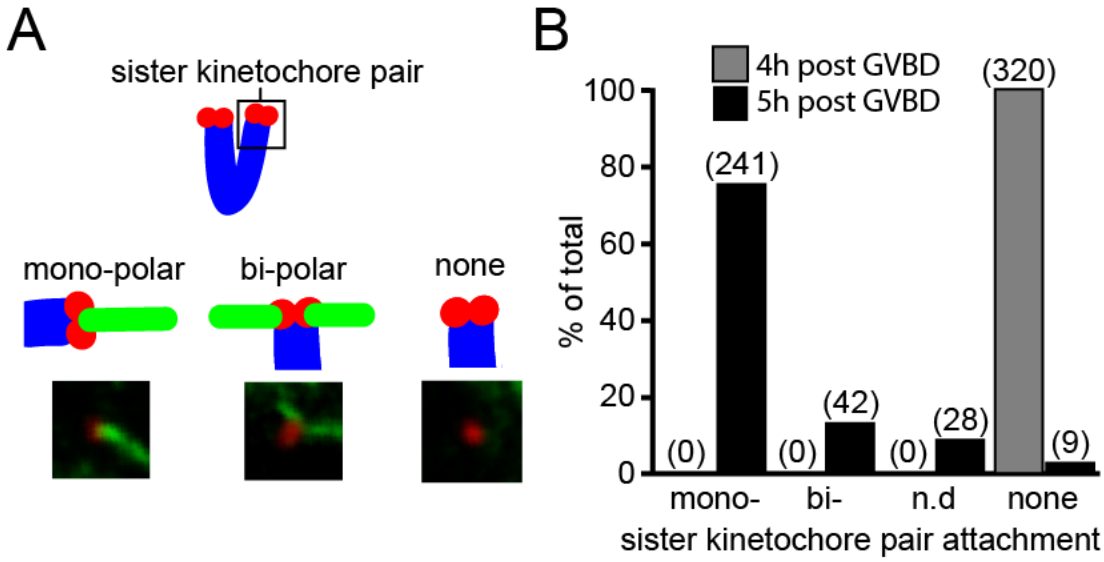

Figure 3.6 - The majority of kinetochores acquire microtubule attachment 4-5 h.

Quantification of kinetochore-microtubule attachments from 8 oocytes fixed at either 4 or 5 h such as those shown in Figure 3.4 *or* Figure 3.5. *Attachment for each sister kinetochore pair was classed as mono-polar attachment (mono-), bi-polar attachment (bi-), non-discernible attachment (n.d.) or as having no attachment (none). Number of sister kinetochore pairs analysed is shown in parentheses.*

3.2.4 DESTRUCTION OF ENDOGENOUS CYCLIN B1 AND SECURIN IN PROMETAPHASE I.

Ca^{2+} stable k-fibres had formed on the majority of kinetochores by 5 h. This timing was of interest because it is some 3 h before anaphase. It would therefore be important to determine if these kinetochore attachments were sufficient to activate the APC, as is predicted by complete kinetochore attachment in studies on somatic cells (Kulukian et al., 2009; Rieder et al., 1995). APC activation should follow after attachment of all kinetochores by microtubules as unattached kinetochores provide the signal that inhibits the APC. However, one might also expect that the timing of APC activation would be more closely associated with that of anaphase.

To determine if the APC was active in oocytes at 5 h the levels of two APC substrates, cyclin B1 and securin, were measured. Synchronized oocytes were collected for western blotting at 4, 5 and 6 h. Fifty oocytes were pooled for each timepoint and the resulting western blot is shown in Figure 3.7 A. Densitometeric analysis was used to determine the relative signal intensity for cyclin B1 and securin at each timepoint and this was ratioed against the loading control (actin) and normalized against cyclin B1 intensity at 4 h (Figure 3.7 B). Both cyclin B1 and securin were found to peak at 5 h, indicating that the APC may have become activated around this time.

3.2.5 DESTRUCTION OF EXOGENOUS CYCLIN B1-GFP IN PROMETAPHASE I.

APC activity could also be determined in real-time, by injection of mRNA encoding cyclin B1-GFP into GV oocytes. Oocytes were imaged for GFP and brightfield at 15 min intervals. During analysis the brightfield images were used to determine the timing of GVBD for each oocyte. Based on this approach the fluorescence data for each oocyte were adjusted such that each had GVBD at 0 h. Traces were then normalized with their maximal fluorescence set to 100% and the data were pooled and plotted as a mean ± S.D. (Methods Section 2.12.6, Figure 3.8 A, Movie 3.1). The peak fluorescence was found to be at 4 h, with degradation of cyclin B1 commencing between 4 and 5 h. The overexpression of cyclin B1 did not appear to impact upon the progression of oocytes through meiosis I as the timing of PBE was not significantly different from that of uninjected controls (cyclin B1-GFP, 7.91 ± 0.62 h, n=77; control, 8.09 ± 0.72 h, n=100; P=0.0692, Mann Whitney U; Figure 3.8 B).

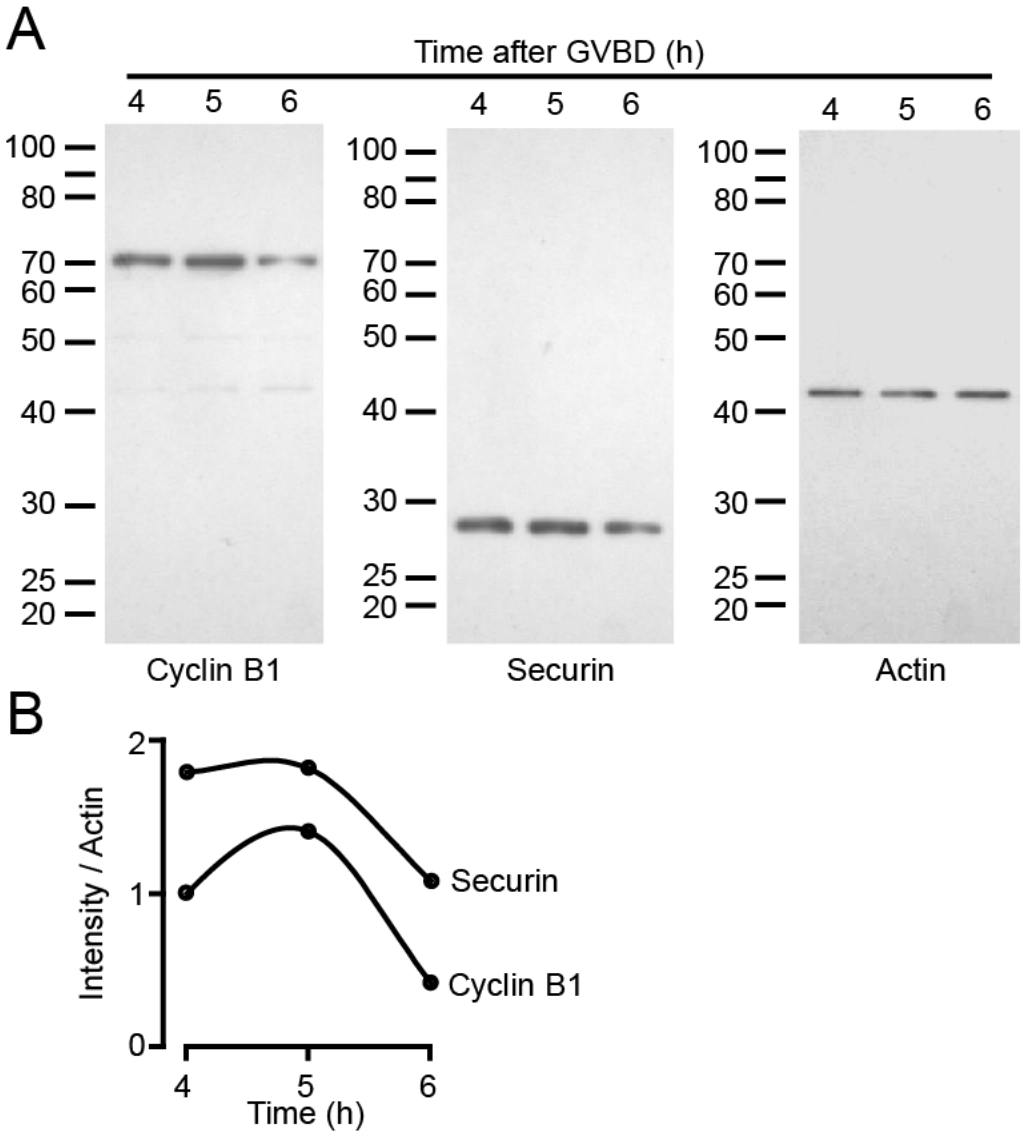

Figure 3.7 - Degradation of endogenous cyclin B1 and securin during prometaphase I.

50 synchronized oocytes were pooled into sample buffer at 4, 5 or 6 h. Samples were separated on an agarose gel and Western blot was used to reveal the levels of cyclin B1, securin and actin in the samples. (A) Images of the Western blot with the 'benchmark' size markers indicated. (B) Densitometeric ratios of cyclin B1 and securin against the loading control actin for each of the timepoints.

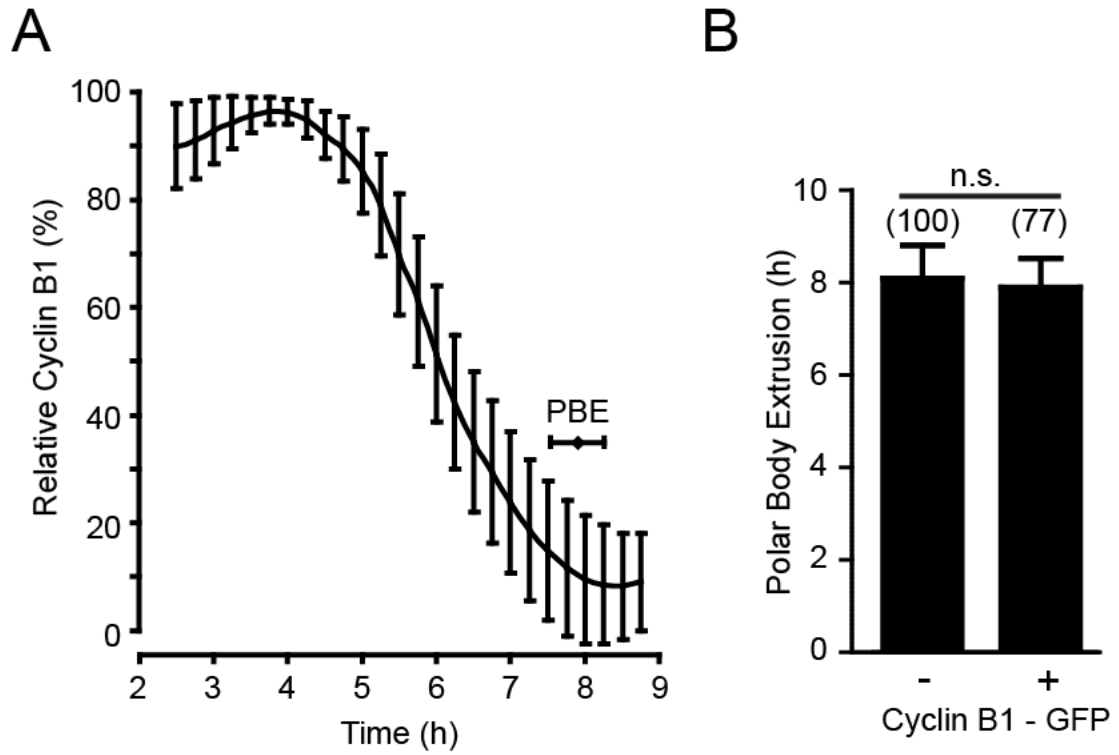

Figure 3.8 - Degradation of cyclin B1-GFP during meiosis I.

(A) Mean fluorescence levels in oocytes expressing cyclin B1-GFP mRNA at the times indicated after GVBD. Maxima are normalized to 100% and the PBE time is indicated (PBE, mean ± standard deviation, n=77). (B) The mean timing of PBE in controls (8.1 ± 0.7 h) or cyclin B1-GFP mRNA injected oocytes (7.9 ± 0.6 h) were not found to be significantly different, P=0.07, t-test. (A-B) Error bars represent standard deviations from the mean. Numbers of oocytes are indicated in parenthesis.

3.2.6 LOSS OF EXOGENOUS MAD2 FROM CHROMOSOMES DURING PROMETAPHASE I

The above work placed the timing of kinetochore-microtubule attachment at ~5 h, and the timing of APC activation was similar. Therefore, it seemed likely that the APC was being activated due to SAC satisfaction in response to microtubule attachment at the kinetochores. To assess this directly oocytes were injected with mRNA encoding Mad2-YFP and H2B-mCherry, and imaged every 30 min by 3D confocal microscopy from 3 h. In whole stack z-projections at 3 h, two discrete Mad2-YFP signals were observed on many of the bivalents (Figure 3.9 A), which were presumed to be kinetochores as they resembled the two CREST signals observed on chromosomes previously (Figure 3.1 B). Moreover endogenous Mad2 immunostaining (next Section) demonstrated co-localisation of Mad2 with kinetochores. When the intensity of these Mad2 kinetochore signals was measured at subsequent timepoints they were found to diminish; the loss was gradual, and first became significantly different from the 3 h timepoint by 5.5 h (3 h, 28.7±15.0, n=16; 5.5 h, 17.9±10.8 n=16; $P<0.05$, ANOVA with Tukey's Multiple Comparison Test; Figure 3.9 B). The loss of signal was not attributed to photobleaching or loss of expression of the Mad2-YFP, but due to removal of Mad2 from the kinetochores because the YFP signal could be maintained for the duration of the experiment by addition of 400nM nocodazole.

3.2.7 TIMING OF LOSS OF ENDOGENOUS MAD2 FROM KINETOCHORES AND APC ACTIVATION.

Live imaging using a YFP-tagged construct demonstrated a loss in Mad2 signal from kinetochores, however it also perturbed meiosis, as no polar bodies were extruded following its expression. I therefore sought to replicate the finding by examining the time at which endogenous Mad2 was lost from kinetochores. Synchronised oocytes were injected with mRNA encoding cyclin B1-GFP and then washed out of milrinone. Brightfield and fluorescent images were recorded at 15 min intervals during maturation. At 4, 5 and 6 h oocytes were removed from the imaging chamber and fixed ('Fix', Figure 3.10 A). After the removal of the 6 h group, 400nM nocodazole was added to the media ('Noc.'), and imaging of the remaining oocytes continued until an attenuation of cyclin B1-GFP degradation was observed, then these oocytes were also fixed. The four groups of oocytes were then processed in parallel by ICC with anti-centromere

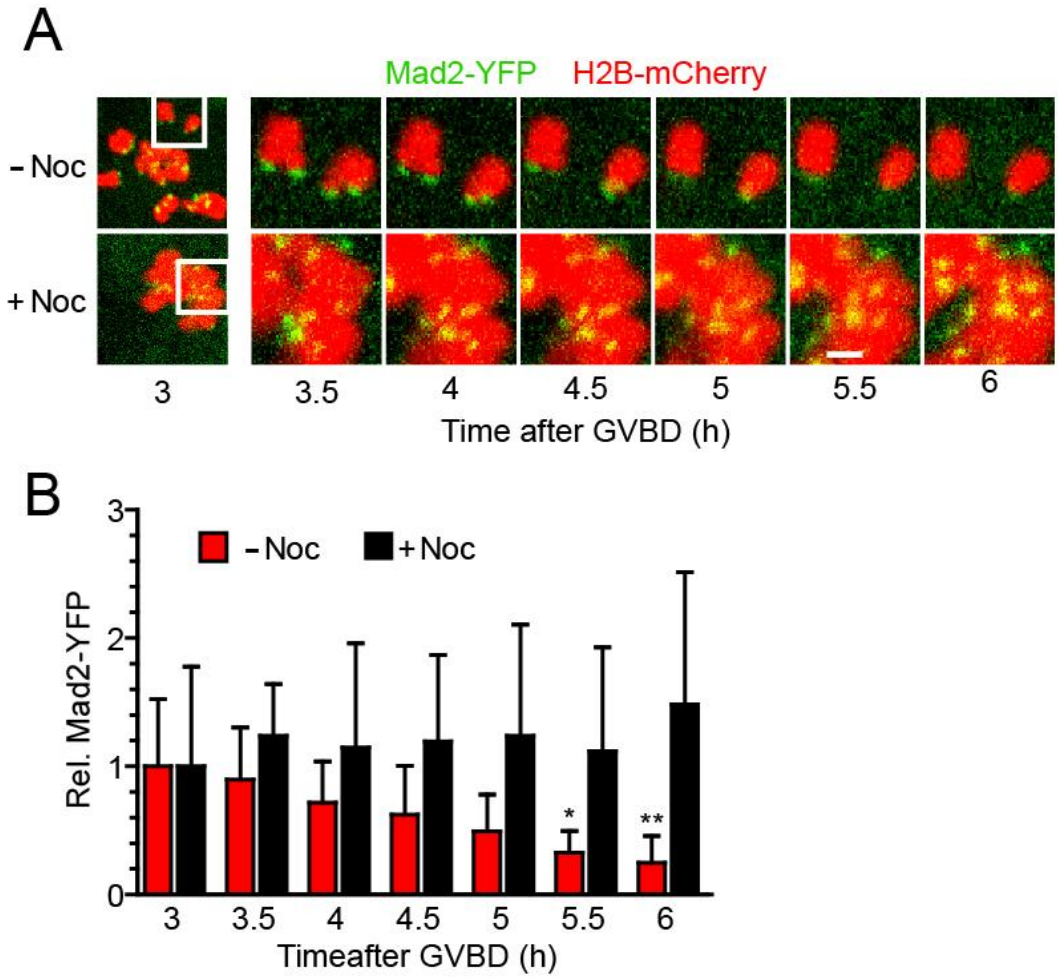

Figure 3.9 - Loss of Mad2-YFP from chromosomes during prometaphase I.

*(A) Representative timelapse images of oocytes microinjected with mRNA encoding for Mad2-YFP and H2B-mCherry and matured with or without nocodazole (400nM). Z-projections from 3D confocal microscopy are shown of the Mad2-YFP (green) on the chromosomes (red) at the times indicated after GVBD. The first image shows all the chromosomes whilst subsequent images follow the chromosomes in the indicated region (white box). n=4 per group, Scale bar represents 1µm. (B) Quantification of the YFP signal from the chromosomes such as those in 'A' n=10-16 per timepoint. Values are relative to the signal at 3 h. *P<0.05, **P<0.01, ANOVA with Tukey's Multiple Comparison Test.*

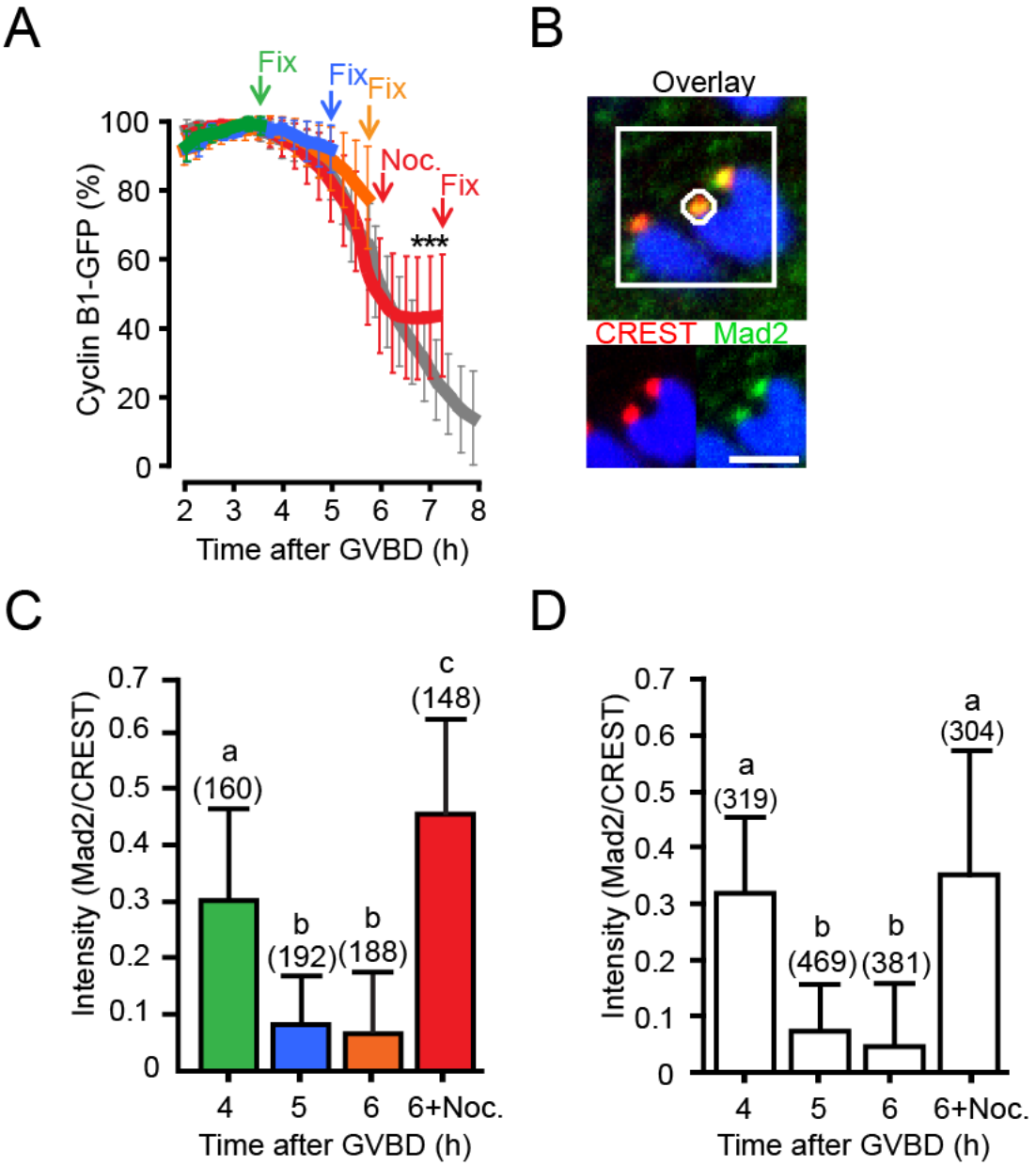

Figure 3.10 - Loss of endogenous Mad2 from kinetochores is coincident with APC activation.

(A) Changes in fluorescence of oocytes expressing cyclin B1-GFP recorded during prometaphase. Groups of oocytes (n=5) were removed from the microscope stage and fixed at the times indicated. Traces are normalized with maxima at 100%. Asterisks indicate significant difference (P<0.02) compared to controls in a separate experiment where no nocodazole was added. (B) Fixed oocytes were fluorescently labelled for

chromatin (blue), CREST (red) and Mad2 (green). The white circle (diameter=12 pixels) was used to define the kinetochore and the white square (width=90 pixels) was used to define the background. Scale bar represents 2µm. (C) For each group of oocytes Mad2/CREST was calculated after respective background subtraction using the areas shown in 'B'. The coloured bars correspond to the curves shown in 'A'. (D) The experiment shown in 'A-C' was repeated, but without injection of cyclin B1-GFP mRNA. (C-D) a,b,c indicate significant difference between groups, P<0.001. Numbers of kinetochores analyzed are shown in parenthesis.

(CREST) and anti-Mad2 antibodies. They were imaged by confocal microscopy using the same acquisition parameters on the same day so that no change in fluorescence was introduced into any group. Using an ImageJ macro the kinetochores from each oocyte were analysed (See Methods Section 2.12.1) such that the signal intensity for Mad2 and CREST was recorded and a background reading was subtracted (Figure 3.10 B). A Mad2/CREST ratio for each kinetochore was then calculated (Figure 3.10 C). A significant drop in this ratio was seen between 4 and 5 h (4 h, 0.30±0.18, n=160; 5 h, 0.08±0.07, n=192; P<0.001) but no further significant drop was witnessed between 5 and 6 h. Mad2 levels could be restored upon addition of nocodazole and reached levels significantly higher than at 6 h (6 h, 0.07±0.09, n=188; nocodazole, 0.45±0.25, n=148; P<0.001). If the experiment was repeated, but without prior injection of cyclin B1-GFP, the results were very similar, showing a significant drop in kinetochore bound Mad2 between 4 and 5 h (4 h, 0.32±0.15, n=320; 5 h, 0.07±0.07, n=469; P<0.001, Figure 3.10 D). Therefore, I conclude that the injection of cyclin B1-GPF was not affecting the timing of loss of Mad2 from the kinetochores. In addition, injection of this concentration of cyclin B1-GFP did not change the timing of PBE (Figure 3.8 B) and so both the readout of cyclin B1 levels (APC activity) and loss of kinetochore Mad2 (SAC activity) were taken as being reliable. Given this, it was possible to conclude that between 4 and 5 h, the switching off of the SAC, as measured by the loss of Mad2 from kinetochores was coincident with the activation of the APC, measured as the start of cyclin B1-GFP degradation.

Taken together, the above data suggest that at around 4-5 h, microtubule attachments form that are sufficient to remove Mad2 from kinetochores. However removal of Mad2 from kinetochores is associated with attachment and not necessarily the generation of tension (Skoufias et al., 2001). Therefore, it is not clear from these data alone whether these k-fibre positive, Mad2 negative, bivalents are under tension. The earlier measurements of inter-kinetochore distances however do suggest that these initial attachments don't add tension, as no significant increase in inter-kinetochore distance was observed between 4 and 5 h (Figure 3.2 B). In summary however, regardless of the extent to which tension is generated, the attachment of microtubules to bivalents established by 5 h appears sufficient to activate the APC. In oocytes there is therefore a large disparity between the time of APC activation and anaphase onset, amounting to around 3 h (APC activation and anaphase being 5 and 8 h respectively).

3.3 MOVIE FIGURE LEGENDS

Movie 3.1 Live cyclin B1-Venus degradation.

An oocyte injected with mRNA encoding for cyclin B1-Venus was imaged using the Biostation IM inverted microscope. Brightfield (left) and fluorescent (right) images are shown at 15 min intervals throughout maturation The time relative to GVBD is indicated (hh:mm). At 00:00 an influx of cyclin B1-Venus is seen into the nucleus followed by the disappearance of the nucleolus and germinal vesicle at 00:15, marking the completion of GVBD. Cyclin B1 can be seen to concentrate slightly on the spindle during maturation and then to decline in intensity prior to PBE (08:15).

3.4 DISCUSSION

The long duration of meiosis I, with its unique function in separating homologous chromosomes as opposed to sister chromatids, sets it apart from the typical somatic division. Given its extraordinary length I wanted to establish the timing of the major cell division events including the formation of the MI spindle, the attachment of the chromosomes to the spindle and the subsequent separation of the chromosomes. In addition I sought to put the timing of these more obvious morphological events into the context of the major cytoplasmic activities that occur during a cell cycle, such as the activity of the SAC and of its target the APC. It seems reasonable to assume that the regulation of MI may differ from that of somatic cells, but the mechanisms and proteins involved remain mostly the same. This makes the regulation of meiosis I interesting as these subtle differences may account for why this particular division often takes place in an error-prone fashion.

The main findings of this chapter were that the timing of microtubule attachment coincides with that of loss of Mad2 from kinetochores and also with the activation of the APC. These events take place ~3 h before anaphase. In addition, it was shown that bivalents can achieve a large degree of congression, stretch and align perpendicular to the spindle equator prior to the formation of the first k-fibres.

3.4.1 INITIAL SPINDLE FORMATION AND BIVALENT ORGANISATION

Examining the timing of the major events in spindle formation allowed four distinct periods to be defined. The first period is discussed here, and subsequent periods in

later sections, in addition these periods are summarised in Figure 3.11. During the first period from 0 to 2 h a spindle formed, but this spindle was not bipolar, and instead had similar length and width. This is likely due to the clustering of microtubule organizing centres (MTOCS) and formation of an apolar microtubule ball amongst the chromosomes reported elsewhere (Brunet and Maro, 2005; Schuh and Ellenberg, 2007). The bivalents within this early spindle were not under tension as judged by the close association of their two sister kinetochore pairs. Measurements of the θ values of the bivalents revealed there was a large variation in direction between bivalents, consistent with there being no spindle poles to bi-orientate between. Bivalent alignment was also poor, in agreement with there being no spindle axis along which the bivalents could congress. This arrangement is thought to result from the outward movement of the bivalents driven by microtubules emanating from the microtubule ball that establishes following GVBD (Calarco et al., 1972; Schuh and Ellenberg, 2007). This arrangement has also been termed a 'rosette' (Viveiros et al., 2004), and is established after individualization of the bivalents following their release from the nucleus at GVBD (Schuh and Ellenberg, 2007).

3.4.2 SPINDLE POLARISATION AND BIVALENT ALIGNMENT, ORIENTATION AND STRETCHING.

During the second period, between 2 and 4 h, there were changes evident in both the spindle and the bivalents. The microtubules developed a spindle shape by elongating in one direction, therefore establishing the direction in which bivalents should orientate. The process of spindle elongation, transforming a microtubule ball with centrally located MTOCS to a highly polarized structure with one distinct MTOC cluster at each pole has been demonstrated to be driven by the motor protein Kinesin 5 (Schuh and Ellenberg, 2007). In addition, other proteins are required for this process of polarization including Aurora Kinase A (Ding et al., 2011), HURP (Breuer et al., 2010), p38α (Ou et al., 2010), Nek2, centrobin (Sonn et al., 2010), NEDD1 (Ma et al., 2010) and PKCδ (Ma et al., 2008). Interestingly the bivalents themselves may not be essential for the process of MTOC re-arrangement and bipolar spindle formation in mouse oocytes as a bipolar spindle can form in their absence (Brunet et al., 1998). During this 2-4 h period the spindle reaches its mature size, as no further significant changes are seen at later timepoints.

An interesting feature of the bivalents at this time was that their kinetochore pairs attain a high degree of separation, a 2.5 fold increase between 2 and 4 h. They also showed greater alignment and θ, making the bivalents appear more similar to those seen later at 5 or 6 h than to those at the earlier time of 2 h. The reason this is of particular interest because no stable k-fibres were observed at 4 h. Given then that bivalents appear to achieve bi-orientation and alignment prior to the attachment of stable k-fibres it seems reasonable to assume that other mechanisms may be at work. In *C. elegans* oocytes bivalents also align and bi-orientate in the absence of k-fibres by recruiting the KLP-19 motor protein (Wignall and Villeneuve, 2009). This pushes bivalents to the spindle mid-zone using microtubules that run alongside them but crucially do not connect with their kinetochores. Non-kinetochore microtubules have also been shown to have an important role in chromosome movement during anaphase I of *C. elegans* oocytes (Dumont et al., 2010) and in anaphase II of mouse oocytes (Deng et al., 2009). It is worth noting therefore that other mechanisms beside those centring on microtubule-kinetochore attachment can be considered. In human somatic cells congression of non-aligned chromosomes is thought to be achieved by sliding along k-fibres belonging to sister chromatids that are already aligned utilizing the motor protein Cenp-E (Cai et al., 2009; Kapoor et al., 2006). If this same mechanism exists in mouse oocytes it could possibly be utilized by non-aligned bivalents to align after the formation of k-fibres on other bivalents (5 h). However, it seems less likely to account for the large degree of alignment observed here in mouse oocytes before any k-fibre formation has been established at 4 h. One possibility is weaker lateral or transient attachments, that are not stable after Ca^{2+} treatment, are sufficient for congression and alignment, and are later converted into more stable kinetochore attachments. This conversion has been demonstrated in yeast, where depolymerisation of microtubules converts lateral to end-on attachment (Maure et al., 2011; Tanaka et al., 2007). This process likely involves the kinetochore protein Dam1. Whether a similar conversion of lateral to end-on attachment can occur in higher eukaryotes, which have no apparent Dam1 homolog is still an open question.

3.4.3 THE TIMING OF K-FIBRE FORMATION, SAC SATISFACTION AND APC ACTIVATION IN MEIOSIS I.

The third period of meiosis I occurred between 4 and 5 h. At this time k-fibres formed, the abundance of the SAC protein Mad2 declined on kinetochores, and the activation

of the APC commenced. The kinetochore attachments however were not necessarily correct with many forming attachments to both poles. Kitajima et al., (2011) demonstrated that bivalents require an average of three attempts to achieve their final bi-orientation state, therefore these initial attachments may be either incorrect, or are readily de-stabilised. Nonetheless, coincident with the formation of the k-fibres, Mad2 levels declined on kinetochores and the APC became activated, suggesting that the SAC is satisfied and sets in motion the events leading to anaphase.

Two other groups have published findings confirmatory to mine on the formation of stable k-fibres during this period of prometaphase in mouse oocytes since I undertook this work. In one study, k-fibres were found to form at 4 h (Hached et al., 2011). In the other k-fibres were observed to change as meiosis I progressed; from as early as 1 h merotelic or lateral attachments were present and by 3 h a small number of amphitelic connections were observed. The proportion of correct k-fibre attachments grew as meiosis progressed, constituting the majority by 5 h (Kitajima et al., 2011). These differences in timing of stable k-fibre formation could be due to the different strains of mice used in the three studies, and also in differences in the sensitivity of the microtubule preserving approach. For instance, in my study stable microtubules appeared quickly between 4 and 5 h, as they did in the study by Hached et al. prior to 4 h. However, in the study by Kitajima et al., calcium stable microtubules were observed at all timepoints. These stable microtubules were also seen radiating out from the spindle into the cytoplasm, even shortly after GVBD, and did not appear to connect kinetochores suggesting that the treatment and fixation method may have preserved laterally-attaching and non-attaching microtubules. An earlier study utilizing electron microscopy to examine microtubule-kinetochore interactions concluded that stable k-fibres did not interact with kinetochores during mid-prometaphase, but did so later in metaphase, within one hour of anaphase (Brunet et al., 1999).

It was important in this study to establish the timing of Mad2 loss from kinetochores alongside the timing of APC activation, as this could help resolve the proposed timing of k-fibre formation. However, it is important to note that although loss of Mad2 is commonly regarded as a readout of proper microtubule attachment (Skoufias et al., 2001), this may not necessarily be the case during meiosis I where the kinetochore unit has a different architecture. It remains possible for instance, that lateral attachment of microtubules and kinetochores causes the loss of Mad2 in mid-prometaphase

observed in this study and in others (Hached et al., 2011; Kitajima et al., 2011). These same lateral attachments may be preserved by the cold- and calcium treatment and represent the fibres which sufficiently satisfy the spindle checkpoint and translate into APC activation. In this case, it is possible that the attachments witnessed by Brunet et al. (1999), in metaphase were the final end-on attachments, but not the initial attachments that were sufficient for activation of the APC. Importantly, whether the stable microtubules shown in mid-prometaphase represent lateral attachments or otherwise it is these attachments that lead to SAC satisfaction. The current study shows in both live and fixed oocytes that loss of Mad2 occurred in mid meiosis I, with data from fixed oocytes pinning the timing between 4 and 5 h.

Previous reports had shown Mad2 loss during maturation on fixed oocytes (Hached et al., 2011; Wassmann et al., 2003) and in one live oocyte (Kitajima et al., 2011). Hached et al., (2011) stated that k-fibre formation and Mad2 loss occurred around 4 h, but no direct evidence was presented to show this. It would be interesting to see how the k-fibres present in mid-prometaphase (this study, Kitajima et al., 2011 and Hached et al., 2011) which are sufficient for loss of Mad2 from kinetochores would appear by detailed electron microscopy as studied by Brunet et al., (1999).

Regardless of the precise nature of the kinetochore-microtubule attachments at 5 h, it appears that they are sufficient to inactivate the SAC and permit APC activity. This was observed by both cyclin B1 fluorescent chimera destruction in live cells and by the loss of endogenous protein in synchronised samples commencing concurrently with formation of the stable k-fibres. The results in this chapter do not prove that the SAC is completely satisfied at this time, only that it is sufficiently satisfied to permit activation of the APC. It is important to make a distinction between the two. It is often assumed that because of early pioneering work demonstrating that attachment of the last kinetochore is a prerequisite for anaphase (Rieder et al., 1995) that the SAC is an efficient on/off switch for the APC. This may hold true for somatic cells, but has not yet been proven in oocytes. In fact evidence is accumulating to the contrary and this point will be discussed further in chapter 4.

3.4.4 CYCLIN B1 DESTRUCTION AND EXIT FROM MEIOSIS I

Finally, the fourth period of meiosis I is characterised by a gradual decline in the levels of cyclin B1 between 5 and 8 h. Although securin degradation was not examined here,

it has been shown in several studies to be degraded with the same timing as cyclin B1 (Homer et al., 2005a; Homer et al., 2005b; Niault et al., 2007; Reis et al., 2007). During this time there are modest improvements in chromosome alignment, orientation and inter-kinetochore distances. Additionally Mad2 levels on kinetochores decline, but not significantly, between 5 and 6 h. The main feature of this time period is therefore the activity of the APC, which following SAC satisfaction at 5 h appears to act as a timer, counting down towards anaphase at 8 h. This 3 h delay is far longer than that seen in most mitotic divisions in which anaphase follows SAC satisfaction almost immediately (Clute and Pines, 1999; Gavet and Pines, 2010). This makes the fourth period of meiosis quite unique, the regulation of the APC and its significance in oocytes is discussed further in chapter 6.

3.4.5 COMPARING RELATIVE TIMINGS

It is worth noting that the profile of fluorescent cyclin or securin destruction can look quite different in differing strains of mice. For instance, when compared to the F1 strain used in this study, the onset of their destruction is several hours later in the MF1 mice used by Homer et al., (2005), commencing at ~ 8 h, with PBE being 3 h later. It is likely therefore that the same variability exists in the timings of other events during meiosis I such as k-fibre formation and SAC satisfaction. As such the absolute timings of events such as SAC satisfaction and the onset of cyclin B1 destruction should not be compared between strains, but rather the timing of these events should be compared relative to each other within each strain. In the study by Hached et al., (2011), the timing of APC activation is not quoted, but they show securin degradation commencing at ~ 6 h, with PBE at ~ 8-9 h. It would also be of interest to know the timing of cyclin B1 or securin destruction in the mouse strain used in the study by Kitajima et al., (2011).

3.4.6 SUMMARY

Collectively the data presented in this chapter show that meiosis I is characterised by distinct phases (Figure 3.11). In the first period, the initial 2 h of meiosis I following GVBD, a spindle is established, this is followed by spindle elongation and bivalent congression in the second period at 2-4 h. During a third period (4-5 h), stable k-fibres form, and these cause loss of Mad2 from kinetochores sufficient to satisfy the SAC, judged by activation of the APC. The last period of meiosis I is the period following SAC satisfaction, during which the APC degrades cyclin B1 and securin, eventually

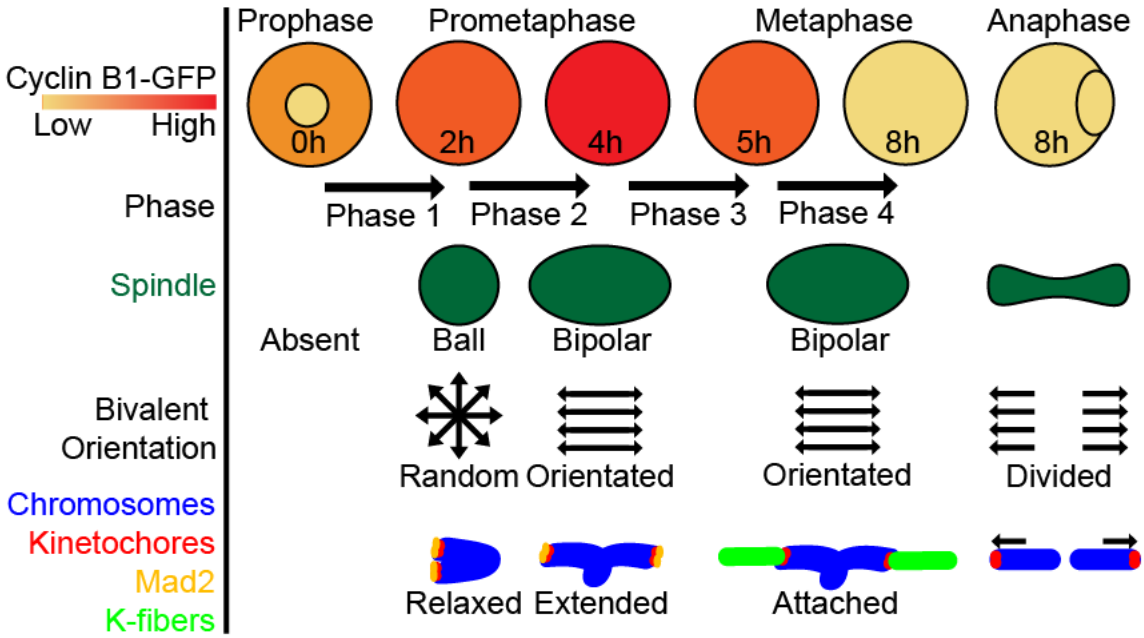

Figure 3.11 - Overview of the timing of events in meiosis I

The timing of many of the events in this chapter are shown relative to each other. Between 2 and 4 hours the spindle elongates, bivalents become orientated perpendicular to the spindle equator, aligned close to the equator and stretched. Between 4 and 5 h stable k-fibres form, Mad2 is lost from kinetochores and APC activity begins. Between 5 and 8 h the cyclin B1 content of the oocyte declines. Finally oocytes undergo anaphase around 8 h.

culminating in anaphase. This unusually long division is likely as a result of the unique needs of the oocyte in faithfully bi-orienting bivalents on an acentriolar spindle.

4 NON-ALIGNED BIVALENTS IN MEIOSIS I

4.1 INTRODUCTION

During the work performed in Chapter 3, it was noticed that in some oocytes not all chromosomes were aligned to the spindle's equatorial plane at the time associated with onset of APC activity. For instance, Figure 3.2 D demonstrates that at 5 and 6 h many chromosomes were a considerable distance from the spindle equator (4-10µm), and Figure 3.3 A shows one such non-aligned chromosome (6h, 4°C). Such occurrences are not restricted to my own work, non-aligned chromosomes can also be seen in mouse oocytes in other studies (Kudo et al., 2006; McGuinness et al., 2009), however these events were not studied in detail in these other works.

I thought the above was an important observation to address because of two related reasons. Firstly, the non-aligned bivalents appeared to be present at times after the onset of APC activity. The implication of this is that the SAC in oocytes may not be sensitive to such displaced chromosomes. This leads to the second reason; given the aneuploidy rate (~2.5%) established in oocytes in this strain of mouse (Figure 5.14), it seemed important to investigate if these non-aligned chromosomes represented a mechanism by which aneuploidy could be generated.

In Chapter 3 it was established that the SAC was satisfied at around 5 h, whilst oocytes did not enter anaphase until 8 h after GVBD. These two events therefore defined the time frame in which I could study non-aligned chromosomes. It is only after SAC satisfaction that non-alignment becomes relevant; earlier in meiosis I the majority of chromosomes would be classed as non-aligned and so it is not surprising that the SAC is active at this time, preventing exit from meiosis I. The investigation into non-alignment was therefore restricted to non-alignment that occurred after the apparent satisfaction of the SAC (or activation of the APC) as this presented the most interesting situation. Why was the SAC permitting APC activation if the oocyte was not ready to enter anaphase?

4.2 RESULTS

4.2.1 NON-ALIGNED CHROMOSOMES ARE A COMMON FEATURE OF METAPHASE I.

I first wanted to establish the prevalence of non-aligned chromosomes. It was important to look for non-alignment during a relevant timeframe, since alignment had been shown to improve with time (Figure 3.2 D). For instance looking at 4 h would no doubt yield many non-aligned chromosomes, however since the SAC is not satisfied at this time and the APC is therefore inactive, this would have no relevance to the generation of aneuploidy. I was therefore only interested in non-alignment that occurred after the activation of the APC, an indication that the SAC had been satisfied. Therefore, oocytes were injected with cyclin B1-Venus mRNA and imaged during maturation until a period of continuous cyclin B1 degradation had been achieved, indicating that the SAC was no longer inhibiting the APC (Figure 4.1 A). At this point cyclin B1-Venus imaging was stopped, Hoechst was added to the media and the oocytes were imaged for chromatin. Since the oocytes had not been moved, it was possible to attribute the chromatin images to individual cyclin B1-Venus traces. It was found that of the oocytes degrading cyclin B1-Venus (n=42, at ~6 h) 43% had chromosomes that were clearly separated from the metaphase plate (Figure 4.1 B).

4.2.2 NON-ALIGNED CHROMOSOMES ARE BIVALENTS

The above data suggested that non-aligned chromosomes were a common feature of meiosis I at times after SAC satisfaction. I next wanted to investigate the nature of the non-aligned chromosomes, starting with the possibility that they were univalents, and not bivalents. This possibility existed because univalents could be derived from prematurely separated bivalents, or univalents that never underwent recombination during prophase. It has been shown in studies on Down Syndrome patients that the origin of the aneuploidy in ~40% of cases is due to there being no recombination between the two copies of chromosome 21, resulting in the presence of two univalents in meiosis I (Lamb et al., 1997a; Lamb et al., 1997b; Lamb et al., 1996). Univalents in meiosis I generated by disruption of the *Sycp3* gene, can interact with the spindle, often becoming bi-orientated (Kouznetsova et al., 2007). Since univalents can be present in MI, and could perceivably be prone to delayed alignment, it seemed

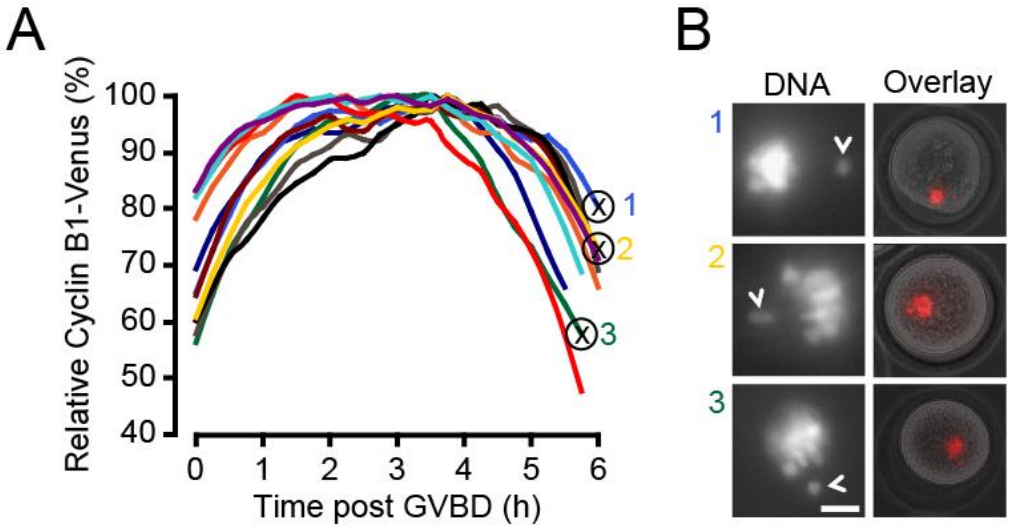

Figure 4.1 - Non aligned chromosomes can be observed following APC activation

(A) Fluorescent traces from oocytes expressing cyclin B1-Venus were normalized with maxima to 100% and plotted against the time after GVBD. (B) Epifluorescent images taken of chromatin from oocytes with corresponding numbers (1-3) in 'A' (left) and whole oocyte brightfield and chromatin overlay (right). Scale bar represents 10µm.

important to establish if the non-aligned chromosomes being observed were univalents or bivalents.

Oocytes were fixed at 5 h and stained for chromatin and CREST before being imaged by confocal microscopy with z-sections 0.5µm apart. This resolution gave a sufficiently detailed view of the kinetochores such that it was possible to determine the nature of the chromosomes. Bivalents would be expected to have a total of 4 kinetochores, which would appear as 2 pairs. Univalents on the other hand would be expected to have just two single kinetochores, relatively close together. In many cases the chromosomes clearly had two very separate kinetochore pairs indicating that they were bivalents (Figure 4.2 A). In other cases the kinetochores had to be more closely examined (Figure 4.2 B-E). In these cases the kinetochore pairs could be distinguished by first applying an outline to one pair (green dashed oval, Figure 4.2 D-E). When the z-section was changed the position of the CREST signal could be seen to change relative to the outline, indicating the presence of two closely positioned kinetochore pairs. In these cases the kinetochores usually occupied around 5 z-sections (2.5µm), which is far greater than is typically occupied by a single kinetochore pair (1-1.5µm). In this way 98% (45/46) of the non-aligned chromosomes were identified as being bivalents with one chromosome being uncertain (Figure 4.2 F).

At this juncture it was necessary to define exactly what constituted a non-aligned bivalent. At advanced times during meiosis I the vast majority of bivalents were found within 4µm of the spindle's equatorial plane (Figure 3.2 D). The definition of non-alignment was therefore established as being bivalents with both kinetochores greater than 4µm from the spindle equator (Figure 4.2 G). Those with one or no kinetochore pairs greater than 4 µm from the spindle equator were considered aligned.

4.2.3 NON-ALIGNED BIVALENTS RECRUIT MAD2

Non-aligned bivalents appeared to be present at a time when the APC was active, this suggested that they were not activating the SAC, or at least not sufficiently to inhibit the APC. I therefore investigated to what extent the non-aligned bivalents recruited Mad2. Synchronised oocytes were fixed at 5 h and stained for Mad2, centromeres and chromatin. As a control, some oocytes were also fixed and stained in parallel but after 30 min treatment with 400nM nocodazole. These two groups of oocytes were then

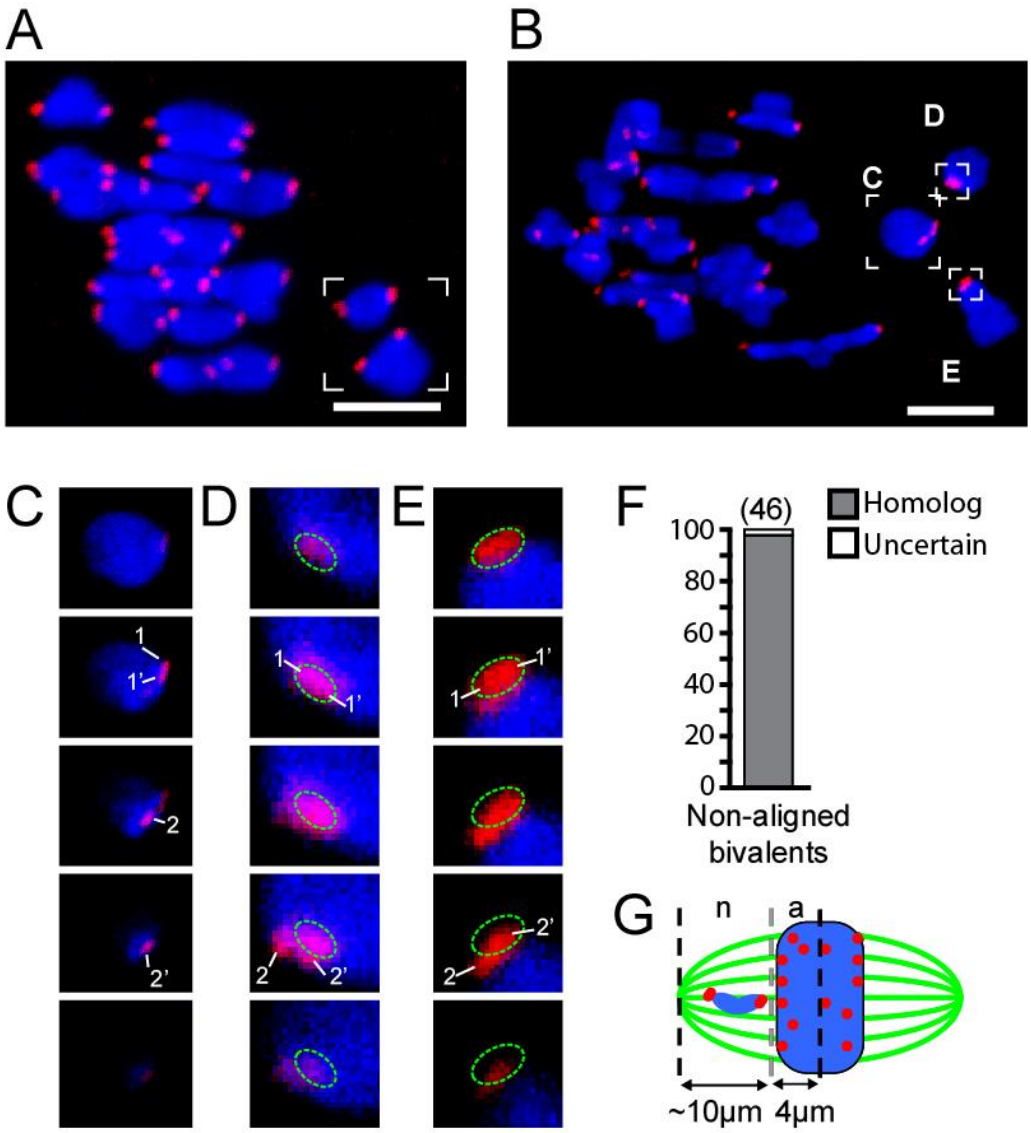

Figure 4.2 - Non-aligned chromosomes are identified as bivalents

(A-E) Fixed oocytes stained for chromatin (blue) and centromeres (red). (A) Whole-oocyte z-projection of an oocyte with non-aligned chromosomes under apparent tension (white boxes). (B) Whole-oocyte z-projection of an oocyte with non-aligned chromosomes in a relaxed form (white boxes). (C-E) individual confocal sections (spaced by 0.5 µm) of the chromosomes indicated by white letters 'C', 'D' and 'E' in figure part 'B'. Green circles show the position of the first sister kinetochore pair. Numbers refer to individual kinetochores (F) Percentage of non-aligned chromosomes identified as bivalents.(G) Non-aligned chromosomes were defined as those with both kinetochore pairs greater than 4µm from the spindle equator 'n' and all other chromosomes were considered to be aligned 'a'.

imaged by confocal microscopy, using the same acquisition parameters throughout to make comparison of Mad2 levels possible.

Analysis of the Mad2 intensity on the kinetochores of non-aligned bivalents, aligned bivalents and those in nocodazole treated oocytes was then performed utilising the same technique used in Figure 3.10. The Mad2/CREST ratios (mean+/-S.D.) on kinetochores of aligned bivalents and on kinetochores in nocodazole treated oocytes were found to be 0.12±0.05 and 0.35±0.10 respectively. These values were comparable with those obtained in previous experiments (5 h, 0.07±0.07; Noc., 0.36±0.23, Figure 3.10 D).

When the kinetochores of non-aligned bivalents were examined they displayed a large range of Mad2 values, some of which were as low as those on aligned bivalents and others that were as high as those in nocodazole treated oocytes. However the mean Mad2 intensity of non-aligned bivalents was found to be significantly different from intensities on both aligned bivalents and those in nocodazole treated oocytes (Non-aligned, 0.16±0.07; $P<0.001$, Tukey's Multiple Comparison Test; Figure 4.3 A). This large range of Mad2 levels prompted me to examine the non-aligned bivalents further. It suggested that non-aligned bivalents might fall into different categories, possibly with some having formed microtubule attachments with correspondingly low Mad2 levels and others having vacant kinetochores, thus attracting more Mad2. In support of this idea, it was evident from examining fixed oocytes that the non-aligned bivalents appeared to be either under tension or in a relaxed state (Figure 4.2 A or B respectively). Bivalents that appeared to be under tension were the ones where the two kinetochore signals were found at opposite ends of the chromatin, and were aligned with the long spindle axis. This was in contrast to bivalents where no tension was apparent; here the kinetochore signals were closer together with the chromatin signal overlapping or to one side.

To test whether the tension across the bivalent correlated with its Mad2/CREST ratio a subset of the oocytes that had been stained for Mad2 and CREST were re-analysed. This time the distance of the bivalent from the equatorial plane was also measured, in addition it was also recorded whether the bivalents appeared to be under tension, for example like those in Figure 4.2 A or in a relaxed form as in Figure 4.2 B. When aligned and non-aligned bivalents were sub-divided on the basis of apparent tension, significant differences were found in the mean amount of Mad2 they recruited. For both

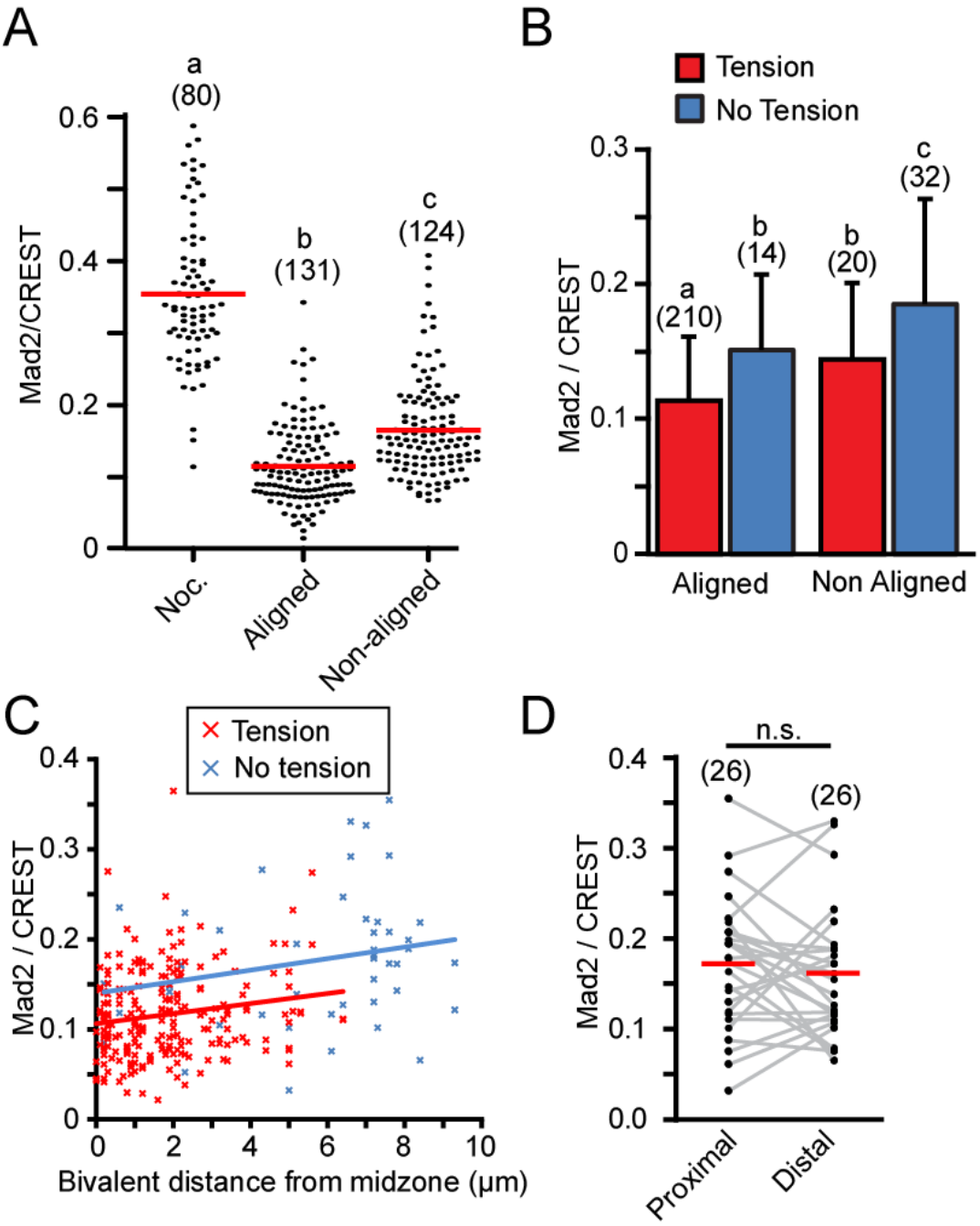

Figure 4.3 - Non-aligned bivalents recruit more Mad2 than aligned bivalents

(A) Mad2/CREST ratio in oocytes treated with or without 400nM nocodazole and fixed at 5 h. Bivalents in oocytes not treated with nocodazole were defined as being either aligned or non-aligned. (B) Mad2/CREST ratios of aligned or non-aligned bivalents, sub-divided into those that appear to be under tension or those that appear relaxed. (C)The same bivalents as in 'B', with Mad2/CREST plotted for each bivalent against its

3

distance from the equatorial plane (D) Comparison of Mad2/CREST ratio between the two kinetochore pairs on the non-aligned bivalents. The kinetochore closer to the pole was denoted as being 'proximal'. (A,D) red lines indicate mean values. (A, C, D) number of bivalents indicated in parenthesis.

aligned and non-aligned bivalents, the presence of tension was associated with less Mad2 on the kinetochore (Aligned: tension, 0.11±0.05; no tension, 0.16±0.06, $P<0.05$; Non-aligned: tension, 0.14±0.06; no tension, 0.18±0.08, $P<0.05$; Tukey's Multiple Comparison Test; Figure 4.3 B).

When Mad2/CREST was plotted against the distance of the bivalents from the spindle equator no correlation (tension $R^2=0.0277$, no tension $R^2=0.0516$) was seen (Figure 4.3 C). However, it could be seen that the appearance of tension across the bivalent was associated with a decrease in Mad2, and this held true for bivalents that were well aligned or those quite distant from the spindle equator.

Finally, I looked for any difference in the Mad2/CREST values between the two kinetochore pairs of a bivalent. If one kinetochore pair recruited more Mad2 than the other this could suggest what type of attachments the non-aligned bivalents had. The kinetochore pair nearest to the spindle pole was termed 'proximal', whilst the other was termed 'distal'. No significant different was seen between the two groups (Proximal, 0.12±0.07, n=26; Distal, 0.11±0.07, n=26; Paired t test; Figure 4.3 D).

Together these data suggest that non-aligned bivalents recruit Mad2 to various extents and that this likely reflects whether the bivalent appears to be under tension or if it is in a relaxed form. These two appearances may be indicative of the microtubule attachments that the non-aligned bivalent has made with the spindle.

4.2.4 NON-ALIGNED BIVALENTS HAVE MICROTUBULE ATTACHMENTS

Loss of Mad2 from kinetochores is temporally coincident with the formation of k-fibres (Chapter 3). Non-aligned bivalents have been shown to have a range of Mad2 levels and to appear under tension or in a relaxed form, suggesting there may also be a variety of attachment statuses. I therefore decided to examine the microtubule-kinetochore attachments on non-aligned bivalents.

Oocytes were fixed following treatment with calcium buffer to preserve the k-fibres, as in Figure 3.5. The oocytes were then stained for tubulin, centromeres and chromatin and imaged by confocal microscopy. When the mean inter-kinetochore distances of the non-aligned bivalents were measured they were found to be significantly different from both aligned bivalents and those in nocodazole treated oocytes (Non-aligned, 4.15±1.55, n=29; Aligned, 5.72±1.56, n=239; Nocodazole, 2.17±0.76, n=33; $P<0.001$,

Tukey's Multiple Comparison Test; Figure 4.4 A). The large range of inter-kinetochore distances reflected a mixture of bivalents that appeared under tension and those that appeared relaxed (Figure 4.4 B).

When tubulin staining was examined on those non-aligned bivalents that could be assessed with a high degree of confidence, the majority of kinetochores were found to be attached to microtubules (22/24, 92%). However when bivalents, as opposed to individual kinetochore pairs were considered, only 7 of 12 non-aligned bivalents were found to be correctly bi-orientated. The remaining 5 bivalents had a variety of attachment errors, such as both sister kinetochore pairs being attached to the same pole (n=1), one kinetochore pair being vacant (n=2), one kinetochore pair attaching to both poles (n=3) or a combination of the above. The mean inter-kinetochore distances of the non-aligned bivalents were found to be significantly greater if the bivalents were bioriented (bioriented, 4.80±0.81, n=7; non-bioriented, 2.83±0.49, n=5; P=0.0007, t test; Figure 4.4 C), and in fact such distances were no different from those achieved by aligned bivalents (Correct, 4.80±0.81, n=7; Aligned, 5.72±1.56, n=239; P>0.05, Dunn's Multiple Comparison Test). In contrast, non-aligned bivalents that were not bioriented had inter-kinetochore distances not significantly different from those observed in nocodazole treated oocytes (Incorrect, 2.83±0.49, n=5; Nocodazole, 2.17±0.76, n=33; P>0.05, Dunn's Multiple Comparison Test).

Finally, Mad2 levels on kinetochore pairs were plotted against inter-kinetochore distance, and separated into two groups (appearance of tension, or no-tension). Both aligned and non-aligned bivalents were included in this analysis. Examination of bivalents that appeared under tension demonstrated that there was a large spread of inter-kinetochore distances (1-7µm), which presumably is a consequence of the large size difference between chromosomes (58-192 Mb, Waterston et al., 2002) and the variation of the position of chiasmata. The same was true of bivalents that did not appear to be under tension. As a consequence of this large variability a bivalent's inter-kinetochore distance did not correlate well with its Mad2 signal (R^2=0.00891, Figure 4.4 D). However, bivalents with apparent tension had consistently lower Mad2/CREST levels than those bivalents lacking tension, and this was true across the range of inter-kinetochore distances. One conclusion that can be drawn from these data therefore is that the appearance of tension across a bivalent is a better predictor of Mad2 recruitment than inter-kinetochore distance is, and this is probably due to the above-

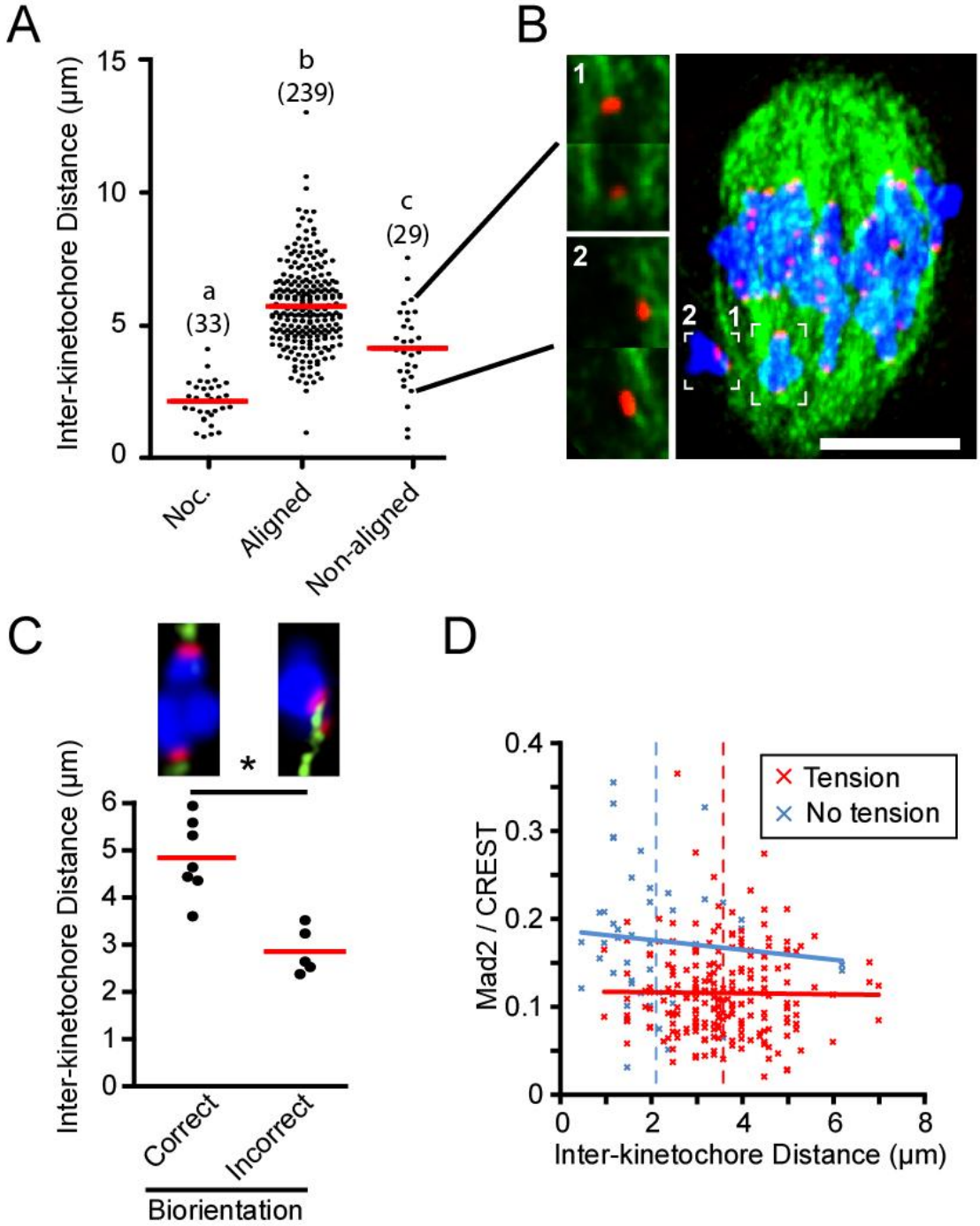

Figure 4.4 - Non-aligned bivalents form microtubule attachments

(A) Inter-kinetochore distances were examined in oocytes treated with or without 400nM nocodazole. The non treatment group was divided into aligned and non-aligned bivalents. Number of bivalents analysed are indicated in parenthesis. (B) Right: A whole z-stack projection of an oocyte fixed following calcium treatment showing tubulin

*(green), centromeres (red) and chromatin (blue). Left: enlarged single confocal z-section images of two non-aligned bivalents (1 and 2 respectively in the image on the right), showing centromeres and tubulin. Black lines indicate to which data point in 'A' those bivalents belong. Scale bar represents 10µm. (C) Inter-kinetochore distances of non-aligned bivalents with correct or incorrect attachments, as judged by their tubulin staining in 'B'. An example of each is shown above. *P=0.0007 (D) Mad2/CREST signal was plotted against Inter-kinetochore distance for aligned and non-aligned bivalents. Bivalents appearing under tension were indicated in red and those appearing relaxed in blue. Solid lines are lines of best fit and dashed lines are mean inter-kinetochore distances. (A,C) Red line indicates mean values.*

mentioned variability in the size of the chromosomes and the random nature of the location of the crossover between homologous chromosomes (Figure 4.4 D).

4.2.5 LIVE IMAGING OF NON-ALIGNED BIVALENTS

The previous data suggested that non-aligned bivalents were likely to be either Mad2 positive and not under tension or to be Mad2 negative and appear taut. This raised the possibility that non-aligned bivalents were in the process of establishing biorientation, before moving back to the spindle equator. The snapshot afforded by fixing oocytes at one particular time could reveal them to be either before or after this process of biorientation, or maybe even transitioning between the two. Therefore to investigate non-alignment further I switched from fixed samples to live imaging.

I injected oocytes with H2B-mCherry mRNA and imaged throughout maturation. The behaviour of the aligned bivalents was examined first. By imaging at 10s intervals it was possible to see aligned bivalents oscillate about the spindle equator with a high frequency (each oscillation lasting around 2-3 min, Movie 4.1). These oscillations, which did not result in any significant displacement of the bivalents from the metaphase plate, were consistent with the chromosome movements reported previously in oocytes (Brunet et al., 1999) and in somatic cells (Jaqaman et al., 2010; Skibbens et al., 1993), and were not the cause of the non-aligned bivalents.

When I looked for non-aligned bivalents they were common, confirming earlier observations (Figure 4.1) and demonstrating that they were not a fixation artefact. When non-aligned bivalents were followed during the timelapse it appeared that in the majority of cases they had never been well aligned to the metaphase plate. However it was not possible to quantify this as the metaphase plate was often poorly defined at earlier times and chromosomes often moved in and out of the focal plane. Oocytes were seen to achieve congression either prior to 5 h (the approximate time of APC activation, Movie 4.2 A) or later than 5 h (Movie 4.2 B).

In order to gain more information on the behaviour of the non-aligned bivalents the kinetochores were imaged in addition to the chromatin. To do this oocytes were injected with CenpC-GFP mRNA, a construct now shown to localise to the centromeres of mouse oocytes (Kitajima et al., 2011), and H2B-mCherry mRNA. Oocytes were imaged during the latter half of maturation by 3D confocal microscopy at ~90s intervals.

Nine non-aligned bivalents were found by such imaging in 12 oocytes, and a representative one is shown in Figure 4.5 A. This non-aligned bivalent was seen to traverse the spindle midzone moving towards the top of the field of view prior to the first frame shown. In frames 1 and 2 both kinetochores of the non-aligned bivalent (arrows) are facing towards the same pole; the bivalent has a low inter-kinetochore distance and is moving away from the spindle equator (Figure 4.5 A, B). During frames 3-6 the bivalent is relatively stationary neither moving away from or toward the spindle equator and the inter-kinetochore distance doubles from ~1-2µm with the kinetochores separating along the spindle axis. In frame 6 the kinetochores appear to face towards opposite poles such that the chromatin lies in-between the two kinetochore signals. Following this the bivalent then moves back towards the spindle midzone, while the inter-kinetochore distance continues to increase to its maximum (frames 7-8). In the subsequent frames (not shown) the bivalent then oscillates on the spindle equator with the same behaviour as the other bivalents that were always aligned there. For the full image sequence see Movie 4.3.

4.2.6 NON-ALIGNED BIVALENTS DO NOT INHIBIT THE APC.

In Figure 4.1 non-aligned bivalents were observed after activation of the APC. The SAC did appear to be sensitive to non-aligned bivalents, as Mad2 levels were higher on non-aligned than on aligned bivalents (Figure 4.3 A). I therefore wanted to test if this increased level of Mad2 produced a sufficient SAC signal to inhibit the APC at all.

Firstly, I examined the timing of anaphase comparing oocytes with or without non-aligned bivalents. The reason for this was that any delay in APC activity brought about by SAC activity should manifest as a delay in anaphase-onset. Oocytes were injected with H2B-mCherry mRNA and imaged for brightfield and H2B from GVBD onwards. The timing of anaphase was calculated and H2B images were examined from 5 h onwards, the time throughout which the APC is active. During this time oocytes were categorised as either having only aligned bivalents, or having at least one non-aligned bivalent that persisted for at least one hour. Interestingly, the mean timing of anaphase was not significantly different between the two groups (Aligned, 8.26±1.06, n=23; Not aligned, 8.25±0.99, n=18; P=0.9745, unpaired t test; Figure 4.6 A-B, Movie 4.4), suggesting the presence of non-aligned bivalents has little impact on APC activity. Secondly I investigated the activity of the APC more directly by looking at the

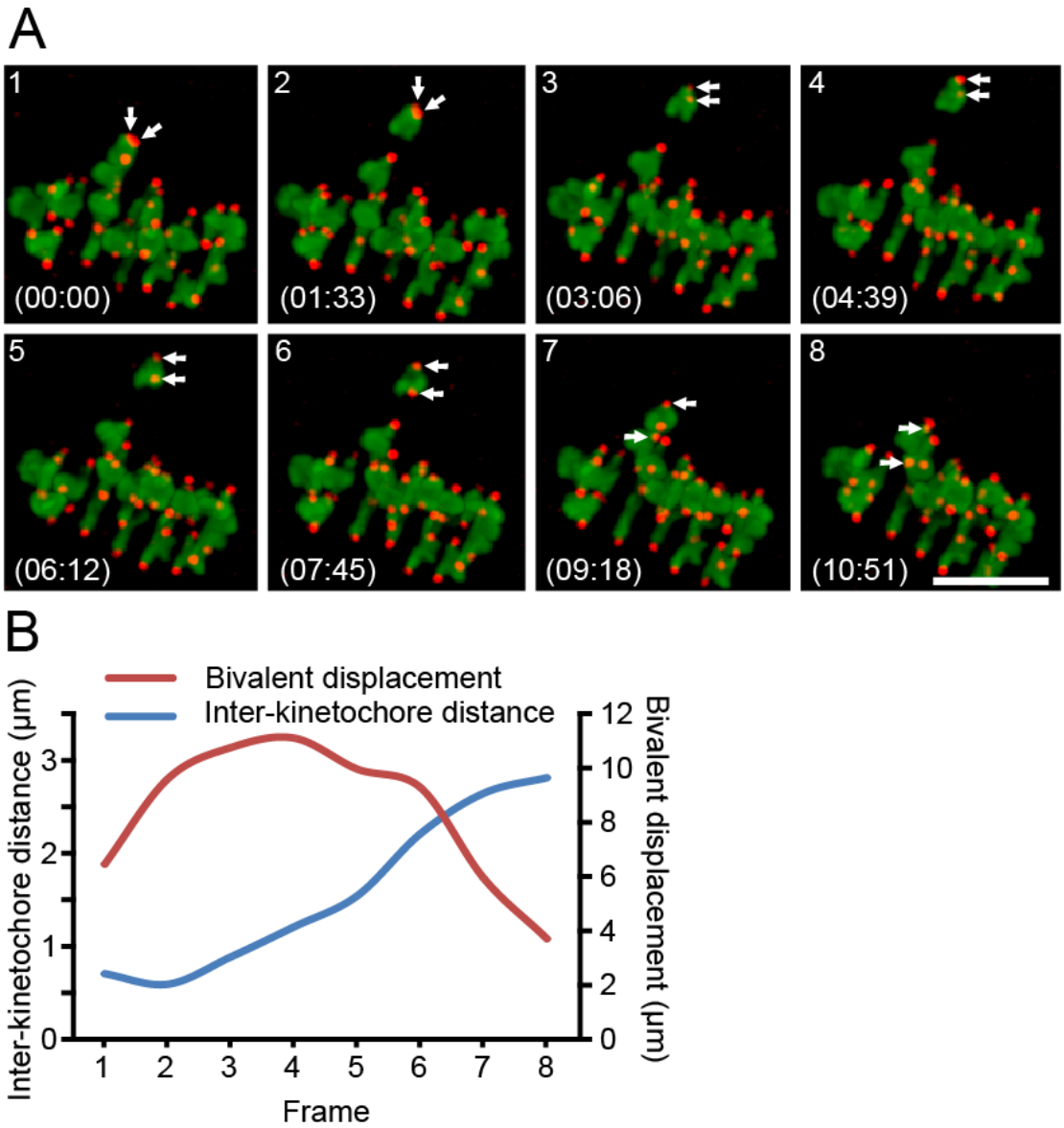

Figure 4.5 - Live imaging of a non-aligned bivalent using CenpC-EGFP to visualise kinetochores.

(A) z-projections of a metaphase plate with one non-aligned bivalent. H2B-mCherry is shown in green and CenpC-EGFP in red. The kinetochores of the bivalent of interest are indicated by arrows. Times shown are mm:ss relative to the first frame shown and the scale bar represents 10µm. (B) Measurements made on the non-aligned bivalent (white arrows) from 'A' are plotted against the frame number. Inter-kinetochore distance is the distance between the two sister kinetochores pairs, and the bivalent displacement is the distance from the midpoint of the two kinetochores to the equatorial plane, which is calculated based on the orientation and position of all the kinetochores.

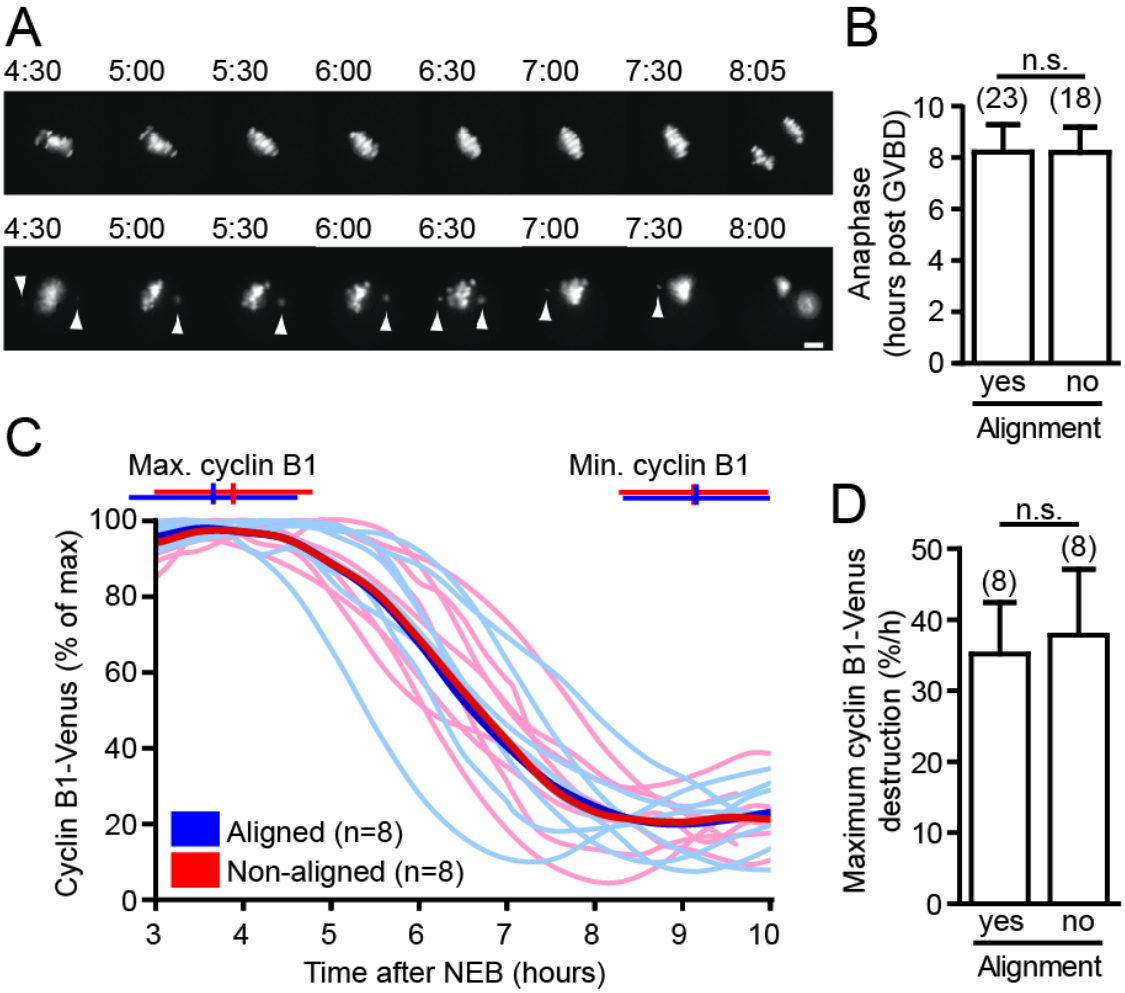

Figure 4.6 - Non-aligned bivalents do not delay anaphase

(A) Typical examples of oocytes having only aligned bivalents (top) or at least one non-aligned bivalent persisting ≥1h (bottom row, arrowhead) during the imaging of H2B-mCherry. Scale bar represents 5 µm. Times (h:mm) are relative to GVBD. (B) The timing of anaphase relative to GVBD in oocytes with or without non-aligned bivalents. (n.s. P=0.9745). (C) Cyclin B1 traces from oocytes expressing cyclin B1-Venus (% of maximum). Oocytes with non-aligned bivalents are shown in red and those only with aligned bivalents in blue. Bold lines indicate mean values. The bars above the traces indicate the mean and S.D. of the time of maximum and minimum cyclin B1-Venus levels. (D) Maximum cyclin B1-Venus destruction rate (mean and S.D.) observed from the oocytes imaged in (C); n.s., P=0.5276. (B,C,D) All error bars represent one standard deviation. Number of oocytes analysed are indicated in parenthesis.

degradation characteristics of cyclin B1-Venus. Oocytes were injected with H2B-mCherry and cyclin B1-Venus mRNA and imaged for brightfield, H2B and cyclin B1 throughout maturation. The same categorisation of oocytes as above was adopted in terms of aligned versus non-aligned bivalents. Figure 4.6 C shows the individual traces of the oocytes from each group (pale colours) as well as the mean values (bold lines). No difference between the two groups was apparent. Comparison of the timing of maximum and minimum cyclin B1-Venus levels also revealed no significant differences (Maximum: Aligned, 3.65±0.95h, n=8; Not aligned, 3.88±0.90h, n=8; P=0.6260, unpaired t test. Minimum: Aligned, 9.16±0.83h, n=8; Not aligned, 9.12±0.85h, n=8; P=0.9417, unpaired t test). Finally, there was also no significant difference in the maximum rate of cyclin B1-Venus destruction achieved in either group (Aligned, 35.17±7.25%/h, n=8; Not Aligned, 37.86±9.28%/h, n=8; P=0.5276, unpaired t test; Figure 4.6 D).

Together these data suggest that non-aligned bivalents, do not manage to significantly alter the activity of the APC or the timing of anaphase, despite the earlier observations that they can have elevated levels of Mad2.

4.2.7 THE FATE OF NON-ALIGNED BIVALENTS

Having established that the non-aligned bivalents fail to delay anaphase it seemed important to also determine their fate during the first meiotic division. If they cannot activate the SAC enough to inhibit the APC then presumably anaphase is no longer coupled to chromosome alignment, raising the possibility that oocytes could undergo anaphase with some bivalents still non-aligned.

Oocytes were injected with both H2B-mCherry and cyclin B1-Venus and imaged by either inverted or confocal microscopy for the duration of meiosis I. When non-aligned bivalents were followed, they were often found to remain non-aligned only transiently, quickly aligning on the metaphase plate and becoming indistinguishable from the other chromosomes. However in some cases the non-aligned bivalent persisted for much longer periods of time (For examples of each, see Movie 4.4 and Movie 4.5). Figure 4.7A shows one such bivalent, indicated by an arrowhead, is present at the time the APC becomes active, at around 5 h and (possibly the same bivalent) is also clearly still

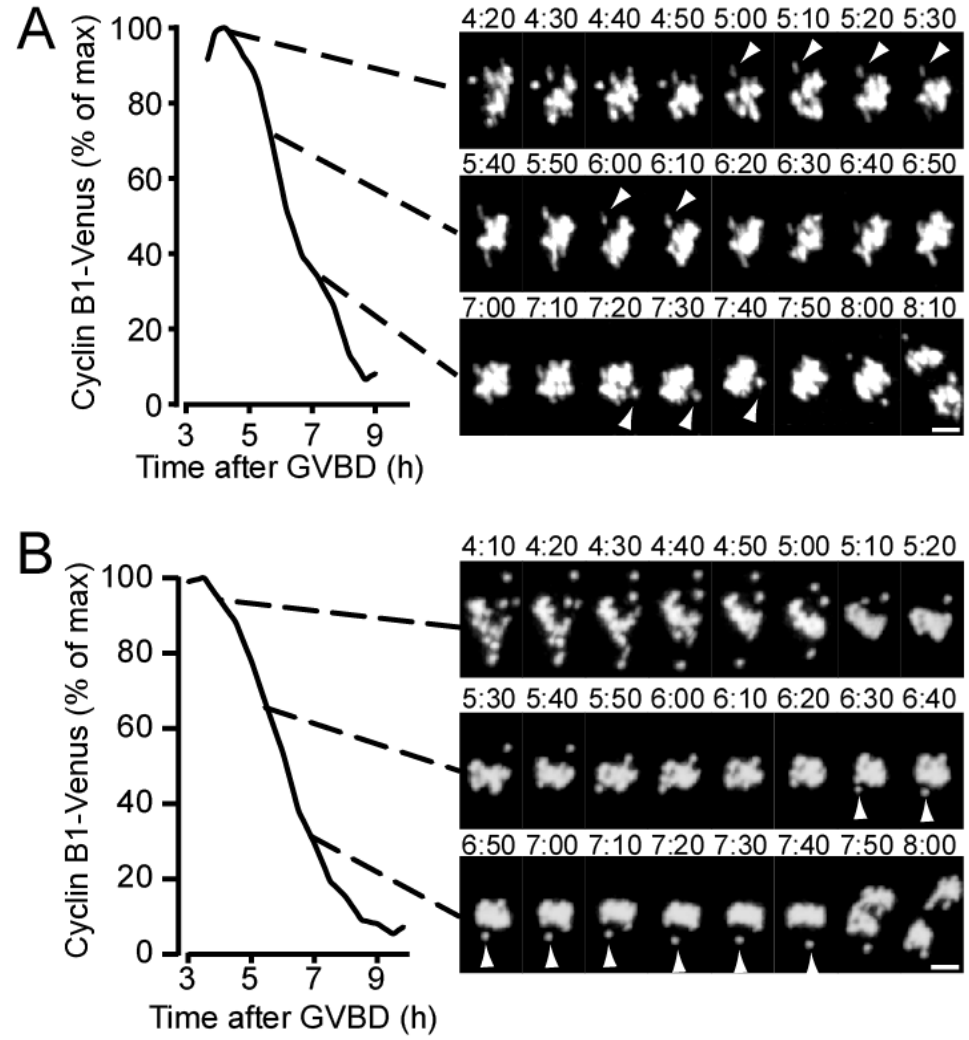

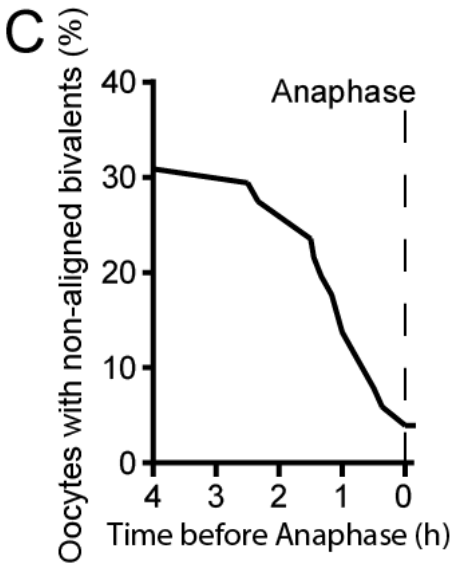

Figure 4.7 - Non-aligned bivalents can persist until anaphase and result in non-disjunction.

(A, B) Oocytes expressing H2B-mCherry and cyclin B1-Venus were imaged through MI. Cyclin B1-Venus is expressed as a percentage of the maximum fluorescence, and plotted against time after GVBD (left) and the corresponding H2B images are shown (right) with time stamps (hh:mm). Arrowheads indicate non-aligned bivalents. (C) The percentage of oocytes with non-aligned bivalents relative to the time before anaphase (dashed line).

non-aligned at later times from 7:20 to 7:40. The bivalent then appears to align at 7:50, shortly before anaphase which was timed at 8:10. During this process the cyclin B1-Venus degradation was continuous, confirming that the APC was not sensitive to this non-aligned bivalent. In this case the oocyte may have aligned its bivalents just before anaphase (Timelapse shown in Movie 4.7, see Movie 4.6 for an oocyte with no non-alignment). In a second example, shown in Figure 4.7 B, a non-aligned bivalent is visible from 6:30 onwards and persists through anaphase. In what appears to be a non-disjunction event, the bivalent moves into the polar body without undergoing segregation. Again, in this oocyte cyclin B1-Venus degradation was un-interrupted and anaphase occurred with normal timing, suggesting that this persisting non-aligned bivalent was unable to inhibit the APC (Timelapse shown in Movie 4.8). A total of 52 oocytes were studied in this way and the time at which the last bivalent aligned on the metaphase plate was determined relative to the timing of anaphase. The vast majority of oocytes (~70%) had all their bivalents aligned three hours prior to anaphase, a time corresponding approximately with 5 h after GVBD, the normal time of APC activation (Figure 4.7 C). The remaining oocytes managed to align all their bivalents during the final three hours with the exception of 2 oocytes (2/52, ~4%) where the non-aligned bivalents apparently underwent non-disjunction as in Figure 4.7 B.

In light of this it seems that oocytes with non-aligned bivalents are unable to delay anaphase significantly, and that they have an approximate three hour window following APC activation in which to properly attach and align all their bivalents on the spindle. Failing to do this, as seen in Figure 4.7 B can result in non-disjunction of bivalents.

4.3 MOVIE FIGURE LEGENDS

Movie 4.1 Aligned bivalents oscillate rapidly on the metaphase plate.

Oocytes injected with H2B-mCherry mRNA were imaged by epifluorescence at 10s intervals. Bivalents were seen to oscillate with high frequency and small displacement about the metaphase plate.

Movie 4.2 Non-alignment is visible by H2B-mCherry epifluorescence.

Oocytes injected with H2B-mCherry mRNA were imaged throughout maturation. (A) Some oocytes aligned all their chromosomes before 5 h. (B) In other oocytes non-alignment persisted after 5 h. (A-B) Time indicates hh:mm post GVBD.

Movie 4.3 Following non-aligned bivalents in 3D with H2B and kinetochore signals.

Oocytes expressing H2B-mCherry (green) and CenpC-EGFP (red) were imaged at 93s intervals from 5 h. A non-aligned bivalent is highlighted in the left image whilst the same images with normal colouration are shown on the right. Time is hh:mm:ss after GVBD and the bar (far left) shows the inter-kinetochore distance of the highlighted bivalent. Arrows indicate the two kinetochores which possibly attach to the same pole at that time.

Movie 4.4 Non-aligned bivalents do not alter the timing of anaphase.

Oocytes expressing H2B-mCherry were imaged during maturation. The timing of anaphase in oocytes in which no non-alignment was observed after 5 h (left) was compared against those in which non-alignment was witnessed after 5 h and which persisted for greater than 1 h (right). Time after GVBD is indicated as hh:mm.

Movie 4.5 Non-aligned bivalents do not alter the timing of anaphase.

Oocytes expressing H2B-mCherry were imaged during maturation. The timing of anaphase in oocytes in which no non-alignment was observed after 5 h (top) was compared against those in which non-alignment was witnessed after 5 h and which persisted for greater than 1 h (bottom). Brightfield (left) and epifluorescent (right) images are shown. Time after GVBD is indicated as hh:mm.

Movie 4.6 Oocyte with no non-alignment.

An oocyte expressing H2B-mCherry and cyclin B1-Venus imaged by confocal microscopy through maturation at 10 min intervals. The brightfield images are in blue, chromatin is shown in red and whole-cell cyclin B1 recordings have been normalized with the maximum value to 100% and are expressed in the green bar (right). Time is indicated in hh:mm after GVBD. This oocyte did not appear to have any non-alignment. Cyclin B1 degradation starts at 4:10.

Movie 4.7 Oocyte with non-alignment.

An oocyte expressing H2B-mCherry and cyclin B1-Venus imaged by confocal microscopy through maturation at 10 min intervals. The brightfield images are in blue, chromatin is shown in red and whole-cell cyclin B1 recordings have been normalized

with the maximum value to 100% and are expressed in the green bar (right). Time is indicated in hh:mm after GVBD. A non-aligned bivalent is present from 4:20-5:10, and another from 5:10-6:30. Cyclin B1 degradation starts at 4:20.

Movie 4.8 Oocyte with non-alignment leading to non-disjunction.

An oocyte expressing H2B-mCherry and cyclin B1-Venus imaged by confocal microscopy through maturation at 10 min intervals. The brightfield images are in blue, chromatin is shown in red and whole-cell cyclin B1 recordings have been normalized with the maximum value to 100% and are expressed in the green bar (right). Time is indicated in hh:mm after GVBD. A non-aligned bivalent is present from 3:40-5:10, and another from 4:30-5:40. What is possibly the same bivalent emerges from the metaphase plate at 6:30 and remains non-aligned until anaphase at 7:50. Cyclin B1 degradation starts at 3:40.

4.4 DISCUSSION

In this chapter the main findings are that non-alignment of bivalents is common in oocytes and that these non-aligned bivalents appear to be in the process of bi-orientating. During this process they may have various incorrect microtubule attachments, and recruit Mad2 to their kinetochores, but this is not sufficient to inhibit the APC. The implications of these findings with regards to aneuploidy in oocytes will be discussed.

4.4.1 NON ALIGNMENT IS A COMMON PHENOMENON IN OOCYTES, BUT NOT SOMATIC CELLS

Studies in somatic cells have shown that APC activation does not occur before the alignment of all chromosomes (Clute and Pines, 1999). Nor does anaphase in either chromosomally stable or unstable cell lines (Thompson and Compton, 2008). Given that the unstable cell lines had wildly varying karyotypes, typically 40-60 chromosomes, mis-segregation of chromosomes was commonplace, however this mis-segregation was never a consequence of non-alignment (instead it typically arises through cells dividing with merotelic attached chromosomes, generating lagging chromosomes at anaphase). This suggests that even in cell lines where the SAC fails to prevent segregation errors, it is still able to delay anaphase until all chromosomes have achieved proper alignment on the metaphase plate. It might therefore be surprising that

non-aligned bivalents are so common in oocytes during a period when the oocyte has committed to anaphase (after APC activation, ~5 h). In the present study the non-aligned bivalents during this period was found in ~30% of oocytes. It is interesting to note that non-aligned bivalents have also been observed in other oocyte studies, although they were not the focus of the respective studies and did not draw comment from the authors (McGuinness et al., 2009; supplementry movie 2, 5.66-9.96 h) (Hached et al., 2011; supplmentary movies 1, 7.5 h and 4, 5.6 h) (Kudo et al., 2006; supplementary movie 1, bottom left, 7 h). It therefore seems that alignment of chromosomes in oocytes is less tightly regulated than in somatic cells.

4.4.2 NON-ALIGNED BIVALENTS, MAD2, TENSION, INTER-KINETOCHORE DISTANCE AND MICROTUBULE ATTACHMENT

Mad2 levels and inter-kinetochore distances of non-aligned bivalents were varied. Most represented those found on aligned bivalents, i.e. Mad2 levels were low and inter-kinetochore stretch was high. However, a smaller number had values tending towards those found in nocodazole treated oocytes. In addition, inter-kinetochore distance appeared to depend on bivalents having correct microtubule attachments. These data gave rise to the hypothesis that non-aligned bivalents were in the process of establishing correct microtubule attachments resulting in a transition from bivalents with lower inter-kinetochore distances and higher Mad2 levels to those with higher inter-kinetochore distances and lower Mad2 levels. It is plausible that initially incorrect attachments caused the non-aligned bivalent to move towards one pole in the first instance, and that following correction of the attachments the bivalent would then move back towards the metaphase plate. It was not possible to test this hypothesis using fixed oocytes however, as the direction in which the bivalent was moving was not evident. It was therefore the examination of live data showing the position of the kinetochores during the alignment of a non-aligned bivalent that appeared to corroborate this idea. An increase in inter-kinetochore distance was seen as the non-aligned bivalents moved back towards the metaphase plate. At this stage the bivalent was assumed to be correctly orientated because a) the two kinetochores faced opposite poles with the chromatin fully between the kinetochores, as would be expected of a bivalent under tension, and b) the bivalent reached the metaphase plate and oscillated in the same way as the bivalents that were already aligned. Data from fixed oocytes showed that an increase in inter-kinetochore distance was also

associated with correct microtubule attachment, adding further weight to the idea that when the bivalents moved back towards the metaphase plate, and their inter-kinetochore distance increased, it was due to having become correctly attached to both spindle poles.

4.4.3 A MODEL FOR CHROMOSOME ALIGNMENT

Based on the data in this chapter a working hypothesis is that initially the bivalent has incorrect attachments as a result of the random nature of microtubule search and capture of kinetochores. This creates a bivalent with one or both kinetochores attaching to a single pole (Figure 4.8). These attachments would be predicted to exert an unbalanced force, moving the bivalent towards that pole. At some point the erroneous microtubule attachments are depolymerised and fresh attachments made, a process known to be dependent on Aurora Kinases (Kitajima et al., 2011). If these new attachments were correct this would cause the two kinetochore pairs to orientate towards opposite poles and the inter-kinetochore distance to increase. Presumably following accumulation of more microtubule attachments, mad2 would be displaced from the kinetochores, reducing observable levels there. A bivalent in such a state may account for those bivalents that are not aligned, yet appear stretched and have lower levels of Mad2, similar to those of aligned bivalents. These non-aligned bivalents, having become correctly attached to both poles may be subject to balanced forces from the microtubules causing them to reach equilibrium at the spindle mid-zone.

4.4.4 NON-ALIGNMENT, APC ACTIVITY AND ANEUPLOIDY

Given that non-aligned bivalents often have incorrect attachments they pose a threat to the ploidy of the oocyte, and potentially the embryo. If the oocyte were to divide without first correcting the erroneous attachments there is a chance the bivalent would segregate intact to one pole. With this in mind, one might expect the oocyte to prevent this by delaying anaphase until the attachments were resolved, as appears to happen faithfully in somatic cells (Thompson and Compton, 2008). Surprisingly this does not appear to be the case in oocytes. No changes were seen in the timing of anaphase or the activity of the APC to suggest that the non-aligned bivalent was exerting an effect. Some non-aligned bivalents did recruit higher levels of Mad2 consistent with that observed following nocodazole treatment, raising the possibility that in oocytes, the SAC signal produced by a single kinetochore is not sufficient to inhibit the APC and

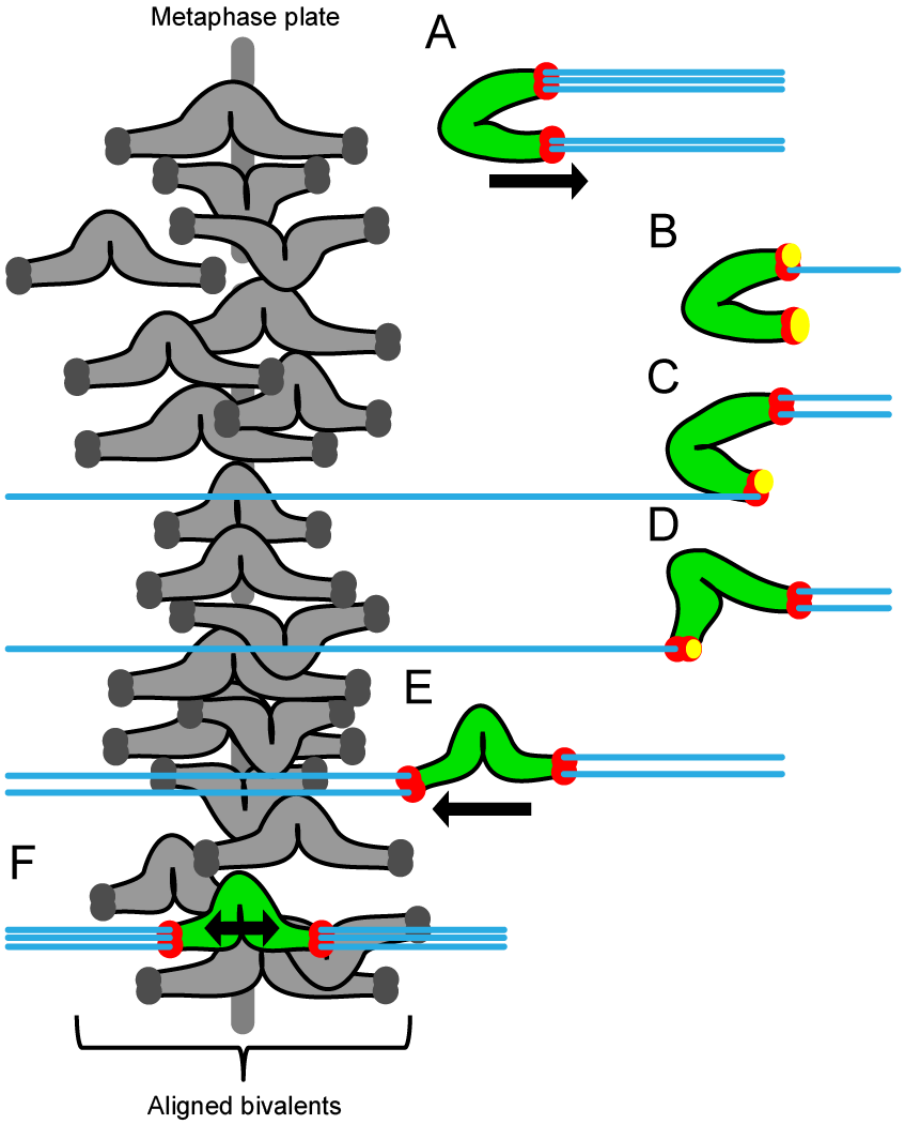

Figure 4.8 - Possible mechanism by which non-aligned bivalents achieve alignment and orientation.

A schematic showing movements (black arrows) of non-aligned bivalents (green) with kinetochores (red), Mad2 (yellow) and microtubules (blue). (A) Non-aligned bivalent moves towards one pole due to unbalanced forces from microtubules. (B) Incorrect attachments are destabilized and kinetochores recruit Mad2. (C-D) New attachments form, inter-kinetochore distance increases and Mad2 levels decline. (E) Microtubule forces are balanced, bivalent bi-orientates and starts moving towards the metaphase plate. (F) Bivalent oscillates on the metaphase plate.

prevent anaphase. A similar conclusion was reached in a study using mice with a high proportion of univalents in MI, where attachment of a majority of the chromosomes was sufficient for anaphase onset (Nagaoka et al., 2011). However, one recent paper suggests that a single bivalent can in fact restrain the APC, at least in an oocyte with half the normal cytoplasmic volume (Hoffmann et al., 2011).

Given that non-alignment does not inhibit the APC in whole oocytes, it is interesting to speculate why. The majority of non-aligned bivalents appear to have k-fibres attaching to both their kinetochores. One possibility then, is that attachment alone is sufficient to satisfy the SAC without a requirement for correct attachments, which can generate tension. There is growing support in mitosis and meiosis for this idea. Firstly, studies of MUG (mitosis with unreplicated genome) cells in which mitosis progresses with only single chromatids, found that cells can exit mitosis without a SAC arrest (Johnson and Wise, 2010; O'Connell et al., 2008). MUG cells also recruit Mad2 in prometaphase and can be arrested by nocodazole, indicative of a functional SAC. However since no tension can be created across sister kinetochores, this suggests that attachment is sufficient to satisfy the SAC. Secondly two studies on tension across sister chromatid pairs found that only intra-kinetochore stretch was required to satisfy the SAC, not inter-kinetochore stretch (Maresca and Salmon, 2009; Uchida et al., 2009). This again suggests that tension across a pair of sisters is not necessary and that attachment is sufficient. Thirdly, growing evidence to favour the ‘attachment is sufficient’ hypothesis is also coming from studies in oocytes. The presence of either a single (LeMaire-Adkins and Hunt, 2000), or multiple univalents (Nagaoka et al., 2011) in MI does not cause a SAC arrest (although this result depends on the stain of mouse studied). A univalent in MI can either bi-orientate, behaving as a pair of sister chromatids would in mitosis or in MII, or it can mono-orientate. There is evidence to suggest that both these scenarios occur, however, what is important is that in some oocytes, there are univalents that are mono-oriented, with both kinetochores attached to one pole, and these univalents fail to activate the SAC.

Returning to the present study, it seems possible then that even if non-aligned bivalents are incorrectly attached and do not appear under tension, that the mere attachment itself is sufficient to satisfy the SAC. However, some kinetochores were vacant and some recruited Mad2 to levels approximating those seen in nocodazole treated oocytes. If some non-aligned bivalents can recruit high levels of Mad2, then

why does this not appear to delay anaphase? Possible explanations are that the Mad2 only exists on the kinetochores transiently as incorrect microtubule attachments are replaced with new attachments. This may in fact delay anaphase, but not enough to cause anaphase to occur outside of the normal spread seen in oocytes with no non-alignment. Another possibility is that the volume of the oocyte, being orders of magnitude greater than a typical somatic cell causes the checkpoint signal to become diluted. In this way it is possible to imagine that the SAC can inhibit the APC easily when all kinetochores recruit Mad2, such as happens at 4 h after GVBD, a time at which the APC is not yet active. However, at 5 h, when only a few kinetochores recruit Mad2 at any one time as they replace their incorrect microtubule attachments, the checkpoint signal is not powerful enough to inhibit all the APCs in the oocyte. Consistent with this is the finding that a single bivalent can delay APC activation in an oocyte with half the normal volume (Hoffmann et al., 2011).

In summary, it remains possible that the oocyte does not respond to non-aligned bivalents as a result of either an ability to recruit enough mad2 to the kinetochores of non-aligned bivalents, or because the SAC signal produced at non-aligned bivalents is insufficient to inhibit APC activity in a whole oocyte volume, or possibly both.

4.4.5 NON-ALIGNMENT AS A RELEVANT MECHANISM FOR GENERATING ANEUPLOIDY

The frequency with which non-aligned bivalents are observed (~30%) make it attractive to speculate that they could be responsible, at least in part for the high aneuploidy rate in mouse oocytes. In the small sample used in this study ~4% of oocytes had a non-disjunction event at anaphase due to a failure to align all bivalents. Although by no means conclusive, this proportion can account for the non-disjunction rate seen in this strain of mouse (2.5%, Figure 5.14 A). This is extremely unlikely to be the sole mechanism by which aneuploidy is generated, but the findings here show that it is a relevant mechanism to consider. This work also shows that regardless of the threat to ploidy, be it a non-aligned bivalent or a univalent, the SAC in oocytes in MI may have inherent weaknesses that prevent it responding to a small number of such problems. This same deficiency in the SAC could also help to exacerbate the increase in aneuploidy seen with maternal age. This increase in aneuploidy has been demonstrated in mice to involve loss of cohesin (Chiang et al., 2010; Lister et al., 2010). It has been suggested by Chiang et al., 2010, that this loss of cohesin could pre-

dispose aged bivalents to making incorrect microtubule attachments as it lessens the restraint that centromeric cohesin normally applies to kinetochore pairs, allowing them to bi-orientate. Given that non-aligned bivalents do not activate the SAC sufficiently to inhibit the APC; it is plausible that other errors involving incorrect attachments in aging oocytes may not do so either.

4.4.6 SUMMARY

In summary, this chapter suggests that in oocytes, although a SAC is present, it does not have the sensitivity of the somatic cell SAC that would allow it to respond to non-alignment of chromosomes. Since non-alignment following APC activation is common this provides one possible mechanism by which non-disjunction evens occur in mouse oocytes.

5 THE EFFECTS OF THE PAN-AURORA INHIBITOR ZM447439 ON MEIOSIS I

5.1 INTRODUCTION

Meiosis I is an error prone cell division, that is unique and highly specialized in many ways (Hunt and Hassold, 2008; Jones, 2008). As discussed in Chapter 4, non-aligned bivalents are a common feature of meiosis I. This, other work (Kitajima et al., 2011) and the high aneuploidy rate resulting from this division suggest that microtubule-kinetochore attachments in meiosis I are seldom initially correct, they take time to finalize, and in some cases fail to be established correctly before the onset of anaphase.

Research in somatic cells has highlighted multiple functions for the Aurora Kinases, with Aurora B in particular having multiple distinct roles as it travels in the CPC. Aurora B regulates both microtubule-kinetochore attachment (Cimini et al., 2006; Knowlton et al., 2006; Liu et al., 2009; Santaguida et al., 2011) and delays anaphase through checkpoint signalling (Cimini et al., 2006; Hauf et al., 2003; Kallio et al., 2002) therefore it is of particular interest in the study of aneuploidy.

Given the high aneuploidy rate generated by oocytes during meiosis I, Aurora Kinase B is of particular interest during this cell division. However, transcripts for an additional Aurora Kinase isoform (Aurora Kinase C) have also been identified in oocytes from humans and mice (Avo Santos et al., 2011; Ding et al., 2011; Shuda et al., 2009; Swain et al., 2008). In these studies Aurora B and C transcripts are found to be present in similar quantities. In somatic cells Aurora C can compensate for loss of Aurora B, indicating potential redundancy (Slattery et al., 2009). Studies of Aurora Kinases in meiosis I have utilized a variety of model organisms, and support the notion that Aurora Kinases are indispensible to the fidelity of meiosis I and proper chromosome segregation (Avo Santos et al., 2011; Ding et al., 2011; George et al., 2006; Sharif et al., 2010; Shuda et al., 2009; Swain et al., 2008; Vogt et al., 2009; Yang et al., 2010). Yang et al., (2010) demonstrate that the role of Aurora B is likely substituted by that of Aurora C in meiosis I in mouse oocytes as Aurora B protein was not detected using antibodies which were demonstrated to be specific to particular isoforms. In addition, Shuda et al., (2009) failed to detect Aurora B protein with a variety of antibodies.

Strategies to study the effects of the Aurora Kinases in oocytes fall into three main categories. Firstly, one could inhibit Aurora Kinases, since various inhibitors exist although none have a high specificity for a particular Aurora isoform. Secondly, one could knockdown Aurora Kinases using morpholino or siRNA. This has the disadvantage that oocytes must be cultured *in-vitro* for long periods, which may affect experimental outcomes. In addition, using these techniques it is not possible to control when in the cell cycle auroras are knocked down. Thirdly, dominant negative constructs could be expressed. Auroras B and C both require the binding partner INCENP; therefore the effects of over-expression of one construct probably would have an effect on both Auroras (Schindler et al., 2012). However, Yang et al., (2010) suggest that only Aurora C is normally present in meiosis I. The interpretation of overexpression of Aurora B therefore requires careful interpretation (Shuda et al., 2009).

Previous studies on mouse oocytes have utilized all of the above three approaches. For instance Swain et al. 2009 used the Aurora Kinase inhibitor ZM447439 to inhibit Aurora Kinases. Shuda et al. 2009 used ZM447439 and then used over-expression of Auroras A, B or C to see which reversed the effects of inhibition. Saskova et al. 2008 utilized knockdown of Aurora A, whereas Yang et al. 2010 used expression of a kinase deficient Aurora C construct to examine its effects on meiosis I. These studies provided insights into the importance of Auroras in meiosis I, however, a feature common to all these studies was that Aurora inhibition (or knockdown/dominant negative expression etc) was for the duration of meiosis I. This seemed to largely block PBE and so the role of the Auroras in the SAC and in preventing aneuploidy was not addressed. To rectify this I decided to use the inhibitor approach, utilizing ZM447439. The inhibitor could be added at any time during meiosis, therefore it might be possible to dissect out the effects of Aurora inhibition that occur during specific parts of meiosis I by an approach in which the timing and length of Aurora inhibition was varied. The long length of meiosis I in mouse oocytes and the fact that they can be synchronised should make this possible with accuracy.

ZM447439 inhibits Auroras by occupying the ATP binding pocket of the kinase domain. It has a similar IC_{50} for both Auroras A and B (Ditchfield et al., 2003), and this specificity likely extends to Aurora C due to the high sequence homology of its kinase domain with Aurora B (Brown et al., 2004). The effects of ZM447439 addition cannot therefore be attributed to a specific Aurora Kinase. However, use of a soluble inhibitor

meant that Aurora Kinases could be inhibited at any time during meiosis I, a feat that cannot be achieved with knockdown or dominant negative expression.

5.2 THE EFFECTS OF ZM447439 ON OOCYTE MEIOSIS I

5.2.1 DOSE DETERMINATION FOR THE USE OF ZM447439 AND NOCODAZOLE

Before beginning experimental work it was first necessary to determine an effective, minimal concentration of both ZM447439 and nocodazole. The Maro group had previously cultured oocytes in nocodazole and found that 0.4µM was an effective, minimal dose to inhibit polar body extrusion and thus could be used as a dose which would sufficiently activate the SAC (Wassmann et al., 2003). ZM447439 had been used previously in mouse oocytes, on mitotic cell lines and in Xenopus egg extracts at concentrations of 1-20 µM (Ditchfield et al., 2003; Gadea and Ruderman, 2006; Jelinkova and Kubelka, 2006; Liu et al., 2009; Swain et al., 2008; Wang et al., 2006). To test which concentration would be effective during mid-prometaphase, a time not previously investigated in mouse oocytes, a range of concentrations were added to the media at 4 h and the effect was measured by the timing of PBE. PBE were scored by eye using a dissection microscope at 30-min intervals. PBE for each group was expressed as a cumulative percentage (Figure 5.1). Comparison of mean PBE times revealed that a ZM447439 concentration of 10µM was most effective in bringing forward the timing of PBE and concentrations greater than 10µM were associated with a drop in the percentage of oocytes able to extrude a polar body. For this reason, a concentration of 10µM was used in all further experiments.

5.2.2 ZM447439 ADDITION IN PROPHASE DOES NOT BLOCK GVBD

Firstly, ZM447439 was tested on GV arrested oocytes to see if it inhibited GVBD. GV intact oocytes were incubated in milrinone containing media supplemented with 10µM ZM447439. After washout of milrinone, but in the continued presence of ZM447439, oocytes were left to mature. They were checked 2 hours after washout for GVBD and 16 hours after washout for the presence of polar bodies. After 2 hours all oocytes had undergone GVBD, but after 16 hours none had extruded polar bodies (n=24). In contrast to this 90% of controls had extruded polar bodies at this time (n=20).

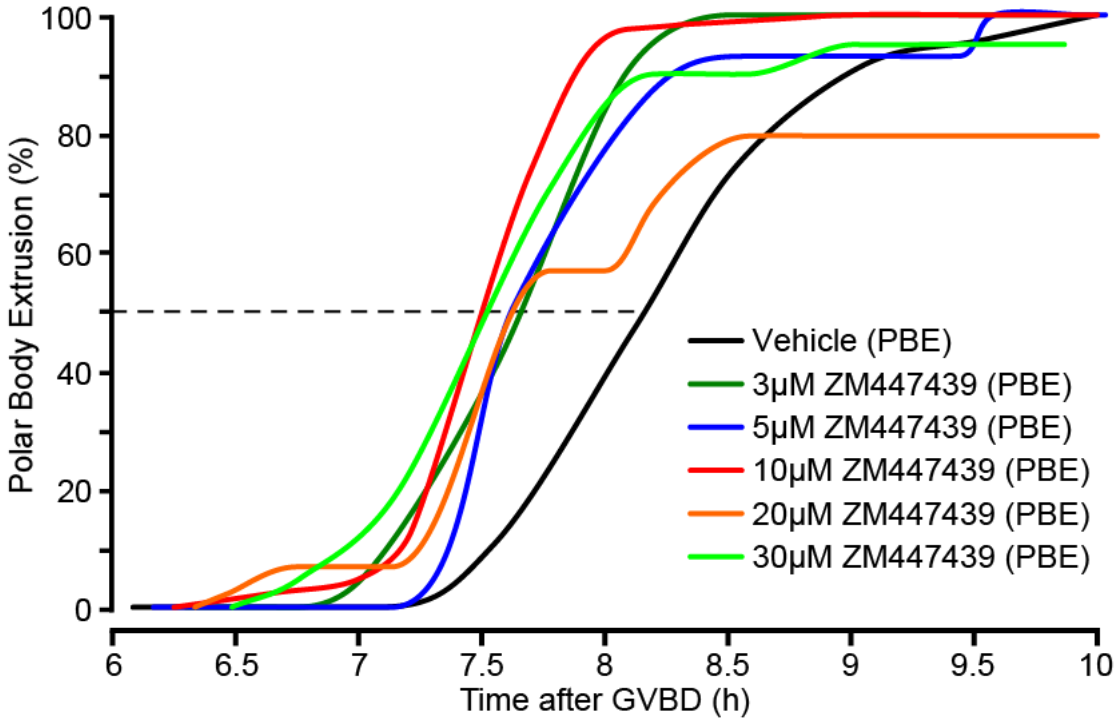

Figure 5.1 - **Percentage PBE following addition of 3-30μM ZM447439.**

The Aurora Kinase inhibitor ZM447439 was added to maturing oocytes at 4 h and oocytes were scored for PBE every 30 min. The cumulative PBE is plotted as a percentage for each concentration tested against the time after GVBD. Each curve is the combination of two separate experiments. ZM447439 was delivered dissolved in DMSO which had a maximal final concentration of 0.1%. Vehicle (n=47), 3μM (n=20), 5μM (n=43), 10μM (n=83), 20μM (n=44), 30μM (n=20). Dashed horizontal line indicates 50% polar body extrusion.

5.2.3 ZM447439 ADDITION FROM GVBD ONWARD CAUSED AN ABORTED POLAR BODY EXTRUSION

Incubation in ZM447439 did not prevent GVBD, but did block PBE (5.2.2), therefore I wanted to determine at what point(s) during maturation the block occurred. To investigate this, oocytes were synchronised in milrinone containing media for 1-2 hours before its thorough washout. ZM447439 was added to the culture media shortly after washout, but before the time of GVBD and oocytes were imaged on the Biostation IM inverted microscope. The microscope was programmed to acquire brightfield images of all oocytes at 15-min intervals. After the experiment was concluded the timing of GVBD for each oocyte was determined from the timelapse image series. The frame during which the largest proportion of oocytes underwent GVBD was considered to be the normal (arithmetic mode) timing of GVBD. Only oocytes that underwent GVBD within one frame of the mode time (mode ± 15 min) were included in further analysis. The pool of oocytes that were analyzed was therefore highly synchronous. Analysis of the time lapse confirmed that in the group treated with ZM447439 no polar bodies were extruded within the 12 hours of imaging (n=64), whereas 94% of vehicle control oocytes extruded polar bodies. The mean time of polar body extrusion in control oocytes was 8.3 ± 0.7h after GVBD (Figure 5.2 A-B, n=69).

Closer examination of the timelapse images revealed that in the oocytes treated with ZM447439 there was a distinctive protrusion of the plasma membrane, which was transient, lasting 30-45 min but which did not lead to cytokinesis. Instead the protrusion receded back into the oocyte. When the mean timing of this aborted polar body extrusion was calculated relative to GVBD it was significantly earlier (7.3 ±1.5h n=64) than that of the proper PBE seen in controls ($P<0.001$, Figure 5.2 B).

Oocytes cultured in ZM447439 attempted to extrude polar bodies earlier than vehicle control oocytes, therefore it was hypothesized that the underlying cellular events governing maturation might be proceeding at an accelerated rate. The failure of the ZM447439 treated oocytes to extrude the polar body could be as a result of a mechanical failure to do so and not because the oocyte had arrested its meiotic progression in response to culture in ZM447439. To test this hypothesis, oocytes were again imaged by timelapse with or without the addition of ZM447439 from the time of GVBD. On this occasion the fluorescent DNA stain Hoechst was added to the media at a final concentration of 3.25µM and an additional image was acquired for each

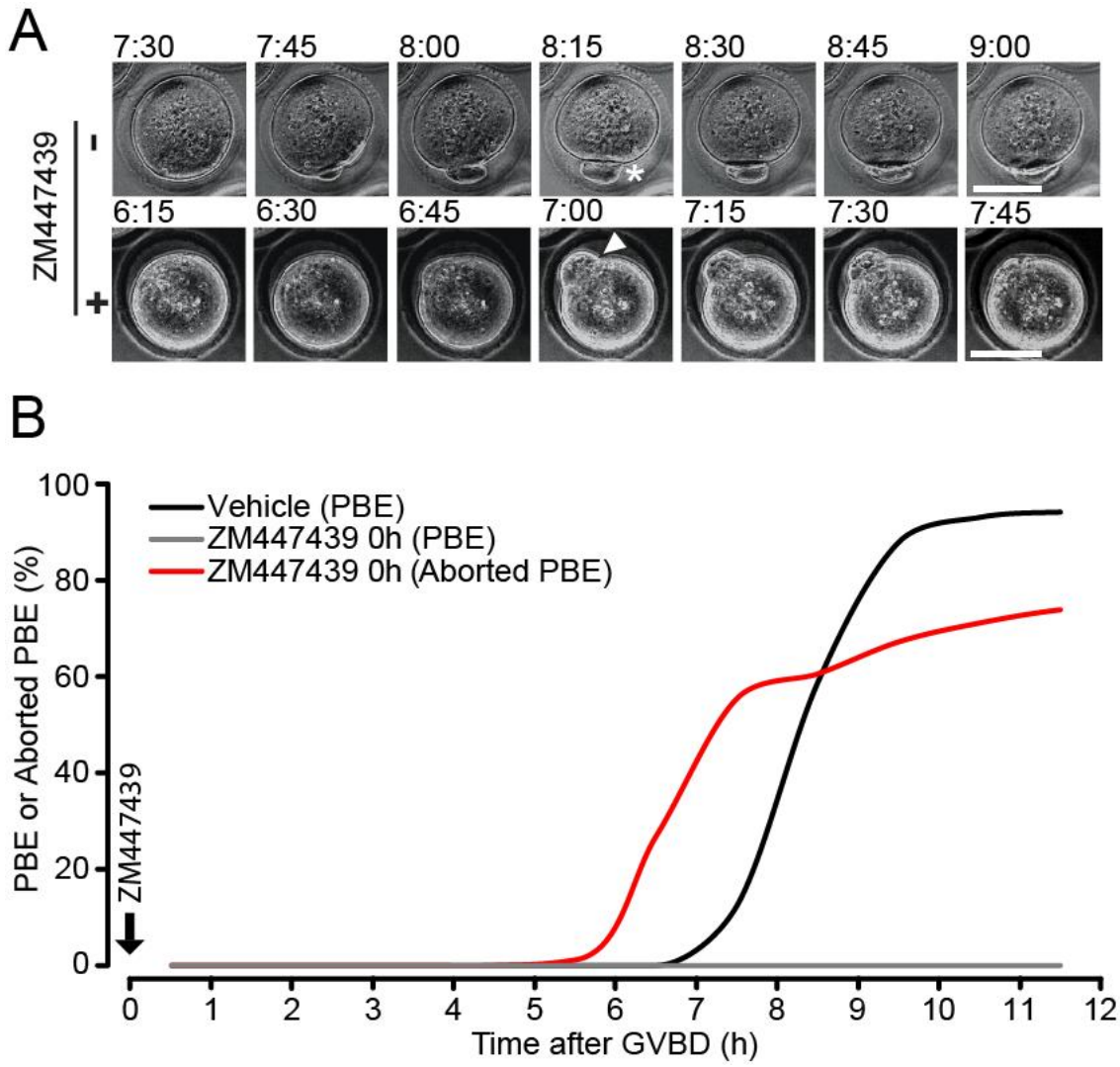

Figure 5.2 - **ZM447439 addition at the time of GVBD results in a block to PBE.**

Synchronized oocytes matured with or without 10µM ZM447439 from 0 h. (A) Representative timelapse images showing complete polar body extrusion (asterisk) in the absence of ZM447439 and the aborted polar body extrusion (arrowhead) in the presence of ZM447439 with the time after GVBD indicated as (h:mm). Scale bar represents 50µm. (B) Cumulative polar body or aborted polar body extrusion percentage with time derived from timelapse images as in 'A'. Vehicle n=69, ZM447439 n=64.

timepoint using low intensity UV light. Analysis of these data showed that in control oocytes an obvious metaphase plate was formed prior to anaphase. At anaphase the control oocytes separated their chromosomes synchronously, such that no lagging chromosomes were ever observed (Figure 5.3 A, n=31). In contrast to this, analysis of the chromosomes in ZM447439 treated oocytes showed that the primary defect was an inability to congress their chromosomes onto a metaphase plate. Second to this was their inability to successfully separate the chromosomes at anaphase. There was a clear enlargement of the area occupied by the chromosomes of ZM447439 treated oocytes, suggesting they were being pulled poleward. This movement occurred concurrently with the attempted polar body extrusion and during this time the chromosomes were found to be in the cleavage furrow. No proper segregation of the chromosomes was observed, nor did the cleavage furrow contract to the point where a polar body was formed (Figure 5.3 A, n=13).

Both the lack of chromosome congression and failure to segregate chromosomes could be quantified. The extent to which chromosomes congressed onto the metaphase plate was quantified by measuring the area occupied by the chromatin in the frame preceding anaphase (~15 min before anaphase) after a threshold was applied to the image to define the edge of the chromatin (Figure 5.3 B). The maximum separation of the chromosomes at anaphase was measured as the greatest distance apart of the chromosomes in direction of the spindle axis (Figure 5.3 C). This analysis revealed a significant increase in ZM447439 treated oocytes of the area occupied by the chromatin prior to anaphase and a significant shortening of the distance between the separating chromosomes (Figure 5.3, D-E, n=10, $P<0.001$).

In conclusion, as the ZM447439 treated oocytes endeavour to extrude a polar body, resulting in a protrusion of the plasma membrane; they also attempted to segregate their chromosomes. This was observed as a stretching movement of the chromosomes along the axis of the spindle. These two events were coincident, suggesting that the underlying processes driving meiosis I were progressing, and that the failure of ZM447439 treated oocytes to extrude polar bodies was due to a failure to segregate chromosomes at anaphase and not an MI arrest.

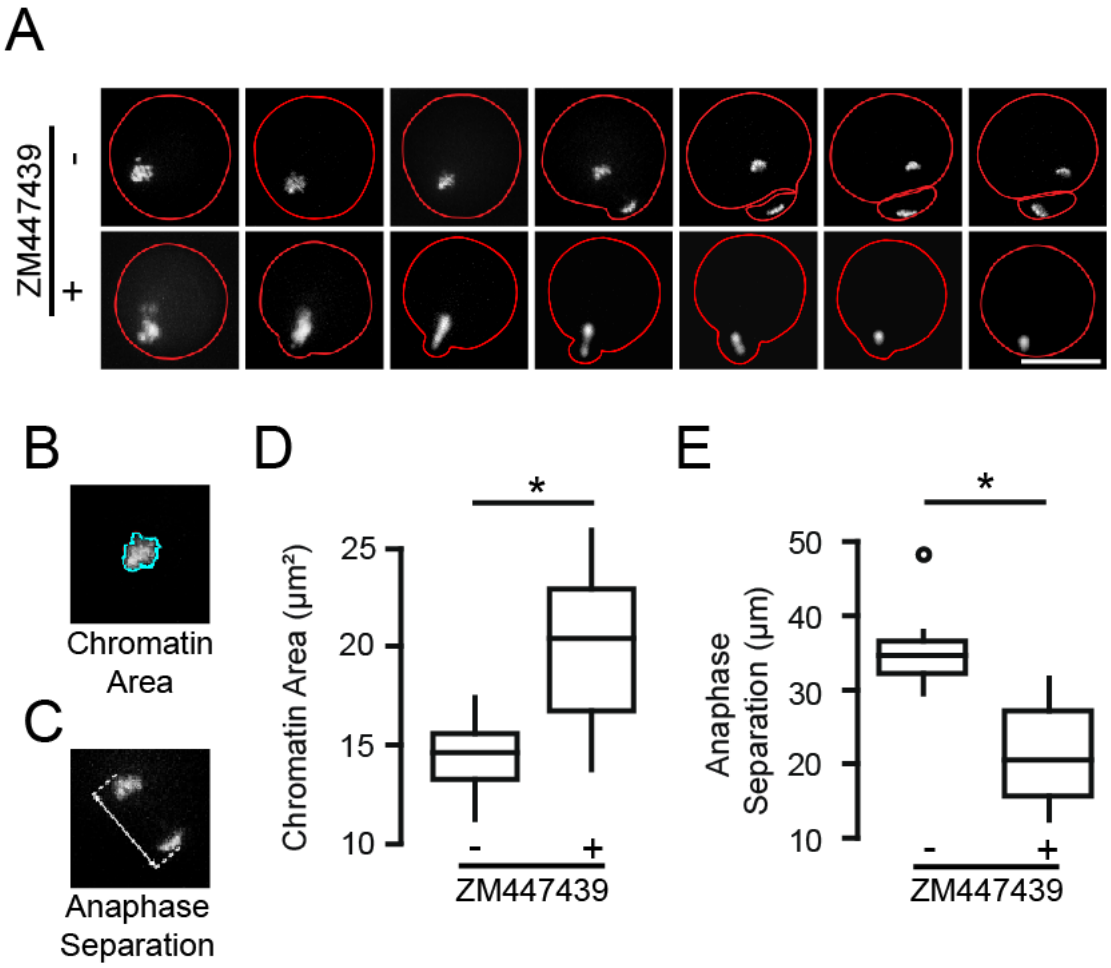

Figure 5.3 - ZM447439 addition from GVBD disrupts chromosome congression and segregation.

*(A) Timelapse (1 image per 15 min) of oocytes matured with or without ZM447439. The position of the oocyte plasma membrane derived from brightfield images are shown in red and chromatin (Hoechst) in grey. Scale bar represents 50µm. (B) The area occupied by the chromatin in the image before anaphase-onset was calculated by applying a threshold to the images (Blue). (C) The maximum separation of the chromosomes was measured at anaphase as the greatest distance apart of the chromosomes along the direction of the spindle. (D) The area occupied by chromatin in oocytes treated with or without ZM447439. (E) The anaphase separation distance in oocytes treated with or without ZM447439. Analysis was performed on 10 oocytes per group. * P<0.001.*

5.2.4 PROMETAPHASE ADDITION OF ZM447439 ACCELERATES PBE

Aurora B is known to have multiple roles during the cell cycle such as in recruiting or phosphorylating kinetochore proteins (Akiyoshi et al., 2009; Ditchfield et al., 2003) in regulating kinetochore-microtubule interactions (Cimini et al., 2006), chromosome alignment (Wang et al., 2006) in regulation of chromosome condensation (Gadea and Ruderman, 2006; Goto et al., 2002) and in cytokinesis (Goto et al., 2003; Steigemann et al., 2009). I therefore decided to use ZM447439 at differing times during meiosis I, instead of inhibiting Aurora Kinases throughout. Oocytes were synchronized in milrinone and following washout were cultured in MEM media inside the imaging chamber of the Biostation IM. Brightfield images were captured every 15 min and ZM447439 was introduced to the media at either 2 or 4 h to give a final concentration of 10µM.

The total percentage of oocytes extruding polar bodies after ZM447439 addition at 4 h was the same as controls (93 vs. 94% respectively). However, addition of ZM447439 at 2 h resulted in a reduction in percentage PBE compared to controls. This difference was not statistically significant (Control, 94%, n=69; ZM447439 2 h, 86%, n=57; P=0.140, Fishers exact test; Figure 5.4). However further analysis showed that 9% of the oocytes in this ZM447439 treated group resorbed their polar bodies after extrusion, accounting for the reduction in PBE from controls (Figure 5.4). The time at which the polar body was resorbed ranged from between 1 to 7.5 h after the time of PBE (Figure 5.5 A-B).

The timelapse images of oocytes treated with or without ZM447439 were analyzed and the timing of PBE calculated relative to GVBD for each oocyte. Vehicle control oocytes extruded polar bodes at 8.3±0.7h after GVBD. When the timings of PBE in oocytes treated with ZM447439 at either 2 or 4 h were compared to those of controls there was found to be a significant, ~1 h shortening of meiosis I with the average PBE being timed at 7.2±0.7h (2 h addition vs. control, P<0.001) and 7.1±0.7h (4 h addition vs. control, P<0.001, Figure 5.6 A-B) respectively. The 2 and 4 h ZM447439 addition groups did not differ significantly from each other (P=0.533). Also shown in Figure 5.6 for comparison is the timing of the aborted PBE in oocytes cultured in ZM447439 from GVBD onwards.

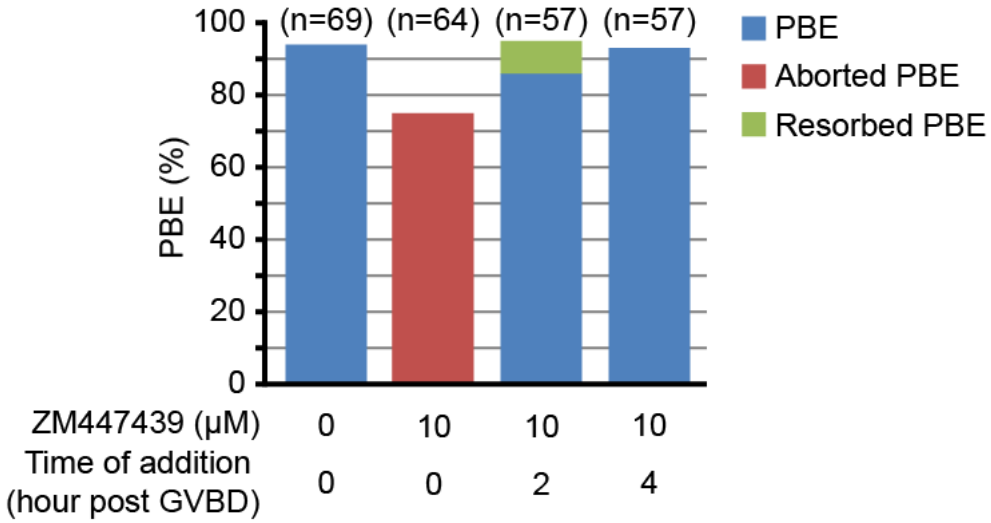

Figure 5.4 - Percentage of PBE after addition of ZM447439 between 0-4 h.

Percentage Polar Body Extrusion for oocytes treated with or without ZM447439 at times throughout early prometaphase I. Proper PBE are indicated in blue whilst aborted PBE and resorbed polar bodies are indicated in red and green respectively. PBE percentage (blue) was not significantly different between groups (Fishers exact test). Numbers of oocytes analyzed per group are indicated in parentheses.

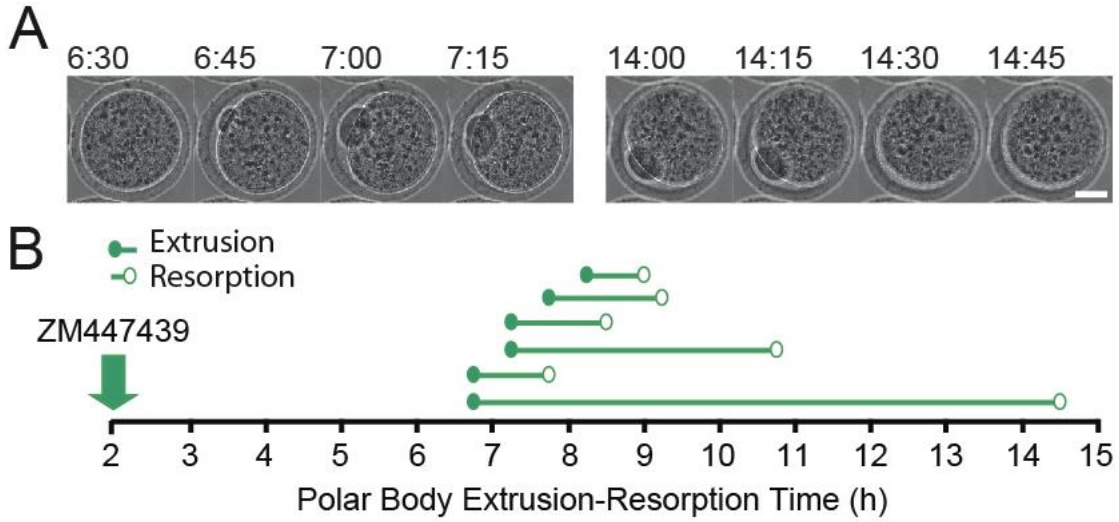

Figure 5.5 - ZM447439 addition at 2 h causes resorption of polar bodies.

(A) Representative brightfield images of an oocyte extruding (left) and then resorbing (right) a polar body in an oocyte that was cultured in ZM447439 from 2 h. Times are hh:mm after GVBD. (B) The timing of extrusion (solid points) and resorption (empty points) of polar bodies in all instances when polar bodies were resorbed following ZM447439 addition at 2 h (6/57 oocytes).

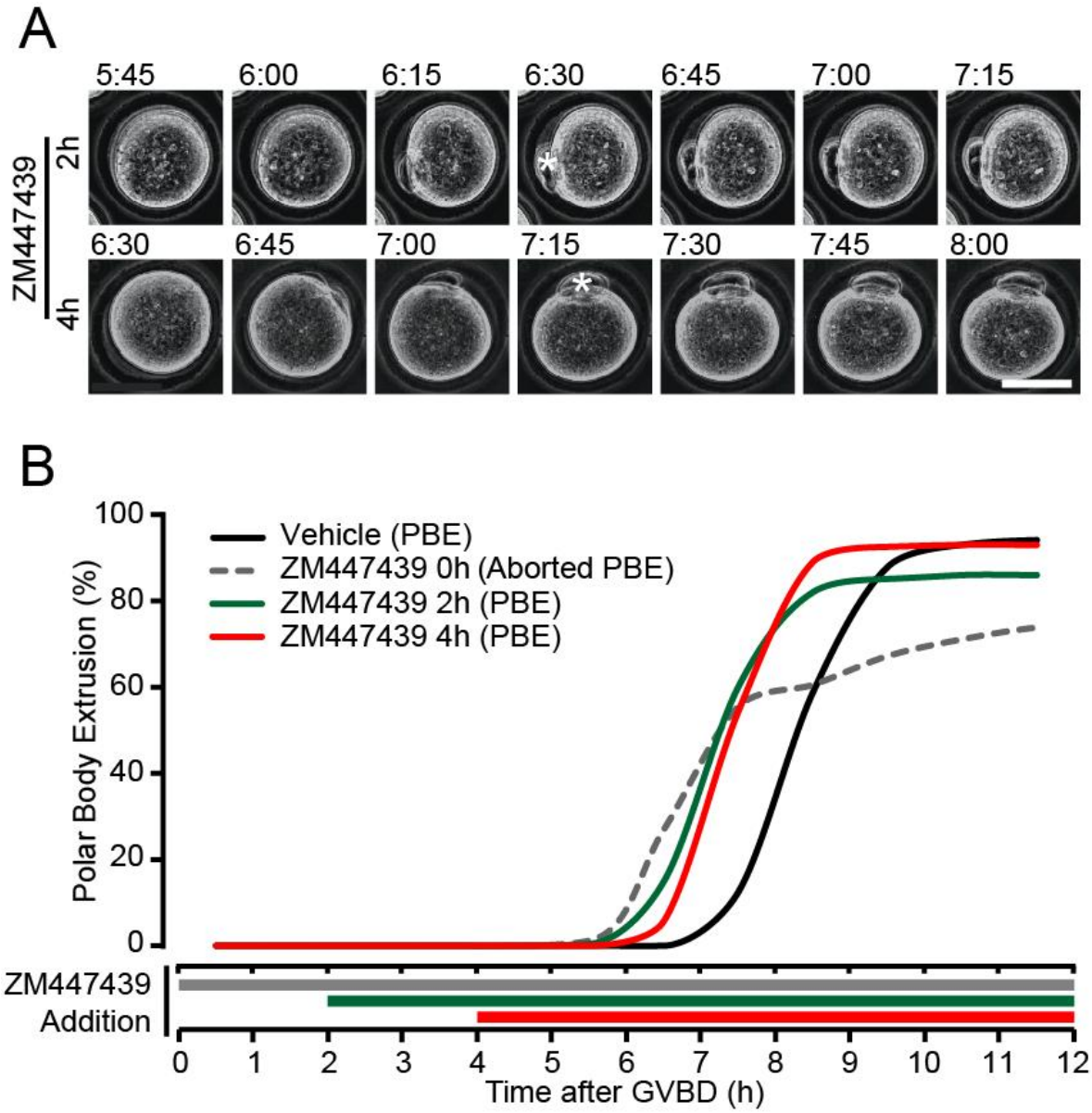

Figure 5.6 - Aurora Kinase inhibition in early prometaphase quickens meiosis I.

(A) Representative brightfield timelapse of oocytes following incubation in 10µM ZM447439 from either 2 or 4 h. Oocytes treated with ZM447439 from these times extruded polar bodies indicated by asterisks. Scale bar represents 50µm. (B) Cumulative polar body extrusion or aborted PBE curves derived from timelapse images as in 'A' (ZM447439 2h, n=57; ZM447439 4h, n=57). Coloured bars denoted 'ZM447439 Addition' show the presence of ZM447439 in the culture media for the respective groups.

In oocytes treated with ZM447439 from 2 h, 9% of polar bodies were resorbed. In order to understand more fully the nature of this resorption, I repeated the experiment using Hoechst to visualize the chromosomes as in Figure 5.3. Imaging by Hoechst did not produce high resolution images, as low levels of UV illumination were used so as to prevent damage to the oocytes. However the images were of sufficient quality to spot aberrant chromosome behaviour. The Hoechst timelapse images revealed that in those oocytes where the polar body was resorbed this was due to incomplete chromosome separation with chromatin still surrounding the cleavage furrow (Figure 5.7 A, n=13). In oocytes that did complete polar body extrusion lagging chromosomes were seen (Figure 5.7 B). In addition, analysis of the oocytes treated with ZM447439 at 4 h showed that 65% (n=13) failed to achieve proper congression before anaphase and 75% (n=15) had lagging chromosomes or chromatin bridges visible during anaphase (Figure 5.7 C n=20).

5.2.5 INCUBATION WITH ZM447439 PREVENTS FORMATION OF A METAPHASE II SPINDLE.

Oocytes treated with ZM447439 from 4 h onwards were fixed at 16 h to determine their progression to metaphase II. At this time control oocytes had formed a metaphase II spindle (Figure 5.8 A). Examination of the ZM447439 treated oocytes, confirmed that the polar body had persisted and contained chromatin, however Aurora Kinase inhibition had prevented formation of a proper metaphase II spindle. Instead a microtubule structure was detected in these oocytes, which did not resemble a metaphase II spindle in size, shape or in the strength of the tubulin staining (Figure 5.8 B). If ZM447439 was washed out of the culture media after polar body extrusion (at 10 h) and oocytes were then matured to MII, a fully formed spindle was observed (Figure 5.8 C). This highlights an essential role for Auroras in assembly of the metaphase II spindle.

5.2.6 ZM447439 EFFECT DEPENDS ON TIMING OF ADDITION

The effects of ZM447439 on oocyte maturation appeared dependent on when it was added. An early time of addition resulted in failed PBE, possibly due to chromatin blocking the cleavage furrow whereas a later time of addition resulted in accelerated PBE. To better define these timing effects oocytes were imaged by timelapse following ZM447439 addition either from GVBD for 2 hours only, or following ZM447439 addition

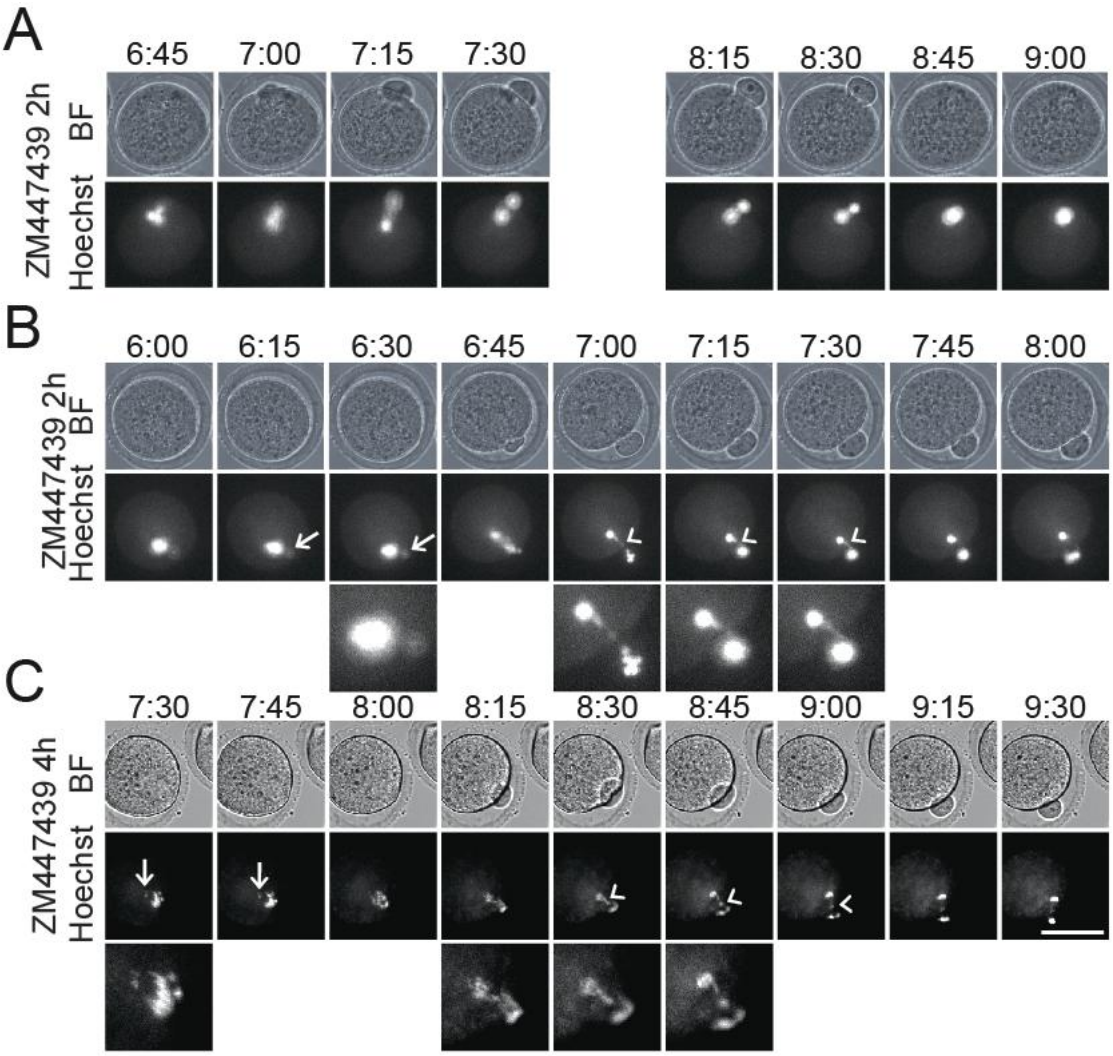

Figure 5.7 - Aurora Kinase inhibition increases non-alignment and lagging chromosomes.

(A) Representative brightfield and Hoechst images of an oocyte with ZM447439 added from 2 h onwards extruding a polar body (left) and then resorbing it (right) at the times indicated (h:mm, n=13). (B) A timelapse showing PBE after ZM447439 addition from 2 h onwards. (C) Representative timelapse showing an oocyte extruding a polar body after incubation in ZM447439 from 4 h. (B-C) Bottom row shows enlargement of Hoechst images, arrows indicated non-aligned chromosomes and arrowheads indicate lagging chromosomes during anaphase. In this group lagging chromosomes or chromatin bridges were common (n=15/20). Scale bars are 50µm.

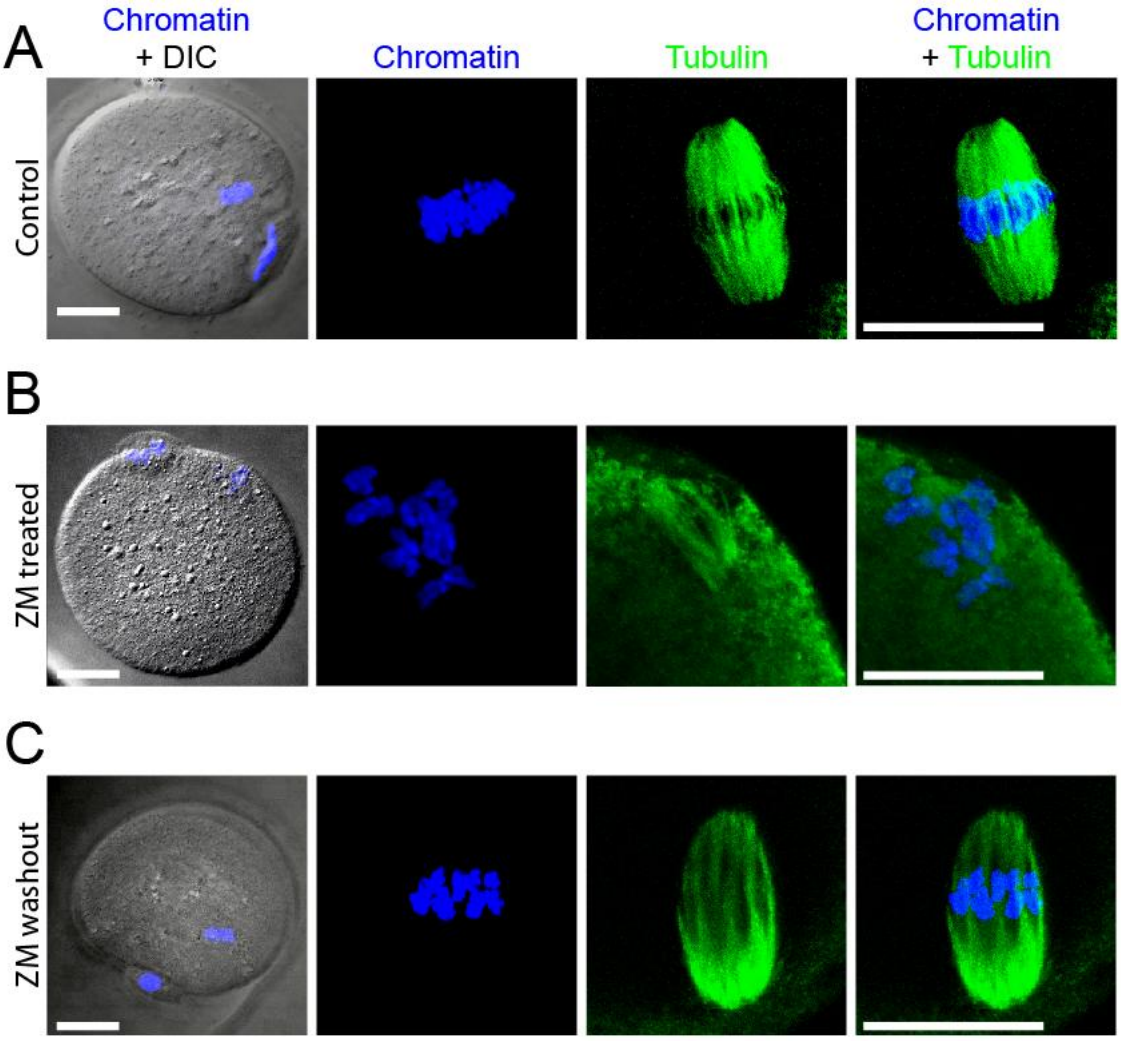

Figure 5.8 - Oocytes treated with ZM447439 from 4 h fail to assemble a normal metaphase II spindle.

Oocytes were cultured in the presence of ZM447439 from 4-10 h and then subjected to either washout of the drug, or continued culture in the drug to 16 h. Control oocytes were subject only to culture in 0.1% DMSO. Oocytes were fixed and stained for tubulin (green) and chromatin (blue). Images are z-projections generated by confocal microscopy, n=5-10 per group, scale bars represent 20µm.

from 6 h (Figure 5.9). The former would determine if Aurora Kinase activity during the first two hours of maturation was essential for further maturation, whilst the latter would help identify during which time period ZM447439 causes the shortening of meiosis I.

Culture of the oocytes in ZM447439 only for the first two hours of maturation caused no significant difference in PBE when compared to controls that were not treated with ZM447439 (ZM447439 0-2 h, 97%, n=75; Control, 94%, n=69; P=0.427, Fishers exact test). In addition the shortening of meiosis I was also abolished under these conditions as meiosis I was significantly delayed when compared to controls (ZM447439 0-2 h, 9.0±0.6h, n=75; Control, 8.3±0.7h, n=69; P<0.001, t-test; Figure 5.9).

The addition of the Aurora Kinase inhibitor from 6 h gave high rates of PBE (95%, n=22) and the timing of this PBE was significantly earlier than controls (ZM447439 6 h, 7.7±0.7h, n=22; Control, 8.3±0.7h, n=69; P<0.001, t-test; Figure 5.9). The reduced duration of meiosis I (measured either by PBE or by attempted PBE) was therefore a feature common to experiments when ZM447439 was in the media from 0, 2, 4 or 6 h onwards. There was no shortening of MI when ZM447439 was added only for the first 2 h of maturation though. Together this suggested that it was the presence of ZM447439 after 2 h that caused the acceleration PBE timing. Further to this, the duration of meiosis I was significantly longer after ZM447439 addition at 6 h than when ZM447439 was added at 4 h (6 h, 7.7±0.7h, n=22; 4 h, 7.1±0.7h, n=57; P<0.001, t-test). This suggested that the influence ZM447439 had in shortening meiosis I occurred mostly between 4 and 6 h, and to a lesser extent after 6 h.

5.2.7 ZM447439 CAN OVERCOME NOCODAZOLE INDUCED ARREST IN MI OOCYTES.

The SAC is important in controlling the timing of MI, as when active, it prevents anaphase by inhibition of the APC (Figure 3.10 A). The above data therefore suggested that Auroras may play an important role in the SAC as the duration of meiosis I is shorter when they are inhibited. This is consistent with the SAC being bypassed and consequently failing to inhibit the APC. To test this idea further I first created a situation in which the SAC was activated. 400nM nocodazole added to the culture media at 4 h blocked PBE in the majority of oocytes (75%, Figure 5.10 A-B). The 25% (n=64) of oocytes extruding polar bodies in nocodazole were delayed significantly when compared to controls (Noc., 11.9±1.5h, n=16; Control, 8.3±0.7h,

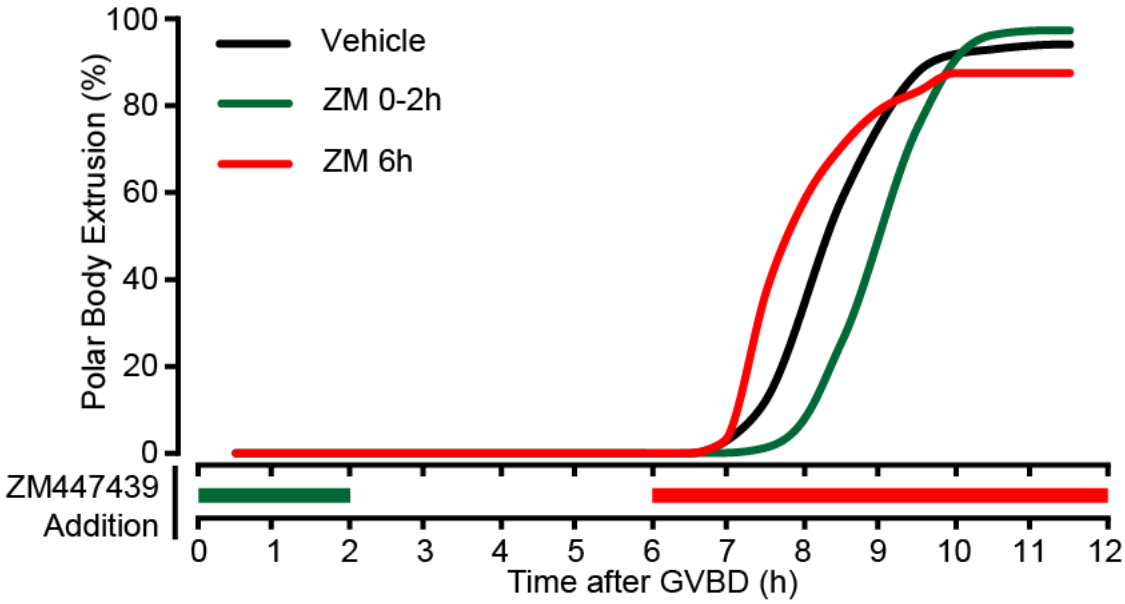

Figure 5.9 - Effect of ZM447439 addition for the first two h of maturation or after 6 h of maturation on PBE timing.

Polar body extrusion is plotted as a cumulative percentage against the time after GVBD. The times of the incubation in media containing ZM447439 are indicated by the coloured bars (0-2 h, green. 6 h onwards, red). ZM447439 0-2h n=75, ZM447439 6h n=22. In the 0-2 h group oocytes were washed out of ZM447439 by repeatedly moving through droplets free of the drug, as described for milrinone washout (Section 2.3.4). Oocytes were then imaged for PBE as per normal. An average timing was used for GVBD when calculating PBE timing as GVBD timing in individual oocytes were unknown.

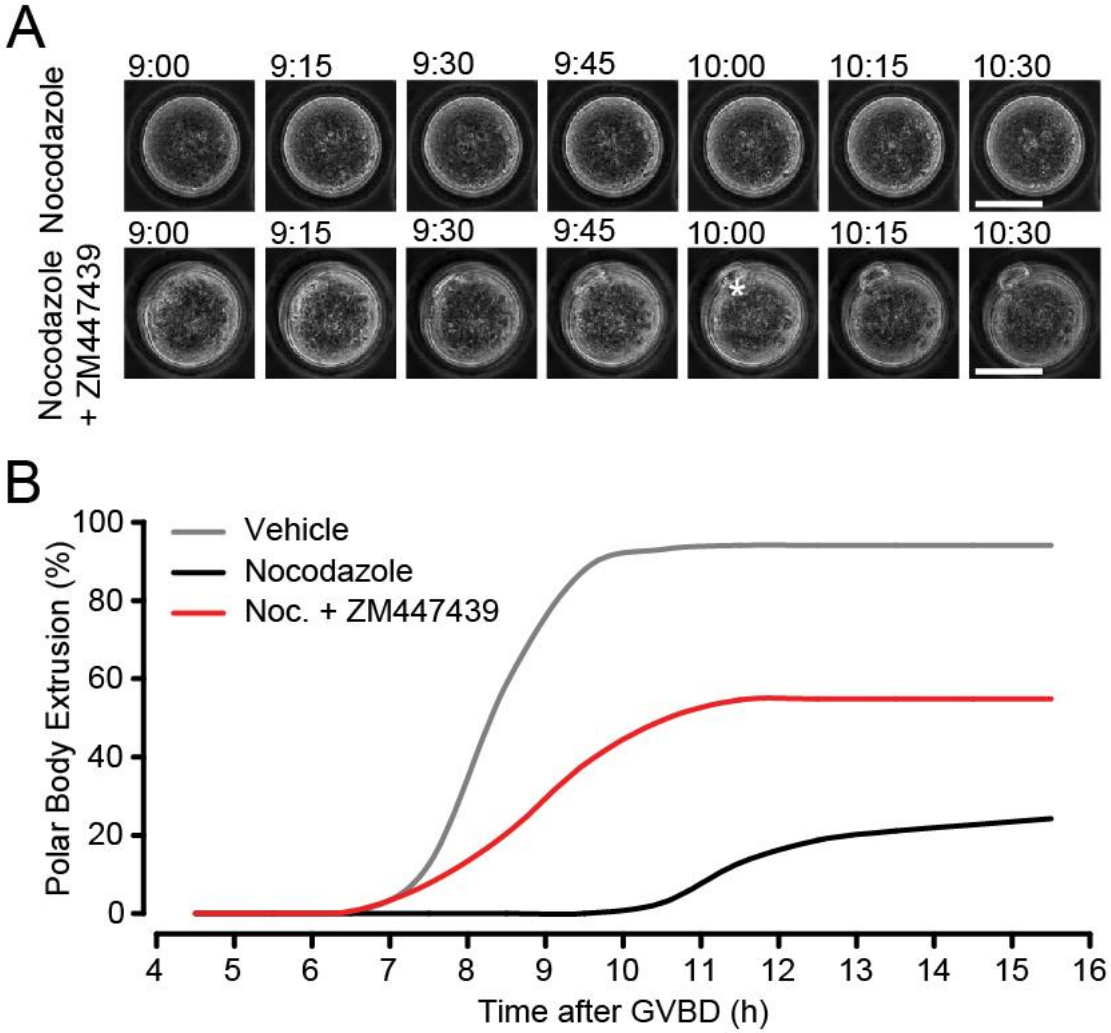

Figure 5.10 - Aurora Kinase inhibition can overcome the SAC.

(A) Representative timelapse images of oocytes incubated in 400nM nocodazole or nocodazole with 10µM ZM447439 from 4 h. Times indicated are hh:mm after GVBD, asterisk indicates complete PBE, scale bars represent 50µm. (B) Cumulative PBE percentage is plotted against time after GVBD for each group. Vehicle n=69, Nocodazole n=64, Nocodazole + ZM447439 n=34.

n=69; P<0.001, t-test; Figure 5.10 B) such that no polar bodies were extruded with normal timing, suggesting that the SAC was activated. Fixation and examination of oocytes arrested in 400nM of nocodazole after ICC for β-tubulin revealed that the metaphase I spindle was very disrupted having lost its barrel-like shape, but was not abolished completely (Figure 5.11 A). This concentration has also been shown to prevent the formation of k-fibres and recruit Mad2 to kinetochores (Figure 3.3 A, Figure 3.10 C-D).

When 10µM ZM447439 was added to the culture media in addition to the nocodazole at 4 h, 55% (n=83) of oocytes were able to overcome the block to PBE. The timing of this PBE, although still delayed compared to controls, was significantly earlier than that seen in the oocytes treated only with nocodazole (Noc. And ZM447439, 8.9±1.1h, n=34; Noc., 11.9±1.5h, n=64; P<0.001, t test; Figure 5.10 B) suggesting that the SAC arrest had been abrogated by the addition of the Aurora Kinase inhibitor. Those oocytes that had extruded polar bodies were fixed at 16 h, a time by which control oocytes had formed a metaphase II spindle (Figure 5.8 A). Staining for tubulin and chromatin revealed that both the oocyte and the first polar body contained chromatin; however the oocyte had not formed a metaphase II spindle (Figure 5.11 B). A metaphase II spindle could be restored by washing out the ZM447439 and nocodazole after the extrusion of the polar body (Figure 5.11 C). This suggested that the concerted effect of ZM447439 and nocodazole prevented a new spindle from assembling.

5.2.8 ADDITION OF ZM447439 REVERSES NOCODAZOLE INHIBITION OF THE APC.

It appeared that in bypassing the block to PBE induced by nocodazole, ZM447439 was able to overcome a SAC arrest. To test this further, the effect of ZM447439 on cyclin B1 degradation was investigated. Cyclin B1 degradation is a consequence of activation of the APC and therefore is a read-out of its activity, and by inference, the inactivity of the SAC. When cyclin B1-Venus mRNA was injected into control oocytes and a fluorescence timelapse was recorded, it was found that there was a peak in fluorescence in mid-prometaphase I. In the latter half of meiosis I cyclin B1-Venus levels declined, reaching their lowest levels around, or just after polar body extrusion (Figure 5.12). Consistent with previous chapters, this demonstrated that in control oocytes the SAC ceased to inhibit the APC at around 4-5 h and consequently APC mediated cyclin B1 degradation commenced from that time. If the experiment was

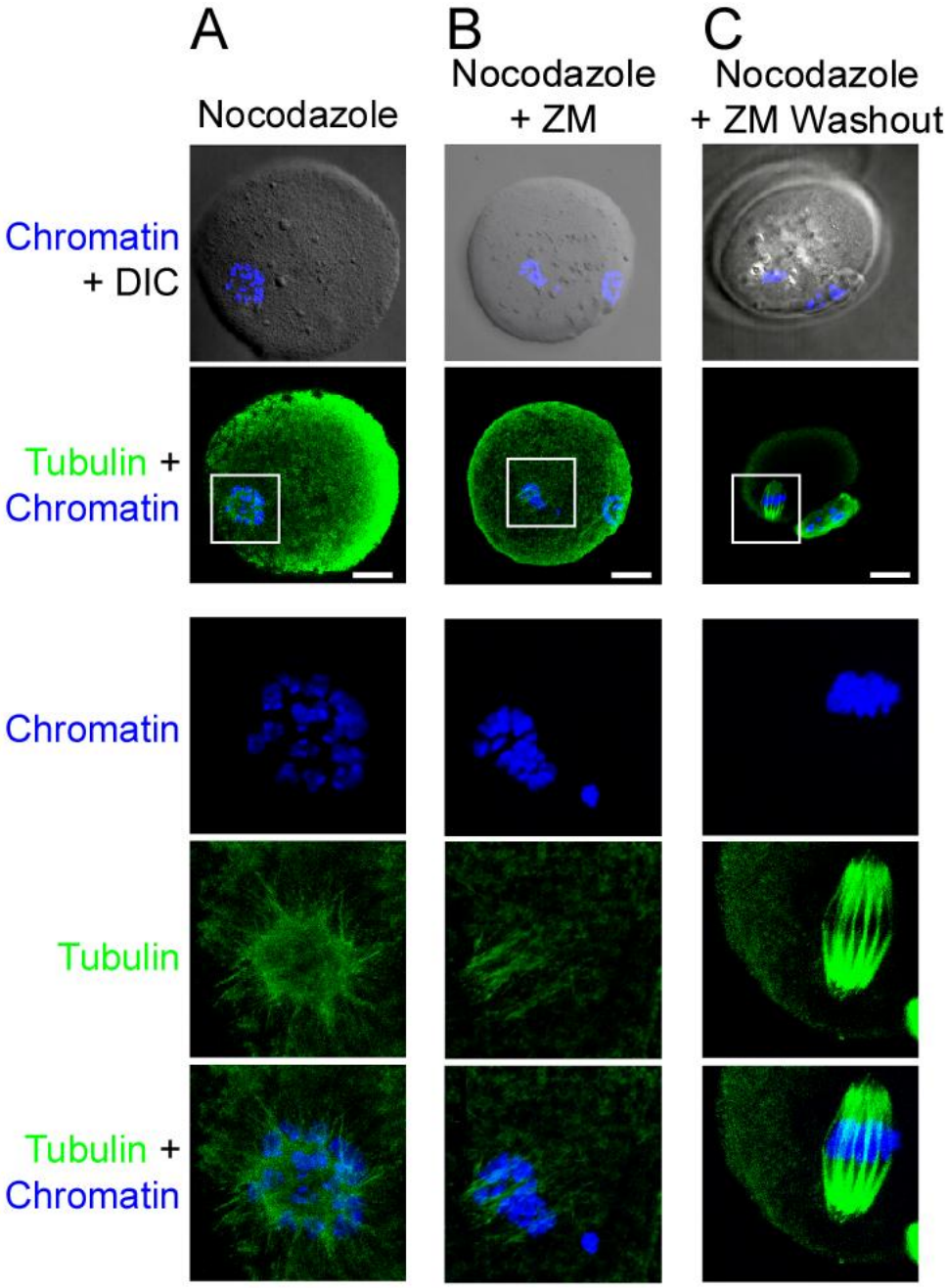

Figure 5.11 - Effects of ZM447439 and nocodazole on spindle formation.

Oocytes were either cultured to MII in the presence of the indicated drug(s) or were washed out of the drugs after polar body extrusion and allowed to reach MII. 16 hours after GVBD, oocytes were fixed and stained for tubulin (green) and chromatin (blue). (A) Nocodazole 400nM. (B) Nocodazole 400nM + ZM447439 10µM. (C) Nocodazole 400nM + ZM447439 10µM, then washout of both drugs after PBE. The white square is enlarged in subsequent images below. n=5-10 per group, scale bars represent 20µm.

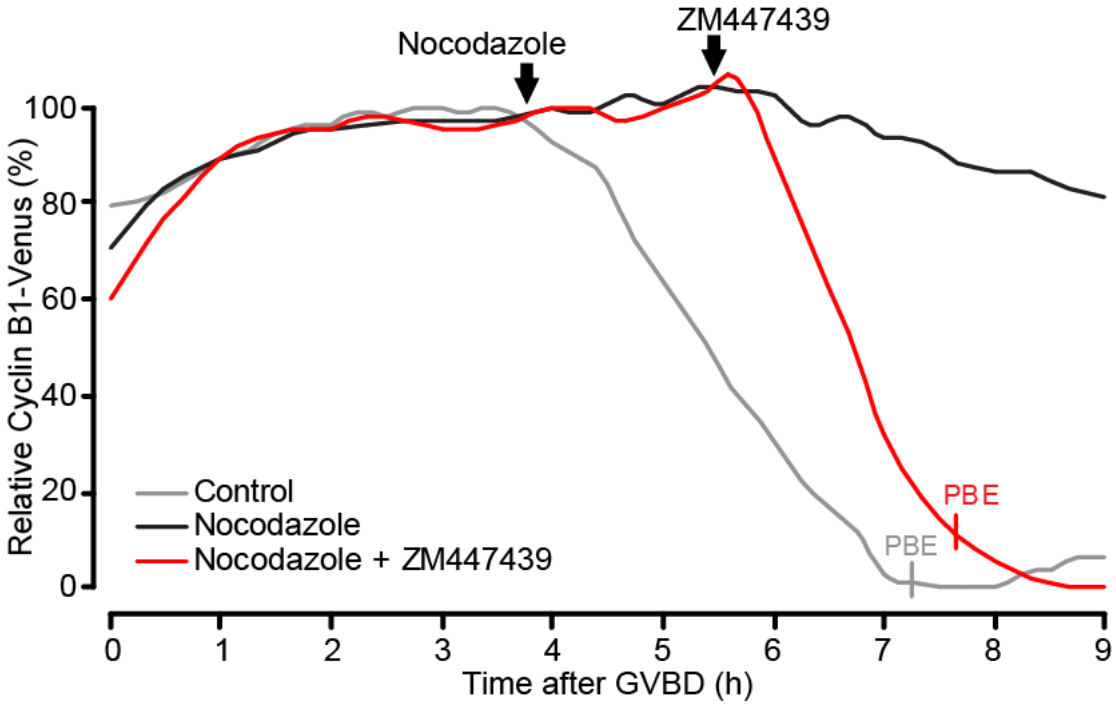

Figure 5.12 - ZM447439 addition initiates cyclin B1 degradation in nocodazole arrested oocytes.

Oocytes injected with mRNA encoding Cyclin B1-Venus were imaged during maturation. The representative traces are from individual oocytes with their maxima normalized to 100%. Nocodazole (400nM, n=9) and ZM447439 (10µM, n=8) were added at the times indicated by arrows. Control n=9.

repeated, but 400nM nocodazole was added at 4 h, it was found that cyclin B1 destruction was prevented. This confirmed that the concentration of nocodazole used was imposing a robust SAC arrest. If following the addition of nocodazole, 10µM ZM447439 was added to the culture media it was possible to see an abrupt drop in the fluorescence of cyclin B1, its decline beginning within 15 min of ZM447439 addition (Figure 5.12).

5.2.9 ZM447439 TREATMENT CAUSES AN INCREASE IN ANEUPLOIDY

Given the previous data, which implied ZM447439 bypassed the SAC, and that oocytes cultured in ZM447439 frequently displayed lagging chromosomes (an indication that at the time of anaphase, not all kinetochore-microtubule attachments had been corrected) it seemed likely that ZM447439 treatment would increase occurrence of aneuploidy in the resulting metaphase II oocytes. To test this hypothesis, oocytes were cultured in ZM447439 from 4 h as in previous experiments. After PBE in-situ chromosome spreads were performed using a modified protocol developed elsewhere (Duncan et al., 2009). Oocytes were washed out of ZM447439 and cultured for 2 hours to allow formation of a metaphase II spindle. At this time 200µM monastrol was added to the culture media for a further 2 hours to collapse the spindle, creating a monopolar spindle which spread out the chromosomes (Figure 5.13). Oocytes were then fixed and stained for CREST and chromatin. Using confocal microscopy, high resolution stacks were generated of the chromosomes and kinetochores. The chromosomes were sufficiently spaced to allow the number of kinetochores to be counted with accuracy. The distance separating planes in the z-axis was sufficiently small (0.5µm) to distinguish between kinetochores that were on top of one another, the typical diameter of the CREST signal being around 1-2µm.

After analysis of 242 in vitro matured control metaphase II oocytes, only 6 oocytes were aneuploid (2.5%). Of these, 3 were hypoploid (<40 kinetochores), and 3 were hyperploid (>40 kinetochores). When 39 oocytes treated with ZM447439 were analyzed 6 were found to be aneuploid (15.4%) a significantly higher proportion than in controls (ZM447439, 15.4%, n=39; Control, 2.5%, n=242; P=0.004, Fisher's Exact Test; Figure 5.14). Of these aneuploid oocytes 6 were found to be hypoploid and none hyperploid.

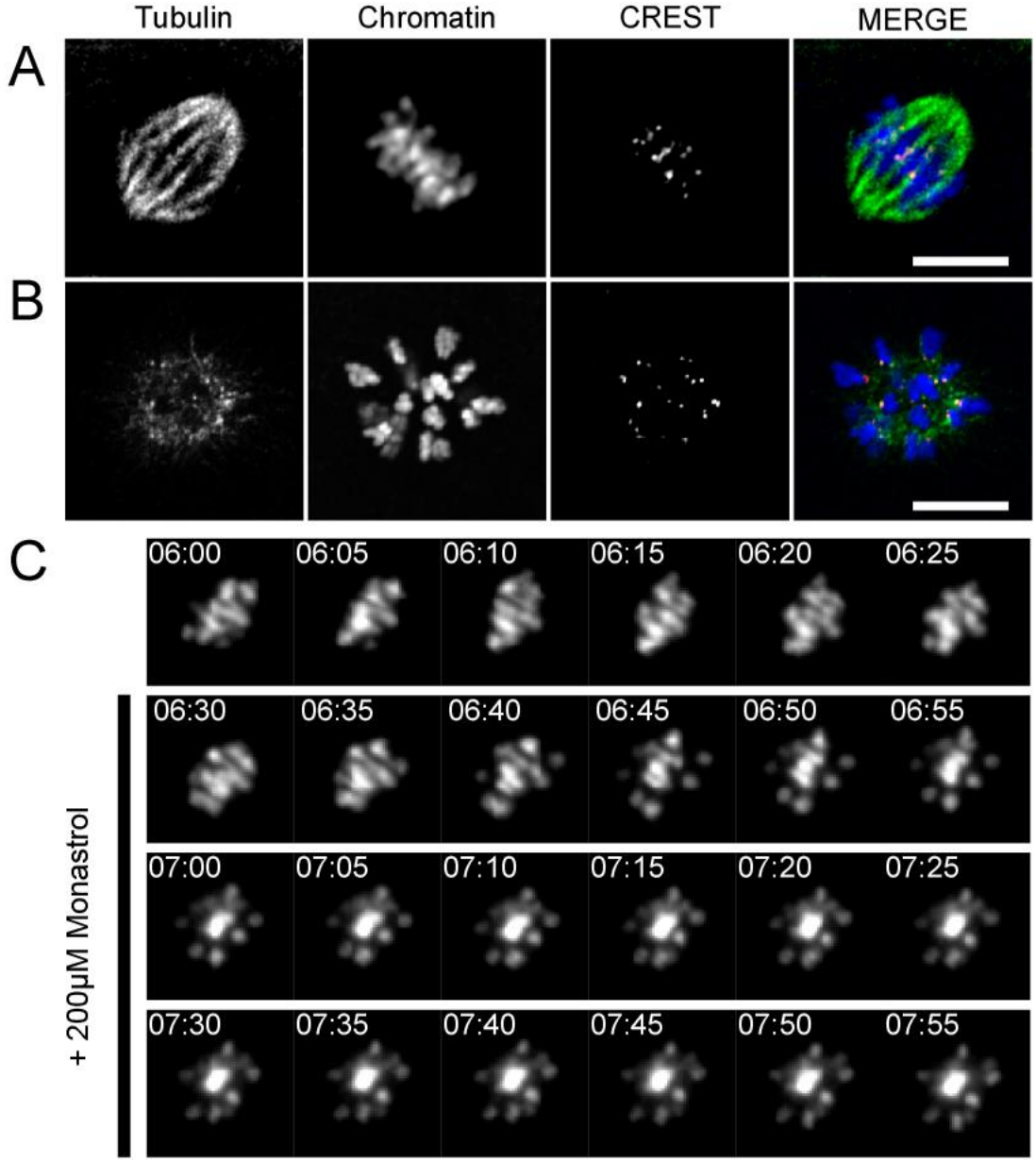

Figure 5.13 - The effect of monastrol treatment on a mouse oocyte spindles.

(A) Images show a single confocal plane through a fixed MII spindle after staining for tubulin, CREST and chromatin. The spindle is bipolar (tubulin), chromosomes are aligned on a metaphase plate (chromatin) and the kinetochores are often clustered together (CREST). (B) A single plane image of a MII spindle fixed after 2h treatment with 200µM monastrol shows an astral spindle, separated chromosomes and better spread kinetochores. Scale bar represents 10µm. (C) A timelapse of a metaphase I oocyte expressing H2B-mCherry. Times are mm:hh after GVBD, monastrol is added at 06:30.

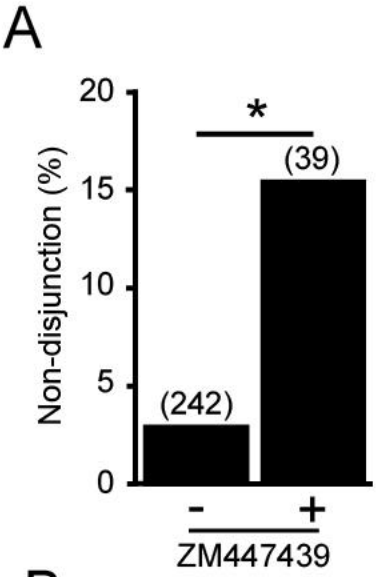

Figure 5.14 - ZM447439 addition increases aneuploidy in mouse oocytes.

*Oocytes incubated with or without ZM447439 from 4 h were washed free of ZM447439 and their chromosome spread in-situ by monastrol treatment before fixation and staining with CREST antiserum and Hoechst. (A) Aneuploidy in oocytes with or without ZM447439 treatment. (Control n=242, ZM447439 n=39, *P=0.004). (B) An intensity z-projection and montage of individual z-sections from one oocyte with each kinetochore numbered. Chromosomes are shown in blue and kinetochores in white. Scale bars represent 10µm.*

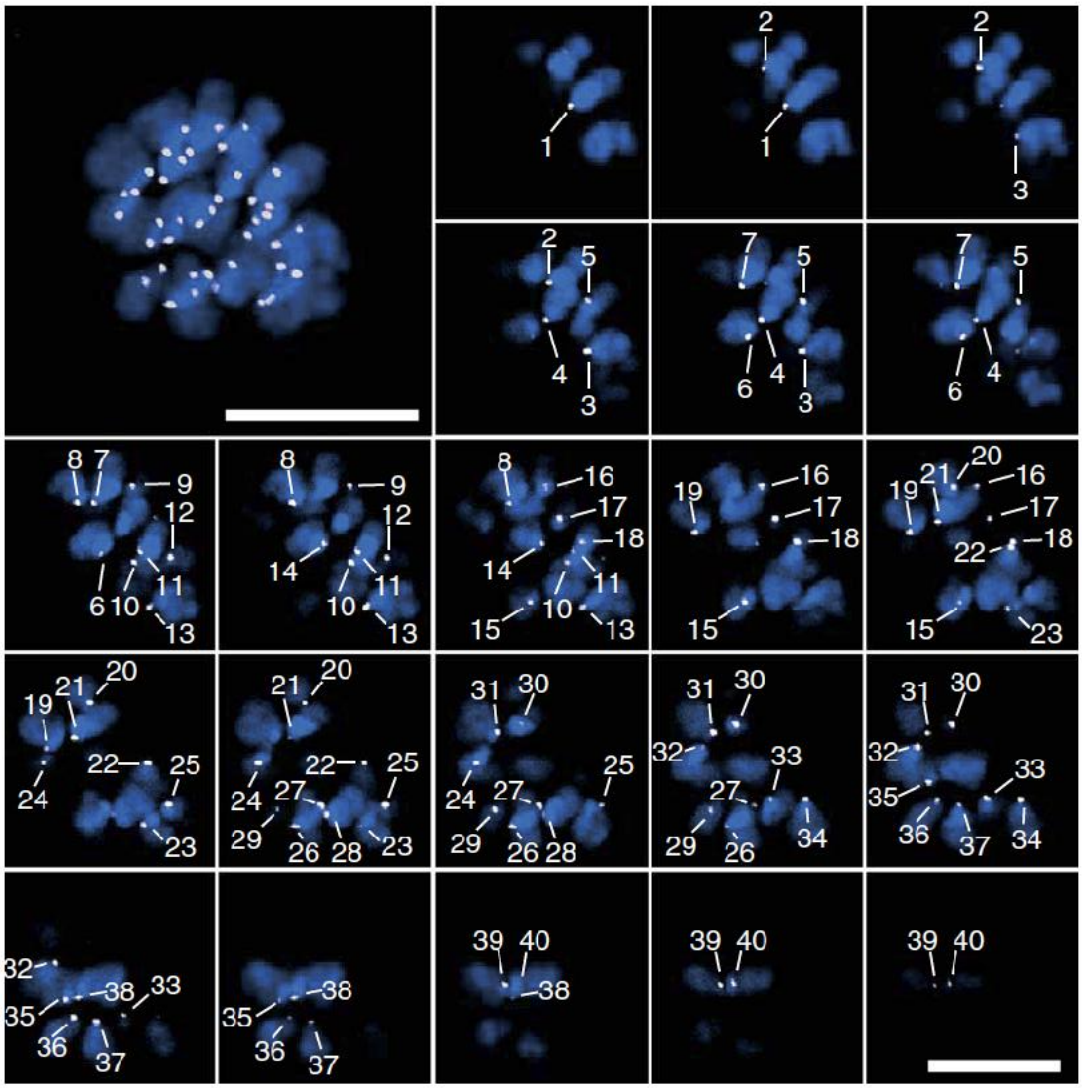

5.3 DISCUSSION

5.3.1 AURORAS ARE NOT REQUIRED FOR GVBD BUT ARE REQUIRED FOR MATURATION.

On the basis of using pharmacological inhibition it seems likely that Auroras are not required for the process of GVBD, but are essential for completion of maturation. This was inferred from the finding that ZM447439 did not block GVBD but blocked oocyte maturation, as has been reported elsewhere in mouse oocytes (Shuda et al., 2009; Swain et al., 2008; Vogt et al., 2009). Possibly because of this block to maturation, the functions of Auroras in MI had not been investigated in previous studies. For instance, the function of Aurora B in the spindle assembly checkpoint which had been reported previously in somatic cells and spermatocytes (Hauf et al., 2003; Kallio et al., 2002; Wang et al., 2006). I therefore decided to dissect the possible roles of Auroras in MI by adding ZM447439 during various temporal windows.

5.3.2 INHIBITION OF AURORAS THROUGHOUT PROMETAPHASE BLOCKS OOCYTE MATURATION.

The observation that maturation was blocked by addition of ZM447439 from GVBD onwards (0 h) was examined in greater detail with timelapse imaging. In this case it was apparent that although oocytes failed to extrude a polar body, an aborted PBE was seen. The timing of this aborted PBE was significantly earlier than the proper PBE seen in controls. This observation lead to the hypothesis that ZM447439 treated oocytes, although not completing MI, were progressing through MI at an accelerated rate.

Analysis of the chromatin prior to anaphase in ZM447439 treated oocytes revealed that the block to PBE was associated with a lack of chromosome congression and a consequent failure to segregate chromosomes. The chromosomes therefore occupied the cleavage furrow, an observation that may account for the failure to complete PBE. This finding is consistent with previous reports demonstrating that chromatin in the cleavage furrow of a mitotic cell has the ability to block cytokinesis, a so called ‘abscission checkpoint’ (Steigemann et al., 2009). The failure to complete polar body extrusion has also been reported in oocytes elsewhere. Oocytes depleted of INCENP, the Aurora B/C binding partner that is required for Aurora B/C activity, exhibit ‘membrane ruffling’ (Sharif et al., 2010). Injection of a kinase deficient Aurora C

construct also causes a failure to complete cytokinesis (Yang et al., 2010). This event is not dissimilar in appearance to the aborted polar body extrusion observed in this study and is accompanied by chromatin in the cleavage furrow. Additionally, Sharif et al., (2010) used the pan-Aurora inhibitor AZD1152 and observed resorption of polar bodies, suggesting cytokinesis failure is not an off target effect of ZM447439, but a consequence of reduced Aurora kinase activity.

One possible explanation for the failed congression and segregation of chromosomes during anaphase is that Aurora Kinase inhibition has prevented the assembly of a functional spindle. This seems likely given that Aurora Kinases are required in order for mouse oocytes to build a functional metaphase I spindle (Swain et al., 2008) and MII spindle (this study). This detrimental effect that Aurora Kinase inhibition has on spindle formation could be due to loss of Aurora A function, which is crucial for the assembly of a bipolar spindle in mitosis (Cowley et al., 2009) and in meiosis I (Ding et al., 2011; Saskova et al., 2008). It could also be due to inhibition of Aurora B which resides on the chromosome arms and centromeres during prometaphase as it travels with the CPC. Aurora B plays a role in chromatin condensation (Goto et al., 2002) during this time as well as in spindle assembly via inhibition of the microtubule destabilizing protein Op18 (Gadea and Ruderman, 2006). The role of Aurora C specifically with regards to spindle assembly in oocytes has been addressed by over-expression of kinase deficient Aurora C, and results in abnormal MI spindle formation (Yang et al., 2010).

In conclusion, Aurora kinase inhibition throughout maturation resulted in a failure to extrude a polar body in spite of an apparent acceleration of meiosis I and this is most likely a consequence of an inability to segregate chromosomes at anaphase. In addition these data demonstrate a role for Aurora kinases in organizing chromosomes onto a metaphase plate.

5.3.3 AURORAS HAVE TEMPORALLY DISTINCT ROLES DURING MATURATION.

The use of ZM447439 throughout maturation had highlighted two different effects, firstly the lack of congression and separation of the chromosomes, and secondly the possible shortening of the duration of meiosis I interpreted from the timing of the aborted polar body extrusion. In order to see if the latter could be examined

independently of the former, ZM447439 was added progressively later during meiosis I at 2 and then at 4 h.

Addition of ZM447439 at 2 h resulted in a small percentage of oocytes resorbing their polar bodies. Imaging with Hoechst revealed that these oocytes had lagging chromosomes at anaphase, which occupied the cleavage furrow. This seemed to be a less severe phenotype than that seen when ZM447439 was added at GVBD and suggested that Auroras had an important role during the first two hours of maturation which impacted on chromosome alignment and segregation.

Addition of ZM447439 at 4 h did not prevent PBE. Timelapse imaging showed that in these oocytes chromosomes frequently lagged at anaphase. However, they were not severe enough to cause resorption of the polar body.

The function of Aurora Kinases which impeded on chromosome alignment, segregation and thus PBE appeared to occur in the first few hours of maturation as a higher rate of polar body extrusion was observed when ZM447439 was added later during maturation. To test this ZM447439 was added from 0-2 h, and it resulted in a percentage PBE matching that of control oocytes. It seemed therefore that there is a period in early maturation during which Auroras are active if a high PBE rate is to be achieved (active either during 0-2 h, or 2 h onwards). This in turn suggests that the role of Auroras during this early period of meiotic maturation is in establishing something that is needed later during meiosis I, for example proper spindle assembly. Aurora inhibition from mid-prometaphase onwards does not undo this function, or at least not to the extent where it can block PBE. Together these data point to a role of Auroras in early prometaphase which likely involves spindle assembly and is distinct from the role of Auroras in the SAC and the timing of anaphase onset which is discussed below.

5.3.4 AURORA KINASE INHIBITION IN EARLY PROMETAPHASE SHORTENS MEIOSIS I.

Interestingly when ZM447439 was added to the media at either 0, 2 or 4 h the accelerated timings underlying meiosis I progression (measure as the time of either PBE or attempted PBE) were very similar, each around 1 hour earlier than in controls. In spite of differing outcomes in terms of cytokinesis, these groups all displayed the same underlying timing governing meiosis I. What was common to these different

experiments was the presence of ZM447439 in the culture media 4 h and onwards. This shortening of meiosis I suggested that Aurora Kinases have a function in delaying anaphase, and that it likely occurs after 4 h.

To further define the period during which ZM447439 caused the shortening of meiosis I the inhibitor was added to the culture media at 6 h. This also caused a quickening of meiosis I, with the timing of polar body extrusion being quicker than controls, but not as pronounced as when ZM447439 was added at 4 h. This suggested that Auroras were delaying meiosis I largely between 4 and 6 h, but also to a lesser extent after 6 h. This point is addressed further in Chapter 6.

The shortening of meiosis I is consistent with abrogation of the SAC. When the effects of ZM447439 addition were tested on nocodazole arrested oocytes, ZM447439 was able to partially rescue PBE rates and timing. In nocodazole arrested oocytes expressing cyclin B1-Venus, ZM447439 addition was also seen to initiate cyclin B1 degradation. These data add further weight to the hypothesis that inhibition of Aurora Kinases was bypassing the SAC and activating the APC. In support of this idea, abrogation of the SAC has been demonstrated in mitosis in the presence of ZM447439 (Ditchfield et al., 2003) or the Aurora inhibitor Hesperadin (Hauf et al., 2003; Santaguida et al., 2011), or following knockdown of Aurora B (Ditchfield et al., 2003). Additionally, Aurora B can maintain the SAC when it is artificially positioned close to kinetochores in somatic cells (Liu et al., 2009).

5.3.5 AURORA KINASES ARE REQUIRED TO CORRECT KINETOCHORE MICROTUBULE ATTACHMENTS

Lagging chromosomes were a common feature of anaphase following Aurora Kinase inhibition; therefore Auroras may have an important role in correcting erroneous attachment in mouse oocytes. Lagging chromosomes are thought to be created when one kinetochore (or sister kinetochore pair in meiosis I) is attached to both spindle poles (Gregan et al., 2011; Thompson and Compton, 2011). If the forces pulling the kinetochore at anaphase are balanced the chromosome remains at the spindle midzone, ultimately either blocking cytokinesis or segregating at random (Thompson and Compton, 2011). Not all erroneous attachments will result in lagging chromosomes, but lagging chromosomes are a readout for erroneous attachment. Consistent with this, previous work in mitosis shows that Aurora B has a role in

destabilizing kinetochore microtubule attachments (Hauf et al., 2003) and that Aurora B inhibition increases merotelic attachments and results in lagging chromosomes (Cimini et al., 2006). In mouse oocytes correction of microtubule-kinetochore attachments has also been shown to depend on Aurora Kinases (Kitajima et al., 2011), specifically Aurora C (Yang et al., 2010).

Work in mitosis showed that removal of incorrectly attached microtubules by Aurora B can be achieved directly through phosphorylation of members of the KMN complex which makes up the outer kinetochore plate (Akiyoshi et al., 2009; Biggins and Murray, 2001; Welburn et al., 2010). This phosphorylation weakens the binding capacity of kinetochores for microtubules. The role of the microtubule depolymerase MCAK is also important in this process (Knowlton et al., 2006). MCAK localizes to centromeres, as well as to spindle poles and to chromatin, during mitosis and meiosis (Kline-Smith et al., 2004; Vogt et al., 2010). In both divisions it translocates along with the CPC to the spindle midzone at the metaphase-anaphase transition. In mouse oocytes MCAK function has been shown to contribute to, but not be essential for, correction of attachment errors (Illingworth et al., 2010).

5.3.6 AURORA KINASES REDUCE ANEUPLOIDY

Given that ZM447439 addition caused a shortening of meiosis I and also generated lagging chromosomes, indicative of the presence of erroneous microtubule-kinetochore attachments, it seemed likely that these two events would culminate in an increase in aneuploidy. Indeed, it was demonstrated that incubation in ZM447439 from 4 h caused a significant, 6-fold increase in aneuploidy. This increase in aneuploidy in response to Aurora Kinase inhibition had not previously been demonstrated in female meiosis I (the cell division most responsible for generating aneuploidy in embryos). The likely reason for this is that use of Aurora inhibitors from prophase onwards or knockdown of Aurora C during meiosis I blocked PBE, preventing aneuploidy analysis. In this study, by using an Aurora Kinase inhibitor during mid-prometaphase, these confounding effects were sidestepped, revealing the role of Auroras in preventing aneuploidy in oocytes in meiosis I.

5.3.7 IS AURORA SAC FUNCTION DIRECT OR INDIRECT?

The ability of ZM447439 to shorten meiosis I is consistent with a bypassing of the SAC. In mitosis Aurora B is known to be able to destabilize erroneous microtubule-kinetochore attachments as discussed above, therefore it is possible that the role of Aurora B (and/or Aurora C in meiosis) in SAC signalling is actually indirect and is downstream of its error correction functions. In this scenario SAC signalling occurs due to the vacant kinetochore created after depolymerisation of erroneously attached microtubules. This vacant kinetochore would recruit SAC components according to the prevailing model of MCC production (Musacchio and Salmon, 2007). However there is evidence to suggest that the SAC signalling role of Aurora Kinases is distinct from that of its attachment-correction function. Under conditions where microtubules are completely depolymerized by nocodazole the SAC can still be bypassed by Aurora Kinase inhibition (Santaguida et al., 2011). The current study is in agreement with this observation. A slightly higher concentration of nocodazole was used compared to the study by Santaguida et al. (400nM vs. 330nM) which was shown to removed cold-stable kinetochore attachments and generate a robust SAC arrest. This arrest was bypassed by addition of ZM447439. Assuming that the role of Aurora Kinases was only in generating vacant kinetochores that in turn generate a SAC signal, then under conditions where kinetochores are already vacant and Mad2 is already present, inhibition of Aurora Kinases would not be expected to bypass the SAC. On the other hand, if Aurora Kinases have an additional function in maintaining the SAC signal directly (for instance by recruiting or phosphorylating SAC proteins), then the SAC signal would cease after inhibition of Aurora Kinases, leading to APC activation. The latter scenario is consistent with the data presented here, where ZM447439 caused rapid activation of the APC under conditions where k-fibres were absent.

5.3.8 SUMMARY

Together the above data suggest that Aurora kinases play multiple distinct roles in meiosis I in oocytes. Inhibition of Auroras during early meiosis I prevents proper chromosome segregation at anaphase and likely results in a failure to extrude the first polar body as a result of improper spindle formation. Meanwhile, Aurora inhibition during mid-prometaphase causes the duration of meiosis I to shorten and generates lagging chromosomes at anaphase, suggesting that Auroras have a role in determining

cell cycle length through the SAC and another role in correcting erroneous microtubule attachments during meiosis I in mouse oocytes.

Due to the nature of the experiments utilizing an Aurora Kinase inhibitor that was not specific to one Aurora kinase family member, it was not possible to attribute the above roles to individual kinases, and the phenotypes described in this chapter could be due to inhibition of any combination of the three kinases potentially present in mouse oocytes. In spite of this it has been possible to tentatively suggest some of the observed effects are attributable to certain kinases, due to what is known of the function of those kinases from other studies.

Finally these data give support to the hypothesis that Aurora Kinases function in SAC signalling directly, as well as indirectly through destabilizing erroneous kinetochore microtubule attachments.

6 CONTROL OF ANAPHASE TIMING AND EXIT FROM MEIOSIS I

6.1 INTRODUCTION

The exit from the first meiosis in oocytes is different from that of somatic cells; it was noted in 1997 that:

> *"… the first meiotic spindle and the metaphase plate appear, morphologically, to be fully formed 3 to 4 h before the onset of the first meiotic anaphase."* (Winston, 1997)

As shown in Chapter 3, k-fibre formation, loss of Mad2 from kinetochores and activation of the APC commenced between 4 and 5 hours after GVBD. APC activation in oocytes therefore appeared to be coupled to SAC satisfaction; as would be predicted based on what is known of the SAC. Whether SAC satisfaction and attainment of a metaphase plate are coupled as tightly as they are in mitosis where APC activation occurs promptly, within 3 minutes of cells reaching metaphase (Clute and Pines, 1999) seems unlikely as non-aligned bivalents which often have incorrect attachments fail to inhibit the APC in oocytes. The bigger difference however seems to be in the duration of APC activity that culminates in anaphase. In this study anaphase did not occur until 3-4 hours after SAC satisfaction. This contrasts with somatic studies, where cyclin B1 degradation is complete within tens of minutes, for instance lasting about 15 minutes in RPE1 cells (Mansfeld et al., 2011). Thus following activation of the APC, the time taken to sufficiently degrade cyclin B1 so as to permit anaphase is around 10 times longer in meiosis I of oocytes than the equivalent period in mitosis.

One remaining question therefore is what controls the duration of meiosis I after satisfaction of the SAC in oocytes? APC activation appears to be coupled to SAC satisfaction as expected, however it is the duration of APC activity that is much longer.

I therefore sought to investigate the activity of the APC in the period following SAC satisfaction, which had been established at 5 h after GVBD (Chapter 3). Exit from mitosis centres around the regulation of Cdk1. Cdk1 activity declines during exit from meiosis I concordantly with the degradation of its activating subunit, cyclin B1 (Hampl and Eppig, 1995). Additionally, studies in mitosis show that there is also significant regulation of Cdk1 by various phosphatases and kinases (Potapova et al., 2009). Therefore when investigating the length of meiosis I exit Cdk1 seemed a good starting

point. In addition, I had noted in chapter 5 that ZM447439 addition at 6 h (after the time of SAC satisfaction), was able to accelerate PBE (Figure 5.9). ZM447439 also appeared to produce higher APC activity than in controls (Figure 5.12). I therefore also decided to investigate the role of the Aurora kinases in MI exit.

6.2 CDK1 IN EXIT FROM MEIOSIS I

6.2.1 CDK INHIBITION CAUSES PREMATURE ANAPHASE ONSET

Following satisfaction of the SAC 5 hours after GVBD it takes the mouse oocyte an additional 3 hours to undergo anaphase in this F1 strain (Chapter 3). This raised the question, why shouldn't anaphase follow as soon as possible after metaphase? One candidate for this delay is Cdk1, which has a high activity during mid-meiosis I but a low activity during meiosis I exit (Hampl and Eppig, 1995). I first decided to test this by inhibiting Cdk1 using the pan-CDK inhibitor roscovitine, which has an IC value of 0.065µM for Cdk1 in vitro and a similar value for Cdk2,Cdk5, Cdk7 and Cdk9 whereas IC values for other major kinases are at least one order of magnitude higher (Bach et al., 2005).

Since an increase in Cdk1 activity is required for the process of GVBD (Solc et al., 2010), failure to undergo GVBD in the presence of roscovitine was used as a functional readout of Cdk1 inhibition. GV oocytes synchronised by arrest in milrinone were washed free and then incubated in M2 media supplemented with various concentrations of roscovitine. After 2 hours the oocytes were assessed for the presence of a germinal vesicle (Figure 6.1). It was found that 30 µM roscovitine was insufficient to completely block GVBD; however 100µM was an adequate concentration. Similar doses of 50-100µM have been used previously to cause a reduction in calcium oscillations in MII mouse eggs (Deng and Shen, 2000) whilst doses of 10 or 50µM have been used to completely inhibit GVBD in starfish or xenopus oocytes respectively (Meijer et al., 1997).

6.2.2 TIMING OF ANAPHASE DEPENDS ON TIMING OF CDK INHIBITION

The established concentration of 100µM was then tested on oocytes during maturation. Synchronised oocytes expressing H2B-mCherry mRNA were imaged at 5 minute

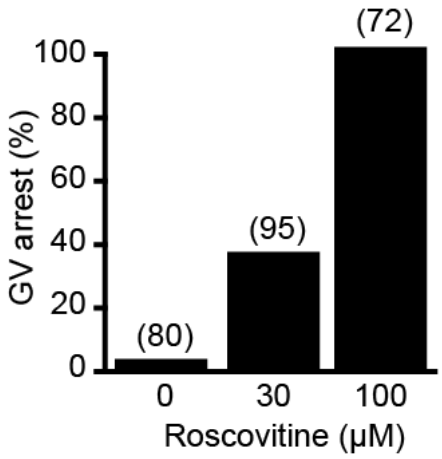

Figure 6.1 - The effect of various doses of roscovitine on GVBD

The percentage of oocytes remaining GV arrested 2 hours after washout from milrinone containing media is shown for different concentrations of roscovitine. Numbers of oocytes are shown in parenthesis.

intervals for mCherry and 100µM roscovitine was added at times between 3 and 7 hours after GVBD. Firstly the oocytes were assessed for their ability to undergo anaphase which was determined from the H2B-mCherry timelapse images (Figure 6.2 A). The main finding was that there was a significant increase in the ability of oocytes to undergo anaphase when roscovitine was added at later timepoints compared to earlier ones. For instance the percentage of oocytes undergoing anaphase increased significantly from 19.2% when roscovitine was added at 3 hours to 70.0% when roscovitine was added at 4 hours post GVBD (3h, n=26; 4h, n=21; P<0.001; Fisher's exact test; Figure 6.2 B). Further non-significant increases in the percentage of oocytes were seen as roscovitine was added later in meiosis I (5h, 86.4%, n=22; 6h, 91.4%, n=35; 7h, 100%, n=10).

These data suggest that the majority of oocytes are incapable of undergoing anaphase before 4 hours, but are capable of anaphase at any timepoint from 4 hours after GVBD onwards. This is in agreement with the fact that k-fibres have been shown to form between 4 and 5 hours after GVBD (Chapter 3) which probably facilitate anaphase.

When the time of anaphase in these oocytes was examined, the outcome also varied depending on when roscovitine was introduced to the media. The timing of anaphase was measured with respect to the addition of the roscovitine, and became progressively shorter as roscovitine was added at later timepoints. As such it was found that anaphase onset required 60±9 minutes when roscovitine was added at 3 hours and only 24±7 minutes following roscovitine addition at 7 hours after GVBD (Figure 6.2 C).

6.2.3 TIMING OF ANAPHASE CAN BE MODIFIED BY CYCLIN B1 LEVELS

To test the above idea further I decided to repeat the addition of roscovitine at 6 hours after GVBD, but after manipulating the cyclin B1 levels in the oocytes. To do this GV oocytes were injected with H2B-mCherry mRNA as before but also with a large injection of cyclin B1-GFP mRNA, estimated to be around 100pg (~100 times greater than used elsewhere in this thesis). This injection caused expression of cyclin B1-GFP that was sufficient to mask any degradation during the time period normally associated with the onset of APC activity (Figure 6.3 A, note that at 4-6 hours GFP intensity continues to rise).

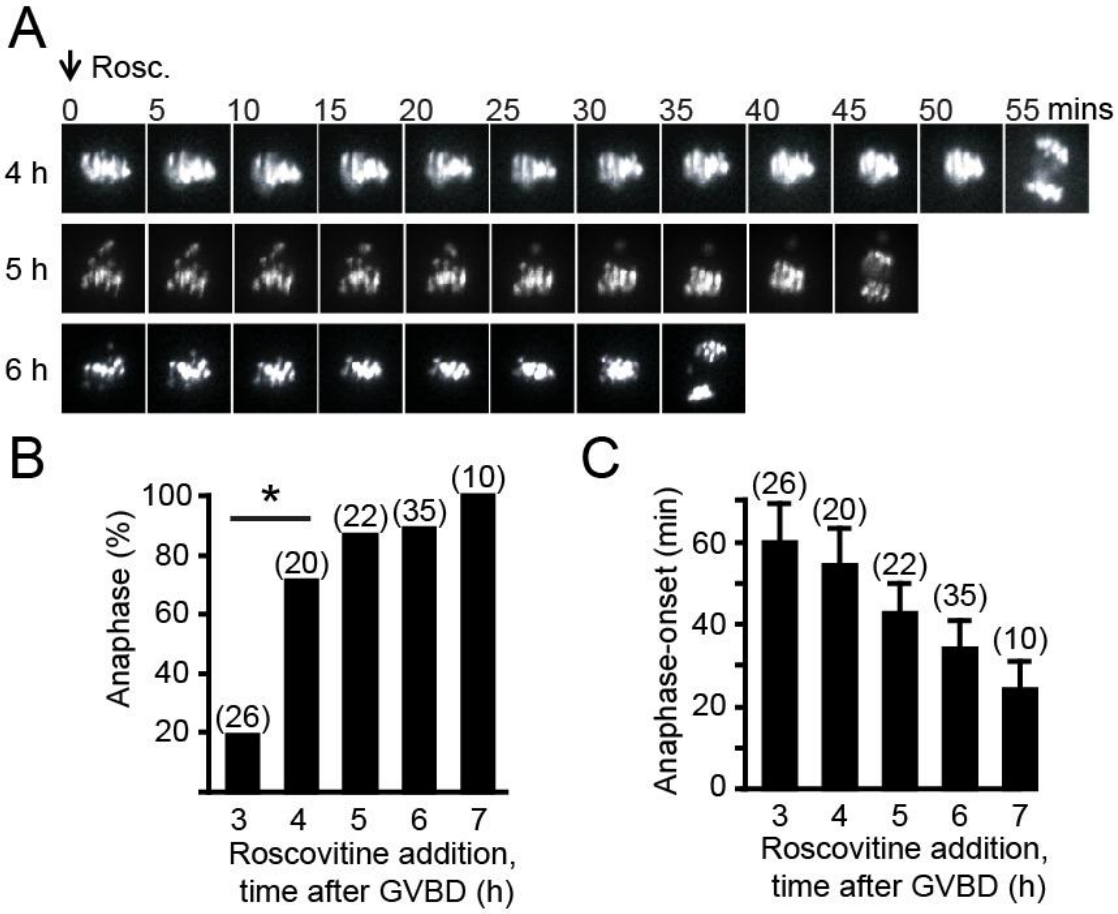

Figure 6.2 - The effect of roscovitine addition to oocytes at various times during Meiosis I

*(A) Timelapse images of oocytes microinjected with H2B-mCherry mRNA and then matured to the indicated time post GVBD. At this time 100µM roscovitine was added to the media. (B) The percentage of oocytes undergoing anaphase when roscovitine was added at the times indicated. *P<0.001. (C) The time taken for oocytes to enter anaphase following the addition of roscovitine to the media at the times indicated. (B,C) number of oocytes imaged is shown in parenthesis.*

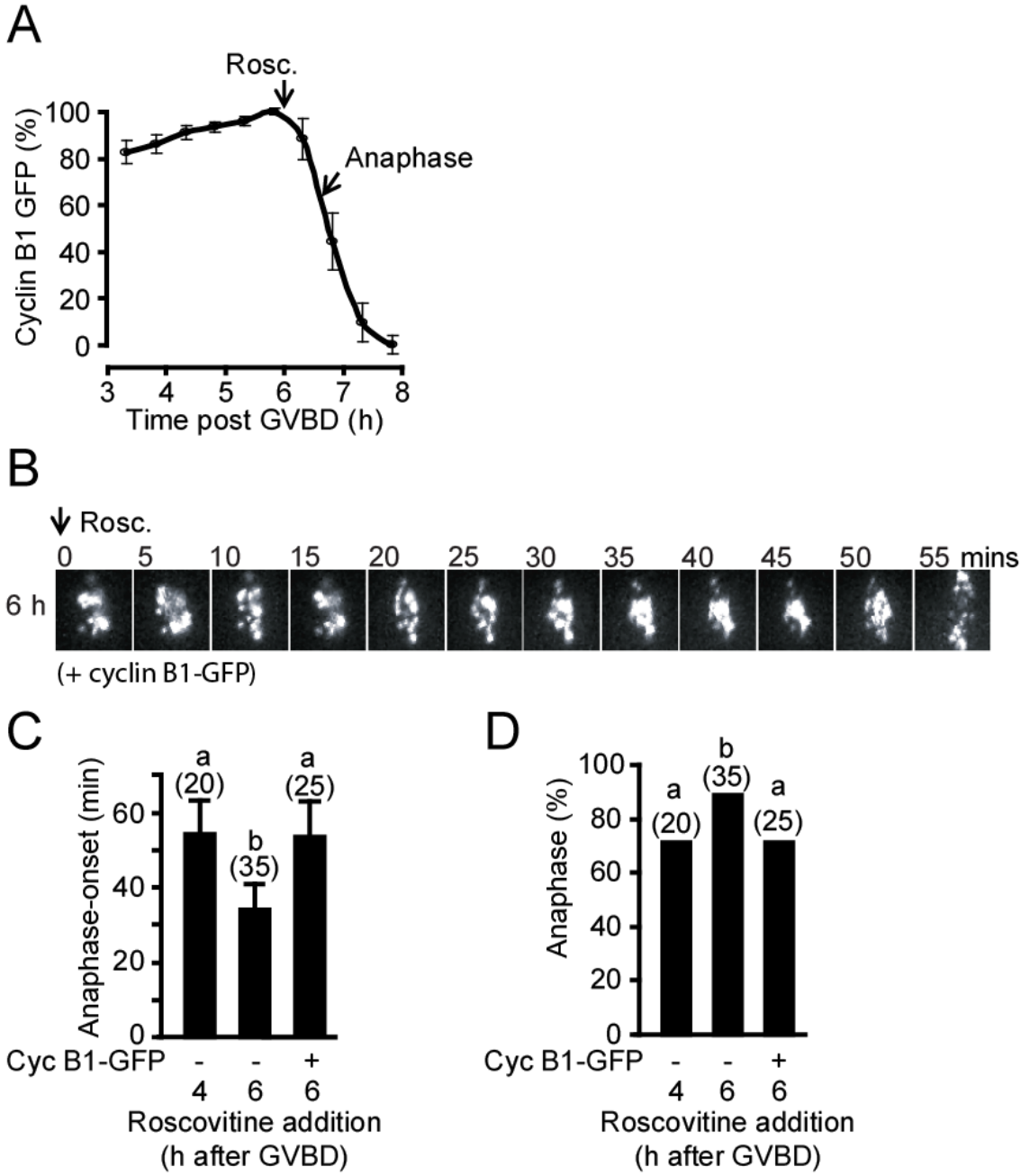

Figure 6.3 - Anaphase in oocytes with high levels of cyclin B1-GFP following roscovitine addition

(A) Relative GFP intensity against time after GVBD in oocytes expressing a large quantity of cyclin B1-GFP. Note there is no decline between 4 and 6 h as there would be in oocytes injected with small amounts of mRNA. n=25 (B) H2B-mCherry timelapse from an oocyte overexpressing cyclin B1-GFP following roscovitine addition at 6 h. (C) The timing of anaphase following roscovitine addition at 4 or 6 h and with or without

5

cyclin B1-GFP overexpression. (D) The percentage of oocytes undergoing anaphase following roscovitine addition at 4 or 6 h and with or without cyclin B1-GFP overexpression. (C,D) the number of oocytes imaged is shown in parenthesis.

When roscovitine was added to these oocytes at 6 hours after GVBD the timing of anaphase was found to be 52±9 minutes later. This timing was significantly later than in oocytes not expressing high levels of cyclin B1 when they were treated with roscovitine at 6 hours after GVBD (6 h with cyclin B1-GFP, 52±9 minutes, n=25; 6 h without cyclin B1-GFP, 34±7 minutes, n=35; P<0.001, Tukey's Multiple Comparison test; Figure 6.3 B, C) but was not significantly different from the timing observed after roscovitine addition to control oocytes at 4 h (6 h with cyclin B1-GFP, 52±9 minutes, n=25; 4 h without cyclin B1-GFP, 55±9 minutes, n=20; P>0.05, Tukey's Multiple Comparison Test). Following cyclin B1-GFP injection, the percentage of oocytes undergoing anaphase was also similar to that of control oocytes treated with roscovitine at 4 hours after GVBD and significantly different from that of control oocytes at 6 hours after GVBD (Figure 6.3 D).

In summary, raising the cyclin B1 levels caused the time taken to enter anaphase to increase, suggesting that the time taken to achieve anaphase may be proportional to cyclin B1 levels and possibly to Cdk1 activity remaining in the oocyte.

6.3 APC ACTIVITY AND EXIT FROM MEIOSIS I

6.3.1 CDK ACTIVITY PREVENTS MAXIMAL APC ACTIVITY

The experiments utilising roscovitine suggested that cyclin B1 levels may have a role to play in controlling the timing of anaphase. It has been established that cyclin B1 is degraded during the latter stages of meiosis I by APC^{Cdc20} (Jin et al., 2010; Reis et al., 2007). Therefore I next decided to look at APC activity during exit from meiosis I.

After addition of roscovitine to oocytes expressing cyclin B1-GFP it was noted that the APC became activated such that the cyclin (an excessive amount) was degraded within 2.7±0.25 h (Figure 6.3 A). In controls the time taken from the onset of APC activity to completion of cyclin B1-GFP destruction was significantly longer at 5.3±2.0 h[a] (P<0.001, Mann Whitney), suggesting that the APC might not be working at its maximal rate during meiotic exit in control oocytes (Figure 6.4 A).

[a] Note that PBE occurs before degradation of cyclin B1-GFP reaches its minimum; therefore this timing is longer than the 3-4 h typically taken for PBE.

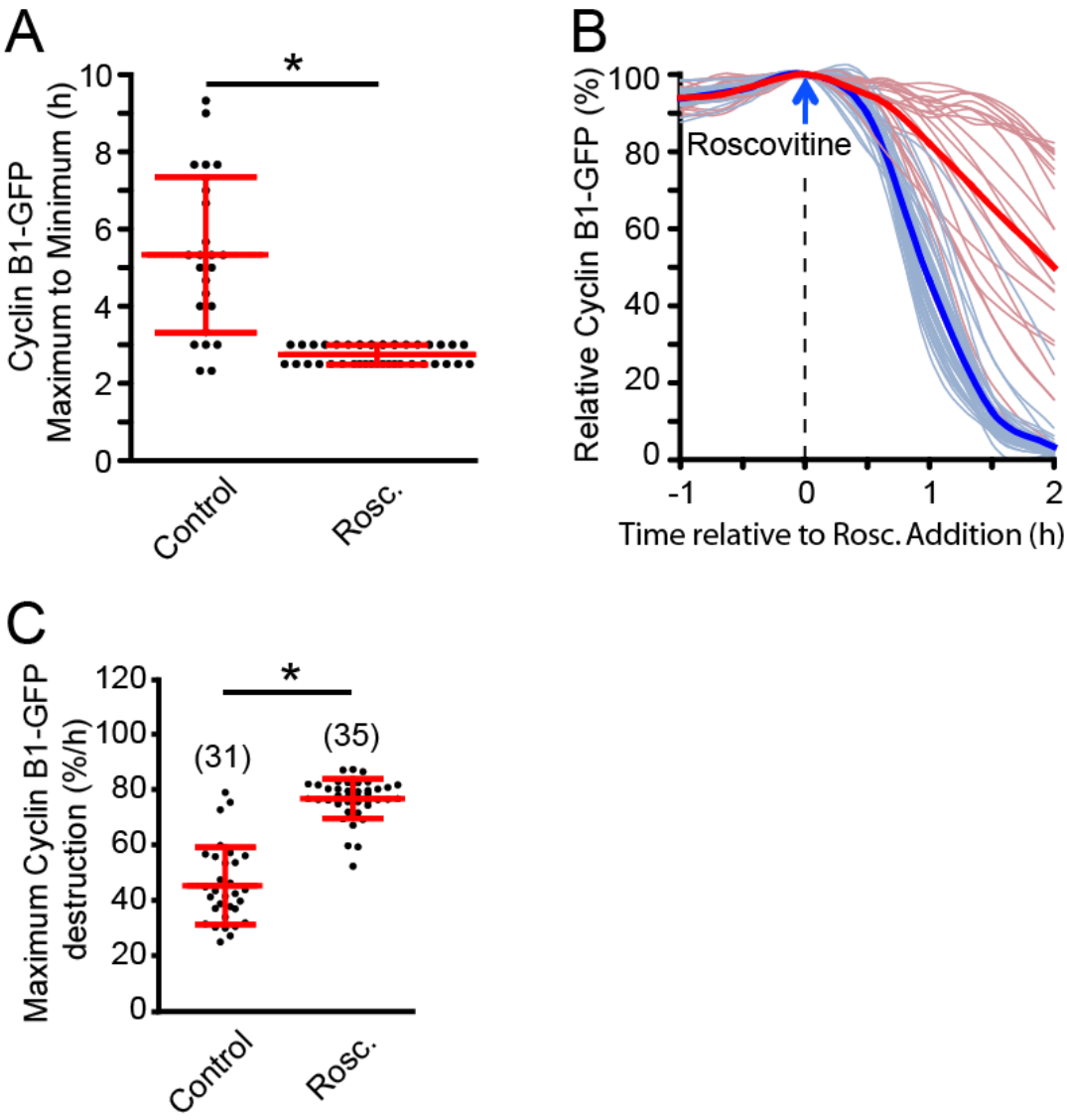

Figure 6.4 - The effect of roscovitine on APC activity

*(A) Comparison of the time taken from the maximum to the minimum cyclin B1 fluorescence levels in oocytes treated with or without roscovitine. Asterisk indicates P<0.001, unpaired t-test. (B) Traces of cyclin B1-GFP in oocytes with (blue) or without (red) the addition of roscovitine were normalized to their maximum fluorescence (100%) and to the time of roscovitine addition or maximal fluorescence for control oocytes (0h). (C) A comparison of the maximal cyclin B1-GFP destruction rates in control oocytes or in oocytes treated with 100µM roscovitine. *P<0.001. Number of oocytes analysed are indicated in parenthesis.*

When cyclin B1-GFP traces from control and roscovitine treated oocytes were normalised with all maxima set to 100% and time 0 it was possible to directly compare the two degradation profiles (Figure 6.4 B). It was readily apparent that the APC was more active under conditions where CDKs were inhibited. The onset of cyclin B1-GFP destruction came soon after roscovitine addition in the experimental group, whereas in controls cyclin B1-GFP destruction onset was more gradual.

A comparison of the maximal rate of cyclin B1-GFP degradation achieved in both groups also indicated that the APC was far more active in the roscovitine treated group (Roscovitine, 77±7 %/h, n=42; control, 46±14 %/h, n=31, *P<0.001, Tukey's Multiple Comparison Test; Figure 6.4 C). Together these data suggest that a) the APC is not maximally active under control conditions and b) that high CDK activity restricts APC activity.

6.3.2 AURORA KINASE ACTIVITY PREVENTS MAXIMAL APC ACTIVITY

I next tested whether the SAC had any role in inhibiting the APC during the exit from meiosis I. As demonstrated in Chapter 5 the Aurora Kinase inhibitor ZM447439 can bypass the SAC. Aurora Kinase B has also been demonstrated to be a part of the SAC pathway, independent of its microtubule destabilising functions, in somatic cells (Ditchfield et al., 2003; Nilsson et al., 2008; Santaguida et al., 2011). Therefore ZM447439 was added to the culture media of oocytes injected with mRNA encoding cyclin B1-GFP at 6 h, whilst they were being imaged. This time was chosen to add the drug because oocytes were already degrading cyclin B1-GFP, giving a pre-addition rate of APC activity against which to compare the effects of ZM447439. As a further control an additional group of oocytes were imaged without the addition of ZM447439. The cyclin B1-GFP traces for the two groups were first normalised such that the maxima were set to 100%. Then the traces were translocated in the y axis such that at the 6 hour timepoint, each trace was equal to 50% of maximal cyclin B1-GFP. This did not change the range of cyclin B1-GFP intensities for the traces, which still had a maximum range of 100%. In this way the two groups could be visualised relative to each other (Figure 6.5 A). The rates of cyclin B1-GFP destruction were then quantified using the 30 minute window before and after the addition of the ZM447439 (or the equivalent time in controls).

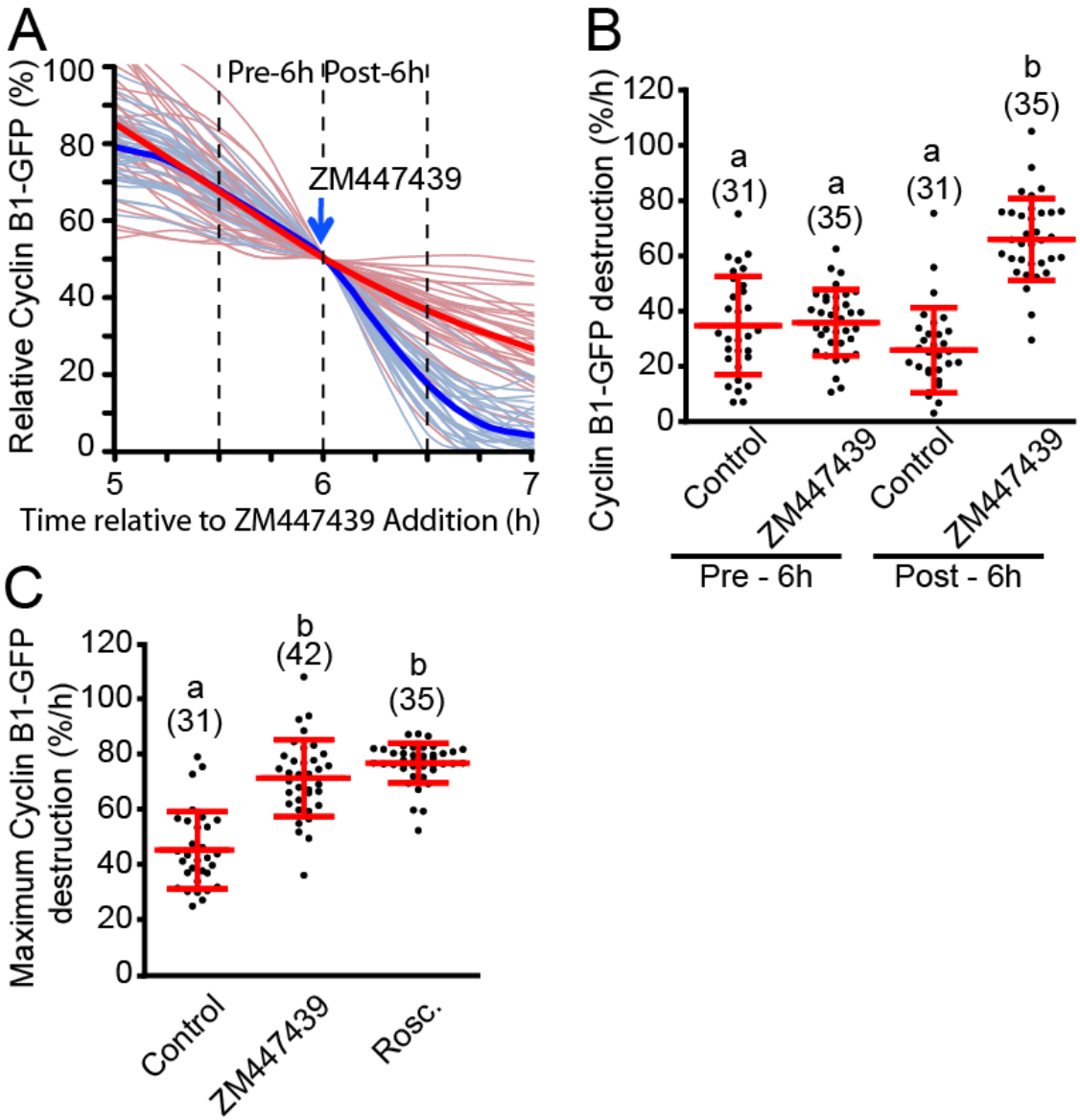

Figure 6.5 - The effect of ZM447439 on APC activity

(A)Traces of cyclin B1-GFP in oocytes treated with (blue) or without (red) ZM447439 at 6 hours after GVBD. Bold line indicates mean of all traces. All traces were normalized with maxima at 100% and minima at 0%, and then translocated such that all traces were at 50% at 6 h. (B) Comparison of the rates of cyclin B1-GFP degradation before and after 6 h in each group, measurements were made in the 30 min periods either side of 6 h indicated by the dashed lines in 'A'. (C) The maximal APC activity from each oocyte in controls, or after addition of roscovitine or ZM447439. Different letters indicate groups differ significantly (P<0.001, ANOVA with Tukey's Multiple Comparison Test).

The rates of cyclin B1-GFP destruction prior to the addition of ZM447439 were not significantly different between the two groups, indicating that the oocytes to which ZM447439 was added were degrading cyclin B1 with normal kinetics before drug addition (ZM pre-6 h, 35.9±12.0%/h n=35; Control pre-6 h, 34.8±17.7%/h, n=31; $P<0.05$, Tukey's Multiple Comparison Test; Figure 6.5 B). However, comparison following 6 h showed that ZM447439 addition caused a significant increase in the rate of cyclin B1 destruction (ZM post-6h, 65.9±14.8%/h, n=35; Control post-6 h, 25.9±15.4%/h, n=31; $P<0.001$, Tukey's Multiple Comparison Test).

When the maximal cyclin B1-GFP degradation rates in oocytes treated with ZM447439 were compared against control oocytes they were also found to be significantly higher (Control, 45.5±14.0%/h, n=31; ZM447439, 71.6±13.9%/h, n=35; $P<0.001$, Tukey's Multiple Comparison Test; Figure 6.5 C). Interestingly, the maximal rate of cyclin B1-GFP degradation after ZM447439 treatment was not significantly different from those observed in oocytes treated with roscovitine (ZM447439, 71.6±13.9%/h, n=35; roscovitine, 77.1±7.2%/h, n=42; $P>0.05$, Tukey's Multiple Comparison Test; Figure 6.5 C).

Together these data provide evidence that suggest the APC is not maximally active during exit from meiosis I and that one or more pathways involving CDKs and Aurora kinases are likely partially inhibiting the APC during this time.

6.4 DISCUSSION

Following establishment of the stable k-fibres the final period of meiosis I is entered. This period is defined by a gradual decline in the APC substrate cyclin B1, indicating that the APC is maintained in an active state during this period. Given then, that the SAC is satisfied and APC active, why doesn't anaphase occur shortly afterwards, for example within minutes of completion of the stable k-fibres? The experiments described in this chapter are the start of an investigation into why the duration of APC mediated cyclin B1 and securin degradation that defines the exit from meiosis I are drawn out for around 3 h or put simply, why anaphase does not follow quickly after SAC satisfaction. At this stage these experiments have generated more questions than answers, and what is presented here is still a work in progress. I have included it in this thesis however because it starts to answer the questions raised by observations in

earlier chapters. As a consequence of the incompleteness of this body of work this discussion is more speculative than the others.

The main findings of this chapter are that CDK inhibition is sufficient for anaphase onset anytime later than 4 h and that the time taken to reach anaphase following CDK inhibition becomes progressively shorter as meiosis I advances. In addition the APC is not maximally active during exit from MI, and APC activity appears to be reduced as a consequence of CDK activity and Aurora kinase activity.

6.4.1 CDK INHIBITION HASTENS ANAPHASE

The observation that anaphase ensues rapidly after the addition of roscovitine has been seen before in mitotic cells (Skoufias et al., 2007). Since anaphase onset occurs sooner following CDK inhibition, this suggests that CDK may have a role in delaying anaphase, even after the apparent satisfaction of the SAC. This is further discussed in section (6.4.4).

A further observation was that the time taken to achieve anaphase following CDK inhibition became progressively shorter as the inhibitor was added at times closer to the normal timing of anaphase (8 h). This decline in the time taken for oocytes to undergo anaphase following roscovitine addition followed a trend, peaking in mid MI, around the time of SAC satisfaction (4 h) and declining as anaphase (8 h) is approached. This trend resembles that of cyclin B1 levels (Figure 3.8) and of Cdk1 activity during exit from meiosis which peak in mid-meiosis and decline as anaphase approaches (Hampl and Eppig, 1995).

Although not by any means the only possibility, one explanation for these observations is as follows: Cdk1 activity at the time of roscovitine addition determines to what extent Cdk1 substrates are phosphorylated (high activity, high phosphorylation). This level of phosphorylation in turn determines the length of time taken for phosphatases to dephosphorylate these Cdk1 substrates (a pre-requisite for anaphase, Potapova et al., 2011). Thus, if Cdk1 activity is low when roscovitine is added, anaphase could occur sooner than if Cdk1 activity were high because it would take the counteracting phosphatases less time to remove the phosphorylation on CDK substrates. Interestingly, exit from mitosis following Cdk1 inhibition can be prevented by the simultaneous inhibition of phosphatase activity (Skoufias et al., 2007).

6.4.2 COULD CYCLIN B1 LEVELS DETERMINE THE TIMING OF ANAPHASE?

Cdk1 is dependent on its binding partner cyclin B1 for activation; it was therefore possible that cyclin B1 levels would dictate the time remaining to anaphase. As mentioned above, cyclin B1 levels declined in step with Cdk1 activity (Hampl and Eppig, 1995). To test the effect of cyclin B1 on the timing of meiotic exit cyclin B1 levels were manipulated by injection of mRNA. This resulted in the time taken for anaphase onset to increase relative to controls with only endogenous cyclin B1. This finding was consistent with the proposed explanation above, it is important to note however that high levels of cyclin B1 may have had many other effects which cannot be accounted for and the hypothesis needs to be tested by other means before any firmer conclusions can be drawn.

Interestingly, one study indicated cyclin B1 is in an approximate 10-fold molar excess of Cdk1 in mouse oocytes (Kanatsu-Shinohara et al., 2000). The increase in the time taken to anaphase following roscovitine is not consistent with this finding. If cyclin B1 were already in excess one might expect Cdk1 activity to be saturated, expression of further cyclin B1-GFP should not increase Cdk1 activity if this were the case. However, there are lines of evidence that suggest Cdk1 activity is sensitive to cyclin levels in mouse oocytes. Injection of Cyclin B1 into GV stage oocytes causes release from GV arrest, an event consistent with an increase in Cdk1 activity (Reis et al., 2006). Additionally, Hampl & Eppig (1995) demonstrated that increasing cyclin B1 levels during MI arrest resulted in increased Cdk1 activity and that all nascent cyclin B1 at metaphase was incorporated into a complex with Cdk1. Thus multiple lines of evidence suggest that cyclin B1 is limiting with regards to Cdk1 activity during oocyte maturation.

6.4.3 THE MITOTIC EXIT NETWORK

An alternative mechanism by which Cdk1 could be regulated is by changes in its phosphorylation status (Chow et al., 2011). Cdk1 requires the presence of activating phosphorylation and removal of inhibitory phosphorylation to be active. This regulation of Cdk1 phosphorylation status is part of the mitotic exit network (MEN) brought about by changes in the activities of various kinases and phosphatases (Potapova et al., 2009; Queralt and Uhlmann, 2008; Toth et al., 2007; Visintin et al., 1998).

During entry into mitosis Cdk1 activity is raised by positive feedback loops. Inhibitory phosphorylation on Cdk1 is removed because Cdk1 inhibits its inhibitory kinase Wee1 and activates its activating phosphatase Cdc25, thus promoting its further activation (Rime et al., 1994; Solc et al., 2010). During exit from M-phase Cdk1 is inhibited by adding back the inhibitory phosphorylation. In cycling *Xenopus* egg extracts inhibitory phosphorylation of Cdk1 and loss of activating phosphorylation have been shown to precede cyclin degradation (Chesnel et al., 2007; D'Angiolella et al., 2007). This suggests that it is not only proteolysis that regulates mitotic exit, but also an interruption to the positive feedback loops that generated the high Cdk1 activity when entering mitosis.

The inhibitory Cdk1 phosphorylation site is the target of Wee1 kinase and Cdc25 phosphatase (Potapova et al., 2009). Cdc25 activity is promoted by Cdk1 phosphorylation upon entry to M-phase, but is inactivated by PP2A activity around the time that Cdk1 activity starts to decline (Forester et al., 2007; Lorca et al., 1992). Wee1 therefore becomes dominant, providing inhibitory phosphorylation of Cdk1 (Chow et al., 2011). Together these events all lead to a rapid feed forward inhibition of Cdk1 which in the in-vitro system takes just 8 minutes (D'Angiolella et al., 2007; Stanford and Ruderman, 2005). In addition, Cdc14 is a major upstream phosphatase involved in inhibition of Cdk1 during mitotic exit. Its down-regulation leads to maintained activity of Cdc25 and Cdk1, blocking exit from mitosis (D'Amours and Amon, 2004; Stegmeier and Amon, 2004; Tumurbaatar et al., 2011).

A Cdk1 inhibitory pathway has been observed in *Xenopus* cell free systems (Chesnel et al., 2007; D'Angiolella et al., 2007), human cell lines (Chow et al., 2011; Potapova et al., 2009; Tumurbaatar et al., 2011), and yeast (Visintin et al., 1998), demonstrating the MEN is conserved; inactivation of the phosphatase Cdc25 and activation of phosphatases Cdc14, Wee1 and Myt1 are common themes. Together these observations suggest a conserved and essential role for phosphatases in mitotic exit.

The importance of phosphatase activity is likely to be similar for mammalian oocytes too, as injection of antibodies to inhibit Cdc14A delays exit from Meiosis I (Schindler and Schultz, 2009). It is not clear however if inhibiting phosphatases delays meiotic exit by preventing Cdk1 inactivation, by preventing dephosphorylation of Cdk1 substrates, or by another mechanism altogether. This point could be tested in future work, possibly by using morpholino knockdown of various phosphatases, to determine which are most

important in meiotic exit and if they can prevent the rapid exit from meiosis brought about by Cdk1 inhibition.

6.4.4 THE APC IS NOT MAXIMALLY ACTIVE FOLLOWING SAC SATISFACTION IN MI

Following inactivation of Cdk1 with roscovitine at 6 h, rapid degradation of a large excess of cyclin B1 was observed. The rate of destruction was significantly greater than that seen during a normal exit from meiosis I. This suggested that the APC has a greater capacity to degrade substrates than is normally used. A similar result was seen after inhibition of Aurora Kinases using ZM447439. During an unperturbed exit from meiosis the process of cyclin B1 destruction takes over 5 h, but could potentially occur in less than 3 h if the APC were fully active.

It would be of interest to know how two different groups of kinases both decrease the activity of the APC. One further experiment would be to test for synergy between the two inhibitors, roscovitine and ZM447439. If there was none, this might suggest that the two were acting on the same pathway, or that either alone gives the maximal APC activity.

Cdk1 is known to have many phosphorylation sites on APC subunits, however, these are considered to increase APC activity (Kraft et al., 2003), therefore it seems unlikely that Cdk1 inhibition would result in increased APC activity through this route. Given that Aurora B (likely C in meiosis) forms part of the SAC, and the SAC is able to restrict APC activity, this seems a more likely route by which these drugs might be acting. Aurora Kinase inhibition has been shown to bypass the SAC (Chapter 5) and thus might reduce SAC inhibition of the APC. Cdk1 might also act via the SAC although less directly, as Cdk activity has been shown to reduce Cdc20 interaction with the APC and increase Mad2 binding to Cdc20, making the SAC more effective in the presence of Cdk1 activity (D'Angiolella et al., 2003).

Careful recordings of APC activity in mouse oocytes have been performed before (McGuinness et al., 2009). In this work McGuinness and colleagues find only a small increase in the rate of APC activation following knockout of the SAC protein Bub1. This appears contrary to the significant increase in SAC activity observed following addition

of ZM447439, and further experimentation will be required to determine the reason for these disparate results.

6.4.5 CYCLIN B1 DESTRUCTION IS INCOMPLETE IN MEIOSIS I

Another possible reason why the APC is regulated differently during MI exit is that oocytes have a requirement to enter immediately into MII following MI. Cyclin B1 degradation during normal exit from meiosis I is incomplete as has been observed many times before (Winston, 1997). There are conflicting accounts of whether Cdk1 activity is also partially retained during the MI to MII transition. Hampl and Eppig (1995) suggest Cdk1 activity remains several fold higher than GV levels, whereas Gorr et al., (2006) suggest it does decline back to GV levels by virtue of separase. In either case, rapid reactivation of Cdk1 is important in oocytes as it allows immediate entry into the next meiotic division, without an intervening S-phase (Perez et al., 2002; Picard et al., 1996; Taieb et al., 2001). In agreement with this, if cyclin B1 is knocked down, oocytes will fail to enter MII (Ledan et al., 2001). Thus the profile of APC activity in exit from female meiosis may be regulated differently to that in mitotic cells. Additionally, the mutual inhibition of Cdk1 and separase may have a role to play in reducing the requirement for cyclin B1 destruction during the MI to MII transition (Gorr et al., 2005; Gorr et al., 2006).

6.4.6 AN EVOLUTIONARY PERSPECTIVE

One more possible reason to explain the long period of APC activity during MI exit is that such a delay to anaphase confers an evolutionary selection advantage. The observation in Chapter 4, that non-aligned bivalents often persisted during this period of meiotic exit, something that has not been observed in somatic cells, raised the intriguing possibility that a slow exit from meiosis I in oocytes would be of benefit to an oocyte, increasing the chances of all bivalents achieving alignment prior to anaphase. If for instance, anaphase occurred at 6 h, ~1 h after SAC satisfaction, aneuploidy levels would be far greater, possibly as high as 30% based on the percentage of oocytes with non-aligned bivalents at that time. With regards to natural selection, it is easy to imagine that there would be a tremendous selection advantage for animals producing oocytes with the correct number of chromosomes. A SAC that was sensitive to incorrect attachment across bivalents would be the best solution, but perhaps the architecture of the mono-orientated sister kinetochore pairs, or the vast cytoplasm that

are unique to MI precluded this sensitivity. The SAC in meiosis utilizes the same basic set of proteins that are used in mitosis but it is possible these proteins may be more suited to generating a checkpoint signal based on cues created by dyads instead of bivalents where the kinetochore structure is different and initial attachments are often incorrect. It may be therefore, that the easiest path to reducing aneuploidy was to evolve a delayed anaphase, specifically in MI of oocytes.

6.4.7 SUMMARY

This chapter has demonstrated that the APC in oocytes is not active at its maximal rate. The mechanism by which APC activity is restrained is unknown, but may involve modulation of the APC by SAC activity and/or by residual Cdk activity. Regardless of the mechanism, the reason why oocytes delay anaphase for several hours following SAC satisfaction is interesting in its own right and could be to do with preserving a proportion of cyclin B1, such that Cdk1 activity can quickly be restored allowing entry into MII, or it is also possible that slow-exit from meiosis I is an evolutionary response to the high aneuploidy rate seen in oocytes. Prolonging meiosis I may be beneficial because it increases fertility by allowing more time for correction of erroneous microtubule attachments that are so common in MI, thus reducing oocyte aneuploidy.

7 GENERAL DISCUSSION

7.1 SUMMARY

The experimental chapters in this thesis have demonstrated that in the F1 stain investigated:

- The loss of Mad2 from kinetochores, the timing of APC activation and the timing of K-fibre formation occur concomitantly between 4 and 5 hours after GVBD.
- Non-aligned bivalents are a common feature during meiosis I.
- Activation of the APC occurs independently of complete chromosome alignment on the spindle, and therefore the SAC does not effectively inhibit the APC in response to some alignment errors.
- Non-aligned bivalents can persist until anaphase causing aneuploidy.
- Non-aligned bivalents are likely to be undergoing a process whereby they achieve bi-orientation, as they have varying microtubule attachments, recruit varying amounts of Mad2 and display movements suggestive of changing microtubule-kinetochore interactions.
- The role of Aurora Kinases has been established as a part of the SAC in meiosis I, as their inhibition bypasses a nocodazole arrest.
- Aurora kinase activity is required to retain ploidy during meiosis I.
- There is a long period of time between SAC satisfaction and anaphase, during this time the rate concentration of cyclin B1 may influence the timing of anaphase.
- The APC is not maximally active after SAC satisfaction; pathway(s) involving Aurora kinases and Cdks restrain its activity.

7.2 DISCUSSION

7.2.1 ANEUPLOIDY IN OOCYTES

A common theme amongst much of the work in the field of oocyte biology is aneuploidy. This is because it is the cause of a large portion of miscarriages, which are estimated to effect around 30% of pregnancies (Wilcox et al., 1988) and is also the cause of genetic disorders such as Down syndrome.

The findings of this thesis are relevant to the aetiology of aneuploidy in two ways. Firstly, for aneuploidy to occur there must be an error of some kind. This could be a failure of homologous chromosomes to recombine during prophase creating univalents in meiosis I (Tease et al., 2002). Univalents could also be generated by a premature loss of arm cohesin, for instance as a consequence the gradual attrition of cohesin during the long prophase arrest, during which time cohesin is not replenished (Revenkova et al., 2010; Tachibana-Konwalski et al., 2010). It has been proposed that the loss of centromeric cohesin could also cause other types of errors, such as promoting merotelic attachment (Chiang et al., 2010, Figure 7.1), although this remains to be demonstrated. Secondly, following the initial error the oocyte must fail to detect this error, or, having detected it, must fail to respond appropriately. In other words there would be an inadequacy in the SAC that would allow the oocyte to pass through the first meiotic division in spite of the potential for aneuploidy.

In this thesis, I have provided evidence for both of the above points. Firstly, I have shown another type of error, non-aligned chromosomes, are common in meiosis I. Secondly I have demonstrated the SAC in oocytes cannot inhibit the APC in response to such errors, thus allowing the error to potentially persist through anaphase, generating aneuploidy. It appears that in this case the erroneous chromosome may be detected, as their kinetochores display elevated levels of Mad2, however, this does not seem to translate into inhibition of the APC.

Whether the SAC on relatively insensitive and does not recruit sufficient Mad2 in response to incorrect or absent attachment on sister kinetochore, or if the subsequent amplification of the SAC signal to a level that can completely inhibit all APCs is deficient is still an open question, and one which should be addressed in the near future. In either case however, it seems that modest errors, such as a small number of misaligned chromosomes do not prevent anaphase. It therefore stands to reason that other potential causes of aneuploidy, such as the presence of univalents, or bivalents that can form incorrect attachments would not sufficiently engage the SAC either.

7.2.2 APC ACTIVITY

Exit from meiosis I seems a relatively underexplored area of oocyte research. Whilst much research has focused on the biochemical pathways active during mitotic exit,

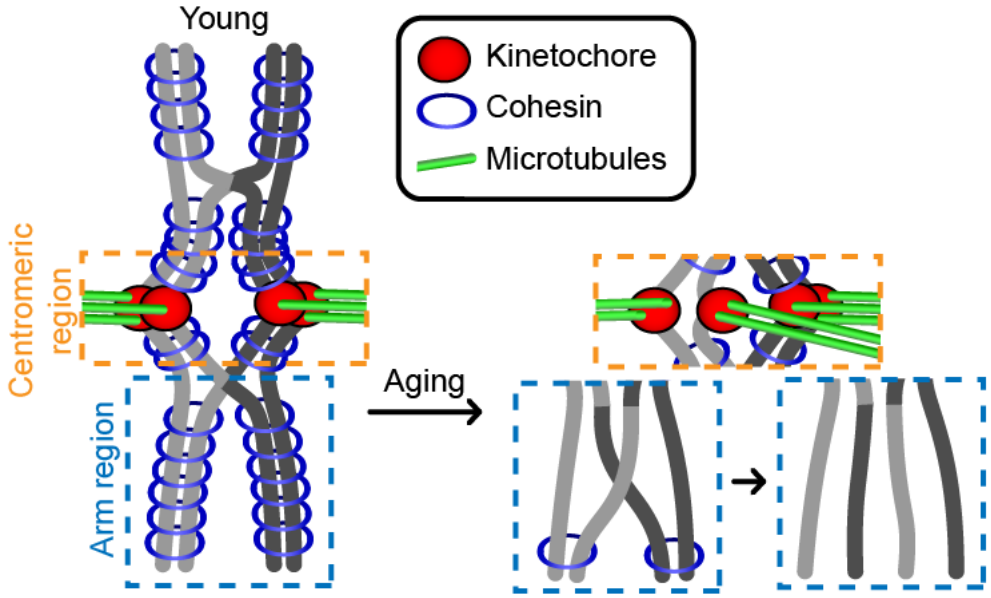

Figure 7.1 - Possible effect of aging on chromosome cohesion and microtubule attachment

Young oocytes with a full complement of cohesin maintain their sister kinetochores as one functional unit, facilitating mono-orientation. Arm cohesin prevents premature separation of homologous chromosomes. In aged oocytes loss of centromeric cohesin could lead to separation of sister kinetochores, potentially permitting their bi-orientation in MI. Loss of arm cohesin could result in the two homologous chromosomes disjoining prematurely.

such as the FEAR and MEN networks (Chesnel et al., 2007; Chow et al., 2011; D'Angiolella et al., 2007; Potapova et al., 2009; Tumurbaatar et al., 2011; Visintin et al., 1998), and the activity of the APC during the same period (Clute and Pines, 1999; Floyd et al., 2008; Lindon and Pines, 2004), the equivalent research has largely not been conducted in oocytes. Given the lengthy duration of meiosis I, and the fact that a large portion of this comes after APC activation (i.e. hours 5-8 of meiosis I in the strain used here), it seems important to better understand the relevance of this period. Potentially, this portion of the cell cycle could be important for staving off aneuploidy by permitting sufficient time for proper chromosome attachment to the spindle. In the absence of a SAC that is sensitive enough to respond to individual kinetochores, such as the one present in somatic cells, the next best defence against aneuploidy may be to elongate the duration of meiosis I. This idea has not yet been tested in oocytes and could form the basis of new research.

8 APPENDIX

8.1 PUBLISHED WORKS CONTAINED IN THIS THESIS

APPENDIX I. DECLARATION OF AUTHORSHIP

Two publications were used in this thesis. My contributions to these publications are outlined below

Lane SI, Chang HY, Jennings PC, Jones KT. The Aurora kinase inhibitor ZM447439 accelerates first meiosis in mouse oocytes by overriding the spindle assembly checkpoint. Reproduction. 2010 Oct;140(4):521-30.

This publication was published in October 2010 and corresponds to the work presented in chapter 5 of this thesis. All experiments were carried out by SL. Experiments were planned by SL and KJ. Data were analysed* and figures prepared by SL. HC and PJ contributed to the discussion.

*PJ was responsible for aneuploidy analysis, corresponding to the data presented in Figure 5.14 A. Experiment was carried out, oocytes were fixed, stained and imaged, and figure was prepared by SL.

Lane SI, Yun Y, Jones KT. Timing of anaphase-promoting complex activation in mouse oocytes is predicted by microtubule-kinetochore attachment but not by bivalent alignment or tension. Development. 2012.

This manuscript has been accepted for publication by the journal Development and represents most of the data presented in Chapters 3, 4 and 6. All experiments were carried out by SL*. Experiments were planned by SL and KJ. Data were analysed and figures prepared by SL.

*YY produced CenpC-GFP mRNA and YY and SL imaged the oocytes used in Figure 4.5. SL planned and analysed the data from the experiment and prepared the figures.

Simon Lane, Candidate Prof. Keith Jones, Principal Supervisor

8.2 BUFFERS AND SOLUTIONS

Notes

- *ddH_2O refers to distilled water from a Milli-Q system (Milli-Q, USA) with a resistivity of 18.2 MΩ.cm at 25°C.*
- *Filter sterilizing and filtering refer to the solution being pushed though a syringe filter or membrane with a pore diameter of 0.2µm (Nalgene/Thermo Fisher Scientific, USA).*

APPENDIX II. PMSG

The PMSG was prepared under sterile conditions by dissolving the lyphoilized hormone in filter sterile Phosphate Buffered Saline solution (PBS, Appendix IV) at a final concentration of 5 IU/0.1ml. The solution was loaded into 1ml syringes which were fitted with a 25 gauge 5/8 inch hypodermic needle before freezing at -80°C until just prior to use when the hormone was gently warmed to room temperature.

APPENDIX III. M2 MEDIA

Component	**g/L**
NaCl	5.533
KCl	0.356
$CaCl_2.2H_2O$	0.252
KH_2PO_4	0.162
$MgSO_4.7H_2O$	0.293
$NaHCO_3$	0.349
Hepes	4.969
Na Lactate	2.610
Na Pyruvate	0.036
Glucose	1.000
BSA	4.000
Penicilin G. K salt	0.060
Streptomycin Sulphate	0.050
Phenol Red	0.010
ddH_2O	To 1L

M2 Media was adjusted to pH 7.2-7.4 and to 283-289 mOsmol and filtered using 0.2µm membranes before being stored at 4°C, as described elsewhere (Quinn et al., 1982).

APPENDIX IV. MEM MEDIA

MEM was prepared by dissolving the content of the sachet (stored at 4°C) in 900ml ddH_2O. 2.2g of $NaHCO_3$ was added and the pH adjusted to 7.4 before making up to 1L with ddH_2O. The Media was stored at 4°C until preparation for use. Before use the media was supplemented with 1/200 volumes of PenStrep solution (Invitrogen, Australia), and 20% Fetal Calf Serum (Invitrogen, Australia) before being filter sterilized.

APPENDIX V. GENERAL BUFFERING SOLUTIONS

25x PVP solution

2.5g of PVP dissolved in 10ml ddH2O

PBS (10x)

NaCl	80g
KCL	2g
Na2HPO4.7H2O	26.8g
KH2PO4	2.4g

pH adjusted to 7.4 with 5M HCl and then made up to 1L with ddH_2O

PBS

10x PBS	5ml
ddH_2O	45ml

Filter sterilized and stored at 4°C.

PBS-PVP (PBS, 1% PVP)

10x PBS	600µl
25x PVP	240µl
ddH_2O	5.16ml

APPENDIX VI. WESTERN BLOTTING SOLUTIONS

PBST (PBS, 0.1% Tween-20)

10x PBS	200ml
10% Tween-20	20ml
ddH_2O	1780ml

PBST-BSA (PBS, 0.1% Tween-20, 3% BSA)

10x PBS	50ml
10% Tween-20	5ml
BSA	15g
ddH_2O	to 500ml

APPENDIX VII. FIXATION SOLUTIONS

3x PHEM Buffer

Pipes	2.72g
Hepes	0.975g
EGTA	0.57g
MgSO4.7H2O	0.304g

Dissolved in ddH_20 and adjusted to pH 7.4 with KOH.

Solution was then made up to 50ml with ddH_20 and filtered before storage at 4°C. Final (1x) concentrations: Pipes 60mM, Hepes 35mM, EGTA 25mM, $MgSO_4.7H_2O$ 4mM.

PHEM-PVP (PHEM Buffer, 1% PVP)

3x PHEM buffer	2ml
25x PVP	240µl
ddH_2O	3.76ml

Fixing Solution (PHEM buffer, 2% Formaldehyde, 0.5% Triton X-100)

3x PHEM buffer	5ml
ddH_2O	8ml
Paraformaldehyde prills	0.3g

Paraformaldehyde prills were dissolved in PHEM buffer to give a 2% solution by heating and stirring and addition of 5M NaOH. This preparation was made in a fume cupboard and then cooled to 4°C. 0.5% volume (75µl) Triton X-100 was added and allowed to dissolve, the solution was then made up to 15ml with ddH_20, filtered and stored at 4°C.

Permeabilization Solution (PBS, 1% PVP, 0.5% Triton X-100)

10x PBS	1ml
Triton X-100	50µl
25x PVP solution	400µl
ddH_2O	8.55ml

2x Calcium Buffer (200mM PIPES pH7.0, 2mM $MgCl_2$, 0.2mM$CaCl_2$, 0.2% Triton X-100)

300mM PIPES pH7.0	10ml
1M $MgCl_2$	3µl
0.5M $CaCl_2$	6µl
Triton X-100	30µl

Made up to 15ml with ddH_2O

This buffer was then filtered and stored at 4°C. Prior to use the buffer was diluted 1:1 with ddH_2O

Calcium Fixation Solution (100mM PIPES pH7.0, 1mM $MgCl_2$, 0.1mM$CaCl_2$, 0.1% Triton X-100, 2% Formaldehyde)

2x Calcium buffer	5ml
4% formaldehyde pH 7.0 in ddH_2O	5ml

This buffer was then filtered and stored at 4°C prior to use. Identical buffers and fixing solutions were also made but without the inclusion of $CaCl_2$ to use as a control.

APPENDIX VIII. IMMUNOFLUORESCENCE SOLUTIONS

Washing Solution (PBS, 1% BSA, 0.1% Tween20)

BSA	100mg
10xPBS	100µl
10% Tween20	100µl
ddH_2O	800µl

Blocking Solution (PBS, 7% Goat Serum, 1%BSA, 0.1% Tween20)

Washing Solution	2.79ml
100% goat serum	210µl

APPENDIX IX. MICROINJECTION SOLUTIONS

HEPES-buffered KCL Solution (140mM KCL, 10mM HEPES pH 7.4)

KCL	1.04g
ddH_2O	99ml
1M HEPES, pH 7.4	1ml

8.3 IMAGING AND FLUOROCHROME INFORMATION

APPENDIX X. SPECTRAL INFORMATION FOR COMMON FLUOROCHROMES

Fluorochrome	Excitation Max (nm)	Emission Max (nm)	Relative brightness
Hoechst	352	461	-
EGFP	488	507	100
Venus	515	528	156
EYFP	514	527	151
mCherry	587	610	47

Table 8.1 Excitation and Emission maxima for commonly used fluorochromes

8.4 IMAGE J MACROS

APPENDIX XI. MAD2 / CREST MEASURMENT MACRO

The following Image J macro script was installed onto the Image J platform and two functions called by using the ‘s’ and ‘l’ keys for ‘Setup’ and ‘Log data’ respectively. Image stacks containing CREST and Mad2 signals were setup using the ‘s’ function, then kinetochores were selected using the point tool and the data logged with the ‘l’ function.

```
print("To use:");
print("Press [s] to setup image");
print("Use the 'point tool' to select kinetochore")
print("Log data by pressing [l]");

macro "KT analysis image setup [s]"
    {
    imagename = getTitle();
    Stack.setDisplayMode("composite");
     Stack.setChannel(1);
     run("Red");
     Stack.setChannel(2);
```

```
13    run("Green");
14    Stack.setChannel(3);
15    run("Blue");
16    run("Channels Tool... ");
17    Stack.setDisplayMode("composite");
18    Stack.setActiveChannels("111");
19    run("Point Tool...", "mark=0 auto-measure label selection=green");
20
21    setTool(7);
22    setSlice(1);
23    print("Setup for [" + imagename + "] complete.");
24    }
25
26 macro "KT analysis log data [l]"
27    {
28    getVoxelSize(width, height, depth, unit);
29    calibration = width;
30    print("x,y calibration =" + calibration);
31    xx = getResult("X", nResults - 1);
32    xx = xx * (1 / calibration);
33    yy = getResult("Y", nResults - 1);
34    yy = yy * (1 / calibration);
35    zz = getResult("Slice", nResults - 1);
36    inf = getInfo("slice.label");
37    inf = split(inf, "/");
38    zs = substring(inf[2], 0, 2);
39    cs = substring(inf[1], 0, 1);
40    goto = (zz-1) * cs;
41    homolognumber = round((nResults / 2) + 0.1);
42    bgpos = newArray(-90, -30, 30);
43    gridX = newArray(0,0,0,1,1,1,2,2,2);
44    gridY = newArray(0,1,2,0,1,2,0,1,2);
45    bgx = -90;
46    bgy = -90;
47    makeOval(xx - 6, yy - 6, 12, 12);
48    setSlice(goto + 2);
49    getStatistics(area, mean);
50    setResult("Channel 2", nResults - 1, mean);
51    crest = mean;
52    setSlice(goto + 3);
53    getStatistics(area, mean);
54    setResult("Channel 3", nResults - 1, mean);
55    mad2 = mean;
56
57    ch2bg = 10000;
58    ch3bg = 10000;
59
60    for(i=0; i < 9; i++)
61       {
62       bgx = gridX[i];
63       bgx = xx + bgpos[bgx];
```

```
64        bgy = gridY[i];
65        bgy = yy + bgpos[bgy];
66        makeRectangle(bgx,bgy,60,60);
67
68        setSlice(goto + 2);
69        getStatistics(area, mean);
70        if(mean < ch2bg)
71           {
72           ch2bg = mean;
73           }
74
75        setSlice(goto + 3);
76        getStatistics(area, mean);
77        if(mean < ch3bg)
78           {
79           ch3bg = mean;
80           }
81        }
82
83        setResult("Channel 2 bg", nResults - 1, ch2bg);
84        setResult("Channel 3 bg", nResults - 1, ch3bg);
85        setResult("Homolog", nResults-1, homolognumber);
86        setFont("Arial", 8, "Bold");
87        setForegroundColor(255,255,255);
88        setBackgroundColor(255,255,255);
89        run("Overlay Options...", "stroke=yellow width=1 fill=yellow set");
90        makeOval(xx - 2, yy - 2, 4, 4);
91        run("Add Selection...");
92        run("Overlay Options...", "stroke=yellow width=1 fill=none");
93        run("Add Selection...");
94        makeText(homolognumber,xx + 3,yy);
95        run("Add Selection...");
96        makeOval(0, 0, 1, 1);
97        setSlice(goto + 1);
98        oneortwo = nResults - (round((nResults / 2) + 0.1) * 2) + 2;
99
100 // Further calculations
101        if(oneortwo == 2)
102           {
103           x2 = getResult("X", nResults - 1);
104           y2 = getResult("Y", nResults - 1);
105           z2 = getResult("Slice", nResults - 1);
106           x1 = getResult("X", nResults - 2);
107           y1 = getResult("Y", nResults - 2);
108           z1 = getResult("Slice", nResults - 2);
109           getVoxelSize(width, height, depth, unit);
110           dz = (z1 - z2) * depth;
111           dx = (x1 - x2);
112           dy = (y1 - y2);
113           iKTd = sqrt(pow(dx, 2) + pow(dy, 2) + pow(dz, 2));
114           setResult("iKTd", nResults - 1, iKTd);
```

```
115            }
116        else{
117            setResult("iKTd", nResults - 1, 0);
118            }
119        moc = (mad2 - ch3bg) / (crest - ch2bg);
120        setResult("Mad2/CREST", nResults - 1, moc);
121            print("logged data for homolog " + homolognumber + ", kinetochore " +
oneortwo);
122    }
```

APPENDIX XII. BIVALENT MEASUREMENT MACRO

The following macro was opened in Image J and appropriate values entered for calibration. The macro was then run and the user directed it to a folder containing .xls files where the 'X', 'Y' and 'Z' (Slice) values of pairs of kinetochores were stored. The macro then outputs the alignment, orientation and inter-kinetochore distance for each bivalent into a separate .xls file.

```
 1 var angle=0;
 2 var bestyet = 0;
 3 var bestyet2 = 100000;
 4 var bestx = 0;
 5 var besty = 0;
 6 var bestz = 0;
 7 var bestscalar = 0;
 8 var ts = 0;
 9 //CALIBRATION ____________________________________________________
10
11 //xy conversion
12                var calibration = 5.99971695;
13 //z plane separation
14                var zcal = 2;
15 //FUNCTIONS_____________________________________________________
16
17 function findangle(vx,vy,vz)
18 {
19 count=0;
20 for(h=1;h<nResults;h=h+2)
21        {
22
23        dx=(getResult("X",h-1)-getResult("X",h))/calibration;
24        dy=(getResult("Y",h-1)-getResult("Y",h))/calibration;
25        dz=(getResult("Slice",h-1)-getResult("Slice",h))*zcal;
26
27        a=(dx*vx)+(dy*vy)+(dz*vz);
28        b=sqrt(pow(vx,2)+pow(vy,2)+pow(vz,2));
29        c=sqrt(pow(dx,2)+pow(dy,2)+pow(dz,2));
30        angle=abs((acos(a/(b*c))*(180/PI))-90);
31        store[count] = angle;
```

```
32        count++;
33        }
34
35 }
36
37 function finddist(planescalar)
38 {
39 for(h=0;h<hs;h++)
40        {
41        k=(2*h);
42
43                    xcen = ((getResult("X",k) - getResult("X",k+1))/calibration)/2 +
(getResult("X",k+1)/calibration);
44                    ycen = ((getResult("Y",k) - getResult("Y",k+1))/calibration)/2 +
(getResult("Y",k+1)/calibration);
45                   zcen = ((getResult("Slice",k) - getResult("Slice",k+1))*zcal)/2 +
(getResult("Slice",k+1)*zcal);
46
47          dist = abs( (bestx*xcen) + (besty*ycen) + (bestz*zcen) + planescalar) / sqrt(
pow(bestx,2) + pow(besty,2) + pow(bestz,2) );
48        store2[h] = dist;
49        }
50 }
51
52
53
54 //DISCOVER TIMPOINTS_____________________________
55
56 rawlocation = getDirectory("Use files in this directory");
57 list = getFileList(rawlocation);
58
59 for(j=0;j<list.length;j++)
60        {
61        testxls = endsWith(list[j], "xls");
62        if(testxls)
63              {
64              ts++;
65              }
66        }
67
68
69 var list2 =  newArray(ts);
70 count2=0;
71 for(j=0;j<list.length;j++)
72        {
73        testxls = endsWith(list[j], "xls");
74        if(testxls)
75              {
76              list2[count2]=list[j];
77              count2++;
78              }
```

```
79        }
80
81
82 //RESULTS TABLE SETUP_____________________
83
84
85
86 newImage("Untitled", "8-bit White", 400, 400, 1);
87 run("Measure");
88 close();
89 run("Clear Results");
90 IJ.renameResults("analysis");
91
92
93
94 //TIMEPOINT CYCLE START_____________________________________
95 for(t=0;t<ts;t++)
96 {
97 open(list2[t]);
98 var hs = nResults/2;
99 var store =  newArray(hs);
100 var store2 =  newArray(hs);
101
102
103//FIND BEST PLANE NORMAL_____________
104
105        for(j=0;j<101;j++)
106        {
107        timea = getTime();
108
109                for(i=0;i<101;i++)
110                {
111                        for(p=0;p<101;p++)
112                        {
113
114                        vz=j-50;
115                        vx=i-50;
116                        vy=p-50;
117
118                        findangle(vx,vy,vz);
119                        Array.getStatistics(store, min, max, mean, stdDev);
120                        if(mean>bestyet){bestx =vx;besty = vy;bestz=vz; bestyet=mean;}
121
122
123                        }
124                }
125
126        print("\\Clear");
127        print("timepoint: " + t+1 + "/" + ts);
128        progress = round((((t*100) + j) / (ts * 100))*1000)/10;
129        print("progress: " + progress + "%  complete");
```

```
130         tsleft = ts - t;
131         jsleft = 50 - j;
132         timeb = getTime();
133         timeforonej = timeb-timea;
134         minleft = floor(((timeforonej * jsleft)+ (timeforonej * 100 * tsleft))/60000);
135         print("Estimated time remaining: " + minleft + " min ");
136
137         }
138
139         findangle(bestx,besty,bestz);
140
141 //FIND MIDZONE_____________________________________________________
142
143         for(g=-10000;g<10000;g++)
144                 {
145                 finddist(g);
146                 Array.getStatistics(store2, min, max, mean, stdDev);
147                 if(mean<bestyet2){bestscalar=g; bestyet2=mean;}
148                 }
149         finddist(bestscalar);
150
151 //iKTd
152
153         Exs = newArray(nResults);
154         Whys = newArray(nResults);
155         Zeds = newArray(nResults);
156         for(i=0;i<nResults;i++)
157                 {
158         Exs[i] = getResult("X",i)/calibration;
159         Whys[i] = getResult("Y",i)/calibration;
160         Zeds[i] = getResult("Slice",i)*zcal;
161                 }
162
163 //output
164
165         selectWindow("Results");IJ.renameResults("temp");
166         selectWindow("analysis");IJ.renameResults("Results");
167
168         name = split(list2[t],"-");
169
170         for(h=0;h<hs;h++)
171                 {
172                 k=h*2;
173                                         iKTd   =   sqrt(pow(Exs[k]-Exs[k+1],2)+pow(Whys[k]-
Whys[k+1],2)+pow(Zeds[k]-Zeds[k+1],2));
174
175                 setResult("Bivalent Number", h, h+1);
176                 setResult(name[0] + " - iKTd", h, iKTd);
177                 setResult(name[0] + " - Alignment dist", h, store2[h]);
178                 setResult(name[0] + " - Alignment angle", h, store[h]);
179                 }
```

```
180
181         selectWindow("Results");IJ.renameResults("analysis");
182         selectWindow("temp");IJ.renameResults("Results");
183 }
```

BIBLIOGRAPHY

Abrieu, A., Magnaghi-Jaulin, L., Kahana, J. A., Peter, M., Castro, A., Vigneron, S., Lorca, T., Cleveland, D. W. and Labbe, J. C. (2001). Mps1 is a kinetochore-associated kinase essential for the vertebrate mitotic checkpoint. *Cell* **106**, 83-93.

Acquaviva, C., Herzog, F., Kraft, C. and Pines, J. (2004). The anaphase promoting complex/cyclosome is recruited to centromeres by the spindle assembly checkpoint. *Nature Cell Biology* **6**, 892-8.

Akiyoshi, B., Nelson, C. R., Ranish, J. A. and Biggins, S. (2009). Analysis of Ipl1-mediated phosphorylation of the Ndc80 kinetochore protein in Saccharomyces cerevisiae. *Genetics* **183**, 1591-5.

Amaro, A. C., Samora, C. P., Holtackers, R., Wang, E., Kingston, I. J., Alonso, M., Lampson, M., McAinsh, A. D. and Meraldi, P. (2010). Molecular control of kinetochore-microtubule dynamics and chromosome oscillations. *Nat Cell Biol* **12**, 319-29.

Avo Santos, M., van de Werken, C., de Vries, M., Jahr, H., Vromans, M. J., Laven, J. S., Fauser, B. C., Kops, G. J., Lens, S. M. and Baart, E. B. (2011). A role for Aurora C in the chromosomal passenger complex during human preimplantation embryo development. *Hum Reprod* **26**, 1868-81.

Bach, S., Knockaert, M., Reinhardt, J., Lozach, O., Schmitt, S., Baratte, B., Koken, M., Coburn, S. P., Tang, L., Jiang, T. et al. (2005). Roscovitine targets, protein kinases and pyridoxal kinase. *J Biol Chem* **280**, 31208-19.

Baltus, A. E., Menke, D. B., Hu, Y. C., Goodheart, M. L., Carpenter, A. E., de Rooij, D. G. and Page, D. C. (2006). In germ cells of mouse embryonic ovaries, the decision to enter meiosis precedes premeiotic DNA replication. *Nat Genet* **38**, 1430-1434.

Basto, R., Scaerou, F., Mische, S., Wojcik, E., Lefebvre, C., Gomes, R., Hays, T. and Karess, R. (2004). In vivo dynamics of the rough deal checkpoint protein during Drosophila mitosis. *Current Biology* **14**, 56-61.

Bedford, L., Paine, S., Sheppard, P. W., Mayer, R. J. and Roelofs, J. (2010). Assembly, structure, and function of the 26S proteasome. *Trends Cell Biol* **20**, 391-401.

Biggins, S. and Murray, A. W. (2001). The budding yeast protein kinase Ipl1/Aurora allows the absence of tension to activate the spindle checkpoint. *Genes Dev* **15**, 3118-29.

Bowles, J., Knight, D., Smith, C., Wilhelm, D., Richman, J., Mamiya, S., Yashiro, K., Chawengsaksophak, K., Wilson, M. J., Rossant, J. et al. (2006). Retinoid signaling determines germ cell fate in mice. *Science* **312**, 596-600.

Boyarchuk, Y., Salic, A., Dasso, M. and Arnaoutov, A. (2007). Bub1 is essential for assembly of the functional inner centromere. *J Cell Biol* **176**, 919-28.

Breuer, M., Kolano, A., Kwon, M., Li, C. C., Tsai, T. F., Pellman, D., Brunet, S. and Verlhac, M. H. (2010). HURP permits MTOC sorting for robust meiotic spindle bipolarity, similar to extra centrosome clustering in cancer cells. *J Cell Biol* **191**, 1251-60.

Brown, J. R., Koretke, K. K., Birkeland, M. L., Sanseau, P. and Patrick, D. R. (2004). Evolutionary relationships of Aurora kinases: implications for model organism studies and the development of anti-cancer drugs. *BMC Evol Biol* **4**, 39.

Brunet, S., Maria, A. S., Guillaud, P., Dujardin, D., Kubiak, J. Z. and Maro, B. (1999). Kinetochore fibers are not involved in the formation of the first meiotic spindle in mouse oocytes, but control the exit from the first meiotic M phase. *J Cell Biol* **146**, 1-12.

Brunet, S. and Maro, B. (2005). Cytoskeleton and cell cycle control during meiotic maturation of the mouse oocyte: integrating time and space. *Reproduction* **130**, 801-11.

Brunet, S., Polanski, Z., Verlhac, M. H., Kubiak, J. Z. and Maro, B. (1998). Bipolar meiotic spindle formation without chromatin. *Curr Biol* **8**, 1231-4.

Bugge, M., Collins, A., Petersen, M. B., Fisher, J., Brandt, C., Hertz, J. M., Tranebjaerg, L., de Lozier-Blanchet, C., Nicolaides, P., Brondum-Nielsen, K. et al. (1998). Non-disjunction of chromosome 18. *Hum Mol Genet* **7**, 661-9.

Buonomo, S. B., Clyne, R. K., Fuchs, J., Loidl, J., Uhlmann, F. and Nasmyth, K. (2000). Disjunction of homologous chromosomes in meiosis I depends on proteolytic cleavage of the meiotic cohesin Rec8 by separin. *Cell* **103**, 387-98.

Cai, S., O'Connell, C. B., Khodjakov, A. and Walczak, C. E. (2009). Chromosome congression in the absence of kinetochore fibres. *Nat Cell Biol* **11**, 832-8.

Calarco, P. G., Donahue, R. P. and Szollosi, D. (1972). Germinal vesicle breakdown in the mouse oocyte. *J Cell Sci* **10**, 369-85.

Carmena, M., Ruchaud, S. and Earnshaw, W. C. (2009). Making the Auroras glow: regulation of Aurora A and B kinase function by interacting proteins. *Curr Opin Cell Biol* **21**, 796-805.

Chan, G. K., Liu, S. T. and Yen, T. J. (2005). Kinetochore structure and function. *Trends Cell Biol* **15**, 589-98.

Chang, D. C., Xu, N. and Luo, K. Q. (2003). Degradation of cyclin B is required for the onset of anaphase in Mammalian cells. *J Biol Chem* **278**, 37865-73.

Cheeseman, I. M., Chappie, J. S., Wilson-Kubalek, E. M. and Desai, A. (2006). The conserved KMN network constitutes the core microtubule-binding site of the kinetochore. *Cell* **127**, 983-97.

Chen, R. H. (2002). BubR1 is essential for kinetochore localization of other spindle checkpoint proteins and its phosphorylation requires Mad1. *J Cell Biol* **158**, 487-96.

Chesnel, F., Bazile, F., Pascal, A. and Kubiak, J. Z. (2007). Cyclin B2/cyclin-dependent kinase1 dissociation precedes CDK1 Thr-161 dephosphorylation upon M-phase promoting factor inactivation in Xenopus laevis cell-free extract. *Int J Dev Biol* **51**, 297-305.

Chi, Y. H., Haller, K., Ward, M. D., Semmes, O. J., Li, Y. and Jeang, K. T. (2008). Requirements for protein phosphorylation and the kinase activity of polo-like kinase 1 (Plk1) for the kinetochore function of mitotic arrest deficiency protein 1 (Mad1). *J Biol Chem* **283**, 35834-44.

Chiang, T., Duncan, F. E., Schindler, K., Schultz, R. M. and Lampson, M. A. (2010). Evidence that weakened centromere cohesion is a leading cause of age-related aneuploidy in oocytes. *Curr Biol* **20**, 1522-8.

Chow, J. P., Poon, R. Y. and Ma, H. T. (2011). Inhibitory phosphorylation of cyclin-dependent kinase 1 as a compensatory mechanism for mitosis exit. *Mol Cell Biol* **31**, 1478-91.

Cimini, D., Wan, X., Hirel, C. B. and Salmon, E. D. (2006). Aurora kinase promotes turnover of kinetochore microtubules to reduce chromosome segregation errors. *Current Biology* **16**, 1711-8.

Clute, P. and Pines, J. (1999). Temporal and spatial control of cyclin B1 destruction in metaphase. *Nat Cell Biol* **1**, 82-7.

Cowley, D. O., Rivera-Perez, J. A., Schliekelman, M., He, Y. J., Oliver, T. G., Lu, L., O'Quinn, R., Salmon, E. D., Magnuson, T. and Van Dyke, T. (2009). Aurora-A kinase is essential for bipolar spindle formation and early development. *Mol Cell Biol* **29**, 1059-71.

Cox, L. J., Larman, M. G., Saunders, C. M., Hashimoto, K., Swann, K. and Lai, F. A. (2002). Sperm phospholipase Czeta from humans and cynomolgus monkeys triggers Ca2+ oscillations, activation and development of mouse oocytes. *Reproduction* **124**, 611-23.

D'Amours, D. and Amon, A. (2004). At the interface between signaling and executing anaphase--Cdc14 and the FEAR network. *Genes Dev* **18**, 2581-95.

D'Angiolella, V., Mari, C., Nocera, D., Rametti, L. and Grieco, D. (2003). The spindle checkpoint requires cyclin-dependent kinase activity. *Genes Dev* **17**, 2520-5.

D'Angiolella, V., Palazzo, L., Santarpia, C., Costanzo, V. and Grieco, D. (2007). Role for non-proteolytic control of M-phase-promoting factor activity at M-phase exit. *PLoS One* **2**, e247.

De Antoni, A., Pearson, C. G., Cimini, D., Canman, J. C., Sala, V., Nezi, L., Mapelli, M., Sironi, L., Faretta, M., Salmon, E. D. et al. (2005). The Mad1/Mad2 complex as a template for Mad2 activation in the spindle assembly checkpoint. *Curr Biol* **15**, 214-25.

DeLuca, J. G., Gall, W. E., Ciferri, C., Cimini, D., Musacchio, A. and Salmon, E. D. (2006). Kinetochore microtubule dynamics and attachment stability are regulated by Hec1. *Cell* **127**, 969-82.

Deng, M., Gao, J., Suraneni, P. and Li, R. (2009). Kinetochore-independent chromosome poleward movement during anaphase of meiosis II in mouse eggs. *PLoS One* **4**, e5249.

Deng, M. Q. and Shen, S. S. (2000). A specific inhibitor of p34(cdc2)/cyclin B suppresses fertilization-induced calcium oscillations in mouse eggs. *Biol Reprod* **62**, 873-8.

Ding, J., Swain, J. E. and Smith, G. D. (2011). Aurora kinase-A regulates microtubule organizing center (MTOC) localization, chromosome dynamics, and histone-H3 phosphorylation in mouse oocytes. *Mol Reprod Dev* **78**, 80-90.

Ditchfield, C., Johnson, V. L., Tighe, A., Ellston, R., Haworth, C., Johnson, T., Mortlock, A., Keen, N. and Taylor, S. S. (2003). Aurora B couples chromosome alignment with anaphase by targeting BubR1, Mad2, and Cenp-E to kinetochores. *J Cell Biol* **161**, 267-80.

Dumont, J., Oegema, K. and Desai, A. (2010). A kinetochore-independent mechanism drives anaphase chromosome separation during acentrosomal meiosis. *Nat Cell Biol* **12**, 894-901.

Dumont, J., Petri, S., Pellegrin, F., Terret, M. E., Bohnsack, M. T., Rassinier, P., Georget, V., Kalab, P., Gruss, O. J. and Verlhac, M. H. (2007). A centriole- and RanGTP-independent spindle assembly pathway in meiosis I of vertebrate oocytes. *Journal of Cell Biology* **176**, 295-305.

Duncan, F. E., Chiang, T., Schultz, R. M. and Lampson, M. A. (2009). Evidence that a defective spindle assembly checkpoint is not the primary cause of maternal age-associated aneuploidy in mouse eggs. *Biol Reprod* **81**, 768-76.

Elowe, S., Hummer, S., Uldschmid, A., Li, X. and Nigg, E. A. (2007). Tension-sensitive Plk1 phosphorylation on BubR1 regulates the stability of kinetochore microtubule interactions. *Genes Dev* **21**, 2205-19.

Enserink, J. M. and Kolodner, R. D. (2010). An overview of Cdk1-controlled targets and processes. *Cell Div* **5**, 11.

Fang, G., Yu, H. and Kirschner, M. W. (1998). The checkpoint protein MAD2 and the mitotic regulator CDC20 form a ternary complex with the anaphase-promoting complex to control anaphase initiation. *Genes Dev* **12**, 1871-83.

Farr, K. A. and Hoyt, M. A. (1998). Bub1p kinase activates the Saccharomyces cerevisiae spindle assembly checkpoint. *Mol Cell Biol* **18**, 2738-47.

Fava, L. L., Kaulich, M., Nigg, E. A. and Santamaria, A. (2011). Probing the in vivo function of Mad1:C-Mad2 in the spindle assembly checkpoint. *EMBO J* **30**, 3322-36.

Floyd, S., Pines, J. and Lindon, C. (2008). APC/C Cdh1 targets aurora kinase to control reorganization of the mitotic spindle at anaphase. *Current Biology* **18**, 1649-58.

Forester, C. M., Maddox, J., Louis, J. V., Goris, J. and Virshup, D. M. (2007). Control of mitotic exit by PP2A regulation of Cdc25C and Cdk1. *Proc Natl Acad Sci U S A* **104**, 19867-72.

Fortune, J. E. (2003). The early stages of follicular development: activation of primordial follicles and growth of preantral follicles. *Anim Reprod Sci* **78**, 135-63.

Gadea, B. B. and Ruderman, J. V. (2006). Aurora B is required for mitotic chromatin-induced phosphorylation of Op18/Stathmin. *Proc Natl Acad Sci U S A* **103**, 4493-8.

Gassmann, R., Holland, A. J., Varma, D., Wan, X., Civril, F., Cleveland, D. W., Oegema, K., Salmon, E. D. and Desai, A. (2010). Removal of Spindly from microtubule-attached kinetochores controls spindle checkpoint silencing in human cells. *Genes Dev* **24**, 957-71.

Gavet, O. and Pines, J. (2010). Progressive activation of CyclinB1-Cdk1 coordinates entry to mitosis. *Dev Cell* **18**, 533-43.

George, O., Johnston, M. A. and Shuster, C. B. (2006). Aurora B kinase maintains chromatin organization during the MI to MII transition in surf clam oocytes. *Cell Cycle* **5**, 2648-56.

Gorr, I. H., Boos, D. and Stemmann, O. (2005). Mutual inhibition of separase and Cdk1 by two-step complex formation. *Mol Cell* **19**, 135-41.

Gorr, I. H., Reis, A., Boos, D., Wuhr, M., Madgwick, S., Jones, K. T. and Stemmann, O. (2006). Essential CDK1-inhibitory role for separase during meiosis I in vertebrate oocytes. *Nat Cell Biol* **8**, 1035-7.

Goto, H., Yasui, Y., Kawajiri, A., Nigg, E. A., Terada, Y., Tatsuka, M., Nagata, K. and Inagaki, M. (2003). Aurora-B regulates the cleavage furrow-specific vimentin phosphorylation in the cytokinetic process. *J Biol Chem* **278**, 8526-30.

Goto, H., Yasui, Y., Nigg, E. A. and Inagaki, M. (2002). Aurora-B phosphorylates Histone H3 at serine28 with regard to the mitotic chromosome condensation. *Genes Cells* **7**, 11-7.

Gregan, J., Polakova, S., Zhang, L., Tolic-Norrelykke, I. M. and Cimini, D. (2011). Merotelic kinetochore attachment: causes and effects. *Trends Cell Biol* **21**, 374-81.

Griffis, E. R., Stuurman, N. and Vale, R. D. (2007). Spindly, a novel protein essential for silencing the spindle assembly checkpoint, recruits dynein to the kinetochore. *Journal of Cell Biology* **177**, 1005-15.

Hached, K., Xie, S. Z., Buffin, E., Cladiere, D., Rachez, C., Sacras, M., Sorger, P. K. and Wassmann, K. (2011). Mps1 at kinetochores is essential for female mouse meiosis I. *Development* **138**, 2261-71.

Hagan, R. S., Manak, M. S., Buch, H. K., Meier, M. G., Meraldi, P., Shah, J. V. and Sorger, P. K. (2011). p31(comet) acts to ensure timely spindle checkpoint silencing subsequent to kinetochore attachment. *Mol Biol Cell* **22**, 4236-46.

Hagting, A., Den Elzen, N., Vodermaier, H. C., Waizenegger, I. C., Peters, J. M. and Pines, J. (2002). Human securin proteolysis is controlled by the spindle checkpoint and reveals when the APC/C switches from activation by Cdc20 to Cdh1. *J Cell Biol* **157**, 1125-37.

Hampl, A. and Eppig, J. J. (1995). Analysis of the mechanism(s) of metaphase I arrest in maturing mouse oocytes. *Development* **121**, 925-33.

Han, S. J. and Conti, M. (2006). New pathways from PKA to the Cdc2/cyclin B complex in oocytes: Wee1B as a potential PKA substrate. *Cell Cycle* **5**, 227-31.

Hardwick, K. G., Weiss, E., Luca, F. C., Winey, M. and Murray, A. W. (1996). Activation of the budding yeast spindle assembly checkpoint without mitotic spindle disruption. *Science* **273**, 953-6.

Hassold, T. and Hunt, P. (2001). To err (meiotically) is human: the genesis of human aneuploidy. *Nat Rev Genet* **2**, 280-91.

Hassold, T., Merrill, M., Adkins, K., Freeman, S. and Sherman, S. (1995). Recombination and maternal age-dependent nondisjunction: molecular studies of trisomy 16. *Am J Hum Genet* **57**, 867-74.

Hauf, S., Cole, R. W., LaTerra, S., Zimmer, C., Schnapp, G., Walter, R., Heckel, A., van Meel, J., Rieder, C. L. and Peters, J. M. (2003). The small molecule Hesperadin reveals a role for Aurora B in correcting kinetochore-microtubule attachment and in maintaining the spindle assembly checkpoint. *J Cell Biol* **161**, 281-94.

Hayden, J. H., Bowser, S. S. and Rieder, C. L. (1990). Kinetochores capture astral microtubules during chromosome attachment to the mitotic spindle: direct visualization in live newt lung cells. *Journal of Cell Biology* **111**, 1039-45.

Herbert, M., Levasseur, M., Homer, H., Yallop, K., Murdoch, A. and McDougall, A. (2003). Homologue disjunction in mouse oocytes requires proteolysis of securin and cyclin B1. *Nature Cell Biology* **5**, 1023-5.

Hewitt, L., Tighe, A., Santaguida, S., White, A. M., Jones, C. D., Musacchio, A., Green, S. and Taylor, S. S. (2010). Sustained Mps1 activity is required in mitosis to recruit O-Mad2 to the Mad1-C-Mad2 core complex. *J Cell Biol* **190**, 25-34.

Hirose, Y., Suzuki, R., Ohba, T., Hinohara, Y., Matsuhara, H., Yoshida, M., Itabashi, Y., Murakami, H. and Yamamoto, A. (2011). Chiasmata promote monopolar attachment of sister chromatids and their co-segregation toward the proper pole during meiosis I. *PLoS Genet* **7**, e1001329.

Hoffman, D. B., Pearson, C. G., Yen, T. J., Howell, B. J. and Salmon, E. D. (2001). Microtubule-dependent changes in assembly of microtubule motor proteins and mitotic spindle checkpoint proteins at PtK1 kinetochores. *Mol Biol Cell* **12**, 1995-2009.

Hoffmann, S., Maro, B., Kubiak, J. Z. and Polanski, Z. (2011). A single bivalent efficiently inhibits cyclin B1 degradation and polar body extrusion in mouse oocytes indicating robust SAC during female meiosis I. *PLoS One* **6**, e27143.

Holt, J. E., Tran, S. M., Stewart, J. L., Minahan, K., Garcia-Higuera, I., Moreno, S. and Jones, K. T. (2011). The APC/C activator FZR1 coordinates the timing of meiotic resumption during prophase I arrest in mammalian oocytes. *Development* **138**, 905-13.

Holt, J. E., Weaver, J. and Jones, K. T. (2010). Spatial regulation of APCCdh1-induced cyclin B1 degradation maintains G2 arrest in mouse oocytes. *Development* **137**, 1297-304.

Homer, H., Gui, L. and Carroll, J. (2009). A spindle assembly checkpoint protein functions in prophase I arrest and prometaphase progression. *Science* **326**, 991-4.

Homer, H. A., McDougall, A., Levasseur, M., Murdoch, A. P. and Herbert, M. (2005a). Mad2 is required for inhibiting securin and cyclin B degradation following spindle depolymerisation in meiosis I mouse oocytes. *Reproduction* **130**, 829-43.

Homer, H. A., McDougall, A., Levasseur, M., Yallop, K., Murdoch, A. P. and Herbert, M. (2005b). Mad2 prevents aneuploidy and premature proteolysis of cyclin B and securin during meiosis I in mouse oocytes. *Genes Dev* **19**, 202-7.

Hornick, J. E., Mader, C. C., Tribble, E. K., Bagne, C. C., Vaughan, K. T., Shaw, S. L. and Hinchcliffe, E. H. (2011). Amphiastral mitotic spindle assembly in vertebrate cells lacking centrosomes. *Curr Biol* **21**, 598-605.

Howell, B. J., Hoffman, D. B., Fang, G., Murray, A. W. and Salmon, E. D. (2000). Visualization of Mad2 dynamics at kinetochores, along spindle fibers, and at spindle poles in living cells. *Journal of Cell Biology* **150**, 1233-50.

Howell, B. J., Moree, B., Farrar, E. M., Stewart, S., Fang, G. and Salmon, E. D. (2004). Spindle checkpoint protein dynamics at kinetochores in living cells. *Current Biology* **14**, 953-64.

Hoyt, M. A., Totis, L. and Roberts, B. T. (1991). S. cerevisiae genes required for cell cycle arrest in response to loss of microtubule function. *Cell* **66**, 507-17.

Hunt, P. A. and Hassold, T. J. (2008). Human female meiosis: what makes a good egg go bad? *Trends Genet* **24**, 86-93.

Hunt, P. A., Koehler, K. E., Susiarjo, M., Hodges, C. A., Ilagan, A., Voigt, R. C., Thomas, S., Thomas, B. F. and Hassold, T. J. (2003). Bisphenol a exposure causes meiotic aneuploidy in the female mouse. *Current Biology* **13**, 546-53.

Illingworth, C., Pirmadjid, N., Serhal, P., Howe, K. and Fitzharris, G. (2010). MCAK regulates chromosome alignment but is not necessary for preventing aneuploidy in mouse oocyte meiosis I. *Development* **137**, 2133-8.

Ito, D., Saito, Y. and Matsumoto, T. (2011). Centromere-tethered Mps1 pombe homolog (Mph1) kinase is a sufficient marker for recruitment of the spindle checkpoint protein Bub1, but not Mad1. *Proc Natl Acad Sci U S A* **109**, 209-14.

Jablonski, S. A., Chan, G. K., Cooke, C. A., Earnshaw, W. C. and Yen, T. J. (1998). The hBUB1 and hBUBR1 kinases sequentially assemble onto kinetochores during prophase with hBUBR1 concentrating at the kinetochore plates in mitosis. *Chromosoma* **107**, 386-96.

Jaqaman, K., King, E. M., Amaro, A. C., Winter, J. R., Dorn, J. F., Elliott, H. L., McHedlishvili, N., McClelland, S. E., Porter, I. M., Posch, M. et al. (2010). Kinetochore alignment within the metaphase plate is regulated by centromere stiffness and microtubule depolymerases. *J Cell Biol* **188**, 665-79.

Jelinkova, L. and Kubelka, M. (2006). Neither Aurora B activity nor histone H3 phosphorylation is essential for chromosome condensation during meiotic maturation of porcine oocytes. *Biol Reprod* **74**, 905-12.

Jelluma, N., Brenkman, A. B., van den Broek, N. J., Cruijsen, C. W., van Osch, M. H., Lens, S. M., Medema, R. H. and Kops, G. J. (2008). Mps1 phosphorylates Borealin to control Aurora B activity and chromosome alignment. *Cell* **132**, 233-46.

Jelluma, N., Dansen, T. B., Sliedrecht, T., Kwiatkowski, N. P. and Kops, G. J. (2010). Release of Mps1 from kinetochores is crucial for timely anaphase onset. *J Cell Biol* **191**, 281-90.

Jia, L., Li, B., Warrington, R. T., Hao, X., Wang, S. and Yu, H. (2011). Defining pathways of spindle checkpoint silencing: functional redundancy between Cdc20 ubiquitination and p31(comet). *Mol Biol Cell* **22**, 4227-35.

Jin, F., Hamada, M., Malureanu, L., Jeganathan, K. B., Zhou, W., Morbeck, D. E. and van Deursen, J. M. (2010). Cdc20 is critical for meiosis I and fertility of female mice. *PLoS Genet* **6**.

Johnson, M. K. and Wise, D. A. (2010). Distribution of kinetochore fragments during mitosis with unreplicated genomes. *Cytoskeleton (Hoboken)* **67**, 172-7.

Johnson, V. L., Scott, M. I., Holt, S. V., Hussein, D. and Taylor, S. S. (2004). Bub1 is required for kinetochore localization of BubR1, Cenp-E, Cenp-F and Mad2, and chromosome congression. *J Cell Sci* **117**, 1577-89.

Jones, K. T. (2008). Meiosis in oocytes: predisposition to aneuploidy and its increased incidence with age. *Human Reproduction Update* **14**, 143-158.

Kallio, M. J., McCleland, M. L., Stukenberg, P. T. and Gorbsky, G. J. (2002). Inhibition of aurora B kinase blocks chromosome segregation, overrides the spindle checkpoint, and perturbs microtubule dynamics in mitosis. *Curr Biol* **12**, 900-5.

Kanatsu-Shinohara, M., Schultz, R. M. and Kopf, G. S. (2000). Acquisition of meiotic competence in mouse oocytes: absolute amounts of p34(cdc2), cyclin B1, cdc25C, and wee1 in meiotically incompetent and competent oocytes. *Biol Reprod* **63**, 1610-6.

Kapoor, T. M., Lampson, M. A., Hergert, P., Cameron, L., Cimini, D., Salmon, E. D., McEwen, B. F. and Khodjakov, A. (2006). Chromosomes can congress to the metaphase plate before biorientation. *Science* **311**, 388-91.

Kapoor, T. M., Mayer, T. U., Coughlin, M. L. and Mitchison, T. J. (2000). Probing spindle assembly mechanisms with monastrol, a small molecule inhibitor of the mitotic kinesin, Eg5. *J Cell Biol* **150**, 975-88.

Katis, V. L., Lipp, J. J., Imre, R., Bogdanova, A., Okaz, E., Habermann, B., Mechtler, K., Nasmyth, K. and Zachariae, W. (2010). Rec8 phosphorylation by casein kinase 1 and Cdc7-Dbf4 kinase regulates cohesin cleavage by separase during meiosis. *Dev Cell* **18**, 397-409.

Keeney, S. and Neale, M. J. (2006). Initiation of meiotic recombination by formation of DNA double-strand breaks: mechanism and regulation. *Biochem Soc Trans* **34**, 523-5.

Kitajima, T. S., Hauf, S., Ohsugi, M., Yamamoto, T. and Watanabe, Y. (2005). Human Bub1 defines the persistent cohesion site along the mitotic chromosome by affecting Shugoshin localization. *Curr Biol* **15**, 353-9.

Kitajima, T. S., Kawashima, S. A. and Watanabe, Y. (2004). The conserved kinetochore protein shugoshin protects centromeric cohesion during meiosis. *Nature* **427**, 510-7.

Kitajima, T. S., Miyazaki, Y., Yamamoto, M. and Watanabe, Y. (2003). Rec8 cleavage by separase is required for meiotic nuclear divisions in fission yeast. *EMBO J* **22**, 5643-53.

Kitajima, T. S., Ohsugi, M. and Ellenberg, J. (2011). Complete kinetochore tracking reveals error-prone homologous chromosome biorientation in mammalian oocytes. *Cell* **146**, 568-81.

Kitajima, T. S., Sakuno, T., Ishiguro, K., Iemura, S., Natsume, T., Kawashima, S. A. and Watanabe, Y. (2006). Shugoshin collaborates with protein phosphatase 2A to protect cohesin. *Nature* **441**, 46-52.

Klein, F., Mahr, P., Galova, M., Buonomo, S. B., Michaelis, C., Nairz, K. and Nasmyth, K. (1999). A central role for cohesins in sister chromatid cohesion, formation of axial elements, and recombination during yeast meiosis. *Cell* **98**, 91-103.

Kline-Smith, S. L., Khodjakov, A., Hergert, P. and Walczak, C. E. (2004). Depletion of centromeric MCAK leads to chromosome congression and segregation defects due to improper kinetochore attachments. *Mol Biol Cell* **15**, 1146-59.

Knowlton, A. L., Lan, W. and Stukenberg, P. T. (2006). Aurora B is enriched at merotelic attachment sites, where it regulates MCAK. *Curr Biol* **16**, 1705-10.

Kotwaliwale, C. and Biggins, S. (2006). Microtubule capture: a concerted effort. *Cell* **127**, 1105-8.

Kouznetsova, A., Lister, L., Nordenskjold, M., Herbert, M. and Hoog, C. (2007). Bi-orientation of achiasmatic chromosomes in meiosis I oocytes contributes to aneuploidy in mice. *Nat Genet* **39**, 966-8.

Kraft, C., Herzog, F., Gieffers, C., Mechtler, K., Hagting, A., Pines, J. and Peters, J. M. (2003). Mitotic regulation of the human anaphase-promoting complex by phosphorylation. *EMBO J* **22**, 6598-609.

Kudo, N. R., Wassmann, K., Anger, M., Schuh, M., Wirth, K. G., Xu, H., Helmhart, W., Kudo, H., McKay, M., Maro, B. et al. (2006). Resolution of chiasmata in oocytes requires separase-mediated proteolysis. *Cell* **126**, 135-46.

Kuliev, A., Cieslak, J. and Verlinsky, Y. (2005). Frequency and distribution of chromosome abnormalities in human oocytes. *Cytogenet Genome Res* **111**, 193-8.

Kuliev, A., Zlatopolsky, Z., Kirillova, I., Spivakova, J. and Cieslak Janzen, J. (2011). Meiosis errors in over 20,000 oocytes studied in the practice of preimplantation aneuploidy testing. *Reprod Biomed Online* **22**, 2-8.

Kulukian, A., Han, J. S. and Cleveland, D. W. (2009). Unattached kinetochores catalyze production of an anaphase inhibitor that requires a Mad2 template to prime Cdc20 for BubR1 binding. *Dev Cell* **16**, 105-17.

Lamb, N. E., Feingold, E., Savage, A., Avramopoulos, D., Freeman, S., Gu, Y., Hallberg, A., Hersey, J., Karadima, G., Pettay, D. et al. (1997a). Characterization of susceptible chiasma configurations that increase the risk for maternal nondisjunction of chromosome 21. *Hum Mol Genet* **6**, 1391-9.

Lamb, N. E., Feingold, E. and Sherman, S. L. (1997b). Estimating meiotic exchange patterns from recombination data: an application to humans. *Genetics* **146**, 1011-7.

Lamb, N. E., Freeman, S. B., Savage-Austin, A., Pettay, D., Taft, L., Hersey, J., Gu, Y., Shen, J., Saker, D., May, K. M. et al. (1996). Susceptible chiasmate configurations of chromosome 21 predispose to non-disjunction in both maternal meiosis I and meiosis II. *Nat Genet* **14**, 400-5.

Lampson, M. A. and Kapoor, T. M. (2005). The human mitotic checkpoint protein BubR1 regulates chromosome-spindle attachments. *Nat Cell Biol* **7**, 93-8.

Ledan, E., Polanski, Z., Terret, M. E. and Maro, B. (2001). Meiotic maturation of the mouse oocyte requires an equilibrium between cyclin B synthesis and degradation. *Dev Biol* **232**, 400-13.

LeMaire-Adkins, R. and Hunt, P. A. (2000). Nonrandom segregation of the mouse univalent X chromosome: evidence of spindle-mediated meiotic drive. *Genetics* **156**, 775-83.

LeMaire-Adkins, R., Radke, K. and Hunt, P. A. (1997). Lack of checkpoint control at the metaphase/anaphase transition: a mechanism of meiotic nondisjunction in mammalian females. *Journal of Cell Biology* **139**, 1611-9.

Li, M., Li, S., Yuan, J., Wang, Z. B., Sun, S. C., Schatten, H. and Sun, Q. Y. (2009). Bub3 is a spindle assembly checkpoint protein regulating chromosome segregation during mouse oocyte meiosis. *PLoS One* **4**, e7701.

Li, R. and Murray, A. W. (1991). Feedback control of mitosis in budding yeast. *Cell* **66**, 519-31.

Li, X. and Nicklas, R. B. (1995). Mitotic forces control a cell-cycle checkpoint. *Nature* **373**, 630-2.

Lindon, C. and Pines, J. (2004). Ordered proteolysis in anaphase inactivates Plk1 to contribute to proper mitotic exit in human cells. *Journal of Cell Biology* **164**, 233-41.

Lindqvist, A., Rodriguez-Bravo, V. and Medema, R. H. (2009). The decision to enter mitosis: feedback and redundancy in the mitotic entry network. *Journal of Cell Biology* **185**, 193-202.

Lister, L. M., Kouznetsova, A., Hyslop, L. A., Kalleas, D., Pace, S. L., Barel, J. C., Nathan, A., Floros, V., Adelfalk, C., Watanabe, Y. et al. (2010). Age-related meiotic segregation errors in mammalian oocytes are preceded by depletion of cohesin and Sgo2. *Curr Biol* **20**, 1511-21.

Liu, D., Vader, G., Vromans, M. J., Lampson, M. A. and Lens, S. M. (2009). Sensing chromosome bi-orientation by spatial separation of aurora B kinase from kinetochore substrates. *Science* **323**, 1350-3.

Liu, D., Vleugel, M., Backer, C. B., Hori, T., Fukagawa, T., Cheeseman, I. M. and Lampson, M. A. (2010). Regulated targeting of protein phosphatase 1 to the outer kinetochore by KNL1 opposes Aurora B kinase. *Journal of Cell Biology* **188**, 809-20.

Lorca, T., Labbe, J. C., Devault, A., Fesquet, D., Capony, J. P., Cavadore, J. C., Le Bouffant, F. and Doree, M. (1992). Dephosphorylation of cdc2 on threonine 161 is required for cdc2 kinase inactivation and normal anaphase. *EMBO J* **11**, 2381-90.

Luo, X., Tang, Z., Xia, G., Wassmann, K., Matsumoto, T., Rizo, J. and Yu, H. (2004). The Mad2 spindle checkpoint protein has two distinct natively folded states. *Nat Struct Mol Biol* **11**, 338-45.

Ma, W., Baumann, C. and Viveiros, M. M. (2010). NEDD1 is crucial for meiotic spindle stability and accurate chromosome segregation in mammalian oocytes. *Dev Biol* **339**, 439-50.

Ma, W., Koch, J. A. and Viveiros, M. M. (2008). Protein kinase C delta (PKCdelta) interacts with microtubule organizing center (MTOC)-associated proteins and participates in meiotic spindle organization. *Dev Biol* **320**, 414-25.

Madgwick, S., Hansen, D. V., Levasseur, M., Jackson, P. K. and Jones, K. T. (2006). Mouse Emi2 is required to enter meiosis II by reestablishing cyclin B1 during interkinesis. *J Cell Biol* **174**, 791-801.

Maldonado, M. and Kapoor, T. M. (2011). Constitutive Mad1 targeting to kinetochores uncouples checkpoint signalling from chromosome biorientation. *Nat Cell Biol* **13**, 475-82.

Mansfeld, J., Collin, P., Collins, M. O., Choudhary, J. S. and Pines, J. (2011). APC15 drives the turnover of MCC-CDC20 to make the spindle assembly checkpoint responsive to kinetochore attachment. *Nat Cell Biol* **13**, 1234-43.

Mao, Y., Desai, A. and Cleveland, D. W. (2005). Microtubule capture by CENP-E silences BubR1-dependent mitotic checkpoint signaling. *Journal of Cell Biology* **170**, 873-80.

Marangos, P. and Carroll, J. (2004). The dynamics of cyclin B1 distribution during meiosis I in mouse oocytes. *Reproduction* **128**, 153-62.

Maresca, T. J. and Salmon, E. D. (2009). Intrakinetochore stretch is associated with changes in kinetochore phosphorylation and spindle assembly checkpoint activity. *J Cell Biol* **184**, 373-81.

Masciarelli, S., Horner, K., Liu, C., Park, S. H., Hinckley, M., Hockman, S., Nedachi, T., Jin, C., Conti, M. and Manganiello, V. (2004). Cyclic nucleotide phosphodiesterase 3A-deficient mice as a model of female infertility. *J Clin Invest* **114**, 196-205.

Matzuk, M. M., Burns, K. H., Viveiros, M. M. and Eppig, J. J. (2002). Intercellular communication in the mammalian ovary: oocytes carry the conversation. *Science* **296**, 2178-80.

Maure, J. F., Kitamura, E. and Tanaka, T. U. (2007). Mps1 kinase promotes sister-kinetochore bi-orientation by a tension-dependent mechanism. *Curr Biol* **17**, 2175-82.

Maure, J. F., Komoto, S., Oku, Y., Mino, A., Pasqualato, S., Natsume, K., Clayton, L., Musacchio, A. and Tanaka, T. U. (2011). The Ndc80 loop region facilitates formation of kinetochore attachment to the dynamic microtubule plus end. *Curr Biol* **21**, 207-13.

McClellan, K. A., Gosden, R. and Taketo, T. (2003). Continuous loss of oocytes throughout meiotic prophase in the normal mouse ovary. *Dev Biol* **258**, 334-48.

McDougall, A. and Levasseur, M. (1998). Sperm-triggered calcium oscillations during meiosis in ascidian oocytes first pause, restart, then stop: correlations with cell cycle kinase activity. *Development* **125**, 4451-9.

McGuinness, B. E., Anger, M., Kouznetsova, A., Gil-Bernabe, A. M., Helmhart, W., Kudo, N. R., Wuensche, A., Taylor, S., Hoog, C., Novak, B. et al. (2009). Regulation of APC/C activity in oocytes by a Bub1-dependent spindle assembly checkpoint. *Curr Biol* **19**, 369-80.

McLaren, A. (2000). Germ and somatic cell lineages in the developing gonad. *Molecular and Cellular Endocrinology* **163**, 3-9.

McLaren, A. (2003). Primordial germ cells in the mouse. *Developmental Biology* **262**, 1-15.

Meijer, L., Borgne, A., Mulner, O., Chong, J. P., Blow, J. J., Inagaki, N., Inagaki, M., Delcros, J. G. and Moulinoux, J. P. (1997). Biochemical and cellular effects of roscovitine, a potent and selective inhibitor of the cyclin-dependent kinases cdc2, cdk2 and cdk5. *Eur J Biochem* **243**, 527-36.

Meunier, S. and Vernos, I. (2011). K-fibre minus ends are stabilized by a RanGTP-dependent mechanism essential for functional spindle assembly. *Nature Cell Biology* **13**, 1406-14.

Monje-Casas, F., Prabhu, V. R., Lee, B. H., Boselli, M. and Amon, A. (2007). Kinetochore orientation during meiosis is controlled by Aurora B and the monopolin complex. *Cell* **128**, 477-90.

Moreno, S., Hayles, J. and Nurse, P. (1989). Regulation of p34cdc2 protein kinase during mitosis. *Cell* **58**, 361-72.

Muhlhauser, A., Susiarjo, M., Rubio, C., Griswold, J., Gorence, G., Hassold, T. and Hunt, P. A. (2009). Bisphenol A effects on the growing mouse oocyte are influenced by diet. *Biol Reprod* **80**, 1066-71.

Musacchio, A. and Salmon, E. D. (2007). The spindle-assembly checkpoint in space and time. *Nat Rev Mol Cell Biol* **8**, 379-93.

Nagaoka, S. I., Hodges, C. A., Albertini, D. F. and Hunt, P. A. (2011). Oocyte-specific differences in cell-cycle control create an innate susceptibility to meiotic errors. *Curr Biol* **21**, 651-7.

Niault, T., Hached, K., Sotillo, R., Sorger, P. K., Maro, B., Benezra, R. and Wassmann, K. (2007). Changing Mad2 levels affects chromosome segregation and spindle assembly checkpoint control in female mouse meiosis I. *PLoS One* **2**, e1165.

Nilsson, J., Yekezare, M., Minshull, J. and Pines, J. (2008). The APC/C maintains the spindle assembly checkpoint by targeting Cdc20 for destruction. *Nat Cell Biol* **10**, 1411-20.

Nixon, V. L., Levasseur, M., McDougall, A. and Jones, K. T. (2002). Ca(2+) oscillations promote APC/C-dependent cyclin B1 degradation during metaphase arrest and completion of meiosis in fertilizing mouse eggs. *Curr Biol* **12**, 746-50.

Norris, R. P., Ratzan, W. J., Freudzon, M., Mehlmann, L. M., Krall, J., Movsesian, M. A., Wang, H., Ke, H., Nikolaev, V. O. and Jaffe, L. A. (2009). Cyclic GMP from the surrounding somatic cells regulates cyclic AMP and meiosis in the mouse oocyte. *Development* **136**, 1869-78.

O'Connell, C. B., Loncarek, J., Hergert, P., Kourtidis, A., Conklin, D. S. and Khodjakov, A. (2008). The spindle assembly checkpoint is satisfied in the absence of interkinetochore tension during mitosis with unreplicated genomes. *J Cell Biol* **183**, 29-36.

Oh, J. S., Han, S. J. and Conti, M. (2010). Wee1B, Myt1, and Cdc25 function in distinct compartments of the mouse oocyte to control meiotic resumption. *Journal of Cell Biology* **188**, 199-207.

Oliveira, R. A., Hamilton, R. S., Pauli, A., Davis, I. and Nasmyth, K. (2010). Cohesin cleavage and Cdk inhibition trigger formation of daughter nuclei. *Nature Cell Biology* **12**, 185-92.

Ou, X. H., Li, S., Xu, B. Z., Wang, Z. B., Quan, S., Li, M., Zhang, Q. H., Ouyang, Y. C., Schatten, H., Xing, F. Q. et al. (2010). p38alpha MAPK is a MTOC-associated protein regulating spindle assembly, spindle length and accurate chromosome segregation during mouse oocyte meiotic maturation. *Cell Cycle* **9**, 4130-43.

Page, S. L. and Hawley, R. S. (2004). The genetics and molecular biology of the synaptonemal complex. *Annu Rev Cell Dev Biol* **20**, 525-58.

Perera, D. and Taylor, S. S. (2010). Sgo1 establishes the centromeric cohesion protection mechanism in G2 before subsequent Bub1-dependent recruitment in mitosis. *J Cell Sci* **123**, 653-9.

Perera, D., Tilston, V., Hopwood, J. A., Barchi, M., Boot-Handford, R. P. and Taylor, S. S. (2007). Bub1 maintains centromeric cohesion by activation of the spindle checkpoint. *Dev Cell* **13**, 566-79.

Perez, L. H., Antonio, C., Flament, S., Vernos, I. and Nebreda, A. R. (2002). Xkid chromokinesin is required for the meiosis I to meiosis II transition in Xenopus laevis oocytes. *Nat Cell Biol* **4**, 737-42.

Peters, J. M. (2006). The anaphase promoting complex/cyclosome: a machine designed to destroy. *Nat Rev Mol Cell Biol* **7**, 644-56.

Pfleger, C. M. and Kirschner, M. W. (2000). The KEN box: an APC recognition signal distinct from the D box targeted by Cdh1. *Genes Dev* **14**, 655-65.

Picard, A., Galas, S., Peaucellier, G. and Doree, M. (1996). Newly assembled cyclin B-cdc2 kinase is required to suppress DNA replication between meiosis I and meiosis II in starfish oocytes. *EMBO J* **15**, 3590-8.

Pines, J. (2011). Cubism and the cell cycle: the many faces of the APC/C. *Nat Rev Mol Cell Biol* **12**, 427-38.

Pinsky, B. A., Nelson, C. R. and Biggins, S. (2009). Protein phosphatase 1 regulates exit from the spindle checkpoint in budding yeast. *Current Biology* **19**, 1182-7.

Potapova, T. A., Daum, J. R., Byrd, K. S. and Gorbsky, G. J. (2009). Fine tuning the cell cycle: activation of the Cdk1 inhibitory phosphorylation pathway during mitotic exit. *Mol Biol Cell* **20**, 1737-48.

Potapova, T. A., Sivakumar, S., Flynn, J. N., Li, R. and Gorbsky, G. J. (2011). Mitotic progression becomes irreversible in prometaphase and collapses when Wee1 and Cdc25 are inhibited. *Mol Biol Cell* **22**, 1191-206.

Queralt, E. and Uhlmann, F. (2008). Cdk-counteracting phosphatases unlock mitotic exit. *Curr Opin Cell Biol* **20**, 661-8.

Quinn, P., Barros, C. and Whittingham, D. G. (1982). Preservation of hamster oocytes to assay the fertilizing capacity of human spermatozoa. *J Reprod Fertil* **66**, 161-8.

Reis, A., Chang, H. Y., Levasseur, M. and Jones, K. T. (2006). APC(cdh1) activity in mouse oocytes prevents entry into the first meiotic division. *Nature Cell Biology* **8**, 539-540.

Reis, A., Madgwick, S., Chang, H. Y., Nabti, I., Levasseur, M. and Jones, K. T. (2007). Prometaphase APCcdh1 activity prevents non-disjunction in mammalian oocytes. *Nat Cell Biol* **9**, 1192-8.

Revenkova, E., Herrmann, K., Adelfalk, C. and Jessberger, R. (2010). Oocyte cohesin expression restricted to predictyate stages provides full fertility and prevents aneuploidy. *Current Biology* **20**, 1529-33.

Riedel, C. G., Katis, V. L., Katou, Y., Mori, S., Itoh, T., Helmhart, W., Galova, M., Petronczki, M., Gregan, J., Cetin, B. et al. (2006). Protein phosphatase 2A protects centromeric sister chromatid cohesion during meiosis I. *Nature* **441**, 53-61.

Rieder, C. L. (2005). Kinetochore fiber formation in animal somatic cells: dueling mechanisms come to a draw. *Chromosoma* **114**, 310-8.

Rieder, C. L. and Alexander, S. P. (1990). Kinetochores are transported poleward along a single astral microtubule during chromosome attachment to the spindle in newt lung cells. *Journal of Cell Biology* **110**, 81-95.

Rieder, C. L., Cole, R. W., Khodjakov, A. and Sluder, G. (1995). The checkpoint delaying anaphase in response to chromosome monoorientation is mediated by an inhibitory signal produced by unattached kinetochores. *J Cell Biol* **130**, 941-8.

Rieder, C. L., Schultz, A., Cole, R. and Sluder, G. (1994). Anaphase onset in vertebrate somatic cells is controlled by a checkpoint that monitors sister kinetochore attachment to the spindle. *J Cell Biol* **127**, 1301-10.

Rime, H., Huchon, D., De Smedt, V., Thibier, C., Galaktionov, K., Jessus, C. and Ozon, R. (1994). Microinjection of Cdc25 protein phosphatase into Xenopus prophase oocyte activates MPF and arrests meiosis at metaphase I. *Biol Cell* **82**, 11-22.

Rischitor, P. E., May, K. M. and Hardwick, K. G. (2007). Bub1 is a fission yeast kinetochore scaffold protein, and is sufficient to recruit other spindle checkpoint proteins to ectopic sites on chromosomes. *PLoS One* **2**, e1342.

Robinson, W. P., Kuchinka, B. D., Bernasconi, F., Petersen, M. B., Schulze, A., Brondum-Nielsen, K., Christian, S. L., Ledbetter, D. H., Schinzel, A. A., Horsthemke, B. et al. (1998). Maternal meiosis I non-disjunction of chromosome 15: dependence of the maternal age effect on level of recombination. *Hum Mol Genet* **7**, 1011-9.

Rosenbusch, B. (2004). The incidence of aneuploidy in human oocytes assessed by conventional cytogenetic analysis. *Hereditas* **141**, 97-105.

Ruchaud, S., Carmena, M. and Earnshaw, W. C. (2007). The chromosomal passenger complex: one for all and all for one. *Cell* **131**, 230-1.

Rudner, A. D. and Murray, A. W. (2000). Phosphorylation by Cdc28 activates the Cdc20-dependent activity of the anaphase-promoting complex. *J Cell Biol* **149**, 1377-90.

Sakuno, T., Tada, K. and Watanabe, Y. (2009). Kinetochore geometry defined by cohesion within the centromere. *Nature* **458**, 852-8.

Sakuno, T., Tanaka, K., Hauf, S. and Watanabe, Y. (2011). Repositioning of aurora B promoted by chiasmata ensures sister chromatid mono-orientation in meiosis I. *Dev Cell* **21**, 534-45.

Salmon, E. D. and Begg, D. A. (1980). Functional implications of cold-stable microtubules in kinetochore fibers of insect spermatocytes during anaphase. *J Cell Biol* **85**, 853-65.

Santaguida, S., Vernieri, C., Villa, F., Ciliberto, A. and Musacchio, A. (2011). Evidence that Aurora B is implicated in spindle checkpoint signalling independently of error correction. *EMBO J* **30**, 1508-19.

Saskova, A., Solc, P., Baran, V., Kubelka, M., Schultz, R. M. and Motlik, J. (2008). Aurora kinase A controls meiosis I progression in mouse oocytes. *Cell Cycle* **7**, 2368-76.

Saurin, A. T., van der Waal, M. S., Medema, R. H., Lens, S. M. and Kops, G. J. (2011). Aurora B potentiates Mps1 activation to ensure rapid checkpoint establishment at the onset of mitosis. *Nat Commun* **2**, 316.

Schindler, K., Davydenko, O., Fram, B., Lampson, M. A. and Schultz, R. M. (2012). Maternally recruited Aurora C kinase is more stable than Aurora B to support mouse oocyte maturation and early development. *Proc Natl Acad Sci U S A*.

Schindler, K. and Schultz, R. M. (2009). The CDC14A phosphatase regulates oocyte maturation in mouse. *Cell Cycle* **8**, 1090-8.

Schramm, S., Fraune, J., Naumann, R., Hernandez-Hernandez, A., Hoog, C., Cooke, H. J., Alsheimer, M. and Benavente, R. (2011). A novel mouse synaptonemal complex protein is essential for loading of central element proteins, recombination, and fertility. *PLoS Genet* **7**, e1002088.

Schuh, M. and Ellenberg, J. (2007). Self-organization of MTOCs replaces centrosome function during acentrosomal spindle assembly in live mouse oocytes. *Cell* **130**, 484-98.

Selesniemi, K., Lee, H. J., Muhlhauser, A. and Tilly, J. L. (2011). Prevention of maternal aging-associated oocyte aneuploidy and meiotic spindle defects in mice by dietary and genetic strategies. *Proc Natl Acad Sci U S A* **108**, 12319-24.

Shah, J. V., Botvinick, E., Bonday, Z., Furnari, F., Berns, M. and Cleveland, D. W. (2004). Dynamics of centromere and kinetochore proteins; implications for checkpoint signaling and silencing. *Current Biology* **14**, 942-52.

Sharif, B., Na, J., Lykke-Hartmann, K., McLaughlin, S. H., Laue, E., Glover, D. M. and Zernicka-Goetz, M. (2010). The chromosome passenger complex is required for fidelity of chromosome transmission and cytokinesis in meiosis of mouse oocytes. *J Cell Sci* **123**, 4292-300.

Shteinberg, M., Protopopov, Y., Listovsky, T., Brandeis, M. and Hershko, A. (1999). Phosphorylation of the cyclosome is required for its stimulation by Fizzy/cdc20. *Biochem Biophys Res Commun* **260**, 193-8.

Shuda, K., Schindler, K., Ma, J., Schultz, R. M. and Donovan, P. J. (2009). Aurora kinase B modulates chromosome alignment in mouse oocytes. *Mol Reprod Dev* **76**, 1094-105.

Sironi, L., Mapelli, M., Knapp, S., De Antoni, A., Jeang, K. T. and Musacchio, A. (2002). Crystal structure of the tetrameric Mad1-Mad2 core complex: implications of a 'safety belt' binding mechanism for the spindle checkpoint. *EMBO J* **21**, 2496-506.

Skibbens, R. V., Skeen, V. P. and Salmon, E. D. (1993). Directional instability of kinetochore motility during chromosome congression and segregation in mitotic newt lung cells: a push-pull mechanism. *J Cell Biol* **122**, 859-75.

Skoufias, D. A., Andreassen, P. R., Lacroix, F. B., Wilson, L. and Margolis, R. L. (2001). Mammalian mad2 and bub1/bubR1 recognize distinct spindle-attachment and kinetochore-tension checkpoints. *Proc Natl Acad Sci U S A* **98**, 4492-7.

Skoufias, D. A., Indorato, R. L., Lacroix, F., Panopoulos, A. and Margolis, R. L. (2007). Mitosis persists in the absence of Cdk1 activity when proteolysis or protein phosphatase activity is suppressed. *J Cell Biol* **179**, 671-85.

Slattery, S. D., Mancini, M. A., Brinkley, B. R. and Hall, R. M. (2009). Aurora-C kinase supports mitotic progression in the absence of Aurora-B. *Cell Cycle* **8**, 2984-94.

Solc, P., Saskova, A., Baran, V., Kubelka, M., Schultz, R. M. and Motlik, J. (2008). CDC25A phosphatase controls meiosis I progression in mouse oocytes. *Dev Biol* **317**, 260-9.

Solc, P., Schultz, R. M. and Motlik, J. (2010). Prophase I arrest and progression to metaphase I in mouse oocytes: comparison of resumption of meiosis and recovery from G2-arrest in somatic cells. *Mol Hum Reprod* **16**, 654-64.

Sonn, S., Oh, G. T. and Rhee, K. (2010). Nek2 and its substrate, centrobin/Nip2, are required for proper meiotic spindle formation of the mouse oocytes. *Zygote* **19**, 15-20.

Stanford, J. S. and Ruderman, J. V. (2005). Changes in regulatory phosphorylation of Cdc25C Ser287 and Wee1 Ser549 during normal cell cycle progression and checkpoint arrests. *Mol Biol Cell* **16**, 5749-60.

Stegmeier, F. and Amon, A. (2004). Closing mitosis: the functions of the Cdc14 phosphatase and its regulation. *Annu Rev Genet* **38**, 203-32.

Steigemann, P., Wurzenberger, C., Schmitz, M. H., Held, M., Guizetti, J., Maar, S. and Gerlich, D. W. (2009). Aurora B-mediated abscission checkpoint protects against tetraploidization. *Cell* **136**, 473-84.

Stemmann, O., Zou, H., Gerber, S. A., Gygi, S. P. and Kirschner, M. W. (2001). Dual inhibition of sister chromatid separation at metaphase. *Cell* **107**, 715-26.

Sudakin, V., Chan, G. K. and Yen, T. J. (2001). Checkpoint inhibition of the APC/C in HeLa cells is mediated by a complex of BUBR1, BUB3, CDC20, and MAD2. *J Cell Biol* **154**, 925-36.

Swain, J. E., Ding, J., Wu, J. and Smith, G. D. (2008). Regulation of spindle and chromatin dynamics during early and late stages of oocyte maturation by aurora kinases. *Mol Hum Reprod* **14**, 291-9.

Tachibana-Konwalski, K., Godwin, J., van der Weyden, L., Champion, L., Kudo, N. R., Adams, D. J. and Nasmyth, K. (2010). Rec8-containing cohesin maintains bivalents without turnover during the growing phase of mouse oocytes. *Genes Dev* **24**, 2505-16.

Taieb, F. E., Gross, S. D., Lewellyn, A. L. and Maller, J. L. (2001). Activation of the anaphase-promoting complex and degradation of cyclin B is not required for progression from Meiosis I to II in Xenopus oocytes. *Curr Biol* **11**, 508-13.

Tam, P. P. L. and Snow, M. H. L. (1981). Proliferation and Migration of Primordial Germ-Cells during Compensatory Growth in Mouse Embryos. *Journal of Embryology and Experimental Morphology* **64**, 133-147.

Tanaka, K., Kitamura, E., Kitamura, Y. and Tanaka, T. U. (2007). Molecular mechanisms of microtubule-dependent kinetochore transport toward spindle poles. *Journal of Cell Biology* **178**, 269-81.

Tanaka, K., Kitamura, E. and Tanaka, T. U. (2010). Live-cell analysis of kinetochore-microtubule interaction in budding yeast. *Methods* **51**, 206-13.

Tang, Z., Shu, H., Oncel, D., Chen, S. and Yu, H. (2004a). Phosphorylation of Cdc20 by Bub1 provides a catalytic mechanism for APC/C inhibition by the spindle checkpoint. *Mol Cell* **16**, 387-97.

Tang, Z., Sun, Y., Harley, S. E., Zou, H. and Yu, H. (2004b). Human Bub1 protects centromeric sister-chromatid cohesion through Shugoshin during mitosis. *Proc Natl Acad Sci U S A* **101**, 18012-7.

Tease, C., Hartshorne, G. M. and Hulten, M. A. (2002). Patterns of meiotic recombination in human fetal oocytes. *Am J Hum Genet* **70**, 1469-79.

Tesse, S., Storlazzi, A., Kleckner, N., Gargano, S. and Zickler, D. (2003). Localization and roles of Ski8p protein in Sordaria meiosis and delineation of three mechanistically distinct steps of meiotic homolog juxtaposition. *Proceedings of the National Academy of Sciences of the United States of America* **100**, 12865-12870.

Thomas, N. S., Ennis, S., Sharp, A. J., Durkie, M., Hassold, T. J., Collins, A. R. and Jacobs, P. A. (2001). Maternal sex chromosome non-disjunction: evidence for X chromosome-specific risk factors. *Hum Mol Genet* **10**, 243-50.

Thompson, S. L. and Compton, D. A. (2008). Examining the link between chromosomal instability and aneuploidy in human cells. *J Cell Biol* **180**, 665-72.

Thompson, S. L. and Compton, D. A. (2011). Chromosome missegregation in human cells arises through specific types of kinetochore-microtubule attachment errors. *Proc Natl Acad Sci U S A* **108**, 17974-8.

Thornton, B. R., Ng, T. M., Matyskiela, M. E., Carroll, C. W., Morgan, D. O. and Toczyski, D. P. (2006). An architectural map of the anaphase-promoting complex. *Genes Dev* **20**, 449-60.

Thornton, B. R. and Toczyski, D. P. (2003). Securin and B-cyclin/CDK are the only essential targets of the APC. *Nature Cell Biology* **5**, 1090-4.

Tighe, A., Staples, O. and Taylor, S. (2008). Mps1 kinase activity restrains anaphase during an unperturbed mitosis and targets Mad2 to kinetochores. *J Cell Biol* **181**, 893-901.

Toso, A., Winter, J. R., Garrod, A. J., Amaro, A. C., Meraldi, P. and McAinsh, A. D. (2009). Kinetochore-generated pushing forces separate centrosomes during bipolar spindle assembly. *J Cell Biol* **184**, 365-72.

Toth, A., Queralt, E., Uhlmann, F. and Novak, B. (2007). Mitotic exit in two dimensions. *J Theor Biol* **248**, 560-73.

Tseng, T. C., Chen, S. H., Hsu, Y. P. and Tang, T. K. (1998). Protein kinase profile of sperm and eggs: cloning and characterization of two novel testis-specific protein kinases (AIE1, AIE2) related to yeast and fly chromosome segregation regulators. *DNA Cell Biol* **17**, 823-33.

Tsurumi, C., Hoffmann, S., Geley, S., Graeser, R. and Polanski, Z. (2004). The spindle assembly checkpoint is not essential for CSF arrest of mouse oocytes. *Journal of Cell Biology* **167**, 1037-50.

Tumurbaatar, I., Cizmecioglu, O., Hoffmann, I., Grummt, I. and Voit, R. (2011). Human Cdc14B promotes progression through mitosis by dephosphorylating Cdc25 and regulating Cdk1/cyclin B activity. *PLoS One* **6**, e14711.

Uchida, K. S., Takagaki, K., Kumada, K., Hirayama, Y., Noda, T. and Hirota, T. (2009). Kinetochore stretching inactivates the spindle assembly checkpoint. *Journal of Cell Biology* **184**, 383-90.

Vanoosthuyse, V. and Hardwick, K. G. (2009). A novel protein phosphatase 1-dependent spindle checkpoint silencing mechanism. *Current Biology* **19**, 1176-81.

Verlhac, M. H., Lefebvre, C., Guillaud, P., Rassinier, P. and Maro, B. (2000). Asymmetric division in mouse oocytes: with or without Mos. *Current Biology* **10**, 1303-6.

Visconti, R., Palazzo, L. and Grieco, D. (2010). Requirement for proteolysis in spindle assembly checkpoint silencing. *Cell Cycle* **9**, 564-9.

Visintin, R., Craig, K., Hwang, E. S., Prinz, S., Tyers, M. and Amon, A. (1998). The phosphatase Cdc14 triggers mitotic exit by reversal of Cdk-dependent phosphorylation. *Molecular Cell* **2**, 709-18.

Viveiros, M. M., O'Brien, M. and Eppig, J. J. (2004). Protein kinase C activity regulates the onset of anaphase I in mouse oocytes. *Biol Reprod* **71**, 1525-32.

Vogt, E., Kipp, A. and Eichenlaub-Ritter, U. (2009). Aurora kinase B, epigenetic state of centromeric heterochromatin and chiasma resolution in oocytes. *Reprod Biomed Online* **19**, 352-68.

Vogt, E., Sanhaji, M., Klein, W., Seidel, T., Wordeman, L. and Eichenlaub-Ritter, U. (2010). MCAK is present at centromeres, midspindle and chiasmata and involved in silencing of the spindle assembly checkpoint in mammalian oocytes. *Mol Hum Reprod* **16**, 665-84.

Wang, Q., Ratchford, A. M., Chi, M. M., Schoeller, E., Frolova, A., Schedl, T. and Moley, K. H. (2009). Maternal diabetes causes mitochondrial dysfunction and meiotic defects in murine oocytes. *Mol Endocrinol* **23**, 1603-12.

Wang, Y., Toppari, J., Parvinen, M. and Kallio, M. J. (2006). Inhibition of Aurora kinases perturbs chromosome alignment and spindle checkpoint signaling in rat spermatocytes. *Exp Cell Res* **312**, 3459-70.

Warren, A. C., Chakravarti, A., Wong, C., Slaugenhaupt, S. A., Halloran, S. L., Watkins, P. C., Metaxotou, C. and Antonarakis, S. E. (1987). Evidence for reduced recombination on the nondisjoined chromosomes 21 in Down syndrome. *Science* **237**, 652-4.

Wassmann, K., Niault, T. and Maro, B. (2003). Metaphase I arrest upon activation of the Mad2-dependent spindle checkpoint in mouse oocytes. *Curr Biol* **13**, 1596-608.

Watanabe, Y. and Nurse, P. (1999). Cohesin Rec8 is required for reductional chromosome segregation at meiosis. *Nature* **400**, 461-4.

Waters, J. C., Chen, R. H., Murray, A. W. and Salmon, E. D. (1998). Localization of Mad2 to kinetochores depends on microtubule attachment, not tension. *Journal of Cell Biology* **141**, 1181-91.

Waters, J. C., Skibbens, R. V. and Salmon, E. D. (1996). Oscillating mitotic newt lung cell kinetochores are, on average, under tension and rarely push. *J Cell Sci* **109 (Pt 12)**, 2823-31.

Waterston, R. H. Lindblad-Toh, K. Birney, E. Rogers, J. Abril, J. F. Agarwal, P. Agarwala, R. Ainscough, R. Alexandersson, M. An, P. et al. (2002). Initial sequencing and comparative analysis of the mouse genome. *Nature* **420**, 520-62.

Wei, L., Liang, X. W., Zhang, Q. H., Li, M., Yuan, J., Li, S., Sun, S. C., Ouyang, Y. C., Schatten, H. and Sun, Q. Y. (2010). BubR1 is a spindle assembly checkpoint protein regulating meiotic cell cycle progression of mouse oocyte. *Cell Cycle* **9**, 1112-21.

Wei, R., Ngo, B., Wu, G. and Lee, W. H. (2011). Phosphorylation of the Ndc80 complex protein, HEC1, by Nek2 kinase modulates chromosome alignment and signaling of the spindle assembly checkpoint. *Mol Biol Cell* **22**, 3584-94.

Weisenberg, R. C. and Deery, W. J. (1981). The mechanism of calcium-induced microtubule disassembly. *Biochem Biophys Res Commun* **102**, 924-31.

Weiss, E. and Winey, M. (1996). The Saccharomyces cerevisiae spindle pole body duplication gene MPS1 is part of a mitotic checkpoint. *Journal of Cell Biology* **132**, 111-23.

Welburn, J. P., Vleugel, M., Liu, D., Yates, J. R., 3rd, Lampson, M. A., Fukagawa, T. and Cheeseman, I. M. (2010). Aurora B phosphorylates spatially distinct targets to differentially regulate the kinetochore-microtubule interface. *Mol Cell* **38**, 383-92.

Westhorpe, F. G., Tighe, A., Lara-Gonzalez, P. and Taylor, S. S. (2011). p31comet-mediated extraction of Mad2 from the MCC promotes efficient mitotic exit. *J Cell Sci* **124**, 3905-16.

Wickramasinghe, D., Ebert, K. M. and Albertini, D. F. (1991). Meiotic competence acquisition is associated with the appearance of M-phase characteristics in growing mouse oocytes. *Dev Biol* **143**, 162-72.

Wignall, S. M. and Villeneuve, A. M. (2009). Lateral microtubule bundles promote chromosome alignment during acentrosomal oocyte meiosis. *Nat Cell Biol* **11**, 839-44.

Wilcox, A. J., Weinberg, C. R., O'Connor, J. F., Baird, D. D., Schlatterer, J. P., Canfield, R. E., Armstrong, E. G. and Nisula, B. C. (1988). Incidence of early loss of pregnancy. *N Engl J Med* **319**, 189-94.

Winston, N. J. (1997). Stability of cyclin B protein during meiotic maturation and the first mitotic cell division in mouse oocytes. *Biol Cell* **89**, 211-9.

Wolf, F., Wandke, C., Isenberg, N. and Geley, S. (2006). Dose-dependent effects of stable cyclin B1 on progression through mitosis in human cells. *EMBO J* **25**, 2802-13.

Wollman, R., Cytrynbaum, E. N., Jones, J. T., Meyer, T., Scholey, J. M. and Mogilner, A. (2005). Efficient chromosome capture requires a bias in the 'search-and-capture' process during mitotic-spindle assembly. *Current Biology* **15**, 828-32.

Woods, L. M., Hodges, C. A., Baart, E., Baker, S. M., Liskay, M. and Hunt, P. A. (1999). Chromosomal influence on meiotic spindle assembly: abnormal meiosis I in female Mlh1 mutant mice. *Journal of Cell Biology* **145**, 1395-406.

Yang, K. T., Li, S. K., Chang, C. C., Tang, C. J., Lin, Y. N., Lee, S. C. and Tang, T. K. (2010). Aurora-C Kinase Deficiency Causes Cytokinesis Failure in Meiosis I and Production of Large Polyploid Oocytes in Mouse. *Mol Biol Cell*.

Yin, S., Wang, Q., Liu, J. H., Ai, J. S., Liang, C. G., Hou, Y., Chen, D. Y., Schatten, H. and Sun, Q. Y. (2006). Bub1 prevents chromosome misalignment and precocious anaphase during mouse oocyte meiosis. *Cell Cycle* **5**, 2130-7.

Zhang, D., Li, M., Ma, W., Hou, Y., Li, Y. H., Li, S. W., Sun, Q. Y. and Wang, W. H. (2005). Localization of mitotic arrest deficient 1 (MAD1) in mouse oocytes during the first meiosis and its functions as a spindle checkpoint protein. *Biol Reprod* **72**, 58-68.

Zhang, D., Ma, W., Li, Y. H., Hou, Y., Li, S. W., Meng, X. Q., Sun, X. F., Sun, Q. Y. and Wang, W. H. (2004). Intra-oocyte localization of MAD2 and its relationship with kinetochores, microtubules, and chromosomes in rat oocytes during meiosis. *Biol Reprod* **71**, 740-8.

Zhang, D., Yin, S., Jiang, M. X., Ma, W., Hou, Y., Liang, C. G., Yu, L. Z., Wang, W. H. and Sun, Q. Y. (2007a). Cytoplasmic dynein participates in meiotic checkpoint inactivation in mouse oocytes by transporting cytoplasmic mitotic arrest-deficient (Mad) proteins from kinetochores to spindle poles. *Reproduction* **133**, 685-95.

Zhang, J., Ahmad, S. and Mao, Y. (2007b). BubR1 and APC/EB1 cooperate to maintain metaphase chromosome alignment. *J Cell Biol* **178**, 773-84.

Zich, J., Sochaj, A. M., Syred, H. M., Milne, L., Cook, A. G., Ohkura, H., Rappsilber, J. and Hardwick, K. G. (2012). Kinase activity of fission yeast mph1 is required for mad2 and mad3 to stably bind the anaphase promoting complex. *Curr Biol* **22**, 296-301.